THE UNIVERSITY *of* EDINBURGH

Alphavirus and flavivirus infection of *Ixodes* tick cell lines: an insight into tick antiviral immunity

Claudia Rückert

Submitted for the degree of Doctor of Philosophy

The University of Edinburgh

2014

Table of contents

Declaration

I declare that all the work included in this thesis is my own except where otherwise stated. No part of this work has been or will be submitted for any other degree or professional qualification.

Claudia Rückert

April 2014

Acknowledgements

First of all, I would like to thank my supervisor **John Fazakerley**, for giving me the opportunity to do this PhD project and for his support and encouragement. I am especially grateful to my 2nd supervisor **Lesley Bell-Sakyi** - thank you for all the effort you put into taking care of us. Thank you for being supportive, proof-reading everything - from abstracts to manuscripts and finally this thesis - and thank you for many invitations and personal favours during these last 3 ½ years.

My sincerest thanks go to **Gerald Barry**, **Rennos Fragkoudis**, **Alain Kohl** and **Finn Grey** for assisting in my supervision. In particular, thank you, **Ger**, for taking the initiative to help me shape my project and guiding me through a crucial phase of my PhD. Similarly, I would like to thank my friend and supervisor **Rennos**, for taking over my supervision and always supporting me. You made me believe in myself as a scientist and helped me decide to pursue this PhD - a choice which despite the many obstacles and moves along the way, I do not regret in the slightest.

Many thanks to **Julio Rodriguez** for help with melanisation experiments and to **Esther Schnettler** for your scientific help, especially with the LGTV work, for your friendship and always being there if I had a scientific problem. Thanks to **Joana Ferrolho** for establishing the SCRV qPCR, which proved extremely useful and to **Sue Jacobs** for her help with SUMOylation experiments and cloning. Many thanks also to **Lisa Stevens** for her help with flow cytometry experiments at Pirbright. Many thanks also to **Anna Moniuszko**, **Pilar Alberdi** and all other co-authors for their work on the co-infection paper including the *E. ruminantium* experiments and to the visiting student **Renata Strouhalová** for her help working on *Ixodes* Relish.

I am grateful to **Sonja Best** and **Esther Schnettler** for providing the Langat virus and antibodies, to **Andres Merits** for SFV reporter constructs, to **Ulrike Munderloh** for provision of tick cell lines, to **Peter Walker** for CxVago antibody and advice, and to **Darren Obbard** for his help with the phylogenetic tree of STAT.

I would also like to thank the Marie Curie Initial Training network **POSTICK** for funding my PhD and also the people involved in the POSTICK project. Thanks to all

the PIs for organising great workshops and meetings, and especially thanks to the other ESRs for forming a great community of PhD students across Europe.

I am most grateful to all the past and present members of the 'Roslin Arbovirus Group' who have contributed to the success of this project and who helped make these last 3 ½ years a great experience. Very special thanks to **Sabine** and **Claire**, you are the best friends one could hope to have while struggling through a PhD - I will miss you sorely when we go our separate ways, Sabine, and I'm already missing you, Clairchen! I wish both of you all the best and will visit you as often as possible. Thank you also, **Mhairi, Stacey** and **Adrian** for all your support and friendship! Important for the preservation of my sanity throughout this PhD were also the members of the **Grey** and **Digard** groups, who made the days at Roslin always a bit more bearable and fun.

I am immensely thankful to the very welcoming community of people at **Pirbright** who helped me through the transition period after our disruptive move. I will never forget the friendliness (and craziness) of this place, the fantastic summer of 2013, the thousands of random Whatsapp messages, movie nights and the brilliant nights at the bar! Thanks also to all our lunch & coffee buddies for the great lunch-time entertainment (although I'll be perfectly happy to never discuss coriander again…).

Finally, I would like to thank my parents **Helga** and **Norbert**, and my brother **Christian**, who have always supported and challenged me, who taught me critical thinking and discussing, who have always let me make my own decisions and become independent, and have thus contributed immensely to the successful completion of my PhD.

"A theory is something nobody believes, except the person who made it. An experiment is something everybody believes, except the person who made it."

(Albert Einstein)

And to all my friends who still face the challenge of finishing their PhD:

*May the force be with yo*u*!*

(George Lucas/Star Wars)

Abbreviations

Ago	Argonaute
ASFV	African swine fever virus
BHK-21	baby hamster kidney cells
BLAST	Basic Local Alignment Search Tool
BSA	bovine serum albumin
BTV	bluetongue virus
C	capsid
CDC	Centers for Diseases Control and Prevention
cDNA	complementary DNA
cds	coding sequence
CG	computed gene
CHIKV	chikungunya virus
CPE	cytopathic effect
CPVI/II	cytopathic vacuole I/II
ct	cycle threshold
d	days
Dcr	Dicer
DD	death domain
DENV	dengue virus
DMSO	dimethylsulphoxide
DNA	deoxyribonucleic acid
dNTP	deoxy-nucleoside triphosphate
dsDNA	double-stranded deoxyribonucleic acid
dsRNA	double stranded ribonucleic acid
DTT	dithiothreitol
E	envelope
EDTA	ethylenediaminetetraacetic acid
EEEV	Eastern equine encephalitis virus
Egf1.0	epidermal growth factor-like 1.0
eGFP	enhanced green fluorescent protein
ER	endoplasmic reticulum
FACS	fluorescence-activated cell sorting
FAF-1	Fas-associated factor 1
FBS	foetal bovine serum
FHV	flock house virus
Fig	figure
g	gram
GFP	green fluorescent protein
GMEM	Glasgow minimal essential medium
GTP	guanosine triphosphate
h	hours
H_2O	water
IFN	interferon
IκB	inhibitor of κB
IKK	IκB kinase
IMD	immune deficiency

JAK	Janus kinase
JEV	Japanese encephalitis virus
Kb	kilobases
KFDV	Kyasanur Forest disease virus
L-15	Leibovitz's L-15
LB broth	Luria-Bertani broth
LGTV	Langat virus
LIV	louping ill virus
LPS	lipopolysaccharide
LRR	leucine-rich repeat
MDA5	melanoma differentiation-associated gene 5
µg	microgram
µl	microlitre
µm	micrometre
ml	millilitre
mRNA	messenger ribonucleic acid
MOI	multiplicity of infection
MTC	mock-treated control
MyD88	myeloid differentiation-88
NBCS	newborn calf serum
NCBI	National Center for Biotechnology Information
NFκB	nuclear factor kappa-light-chain-enhancer of activated B cells
nsP	non-structural protein (of alphaviruses)
NTC	non-treated control
OHFV	Omsk haemorrhagic fever virus
ONNV	O'nyong-nyong virus
ORF	open reading frame
PAMP	pathogen-associated molecular pattern
PAP	phenoloxidase activating protein
PAZ	Piwi/Argonaute/Zwille
PBS	phosphate buffered saline
PBSA	phosphate buffered saline with 0.75 % bovine serum albumin
PCR	polymerase chain reaction
PFU	plaque-forming unit
p.i.	post-infection
piRNA	PIWI-interacting RNA
PIWI	P-element induced wimpy testis in *Drosophila*
PGN	peptidoglycan
PGRP	peptidoglycan recognition proteins
PM	plasma membrane
PO	phenoloxidase
POWV	Powassan virus
PPO	pro-phenoloxidase
PRR	pattern recognition receptor
P/S	penicillin/streptomycin
qPCR	quantitative real-time PCR
RdRP	RNA-dependent RNA polymerase
Rel	Relish

RIG-I	retinoic acid-inducible gene-I
RISC	RNA-induced silencing complex
RHD	Rel homology domain
Rluc	*Renilla* luciferase
RNA	ribonucleic acid
RNAi	RNA interference
RT	room temperature
RT-PCR	reverse-transcriptase PCR
RVFV	Rift Valley fever virus
SCRV	St Croix River virus
SD	standard deviation
SFV	Semliki Forest virus
SFTSV	severe fever with thrombocytopenia syndrome virus
SINV	Sindbis virus
siRNA	small interfering RNA
S.O.C. medium	Super Optimal broth with Catabolite repression
SOCS	suppressor of cytokine signalling
ssRNA	single-stranded ribonucleic acid
ss(+)RNA	single-stranded positive sense ribonucleic acid
ss(-)RNA	single-stranded negative sense ribonucleic acid
STAT	signal transducer and activator of transduction
TBEV	tick-borne encephalitis virus
TIR	Toll-interleukin 1-receptor homology
TLR	Toll-like receptor
TPB	tryptose phosphate broth
U	units
UTR	untranslated region
UV	ultra-violet
VEEV	Venezuelan equine encephalitis virus
VRP	virus replicon particle
VSV	vesicular stomatitis virus
WEEV	Western equine encephalitis virus
WNV	West Nile virus
wt	wild type

Abstract

Arthropod-borne viruses, arboviruses, have the ability to replicate in both vertebrates and invertebrates and are transmitted to susceptible vertebrate hosts by vectors such as mosquitoes and ticks. Ticks are important vectors of many highly pathogenic arboviruses, including the flavivirus tick-borne encephalitis virus (TBEV) and the nairovirus Crimean-Congo haemorrhagic fever virus. In contrast, alphaviruses are principally mosquito-borne and have been isolated only rarely from ticks; ticks have not been implicated as their vectors. Nevertheless, the alphavirus Semliki Forest virus (SFV) replicates in cell lines derived from many different tick species, including those of the genus *Ixodes*, which includes vectors of TBEV and its less-pathogenic relative Langat virus (LGTV). In vertebrate cells, arboviruses generally cause cytopathic effects; however, arbovirus infection of arthropod cells usually results in a persistent low-level infection without cell death. While little is known about antiviral immunity in tick cells, the immune system of other arbovirus vectors such as mosquitoes has been studied extensively over the last decade. In insects, pathways such as RNA interference (RNAi), JAK/STAT, Toll, Imd and melanisation have been implicated in controlling arbovirus infection, with RNAi being considered the most important antiviral mechanism. In tick cells, RNAi has been shown to have an antiviral effect, but current knowledge of other immunity pathways is limited and none have been implicated in the antiviral response. In the present study, SFV and LGTV replication in selected *Ixodes* spp. tick cell lines was characterised and the *Ixodes scapularis*-derived cell line IDE8 was identified as a suitable cell line for this project. Potential antiviral innate immunity pathways were investigated; putative components of the tick JAK/STAT, Toll and Imd pathways were identified by BLAST search using available sequences from well-studied arthropods including the fruit fly *Drosophila melanogaster*. Using gene silencing, an attempt was made to determine whether these pathways play a role in controlling SFV and LGTV infection in tick cell lines. Selected genes were silenced in IDE8 cells using long target-specific dsRNA and cells were subsequently infected with either SFV or LGTV. Effects of gene silencing on virus replication were assessed by quantitative real time PCR (qPCR) or luciferase reporter assay. Effects on infectious virus production were measured by plaque assay. Replication of the orbivirus St Croix

River virus (SCRV), which chronically infects IDE8 cells, was also quantified by qPCR after silencing of selected genes. Interestingly, SFV or LGTV infection of IDE8 cells resulted in a significant increase in SCRV replication, possibly as a result of interference with antiviral pathways by SFV and LGTV or possibly due to diversion of cellular responses from sole control of SCRV. No evidence for an antiviral role for the JAK/STAT or Toll pathways was found in IDE8 cells. However, an antiviral effect was observed for protein orthologues putatively involved in the RNAi response. Argonaute proteins play an important role in translation inhibition and target degradation mediated by RNAi, and silencing of selected Argonaute proteins resulted in a significant increase in SFV and SCRV replication. The carboxypeptidase CG4572 is essential for an efficient antiviral response in *D. melanogaster*, and supposedly involved in the systemic RNAi response. A putative tick orthologue of CG4572 was identified and this appeared to be involved in the antiviral response in IDE8 tick cells. When expression of CG4572 was silenced and cells subsequently infected with SFV or LGTV, replication of both viruses was significantly increased. In addition, it was shown that three mosquito orthologues of CG4572 also had an antiviral role against SFV in *Aedes* mosquito cells. In conclusion, of the tick cell lines investigated, IDE8 provided a suitable model system for investigating tick cell responses against arboviruses and new insight into the nature of the tick cell antiviral response was gained.

1. Introduction

1.1 INTRODUCTION

Little is known about tick immunity and in particular the responses of tick cells to virus infection. This chapter will introduce arthropod-borne viruses (arboviruses), their arthropod vectors with an emphasis on ticks, and what is known about the arthropod immune response to arbovirus infection.

1.2 ARBOVIRUSES

Arboviruses pose an increasing threat to both human and animal health worldwide. Due to environmental change and globalisation, arboviral vectors, such as mosquitoes and ticks, are invading new geographic regions (Charrel et al., 2007; Jaenson et al., 2012; Medlock et al., 2013; Weaver and Reisen, 2010). In particular, global distribution of the Asian tiger mosquito *Aedes (Stegomyia) albopictus* has greatly increased since 1980, facilitating the spread of mosquito-borne pathogens (Charrel et al., 2007). Most arboviruses belong to the *Bunyaviridae*, *Flaviviridae*, *Togaviridae* and *Reoviridae* families of RNA viruses (Table 1.1) (Hollidge et al., 2010). A small number of arboviruses belong to virus families which are in the majority not vector-borne including for example the tick-borne Thogoto virus (*Orthomyxoviridae*) (Haig et al., 1965) and Barur virus (*Rhabdoviridae*) (Butenko et al., 1981). The only known arbovirus with a DNA genome is the tick-borne African swine fever virus (ASFV) of the family *Asfarviridae*, which is highly pathogenic in pigs (Dixon et al., 2013). Viruses with RNA genomes generally have a high mutation rate (Holland and Domingo, 1998) and arboviruses often have a very broad host range resulting in high zoonotic potential. It is thus not surprising that highly pathogenic arboviruses such as chikungunya virus (CHIKV) (Chhabra et al., 2008; Renault et al., 2007), severe fever with thrombocytopenia syndrome virus (SFTSV) (Yu et al., 2011; Zhao et al., 2012), Heartland virus (McMullan et al., 2012; Savage et al., 2013) and possibly a new dengue virus (DENV) serotype (Normile, 2013), among others, have emerged or re-emerged over the past decade. CHIKV showed the impact of adaptation to arthropod vectors on arbovirus spread.

Table 1.1: Arbovirus families, representatives of medical, veterinary or scientific importance and their primary vectors. Vector group is indicated by * mosquito, # tick, § sand fly, † midge.

Family (genome)	**Genus**	**Important representatives**	**Primary Vector**	**References**
Flaviviridae (ss(+)RNA)	*Flavivirus*	dengue virus	*Ae. aegypti* *	(Gould and Solomon, 2008)
		West Nile virus	*Culex* spp.*	(Gould and Solomon, 2008)
		yellow fever virus	*Aedes* spp.*	(Gould and Solomon, 2008)
		Japanese encephalitis virus	*Aedes* spp.*	(Gould and Solomon, 2008)
		St Louis encephalitis virus	*Culex* spp.*	(Gould and Solomon, 2008)
		tick-borne encephalitis virus	*Ixodes* spp.#	(Gould and Solomon, 2008)
		Kyasanur Forest disease virus	*Haemaphysalis* spp.#	(Gould and Solomon, 2008)
Togaviridae (ss(+)RNA)	*Alphavirus*	chikungunya virus	*Aedes* spp.*	(Hollidge et al., 2010)
		Venezuelan equine encephalitis virus	*Aedes spp.**	(Hollidge et al., 2010)
		Semliki Forest virus	*Aedes* spp.*	(Mathiot et al., 1990)
		O'nyong nyong virus	*Anopheles* spp.*	(Williams et al., 1965)
Rhabdoviridae ss(-)RNA	*Vesiculovirus*	vesicular stomatitis virus	*Phlebotominae*§	(Letchworth et al., 1999)
		Chandipura virus	*Phlebotomus* spp.§	(Menghani et al., 2012)
		bovine ephemeral fever virus	*Culicoides* spp.†	(Nandi and Negi, 1999)
Bunyaviridae (ss(-)RNA segmented)	*Orthobunyavirus*	La Crosse virus	*Ae. triseriatu.**	(Hollidge et al., 2010)
		Oropouche virus	*Culicoides* spp.†	(Carpenter et al., 2013)
		Schmallenberg virus	*Culicoides* spp.†	(Carpenter et al., 2013)
	Phlebovirus	Rift Valley fever virus	*Aedes* spp.*	(Hollidge et al., 2010)
		Heartland virus	*Amblyomma* spp. (unclear)#	(Savage et al., 2013)
	Nairovirus	severe fever with thrombo-cytopenia syndrome virus	*Haemaphysalis* spp. (unclear)#	(Zhang et al., 2012)
		Uukuniemi virus	*Ixodes* spp.#	(Hubalek and Rudolf, 2012)
		Crimean-Congo haemorrhagic fever virus	*Hyalomma* spp.#	(Labuda and Nuttall, 2004)
		Nairobi sheep disease virus	*Rhipicephalus appendiculatus*#	(Labuda and Nuttall, 2004)
Orthomyxoviridae (ss(-)RNA segmented)	*Thogotovirus*	Thogoto virus	*Rhipicephalus* spp.#	(Haig et al., 1965)
Reoviridae (dsRNA segmented)	*Orbivirus*	bluetongue virus	*Culicoides* spp.†	(Maclachlan and Guthrie, 2010)
		African horse sickness virus	*Culicoides* spp.†	(Maclachlan and Guthrie, 2010)
		Tribeč virus	*Ixodes* spp.#	(Chumakov, 1963)
	Coltivirus	Colorado tick fever virus	*Dermacentor andersoni*#	(Attoui et al., 2005)
Asfarviridae (dsDNA)	*Asfivirus*	African swine fever virus	*Ornithodoros* spp.#	(Dixon et al., 2013)

In the 2005-2006 outbreak of chikungunya fever on the Indian Ocean island of La Reunion, rapid replication and dissemination of this infection was associated with a single point mutation in the viral envelope glycoprotein which adapted the virus to replicate in and to be disseminated by anthropophilic *Ae. albopictus* mosquitoes (Vazeille et al., 2007).

Arboviruses are not transmitted simply through the contaminated mouthparts of ectoparasitic arthropods, but have the ability to replicate in both vertebrates and invertebrates. Arboviruses cycle between vertebrate hosts and invertebrate vectors such as mosquitoes, biting midges or ticks in what is often referred to as the 'enzootic cycle' (Fig 1.1). This alternation between hosts can be of great importance to the genome stability of the arbovirus (Moutailler et al., 2011).

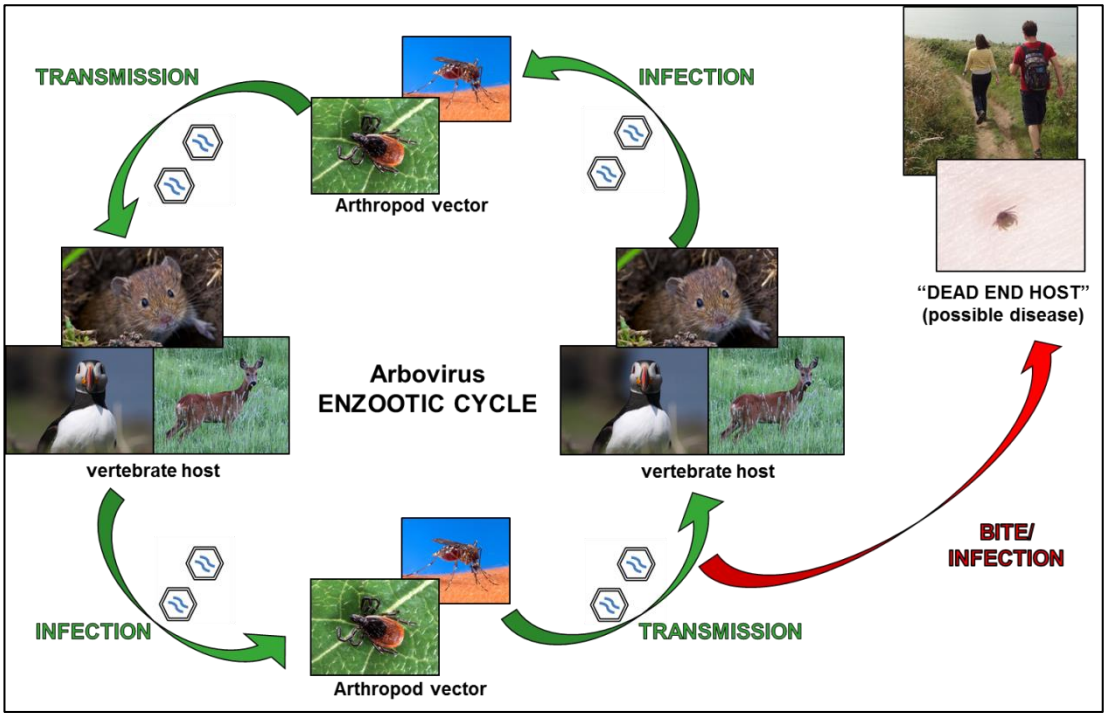

Figure 1.1: Natural enzootic cycle of arboviruses: Viruses circulate between arthropods and small mammals or birds serving as natural reservoirs. Sometimes humans become infected, possibly as dead-end hosts that are susceptible to disease.

The most common route by which arthropod vectors are infected with arboviruses is horizontal oral transmission, which occurs when a vector feeds on a viraemic vertebrate host. The virus is taken up with the blood-meal. If the virus can cross the

midgut barrier, and is not eliminated by the arthropod immune system, it replicates and disseminates in the vector and high titres of infectious virus are released into the arthropod saliva, so that it can be passed to the next vertebrate host on which the arthropod feeds (Weaver and Reisen, 2010). The possibility of non-viraemic transmission of arboviruses between co-feeding ticks has also been proposed for a number of different viruses and may play an important role for the 'survival' of tick-borne viruses in nature (Havlikova et al., 2013; Labuda and Randolph, 1999). Many arboviruses can also be transmitted vertically, transovarially, transstadially or both. Transovarial transmission is the infection of eggs in the female's ovaries resulting in infected male and female offspring. Transstadial transmission occurs between developmental stages and is essential for virus transmission by (some) hard ticks which only feed once per life stage. Another route of infection is horizontal venereal transmission from a vertically infected male to an uninfected female (Weaver and Reisen, 2010). Many arboviruses persistently infect their arthropod vector and can also ensure continuous replication by both transovarial and transstadial transmission.

Occasionally, arthropod vectors transmit the virus to hosts which generally do not pass on the virus, so-called dead-end hosts. There are a number of possible reasons why a host constitutes a dead-end, including insufficient levels of viraemia for infection of other vectors or specific behaviour; for example, a human might notice a tick, remove and kill it, and thus stop the virus transmission cycle. Dead-end hosts could be humans, for example, who may develop disease symptoms varying from mild febrile illness to fatal encephalopathy or haemorrhagic fever. Some arboviruses, such as DENV and CHIKV, have evolved to be transmitted efficiently between human hosts and the anthropophilic mosquitoes *Ae. aegypti* and *Ae. albopictus*, causing outbreaks of disease especially in urbanised areas (Chen and Vasilakis, 2011; Weaver and Reisen, 2010).

All arboviruses have to deal with at least two very different immune systems and, while research into and knowledge of arbovirus-host interactions in vertebrate systems is well developed, knowledge of vector antiviral responses has been gained principally over the last ten years and mainly for mosquitoes (Fragkoudis et al., 2009; Kingsolver et al., 2013; Merkling and van Rij, 2013). The present study aimed

to examine arthropod-virus interactions, focusing on arboviruses belonging to the families *Togaviridae* (Semliki Forest virus, genus *Alphavirus*) and *Flaviviridae* (Langat virus, genus *Flavivirus*). In addition to these two arboviruses, St Croix River virus (SCRV) of the *Reoviridae* (genus *Orbivirus*), which is believed to be a tick-only virus and persistently infects a number of tick cell lines, was investigated. All three virus groups will be introduced in the following sections.

1.2.1 Alphaviruses

Alphavirus is a genus of the family *Togaviridae*. Alphaviruses are single-stranded, positive-sense RNA (ss(+)RNA) viruses with a genome size of approximately 12 kilobases (kb). Alphaviruses have a variety of hosts including insects, fish, amphibians, reptiles, birds, rodents, horses and humans and they can be found on all continents except Antarctica (Powers et al., 2001). They are mostly transmitted by mosquitoes and include highly pathogenic encephalitic viruses such as Western-, Eastern- and Venezuelan equine encephalitis viruses (WEEV, EEEV and VEEV respectively) (Zacks and Paessler, 2010). Other alphaviruses, such as CHIKV and Ross River virus, are known to cause febrile illness and arthralgia, but in rare cases they can also cause encephalitis (Zacks and Paessler, 2010). There is one alphavirus, Eilat virus, which is only known to infect insect cells and it has been suggested that it lost its ability to infect vertebrate hosts (Nasar et al., 2012). There are also alphaviruses which infect fish and cause severe economic losses especially to the salmon and trout industry (McLoughlin and Graham, 2007). No arthropod vector of these salmonid alphaviruses has been identified with certainty, but the salmon louse *Lepeophtheirus salmonis* (*Crustacea*; subclass *Copepoda*) has been implicated as a potential vector in virus transmission (Petterson et al., 2009). Another area of research is aimed at using alphaviruses as vectors for gene therapy (Lundstrom, 2009).

While alphaviruses are not known to be transmitted by ticks, Sindbis virus (SINV) has been isolated from both ticks and mites (Al-Khalifa et al., 2007; Strauss and Strauss, 1994) and Semliki Forest virus (SFV) (Smithburn, 1944) has been isolated from ticks of several different species in Kenya (Lwande et al., 2013); virus may have been present in the blood-meal without infecting the ticks.

Laboratory strains of the two viruses regularly studied in alphavirus research, SINV and SFV, are considered not to cause disease in humans; however, there has been one fatal case of encephalitis associated with a laboratory strain of SFV and natural variants of the two viruses have been reported to cause disease in humans (Strauss and Strauss, 1994). Northern European SINV strains can cause polyarthritis and SFV strains in Central Africa can cause severe headaches, fever, myalgia and arthralgia (Strauss and Strauss, 1994).

SFV is transmitted by mosquitoes of the *Aedes* genus and replicates in many mosquito and mammalian cell lines. However, SFV has also been shown to infect tick cell lines from a number of different species (Barry et al., 2013; Pudney, 1987). While SFV generally causes rapid cytopathic effect (CPE) in infected mammalian cells, SFV infection of mosquito and tick cells does not cause visible CPE (Brown, 1984; Leake et al., 1980; Peleg, 1968). After an initial peak, SFV production in mosquito cells is reduced to a low level persistent infection by 4 days post-infection (p.i.) (Fragkoudis et al., 2008). SFV is a useful model virus to study arbovirus infection of vertebrate and invertebrate cells, due to its easy propagation, rapid replication and the availability of many different reporter virus constructs.

SFV genome organisation and replication

Alphavirus particles have a size of approximately 70 nm and are enveloped. The envelope is a lipid bilayer derived from the plasma membrane (PM) of a host cell and it is covered with 80 spikes, each composed of three heterodimers of the viral E1 and E2 glycoproteins (Paredes et al., 1993) (Fig 1.2A). The capsid is icosahedral (T=4) and assembled out of 240 copies of a single capsid protein (Strauss and Strauss, 1994; Vogel et al., 1986). Enclosed in this capsid is the ss(+)RNA genome (Fig 1.2B) of approximately 11.7 kb, which is capped at the 5’ end and polyadenylated at the 3’ end. The genome encodes nine functional proteins from two open reading frames (ORFs). At the 5’ end one ORF, which corresponds to approximately two-thirds of the genome, encodes the four non-structural proteins (nsP1-4) while another ORF at the 3’ third of the genome encodes the five structural proteins: capsid (C), the envelope glycoproteins (E1-3) and 6K. The precursor of E2 and E3 is referred to as

p62. Transcription of the ORF encoding the structural proteins is under the control of an internal subgenomic (26S) promoter (Strauss and Strauss, 1994).

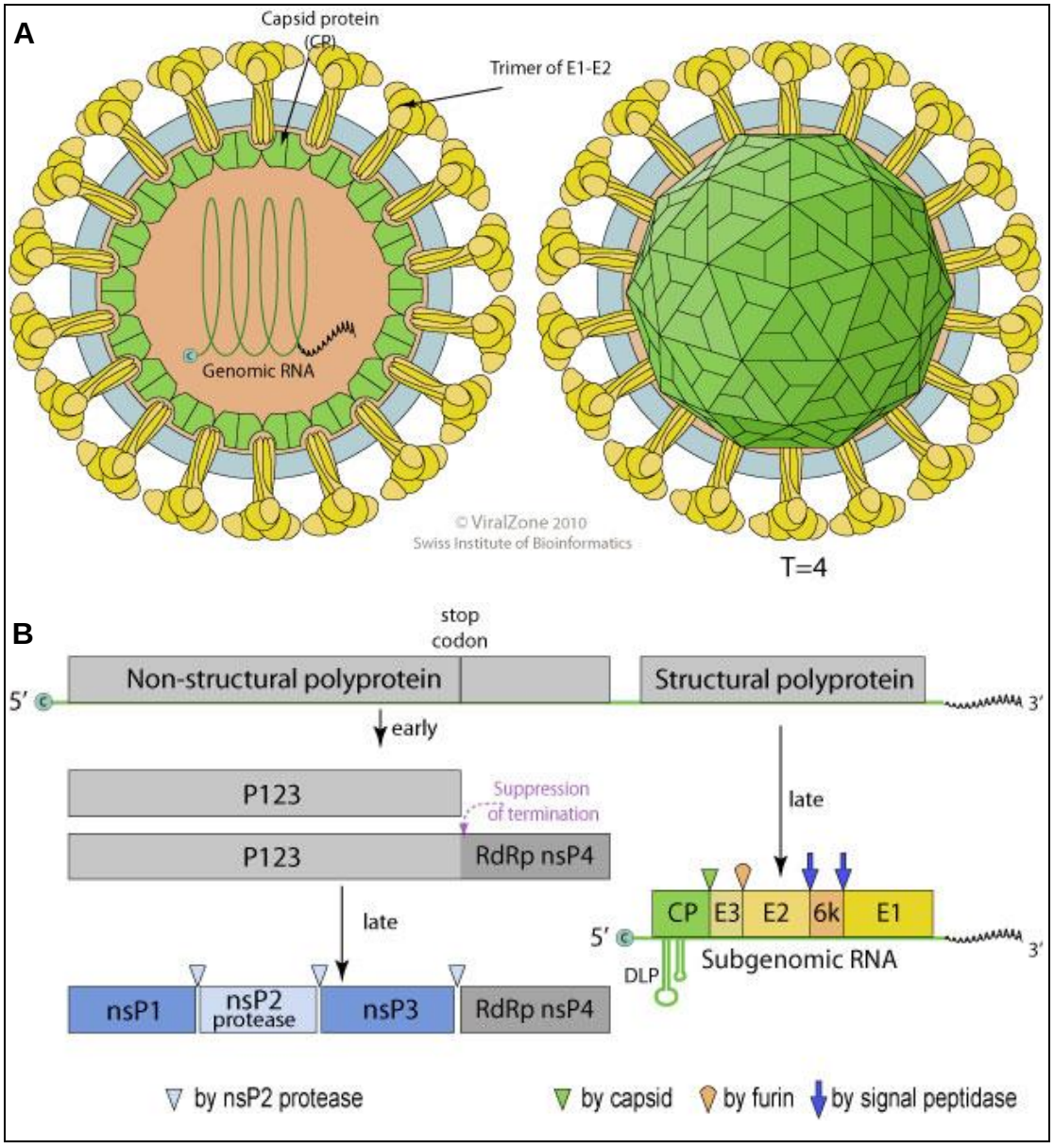

Figure 1.2: Alphavirus particle structure (A) and genome organisation (B). (Taken from the website Viralzone http://viralzone.expasy.org/ of the Swiss Institute of Bioinformatics)

The first step in SFV infection is attachment to a cell surface receptor through the receptor-binding domains of the E2 glycoprotein (Smith et al., 1995; Strauss and Strauss, 1994). The receptor to which SFV binds remains unknown in both vertebrate host and arthropod vector, but a number of possible receptors have been suggested

for alphaviruses, including the class I major histocompatibility complex (Helenius et al., 1978), laminin (Wang et al., 1992), NRAMP (Rose et al., 2011), C-type lectins (Klimstra et al., 2003) and heparan sulphate in cultured cells (Klimstra et al., 1998). Upon attachment, SFV enters the cell via clathrin-mediated endocytosis (DeTulleo and Kirchhausen, 1998). Entry into the cytosol is facilitated by alteration of the three-dimensional structure of the spike protein due to the acidic environment of the endosome. The E1 spike protein enables fusion of the virus envelope with the endosome membrane (Glomb-Reinmund and Kielian, 1998). It has been suggested that due to the acidic conditions of the endosome, capsid conformation changes and ribosomal binding sites are revealed. Thus, after release of the nucleocapsid into the cytosol, ribosomes bind to these sites and the RNA is uncoated in the cytoplasm (Singh and Helenius, 1992).

Upon binding of ribosomes to the viral genomic RNA, the four nsPs are translated as a polyprotein (Takkinen, 1986); however, due to a 'leaky' stop-codon in nsP4 two polyproteins are produced, P123 and P1234, reducing the amount of redundant nsP4. The C-terminus of nsP2 has a papain-like protease domain and processes the polyprotein into its individual components (Merits et al., 2001). While all nsPs are required at the site of replication, they also localise to different cellular compartments. nsP1 predominantly localises to the PM and induces membrane invaginations, referred to as spherules, which serve as the site of virus replication (Spuul et al., 2010). Large proportions of nsP2 translocate to the nucleus and mediate shut-off of host transcription and antagonise the antiviral interferon response (Akhrymuk et al., 2012; Breakwell et al., 2007). Aggregates of nsP3 appear to form in the cytoplasm, and this viral protein is important in the disruption of the formation of antiviral stress granules (Panas et al., 2012). nsP4 is the viral RNA-dependent RNA polymerase (RdRP) and abundant nsP4 in the cytoplasm that is not required for replication is degraded by the proteasome (Spuul et al., 2010).

Replication of the SFV genome is facilitated by nsP4 as the viral RdRP and takes place in cytoplasmic replication complexes which are associated with cellular membranes (Friedman et al., 1972; Grimley et al., 1972; Salonen et al., 2005). Initially, spherules form at the PM and replication is mediated by nsP4 and the polyprotein P123, before the latter is cleaved into nsP1-3 and the replication

complexes (spherules) are transferred to the membranes of small cytoplasmic vesicles in a manner dependent on phosphatidylinositol3-kinase (Figure 1.3).

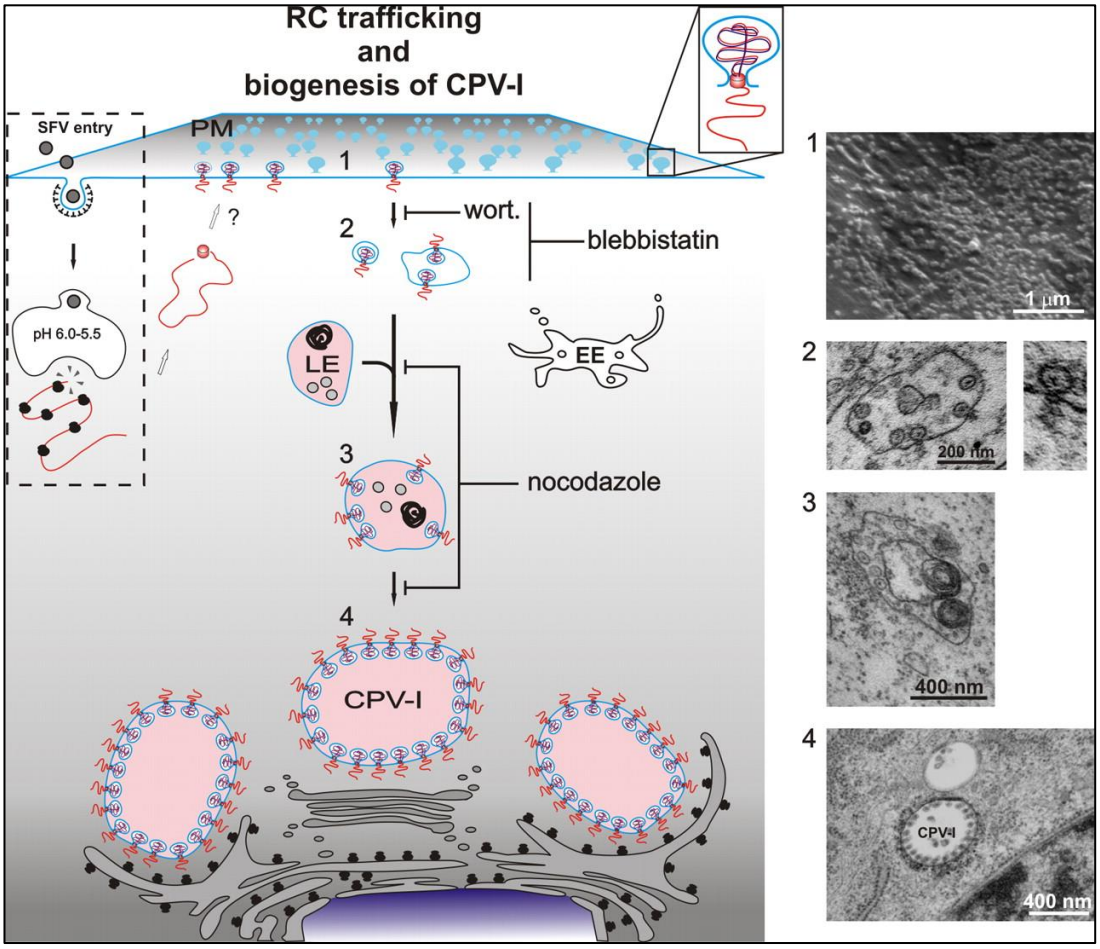

Figure 1.3: Proposed model of localisation of alphavirus replication complexes (RC) during the course of infection. Initial spherules are formed at the PM (1), then internalised by small vesicles (2) which fuse with late endosomes (LE) to larger vesicles (3) which are transported to the peri-nuclear region and eventually form large CPV-I as the major sites of virus replication (Taken from Spuul et al., 2010).

These vesicles then fuse with late endosomes and eventually form virus-induced type I cytopathic vacuoles (CPV-I) typical for alphavirus replication (Grimley et al., 1968). All nsPs are essential for virus replication; however, the specific function of nsP3 remains unclear. The viral polymerase nsP4 uses the genomic ss(+)RNA strand as a template to create antigenomic single-stranded negative sense RNA (ss(-)RNA). This ss(-)RNA serves as a template for both genomic and subgenomic RNA. Minus

strand synthesis has been shown to be mediated by nsP4 and the polyprotein P123, whereas plus strand synthesis is mediated by the cleaved individual non-structural proteins (Shirako and Strauss, 1994). During replication, double-stranded RNA (dsRNA) intermediates occur which are recognised by the host cell as foreign and can trigger antiviral responses. SFV nsP1 has both guanine-7-methyltransferase and guanylyl activity and thus mediates capping and methylation of newly synthesised viral ss(+)RNA (Ahola and Kaariainen, 1995; Laakkonen et al., 1994). nsP2 is important during replication due to its functions as an RNA helicase and an RNA 5' triphosphatase (Gomez de Cedron et al., 1999).

The structural proteins of SFV are translated late in infection as a single polyprotein from the messenger RNA (mRNA) of the subgenomic ORF. The capsid protein is released autocatalytically. Upon translation of the signal sequence in p62, the translation process is translocated to the endoplasmic reticulum (ER) where the cellular enzyme signalase cleaves the polyprotein into its individual components with the exception of the E2 precursor p62 which is cleaved late in the secretory pathway by a cellular furin-like protease (Garoff et al., 1990; Zhang et al., 2003). The envelope glycoproteins are transported to the Golgi apparatus for post-translational modification and maturation before they are transported to the PM. The genomic RNA has packaging signals in the sequence encoding nsP2 to facilitate encapsidation of the RNA genome (Frolova et al., 1997). The cytoplasmic tail of E2 then interacts with the nucleocapsid mediating budding and release of new virus particles (Strauss and Strauss, 1994).

SFV reporter constructs

The genome of SFV is easily manipulated. Insertion of luciferase reporter genes or genes encoding fluorescent proteins, such as enhanced green fluorescent protein (eGFP), ZsGreen and DsRed, is possible at different sites of the genome. Different genetic modification strategies have been used in the past. Fluorescently-labelled reporter viruses have been engineered by insertion of the green fluorescent protein (GFP) into the SFV genome, either into the structural ORF (Fig 1.4A) (Fragkoudis et al., 2007) or as a fusion protein with nsP3, named SFV4(3F)-GFP (Tamberg et al., 2007). The viruses SFV4(3F)-dsRed and SFV4(3F)-ZsGreen (Fig 1.4B) were

generated in the same manner as SFV4(3F)-GFP. These viruses were stable and replication was only mildly reduced compared to wild type (wt) SFV (Tamberg et al., 2007). In a different study, the coding sequence for a luciferase enzyme derived from the sea pansy (*Renilla reniformis*), referred to as *Renilla* luciferase (*Rluc*), was inserted into the SFV genome behind nsP3; however, it was not inserted as a fusion protein, but with a highly efficient cleavage site. This virus was named SFV4(3H)-*Rluc* (Kiiver et al., 2008) (Fig 1.4C). Another possibility for creating SFV reporter viruses is to insert a duplicated subgenomic promoter followed by the gene of interest. Generally, this results in a slightly less stable virus as the inserted region is of no benefit to the virus and is not directly linked to essential regions of the genome (Tamberg et al., 2007).

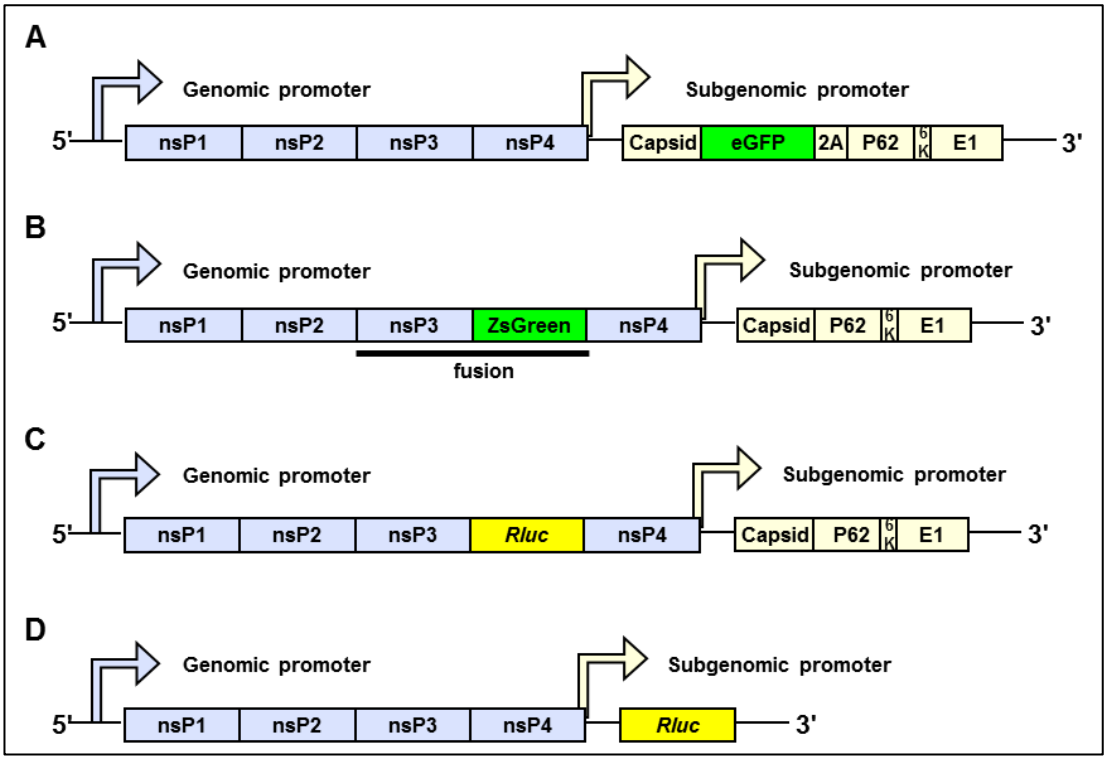

Figure 1.4: Examples of SFV reporter constructs. (A) SFV4-steGFP has GFP inserted into the structural ORF. (B) SFV4(3F)-ZsGreen expresses a ZsGreen-nsp3 fusion protein. (C) SFV4(3H)-*Rluc* has *Rluc* inserted into the non-structural ORF. (D) SFV1-*Rluc* is a replicon expressing *Rluc* under the subgenomic promoter.

By deletion of the subgenomic ORF encoding the structural proteins an SFV replicon can be generated (Fig 1.4D). When *in vitro*-transcribed and transfected into cells, this

RNA will produce non-structural proteins and replicate, but in the absence of structural proteins it cannot be packaged into new virions and therefore cannot infect new cells (Liljestrom and Garoff, 1991). By co-transfecting RNA encoding the structural proteins, it is possible to generate virus replicon particles (VRPs) that can undergo a single round of infection (Berglund et al., 1993; Smerdou and Liljestrom, 1999). Instead of deleting the subgenomic promoter, reporter genes such as eGFP and *Rluc* can be inserted in place of the structural proteins resulting in reporter VRPs.

1.2.2 Flaviviruses

Flaviviruses are ss(+)RNA viruses with a genome of approximately 11 kb (Kaufmann and Rossmann, 2010). They form enveloped, spherical particles, typically ranging from 40-65 nm in size (Fig 1.5). The family consists of more than 75 different viruses, of which at least 56 are arthropod-borne. There are 40 mosquito-borne flaviviruses, including the highly pathogenic DENV, West Nile virus (WNV) and Japanese encephalitis virus (JEV). Although the majority of flaviviruses are mosquito-borne, there are also at least 16 tick-borne flaviviruses (Hollidge et al., 2010). These include viruses of high pathogenicity in humans such as tick-borne encephalitis virus (TBEV) and Powassan virus (POWV) (Labuda and Nuttall, 2004), but also viruses of veterinary importance, including louping ill virus (LIV) (Jeffries et al., 2014). While TBEV, LIV and POWV usually cause symptoms ranging from mild febrile illness to severe encephalitis, there are also tick-borne flaviviruses that can cause haemorrhagic fever such as Omsk haemorrhagic fever virus (OHFV) and Kyasanur forest disease virus (KFDV) (Gritsun et al., 2003). Langat virus (LGTV) is a close relative of TBEV that has not been found to naturally infect humans and is considered to be of low pathogenicity (Dobler, 2010). It was first isolated from *Ixodes granulatus* ticks in Malaysia (Smith, 1956) and later from *Haemaphysalis papuana* in Thailand (Bancroft et al., 1976). LGTV was used to vaccinate against TBEV in the past; the vaccine was efficacious against most TBEV strains in initial studies (Il'enko et al., 1968), but was not protective in some endemic areas and was not considered safe enough due to the rare occurrence of encephalitis after vaccination (Stephenson, 1988). While TBEV requires to be handled in a

containment level 3 (CL3) laboratory, LGTV is safe to handle in CL2 laboratories and was thus used in the present study instead of TBEV.

Genome organisation and replication

The flavivirus genome consists of one large ORF encoding a polyprotein which is processed into three structural (C, prM, E) and seven non-structural (NS1, NS2A, NS2B, NS3, NS4A, NS4B, NS5) proteins (Fig 1.5). The genome has a 5' cap, but no 3' poly-(A) tail (Kaufmann and Rossmann, 2010). The ORF is flanked by the 5' untranslated region (UTR) and the 3'UTR which fold into complex and important secondary structures (Tumban et al., 2010).

Upon attachment of the flavivirus particle to the host cell it is internalised by clathrin-dependent endocytosis. The low pH in endosomes induces the process of uncoating, in which the virus envelope fuses with the endosomal membrane to release the viral genome into the cytoplasm of the host cell. NS3 and NS5 assemble together with other viral and host proteins to form the replication complex in association with ER membranes; NS5 is the RdRP and facilitates replication of the viral genome (Kaufmann and Rossmann, 2010). The structural proteins C, prM and E are expressed, and assembly of virions occurs at the ER where newly synthesised proteins and viral RNA form immature virus particles that bud into the ER and during this process gain a lipid envelope. Following assembly, immature virions transit from the ER, through the trans-Golgi network to the cell surface and undergo a protease- and pH-dependent process of maturation. The released virions are mature and ready to infect new host cells (Kaufmann and Rossmann, 2010).

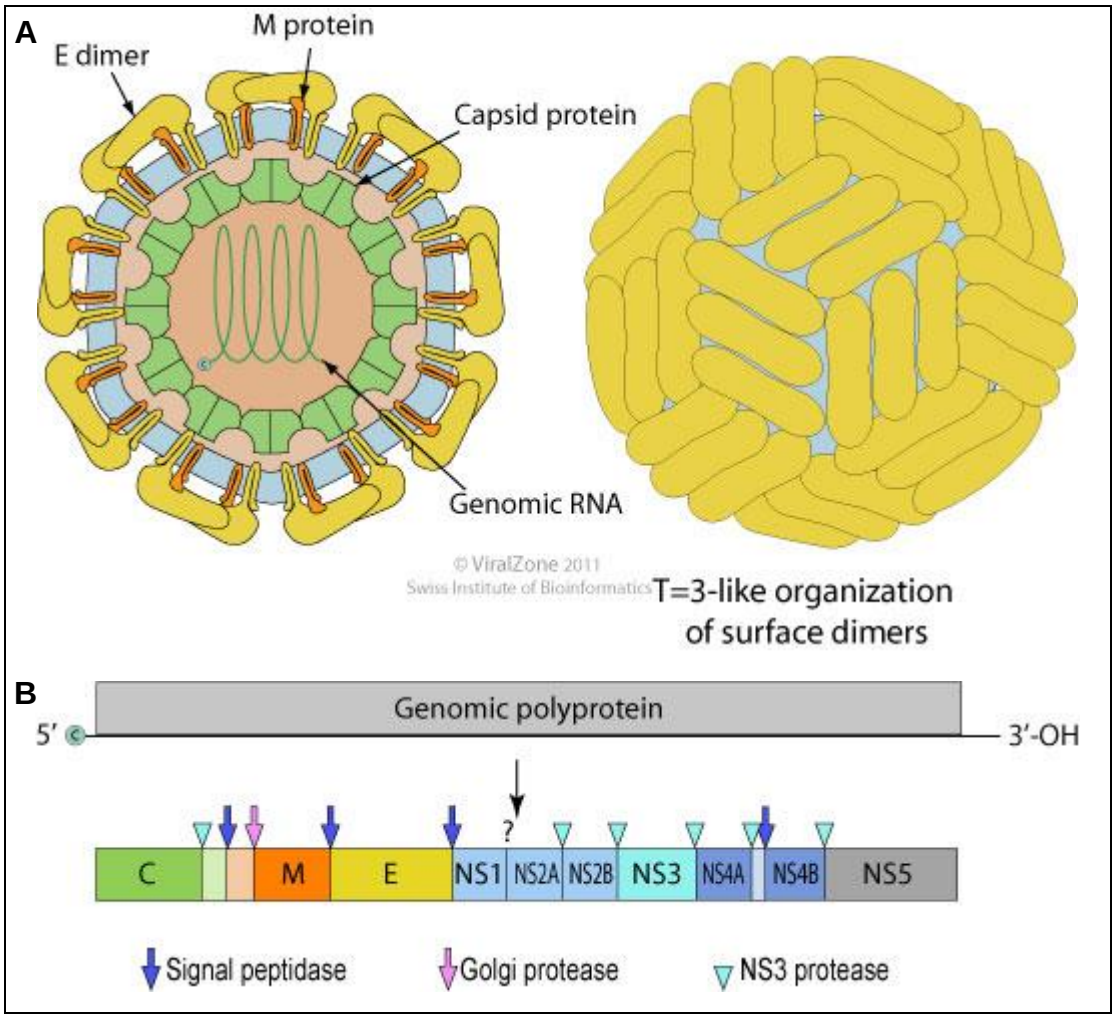

Figure 1.5: Flavivirus particle (A) and genome organisation (B). (Taken from the website Viralzone http://viralzone.expasy.org/ of the Swiss Institute of Bioinformatics)

1.2.3 Orbiviruses

The genus *Orbivirus* is a member of the family *Reoviridae* and its genome consists of 10 segments of dsRNA. Orbivirus particles are non-enveloped and consist of an inner core and an outer surface capsid (Patel and Roy, 2013). The orbivirus genome encodes four distinct non-structural (NS1-4) and seven distinct structural (VP1-7) proteins, with the exception of SCRV which has a stop codon in the ORF of the newly discovered NS4 (Belhouchet et al., 2011; Ratinier et al., 2011). The replication complex consists of an RdRP to replicate the genome, a capping enzyme and an RNA helicase to separate the dsRNA into ssRNA. The virus core is assembled in the so-called viral inclusion body and serves to concentrate components of core

assembly. The assembled core particles are then trafficked on exocytotic vesicles while the outer capsid proteins complete the virus particle. The virus leaves the cell by either budding or host cell lysis. In insect cells no lysis of infected cells is observed (Patel and Roy, 2013).

The type species of the genus is bluetongue virus (BTV), which is of high veterinary importance worldwide. However, there are many other economically important viruses, including African horse sickness virus, equine encephalosis virus and epizootic haemorrhagic disease virus, all of which are transmitted by *Culicoides* spp. biting midges (Maclachlan and Guthrie, 2010). Although many orbiviruses are midge-borne, there are also mosquito- and tick-borne orbiviruses. Peruvian horse sickness virus and Yunnan virus are likely to be transmitted by mosquitoes (Attoui et al., 2009) and Great Island virus is a tick-borne orbivirus of seabirds (Nunn et al., 2006). SCRV is an orbivirus that was isolated from an *Ixodes scapularis* tick cell line (Attoui et al., 2001) and is considered a "tick only" virus as it could not infect any of the mammalian and mosquito cells tested (Bell-Sakyi and Attoui, 2013). It has also been detected in two cell lines of the tick species *Rhipicephalus appendiculatus* (Alberdi et al., 2012) and SCRV could be passaged from the infected *I. scapularis* cell line IDE8 to another *I. scapularis* cell line ISE6 and subsequently to the *Rhipicephalus sanguineus* cell line RSE8 (Bell-Sakyi and Attoui, 2013).

1.2.4 Vectors of arboviruses

Many arboviruses are transmitted by insects of the order *Diptera* (flies), which includes for example mosquitoes, biting midges and phlebotomine sand flies. Many arboviruses of high importance for public health are transmitted by mosquitoes, especially those of the genera *Culex* and *Aedes*[1] (Table 1.1). While *Culex* spp. are important vectors of for example WNV, the yellow fever mosquito *Aedes aegypti* and the Asian tiger mosquito *Ae. albopictus* are particularly important vector species,

[1] The genus *Aedes* has recently been reorganised, so that the medically important vector species are now of the genus *Stegomyia* - thus the correct taxa for the well-known vector species *Ae. aegypti* and *Ae. albopictus* are now *Stegomyia aegypti* and *Stegomyia albopicta*, respectively (Reinert, J.F., Harbach, R.E., Kitching, I.J., 2009. Phylogeny and classification of tribe Aedini (Diptera: Culicidae). Zool J Linn Soc-Lond 157, 700-794); however, as this change has not been implemented by most scientists in the field of arbovirology, the more common names *Ae. aegypti* and *Ae. albopictus* will be used throughout this thesis for simplicity and clarity.

responsible for example for the transmission of DENV, CHIKV and yellow fever virus (Gould and Solomon, 2008; Hollidge et al., 2010). The two species are closely related and have an almost identical appearance (Fig 1.6).

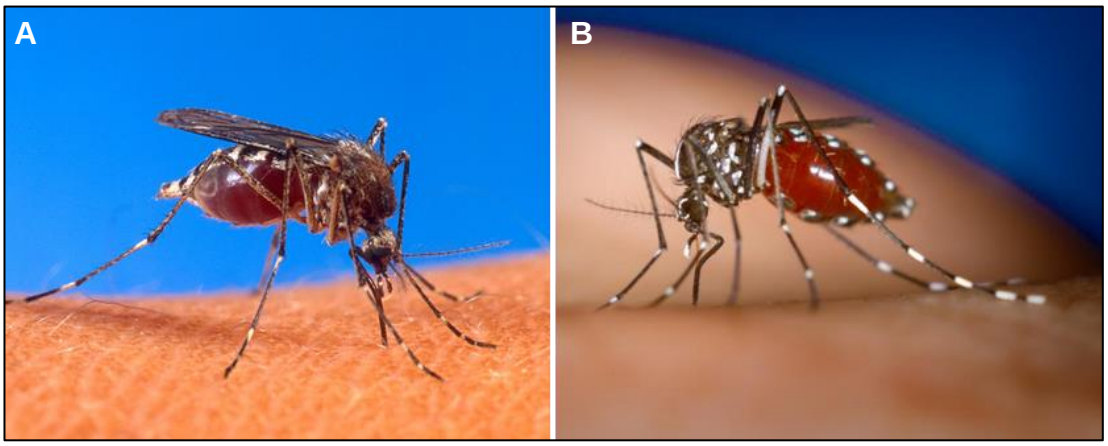

Figure 1.6: Two important arthropod vector species: (A) *Ae. aegypti*, the yellow fever mosquito, and (B) *Ae. albopictus*, the Asian tiger mosquito, towards the end of a bloodmeal (taken from the CDC Public Domain).

The pattern of white stripes is slightly more pronounced in the Asian tiger mosquito and it is also of slightly stronger build. However, the main difference between the two vector species is their habitat and lifestyle - *Ae. aegypti* is a tropical and subtropical mosquito sensitive to temperate climate and is perfectly adapted to completing its life cycle in urbanised areas. *Ae. aegypti* mosquitoes prefer to feed on and live in close proximity to humans, and usually only fly an average of 400 m (WHO dengue control; http://www.who.int/denguecontrol/mosquito/en/). Artificial containers such as buckets or tyres where water can accumulate are suitable for deposition of their desiccation-resistant eggs and, once filled with water, development of larvae. From its African origin, *Ae. aegypti* has increased its distribution to most tropical and subtropical areas of the world (Barrett and Higgs, 2007). While *Ae. albopictus* mosquitoes can follow a life cycle similar to that of *Ae. aegypti* in cities, they are also abundant in more rural areas. *Ae. albopictus* mosquitoes are generally sturdier than *Ae. aegypti* and can fly longer distances. They are also more resistant to cool temperatures and can survive in temperate climates. The ability to survive in temperate climates and the increase in international trade of

goods (in particular scrap tyres) have enabled *Ae. albopictus* to become a successful invasive species in the U.S. and Europe, introducing the risk of establishment of arboviruses such as CHIKV (Medlock et al., 2012). There have been an increasing number of cases of autochthonous infections with CHIKV and DENV in Southern Europe over the last four years (Grandadam et al., 2011; La Ruche et al., 2010; Tomasello and Schlagenhauf, 2013).

Biting midges are known to transmit a number of arboviruses of veterinary importance, such as BTV, Akabane virus and Schmallenberg virus, but only one midge-transmitted virus of public health importance is known to date; the midge species *Culicoides paraensis* is considered the primary vector of Oropouche virus, an orthobunyavirus of Central and South America which causes a febrile illness often associated with headache, arthralgia and, rarely, meningitis (Carpenter et al., 2013). However, midges play an important role in spreading diseases of veterinary importance, especially due to their small size which allows passive wind-facilitated movement of large populations across and between countries (Gloster et al., 2008; Hendrickx et al., 2008).

Sand flies (*Phlebotominae*) are mostly known as the principal vectors of parasites in the genus *Leishmania* (Ready, 2013), yet they also transmit arboviruses, mainly of the genera *Phlebovirus* including Toscana virus, sandfly fever Sicilian virus and Punta Toro virus, *Vesiculovirus* including Chandipura virus, and *Orbivirus* including Changuinola virus. Most arboviruses transmitted by sand flies are considered neglected, despite the large number of virus species of low pathogenicity endemic to Southern Europe, which could spread to more temperate regions (Depaquit et al., 2010). Another common arbovirus threat is the emergence of new viruses with higher pathogenicity. In India, Chandipura virus, which was described in the 1960s (Bhatt and Rodrigues, 1967), recently re-emerged as a tropical pathogen with devastating outbreaks of disease in children (Menghani et al., 2012).

Besides dipteran insects, the other major group of arbovirus vectors are ticks, which are the main focus of the present study and are introduced in more detail in the following section.

1.3 TICKS AND TICK-BORNE DISEASES

Ticks are obligate ectoparasites which transmit many highly pathogenic arboviruses, bacteria and protozoan parasites worldwide. In the context of climate change and globalisation, tick-borne diseases pose an increasing risk for animals and humans. Ticks are haematophagous arthropods belonging to the class Arachnida (subphylum Chelicerata; subclass Acari) and are closely related to mites, spiders and scorpions. While both arachnids and insects are arthropods, they represent two distinct classes under two different subphyla, Chelicerata and Hexapoda, and are evolutionarily more distant than is often assumed.

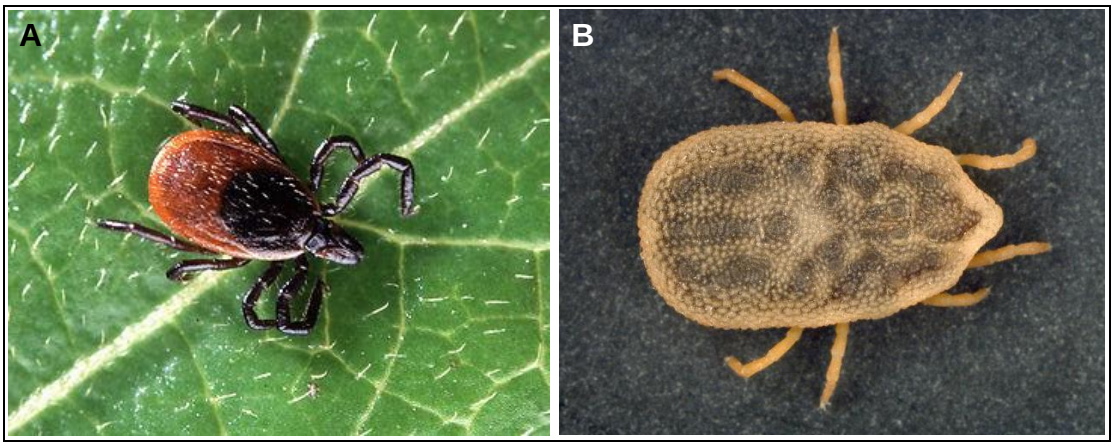

Figure 1.7: Images of an adult hard tick, *I. scapularis*, the American deer tick (A) and an adult soft tick, *Carios kelleyi,* the "Bat Tick" (B). The *I. scapularis* image was taken from the public domain (released by Scott Bauer, U.S. Department of Agriculture) and the *C. kelleyi* image was taken from the Public Health Image Library of the CDC (http://phil.cdc.gov).

There are two main families of ticks - soft ticks, Argasidae, and hard ticks, Ixodidae (Fig 1.7). They differ in many aspects, the primary difference being the sclerotised dorsal scutum of ixodid (hard) ticks. There are 193 currently recognised species of soft ticks belonging to four genera, namely *Argas*, *Carios*, *Ornithodoros* and *Otobius*. Currently, there are 243 species of the *Ixodes* genus and another 459 species of hard ticks belonging to 13 genera, namely *Amblyomma*, *Anomalohimalaya*, *Bothriocroton*, *Cosmiomma*, *Cornupalpatum*, *Compluriscutula*, *Dermacentor*, *Haemaphysalis*, *Hyalomma*, *Margaropus*, *Nosomma*, *Rhipicentor* and *Rhipicephalus* (Guglielmone et al., 2010). A third family of ticks, the Nuttalliellidae, is monotypic

and contains the single species *Nuttalliella namaqua* which has characteristics of both soft and hard ticks and is considered the missing link between the two families (Mans et al., 2011).

Ticks typically have four different stages in their life cycle, developing from an egg through to a larva, a nymph and finally to an adult. The length of these stages, the process of moulting and the number of hosts that ticks feed on during their life cycle varies between genera and species (Walker et al., 2003). Soft ticks have multiple nymphal stages with feeds and moults in between these stages. Adult soft ticks feed multiple times for short periods (several hours) and females lay small batches of eggs after each feed, whereas hard ticks generally feed once per life cycle stage staying attached for 3-14 days and, after feeding, adult female ticks lay one large batch of eggs and then die (Walker et al., 2003).

Depending on the species, hard ticks feed on one, two or three hosts during the life cycle. The present study focusses mainly on hard ticks of the species *Ixodes ricinus* and *I. scapularis*, vectors of various pathogens in Europe and North America, respectively. Both *I. ricinus* and *I. scapularis* are three-host ticks. Three-host *Ixodes* spp. ticks usually have a life cycle spanning 2-3 years in temperate latitudes (Fig 1.8). Initially an engorged adult female tick drops off its host and lays eggs. These eggs hatch into six-legged larvae which typically overwinter in the larval stage and feed on their first host in the following spring (often rodents or other small mammals). After feeding on the first host, larvae will drop off and moult into nymphs. These nymphs will typically feed again in the next year and moult into adults after dropping off the second host (usually a rodent or lagomorph). In the third year, adult ticks attach to the third host (often larger mammals like deer, cattle or sheep) for feeding. Most hard tick species (*Metastriata*) will mate on the host with male ticks copulating with partially-engorged female ticks, which will then fully engorge and drop off the host to lay eggs. However, *Ixodes* spp. ticks (*Prostriata*) will often mate off-host (Walker et al., 2003).

The three hosts are not necessarily of a different species and can in some cases even be the same individuals. Humans can serve as host for any stage of the tick life cycle (Centers for Disease Control and Prevention, http://www.dpd.cdc.gov/dpdx), but for humans the tick rarely has an opportunity to completely engorge as the host will

notice and remove it; humans are thus generally dead-end hosts for ticks and consequently tick-borne pathogens.

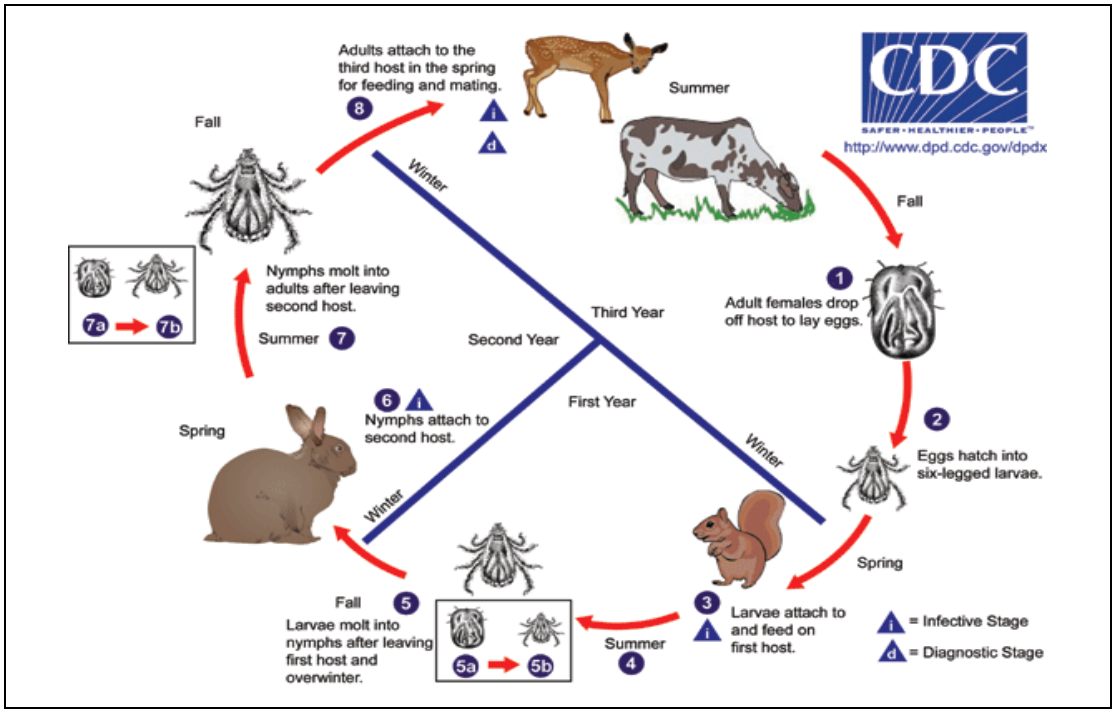

Figure 1.8: The life cycle of three-host hard ticks such as ticks of the genera *Ixodes* and *Dermacentor* in temperate climate (Image: Centers for Disease Control and Prevention). The life cycle of three-host ticks spans two or three years. (1) Adult females lay egg batches after feeding. This usually occurs in autumn and eggs hatch into larvae and overwinter (2). In the following spring larvae feed on the first host (3), usually small mammals such as rodents. In late summer or autumn engorged larvae will moult into nymphs and overwinter in this stage (4-5). The following spring nymphs will feed on the second host (6) and moult into adults after leaving the second host in summer (7). Adult ticks then may overwinter and feed on the third host during the next spring (8), or they feed in late summer/autumn of the same year and lay eggs in autumn.

1.3.1 Ticks as vectors of pathogens

Ticks are vectors of a number of human and animal pathogens. Bacterial pathogens transmitted by ticks include *Borrelia burgdorferi*, the causative agent of Lyme disease (Stricker and Johnson, 2011), and various *Anaplasma* and *Ehrlichia* species which can cause disease in humans, livestock and/or companion animals (Ismail et al., 2010). Important protozoan parasites transmitted by ticks are *Babesia*, of which some species can cause a malaria-like disease in humans (Chauvin et al., 2009), and *Theileria*, an economically important parasite of ruminants (Morrison, 2009). Bovine babesiosis in Europe is caused by the parasite *Babesia divergens* and is transmitted

by the tick *I. ricinus*. It causes significant loss to the cattle industry and has zoonotic potential (Zintl et al., 2003). Economically important parasitic diseases are also caused by *Babesia caballi* and *Theileria equi* which are the causative agents of equine piroplasmosis, a disease of horses present in most countries of the world (Wise et al., 2013).

Another large group of pathogens that can be transmitted by ticks are arboviruses, with over 40 tick-borne arboviruses belonging to at least 6 virus families (*Asfar-*, *Reo-*, *Rhabdo-*, *Orthomyxo-*, *Bunya-*, *Flaviviridae*) including the only known arthropod-borne DNA virus, ASFV (Labuda and Nuttall, 2004). Recently, ticks of the species *Rhipicephalus (Boophilus) decoloratus* have also been implicated in the transmission of another large DNA virus, lumpy skin disease virus (*Poxviridae*) (Tuppurainen et al., 2013; Tuppurainen et al., 2010). Some mosquito-borne viruses have also been isolated from ticks (Al-Khalifa et al., 2007; Lwande et al., 2013) and the mosquito-borne flavivirus WNV can be experimentally transmitted by soft ticks of the species *Ornithodoros moubata* (Lawrie et al., 2004b). While there is some evidence for infection and transstadial transmission of WNV in hard ticks fed on infected rodents, transmission of WNV by hard ticks was not observed (Anderson et al., 2003).

Tick-borne viruses regularly cause devastating medical crises or economic losses to farmers. Highly pathogenic tick-borne viruses include TBEV which is endemic in large parts of Europe and Asia and can cause fatal encephalitis (vector: *Ixodes* spp.) (Dobler, 2010) and the bunyavirus Crimean-Congo haemorrhagic fever virus (CCHFV) causing haemorrhagic fever with a mortality rate of up to 30% in areas of Africa, Asia and Europe (vector: *Hyalomma* spp.) (Leblebicioglu, 2010). Tick-borne viruses with high economic impact include Nairobi sheep disease virus, a highly pathogenic virus of sheep and goats in Africa (Lasecka and Baron, 2013), and ASFV which is endemic in Africa, the Middle East and is currently causing increasing numbers of outbreaks in Russia and Eastern Europe (Gogin et al., 2013; Oura, 2013). Ticks transmit at least 16 viruses belonging to the *Flaviviridae* (Hollidge et al., 2010; Kuno et al., 1998), over 30 belonging to the *Bunyaviridae* and some members of the *Reoviridae* (Labuda and Nuttall, 2004). In Europe alone, there are at least 27 known

tick-borne viruses of varying medical and economic importance (Hubalek and Rudolf, 2012). With globalisation and climate change many of these viruses threaten to become endemic in new areas of Europe, and across the globe new viruses emerge such as the highly pathogenic SFTSV in regions of China (Yu et al., 2011; Zhao et al., 2012) and a related virus named Heartland virus in the United States (McMullan et al., 2012).

1.3.2 Tick cell lines

A large number of mammalian clonal cell lines are available and have been used in research studies based on mammalian systems for many decades. Despite the establishment of the first tick cell lines in the 1970s (Varma et al., 1975), until recently it was more common to use live ticks in tick research. To date more than 50 tick cell lines have been established from 14 ixodid and two argasid tick species (Bell-Sakyi and Attoui, 2013) and cell lines have gained more and more importance in tick research over the last 20 years. Tick cell lines have been used to isolate a number of pathogens of medical and veterinary importance from field/clinical samples, including for example the intracellular bacteria *Anaplasma phagocytophilum*, a pathogen of sheep, dogs, horses and humans, and *Anaplasma marginale*, a bovine pathogen (Dyachenko et al., 2013; Passos, 2012).

Most tick cell lines (reviewed by Bell-Sakyi et al., 2012 and Bell-Sakyi et al., 2007) were established from developing embryos released from eggs, resulting in a mixture of embryonic cells. Some other continuous cell lines were derived from primary cultures of moulting nymphal tissues or moulting larval explants. Tick cell lines are thus usually heterogeneous cultures of at least two but often more different cell types. Attempts to generate clonal cell lines from established cultures have failed (Munderloh et al., 1994), possibly because the heterogeneity of the culture is essential for growth and survival. Interestingly, the number of chromosomes can vary between individual cells in a culture, suggesting a gain or loss of chromosomes without affecting cell viability. Tick cells generally grow at temperatures between 28ºC and 34ºC, but some cell lines will also grow at 37ºC and most cell lines can be kept at cool temperatures (15ºC or even 4ºC) to slow down growth for longer periods. The cell lines used in the present study generally prefer a slightly acidic pH

of the culture medium, but the *I. scapularis* cell line IDE8 and some other cell lines also tolerate neutral or alkaline pH. All cell lines are normally grown in sealed containers, such as flat-sided tubes or non-ventilated flasks. Some cell lines can tolerate short-term cultivation in unsealed containers such as multiwell plates. While tick cells generally are not strongly adherent, the *I. scapularis* cell lines used in the present study, IDE8 and ISE18 (Munderloh et al., 1994), are strongly adherent unless cell density of the culture is very high, and the *I. ricinus* cell line used in the present study, IRE11 (Simser et al., 2002), is weakly adherent. Some tick cell lines, including ISE18, grow in three dimensions, forming large clumps instead of an even distribution across the tube or flask. Culture growth is slow compared to most mammalian or mosquito cell lines and high densities of cells or infrequent subculture is not detrimental to the culture in contrast to most mammalian and mosquito cells.

Arbovirus infection of tick cell lines

Tick cell lines have been used to study arboviruses, both tick- and mosquito-borne, for five decades (reviewed by Bell-Sakyi et al., 2012). At least 38 tick-borne and 16 mosquito-borne arboviruses have been propagated in tick cell lines to date, particularly of the major arbovirus groups *Bunya*-, *Flavi*-, *Reo*- and *Togaviridae*. Early studies investigated the ability of different arboviruses to replicate and produce virus in tick cell lines. Leake and colleagues showed that (among other viruses) SFV, LGTV and LIV could infect the *R. appendiculatus* cell line RA243 and that the cells produced infectious virus with differences in their growth kinetics (Leake et al., 1980). While SFV grew rapidly to high titres (peak at day 1 p.i.) and was reduced to very low level of virus production within two weeks, LGTV and LIV grew slightly slower (peak at 3 and 4 days p.i., respectively) and did not reach as high levels of virus production as SFV. However, levels of LGTV and LIV production remained stable at a rather high level (>10000 plaque forming units (PFU)/ml). In fact, it was also shown that a persistent infection of RA243 cells with LIV could be established over a period of 90 weekly subcultures, showing little change in virus production or plaque size over the experimental period (Leake et al., 1980). Recently, it was observed that a persistent infection with SFV could be established in the *R. decoloratus* cell line BDE/CTVM14, with infectious virus still produced after one

year (Bell-Sakyi et al., 2012). In 1987, Pudney presented a comprehensive summary on infection of selected tick cell lines with different arboviruses (Pudney, 1987). All but one (Middleburg virus) of nine alphaviruses infected RA243 cells as measured by production of infectious virus particles. Of the flaviviruses investigated, the seven tick-borne viruses used grew in all tick cell lines tested and four of the five tested mosquito-borne flaviviruses grew in at least one of the tick cell lines (the exception being DENV2). Seven mosquito-borne bunyaviruses were tested, yet only Bunyamwera virus grew in tick cells and only to very low levels. Of 13 tick-borne bunyaviruses nine grew in at least one of the tick cell lines used. All of seven tested orbiviruses grew in tick cells. More recent studies have also shown replication of viruses such as Alkhumra haemorrhagic fever virus (Madani et al., 2013) and CCHFV (Bell-Sakyi et al., 2012) in a number of tick cell lines.

The cell lines used in the present study (ISE18, IDE8 and IRE11) have not been used extensively in the study of arboviruses. No studies on arbovirus infections of ISE18 and IRE11 cells have been published to date. The cell line IDE8 has been used extensively for the isolation and study of tick-borne bacteria (Bell-Sakyi et al., 2007; Cabezas-Cruz et al., 2013; Silaghi et al., 2011; Zweygarth et al., 2008) and also for the protozoan *Babesia bigemina* (Ribeiro et al., 2009), yet only one study using an arbovirus, namely SFV, to infect IDE8 cells has been published to date (Barry et al., 2013). However, another *I. scapularis*-derived cell line, ISE6 (Kurtti et al., 1996), has been shown to support replication of Dugbe virus, Hazara virus (Garcia et al., 2005), WNV, TBEV, POWV, Negishi virus, LIV and LGTV (Lawrie et al., 2004a) and has been used to study infection with LGTV in more detail (Offerdahl et al., 2012). In the latter study, LGTV production peaked at 2 days p.i. and remained at a high level. In fact, LGTV infection of ISE6 cells resulted in a persistent infection over one year with little change in virus production. TBEV was also grown in the *I. scapularis* cell line IDE2, but virus production was low in IDE2 compared to the *I. ricinus* cell lines IRE/CTVM18, 19 and 20 (Ruzek et al., 2008).

The disadvantage of a cell line system for experimental use is that it does not necessarily fully reflect what would happen in an *in vivo* scenario. Many processes may only occur in specific cell types or organs, or they might require a combination

of events in multiple organs. There might also be differences during particular stages of development. In particular, when investigating vector-pathogen interactions, the interplay of the two may vary immensely between organs. Immune responses in the midgut may vary significantly to those of the salivary glands for example. While it is important to keep this in mind, there are numerous advantages of working with cell lines as opposed to whole ticks. Firstly, it is easier to set up relatively frequent large scale experiments in a cell culture system, testing multiple conditions at the same time. Furthermore, cell culture systems allow more standardised techniques with less confounding factors compared to whole animals. One major advantage of cell lines is that an animal facility with animals such as rabbits for tick feeding is not necessary. While there are established *in vitro* feeding techniques for several tick species (Krober and Guerin, 2007), it has so far not been possible to keep laboratory tick colonies for the full life cycle on *in vitro* feeding systems without detrimental effects on tick viability (John Andrade, personal communication). These feeding systems are only used for experiments to reduce variability and allow, for example, application of very specific concentrations of drugs or pathogens in a blood meal (Krober and Guerin, 2007).

Endogenous microorganisms in tick cells

An interesting observation is the presence of endogenous microorganisms in many tick cell lines. Endosymbiotic bacteria have been found in ticks (Scoles, 2004) and established tick cell lines (Mattila et al., 2007; Najm et al., 2012; Simser et al., 2001). Reovirus-like particles were observed by electron microscopy (EM) in a *R. appendiculatus* cell line over 25 years ago (Munz et al., 1987), but the first virus that was sequenced from a tick cell line (*I. scapularis* IDE2) was SCRV (Attoui et al., 2001). Recently, it has become apparent that in fact most (possibly all) of the existing tick cell lines harbour endogenous viruses (Alberdi et al., 2012; Bell-Sakyi and Attoui, 2013). At least 25 tick cell lines appear to be persistently infected with reovirus-like particles, and some nairovirus sequences were detected using pan-nairovirus primers (Alberdi et al., 2012). As many of these cell lines are derived from surface-sterilised egg batches, it indicates vertical transmission of these viruses in ticks and the possibility that many ticks in nature are persistently infected with

endogenous viruses which may not be transmitted to mammalian hosts. While there is little evidence for the presence of 'tick only' viruses in whole ticks, some older studies visualised so-called 'glycogen granules' (Binnington and Lane, 1980; Jaworski et al., 1983) which in fact have the appearance of viruses (Bell-Sakyi and Attoui, 2013). How these endogenous viruses may interact with superinfecting arboviruses remains unknown.

1.4 ARTHROPOD ANTIVIRAL IMMUNITY[2]

Ticks are vectors of many human and animal pathogens as described above. Vector competence of ticks is probably tightly linked to tick-pathogen interaction. Despite the importance of understanding tick-pathogen interactions, very little is known about how ticks and tick cells respond to virus infection. Responses against bacteria and protozoa include phagocytosis by tick haemocytes. This seems to be associated with a complement-like system. Some antimicrobial peptides such as defensins and lysozymes have been found but these are mostly single discoveries distributed among a wide range of different tick species. So far, no tick species has been properly characterised with respect to its innate defences to a series of infectious agents. For example, there has been no experimental investigation of whether ticks use melanisation or coagulation of tick haemolymph as defence mechanisms against microorganisms (reviewed by Hajdusek et al., 2013; Kopacek et al., 2010).

Ability to cross the midgut barrier is often an important factor in determining vector competence for an arbovirus (Arias-Goeta et al., 2013; Black et al., 2002; Moudy et al., 2007; Smith et al., 2008). Once the virus has crossed the midgut barrier, it has to disseminate to the salivary glands and from there to the next susceptible host. Unlike mammalian systems, where virus infections are usually cleared by the immune system, sometimes at great cost to the host, arthropods generally do not eliminate virus, but they control it and keep it at a low level. There are many different mechanisms known to play a role in controlling arbovirus replication in insects. These are summarised in Fig 1.9 and described in the following sections. However, knowledge about these mechanisms in ticks is limited.

[2] Parts of this chapter were used as a draft for a short review, which was submitted in February 2014 to the Springer journal VirusDisease (Rückert et al. 2014, in press, attached at the end of this thesis).

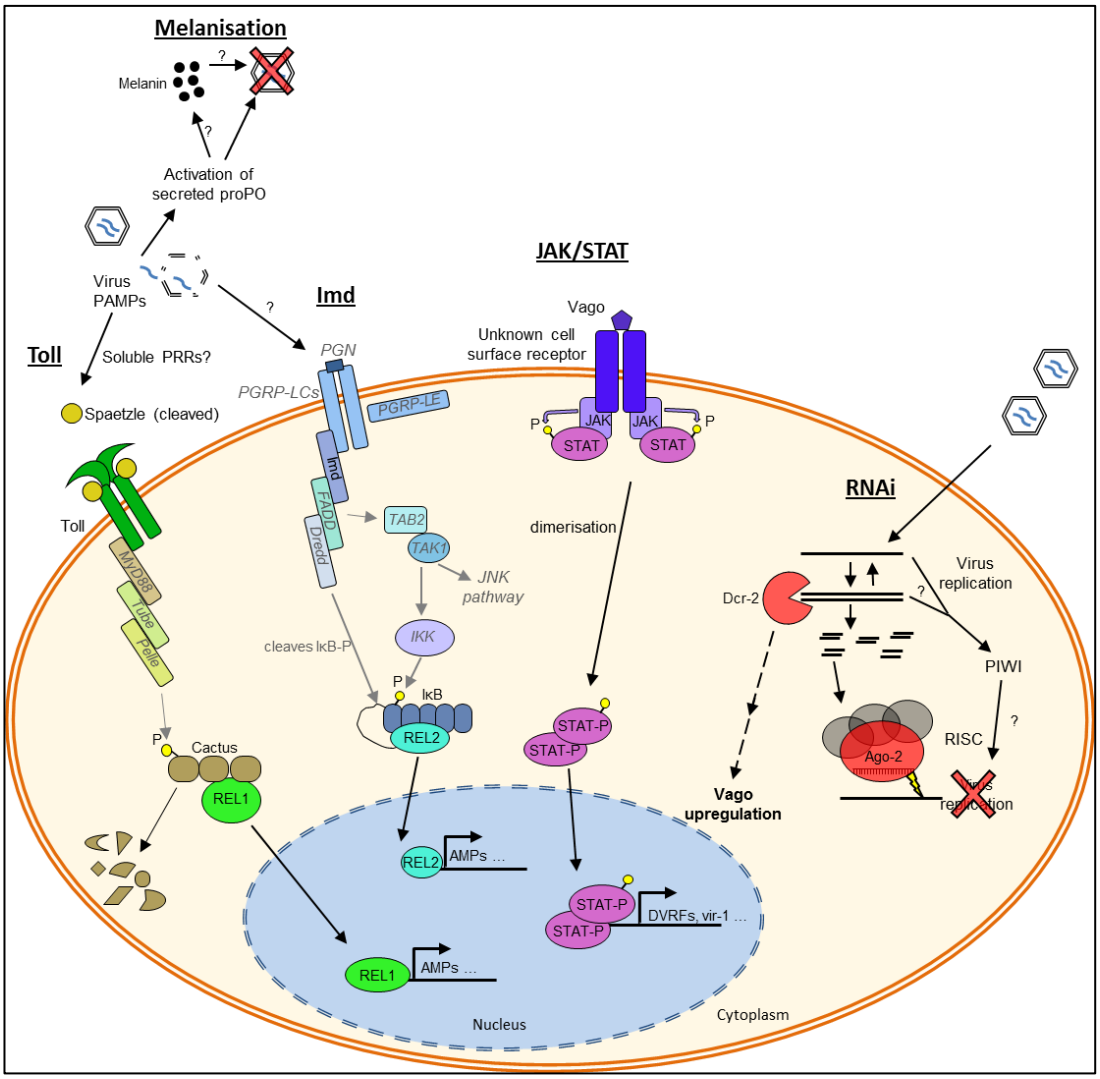

Figure 1.9: Innate immunity pathways in mosquitoes - gaps in current knowledge were filled using information known for *Drosophila* (shown in grey). **Toll**: PAMPs are recognised by extracellular PRRs which activate a proteolytic cascade leading to activation of the cytokine spaetzle by cleavage. Active spaetzle binds to the Toll receptor resulting in its dimerisation and intracellular recruitment of MyD88, Tube and Pelle. This interaction initiates phosphorylation of Cactus, probably mediated by the kinase Pelle. Phosphorylated Cactus is degraded and REL1 translocates to the nucleus and activates transcription of effector genes. **Imd**: Binding of peptidoglycan of gram-negative bacteria to PRGP receptors activates Imd and a signal transduction cascade results in phosphorylation of IκB by IκB-kinase (IKK). IκB is then proteolytically cleaved off REL2, which translocates to the nucleus and activates transcription of AMPs. For both Toll and Imd it is unclear how these pathways are activated by viruses, but possible activating factors are virus or debris associated PAMPs. **JAK/STAT**: Binding of the virus-induced cytokine Vago to an unknown cell surface receptor activates JAK, which in turn phosphorylates STAT. STAT-P dimerises and translocates to the nucleus as a transcription factor. **RNAi**: Viral dsRNA molecules are recognised by Dcr-2 which cleaves the long dsRNA into 21 nt viRNAs. The viRNAs are incorporated into the RISC. The passenger strand of the viRNA is degraded and the RISC targets the viral genome/mRNA using the guide strand. Ago-2 slices the complementary target mRNA and inhibits synthesis of viral proteins. **Melanisation**: Mosquito pro-PO is activated by microorganisms such as bacteria and in some cases viruses. Activation of PO leads to the formation of melanin and in some cases PO activity is responsible for a reduction in infectious virus (whether or not this is due to melanin is not known). (Figure adapted from Rückert et al. 2014, in press).

1.4.1 RNA interference

Among arbovirus vectors, mosquitoes are probably the most thoroughly studied group with regard to their antiviral responses. RNA interference (RNAi), identified in mosquitoes over ten years ago (Hoa et al., 2003; Keene et al., 2004; Sanchez-Vargas et al., 2004), is considered to be the most important antiviral mechanism (Blair, 2011). There are three major types of small RNA systems - the microRNA (miRNA), the PIWI-interacting RNA (piRNA) and the small interfering RNA (siRNA) pathways, all of which can play a role in arthropod antiviral defences (reviewed by Donald et al., 2012; Vijayendran et al., 2013). While the generation of exogenous siRNAs has been implicated in antiviral defences in arthropods, miRNAs and piRNAs have mainly been associated with regulation of gene expression and control of transposons in germlines (reviewed by Asgari, 2013; Ishizu et al., 2012)); however, recently their role in virus infection has become more apparent. Numerous small RNA profiles of arbovirus-infected mosquitoes or mosquito cells have been published (Hess et al., 2011; Leger et al., 2013; Myles et al., 2008; Siu et al., 2010; Vodovar et al., 2012) and have provided insights into the importance of the different small RNA pathways during arbovirus infection. Knowledge gained about antiviral RNAi over the last decade has also led to new techniques for virus discovery. It was shown that nearly complete virus genomes can be assembled by sequencing of small RNAs derived from invertebrates (Wu et al., 2010). Both siRNAs and piRNAs were found to match viral genomes.

siRNAs

While there is both an endogenous (Czech et al., 2008; Ghildiyal et al., 2008; Okamura et al., 2008) and an exogenous (Blair, 2011; Sanchez-Vargas et al., 2004) siRNA pathway in insects, the exogenous pathway is predominantly associated with antiviral RNAi. There has been one report of SINV infection inducing a novel class of endogenous siRNAs, but it is not clear whether this is of benefit for the virus or the vector (Adelman et al., 2012). The exogenous siRNA pathway is considered to be the most important antiviral mechanism in arbovirus vectors such as mosquitoes (Blair, 2011). The mechanism in mosquitoes is very similar to the one described for the model organism *D. melanogaster* (reviewed by Donald et al., 2012; Fragkoudis et

al., 2009). Upon infection, RNA viruses introduce or generate foreign dsRNA in the arthropod cell either as replication intermediates, as part of their dsRNA genome or as secondary structures of their ssRNA genome. dsRNA is recognised as a pathogen-associated molecular pattern (PAMP) by Dicer-2 (Dcr-2). In association with R2D2, Dcr-2 cleaves dsRNA into virus-induced small interfering RNAs, designated viRNAs, which are predominantly 21 nt long. The viRNAs are then incorporated into the RNA-induced silencing complex (RISC) with Argonaute-2 (Ago-2) as its integral protein. Ago-2 is also called the Slicer protein. Slicer activity is essential for an efficient RNAi response against flaviviruses (Chen et al., 2011) and probably other arboviruses. One strand, the passenger strand, of the viRNA is degraded and the RISC uses the remaining guide strand to target complementary RNA including potentially viral mRNA and genomes. Upon interaction with a complementary RNA, Ago-2 slices the target. In the case of mRNA this in turn inhibits synthesis of viral proteins. It has been suggested that Dcr-2 is also involved in signalling. Like RIG-I or Mda-5 in mammalian cells, Dcr-2 detects dsRNA as foreign and activates signalling which, at least in mosquitoes, results in increased expression of Vago, a cytokine with an interferon-like function (Paradkar et al., 2012).

Systemic spread of the RNAi response and amplification of small RNAs is an important aspect of antiviral RNAi in plants and the nematode *Caenorhabditis elegans* (Nematoda) (Smardon et al., 2000; Voinnet, 2005; Yang et al., 2004). In *D. melanogaster* it has been shown that systemic spread of the RNAi response is essential for an efficient antiviral response and components of the dsRNA uptake machinery have been identified (Karlikow et al., 2014; Saleh et al., 2009). To date no protein with RdRP activity for amplification of small RNAs has been identified in insects. One report of a *Drosophila* protein with RdRP activity was subsequently retracted because the measured RdRP activity was found to be an artefact (Lipardi and Paterson, 2009, 2011); however, it was proposed that reverse transcription of viral RNA by retrotransposons may result in viral cDNA elements serving as a template for the generation of new viRNAs (Goic et al., 2013). In *Ae. albopictus* U4.4 cells it has been shown that siRNAs can spread through the culture if there is cell-to-cell contact, but cannot spread freely through the culture medium (Attarzadeh-Yazdi et al., 2009).

While RNAi in mosquitoes is relatively well-characterised, little is known about RNAi in other arbovirus vectors. RNAi has been identified as an antiviral mechanism in tick cells (Garcia et al., 2005; Garcia et al., 2006) and has been used as a tool for knockdown of gene expression in tick and tick-borne disease research for over a decade (Barry et al., 2013; de la Fuente et al., 2007), but the detailed mechanisms are not well understood. For the two tick species *I. scapularis* and *Rhipicephalus (Boophilus) microplus*, components of the RNAi pathway have been identified by comparative genomics (Kurscheid et al., 2009). For both species, putative Dcr-1, Ago-1 and Ago-2 as well as orthologues of many proteins involved in dsRNA uptake and systemic RNAi in *D. melanogaster* have been identified (Kurscheid et al., 2009). However, it remains unknown if these tick proteins exhibit the expected Dcr-1, Ago-1 and Ago-2 activity in ticks. Another study by Schnettler and colleagues has shown that there are additional Ago and Dcr proteins in *I. scapularis* (Esther Schnettler, personal communication). Four orthologues similar to Ago-2 (namely Ago-16, Ago-30, Ago-68 and Ago-96) and one orthologue similar to Ago-1 (namely Ago-78) were identified. In addition, two Dcr-like orthologues were identified: one with similarity to Dcr-1 and the other with unclear relation. All these Ago and Dcr orthologues are expressed in the cell line IDE8 (Schnettler et al. 2014, submitted). Kurscheid et *al*. also proposed that an RdRP responsible for amplification of the RNAi response is present in ticks (Kurscheid et al., 2009). However, there is no experimental evidence for this and while the application of dsRNA for knockdown of gene expression in ticks indicates efficient systemic RNAi (de la Fuente et al., 2007), the detailed mechanisms remain unknown.

Another large group of arbovirus vectors are midges, transmitting many economically important viruses affecting animal health, such as BTV (Maclachlan, 2011; Wilson and Mellor, 2009) and Schmallenberg virus (SBV) (Garigliany et al., 2012). Despite the current lack of a published genome, RNAi has recently been shown to target replication of BTV and SBV in *Culicoides* cells in a manner similar to other arbovirus vectors (Schnettler et al., 2013b).

Many insect and plant viruses have developed strategies to counteract RNAi, such as suppression and evasion of the RNAi response (reviewed by Donald et al., 2012).

For a summary of known suppressors of RNAi expressed by insect and plant viruses, see http://viralzone.expasy.org/all_by_protein/891.html (Masson et al., 2013). One interesting observation is that while some arboviruses do have RNAi evasion strategies (Siu et al., 2010), they generally do not encode efficient suppressors of RNAi. Strong suppression of the antiviral RNAi response could be detrimental to vector survival (Cirimotich et al., 2009; Myles et al., 2008) and thus to the transmission of the arbovirus. The only arboviruses known to encode suppressors of RNAi are flaviviruses. WNV encodes a subgenomic RNA in the 3' untranslated region of its genome, subgenomic flaviviral RNA (sfRNA); this sfRNA acts as an RNAi suppressor in both mammalian and insect cells (Schnettler et al., 2012). TBEV and LGTV also appear to express sfRNAs which suppress the RNAi response in tick cells (Esther Schnettler, personal communication). The NS4B protein of another flavivirus, DENV-2, has also been shown to act as a suppressor of mammalian and insect RNAi (Kakumani et al., 2013).

miRNAs

Among all the classes of small RNAs, miRNAs may be considered the most important for the cell as miRNAs are important regulators of gene expression in different tissues and developmental stages (Asgari, 2013). In *Drosophila melanogaster* the ratio of genes expressing miRNAs to genes expressing proteins is roughly 1:100 (Lai et al., 2003). miRNAs are ~22 nt in length and are found in most eukaryotic cells; their biogenesis in insects has been reviewed extensively (Asgari, 2013; Behura, 2007; Lucas and Raikhel, 2013). It is widely believed that the mechanism of biogenesis is conserved among insects, including arbovirus vectors such as mosquitoes and midges. A number of miRNAs have been identified in mosquitoes of different species (Gu et al., 2013; Li et al., 2009; Puthiyakunnon et al., 2013; Skalsky et al., 2010; Thirugnanasambantham et al., 2013; Winter et al., 2007) and their presence in midges is to be expected. In ticks, however, our knowledge of small RNAs is limited. So far only 49 miRNAs have been identified in the *I. scapularis* genome by the miRNA database miRBase (Griffiths-Jones et al., 2006). In ticks of the species *Haemaphysalis longicornis* miRNAs are expressed in the salivary glands with differences in the expression pattern during blood-feeding (Zhou

et al., 2013). In *R. microplus* both conserved miRNAs and tick-specific miRNAs have been identified (Barrero et al., 2011) and, as in other arthropods, the pattern of expression of the *R. microplus* miRNA changes during developmental stages and in different organs. Whether or not the pathway components are entirely conserved remains unknown.

For those vector species in which miRNAs have been identified, we know that they play an important role in development and regulation of gene expression in the uninfected organism (Barrero et al., 2011; Puthiyakunnon et al., 2013; Zhou et al., 2013); whether they are involved in antiviral responses against arboviruses remains unknown. In *D. melanogaster* a number of miRNAs have been implicated in regulating immune responses (reviewed by Asgari, 2013; Vijayendran et al., 2013), such as miR-8 (Choi and Hyun, 2012) and the let-7 miRNA (Garbuzov and Tatar, 2010) which are involved in regulation of antimicrobial peptides. Recently, miRNAs involved in controlling responses such as melanisation have also been predicted by a computational approach in the mosquito species *Anopheles gambiae* (Thirugnanasambantham et al., 2013), the vector of the alphavirus O'nyong-nyong virus (ONNV) (Williams et al., 1965) and the protozoan parasite *Plasmodium falciparum* (Mitri and Vernick, 2012). In *Ae. aegypti* mosquitoes, miRNAs are responsible for gene expression changes after a blood-meal, and one of these (aae-miR-375) regulates immune-related genes such as *cactus* and *REL1* (Hussain et al., 2013). During infection of *Ae. aegypti* mosquitoes with the intracellular bacterium *Wolbachia*, the bacterium uses a host miRNA to regulate a methyltransferase, which contributes to inhibition of DENV replication (Zhang et al., 2013). These findings suggest that there may be miRNAs in other arthropods that contribute to modulating the antiviral response. In addition, an intriguing observation is that WNV encodes a miRNA that can modulate host gene expression (Hussain et al., 2012).

piRNAs

piRNAs are 24-32 nt in length and are distinct from other small RNAs as their production is Dicer-independent (Vagin et al., 2006) and they do not generally form hairpins or other secondary structures during biogenesis. The biogenesis of piRNAs is reviewed by (Ishizu et al., 2012; Siomi et al., 2011). The detailed mechanism of

piRNA biogenesis is not entirely clear and appears to vary significantly between germline and somatic cells (Handler et al., 2013), and between *Drosophila* and mosquitoes (Donald et al., 2012). While PIWI-mediated RNAi has been described as a mechanism of protection against transposable elements in germline cells of some arthropods and vertebrates, it has recently also been implicated in mosquito antiviral immunity. Increasing knowledge about the piRNA pathway in mosquitoes reveals many apparent differences from that in *Drosophila* (Donald et al., 2012) and virus-derived piRNAs have been shown to be produced both in the *Aedes* mosquito soma (Morazzani et al., 2012) and in the cell lines U4.4, C6/36 (*Ae. albopictus*) and Aag2 (*Ae. aegypti*) upon infection with SINV (Vodovar et al., 2012). Virus-derived piRNAs were also observed in C6/36 cells infected with the bunyavirus La Crosse virus (Vodovar et al., 2012). In another study, both U4.4 and Aag2 cells produced piRNAs after infection with SFV and knockdown of one of the PIWI proteins, PIWI4, resulted in an increase in SFV replication, demonstrating that activity of a PIWI protein was involved in controlling arbovirus replication (Schnettler et al., 2013a). The flavivirus DENV was also shown to induce virus-specific piRNAs after infection of *Ae. aegypti* mosquitoes (Hess et al., 2011; Scott et al., 2010). In addition, PIWI-mediated RNAi has been observed in Aag2, U4.4 and C6/36 cells infected with the bunyavirus Rift Valley fever virus (Leger et al., 2013). All three cell lines were shown to produce viRNAs with a PIWI signature, in particular late in infection after the peak of 21 nt viRNA production. In summary, progress in the field of piRNAs has revealed the importance of a PIWI-mediated response in the antiviral response of mosquitoes. The piRNA pathway is conserved between vertebrates and other arthropods suggesting that it is likely to be present in ticks. However, no studies investigating the tick PIWI-mediated RNAi response have been published to date.

1.4.2 Antiviral responses triggered by innate immunity signalling pathways

While RNAi is an important and essential component of the antiviral response, there is evidence for the involvement of several other innate immunity pathways in controlling arbovirus infections in arthropod vectors. All of the three major innate immunity signalling pathways in insects, namely Janus kinase/signal transducer and

activator of transcription (JAK/STAT), Toll and Immune deficiency (Imd), have been implicated in antiviral defences in insects (reviewed by (Fragkoudis et al., 2009; Kingsolver et al., 2013; Merkling and van Rij, 2013)). All three pathways also play a role in development and especially in immune responses to other pathogens. These pathways are very well-studied in *Drosophila*, but less so in arbovirus vectors. In mosquitoes it is largely assumed that mechanisms are very similar to those in *Drosophila* and components of the pathways are found in the published mosquito genomes. A comparative genomic study of *D. melanogaster*, *A. gambiae* and *Ae. aegypti* examined the evolutionary dynamics of immunity genes in higher insects (Waterhouse et al., 2007). In ticks, knowledge about immunity pathways is generally very limited; however, immune responses against bacteria have been studied in some detail (Kopacek et al., 2010; Liu et al., 2012) and the knowledge gained about bacterial defences may provide a basis for studies on antiviral defence mechanisms.

The JAK/STAT pathway

Among arbovirus vectors, the JAK/STAT pathway and its antiviral activity have been characterised predominantly in mosquitoes. JAK/STAT pathway activation inhibits replication of the flaviviruses DENV (Souza-Neto et al., 2009) and WNV (Paradkar et al., 2012) in *Ae. aegypti* mosquitoes and *Culex quinquefasciatus* Hsu mosquito cells, respectively. Upon flavivirus infection, mosquito Dcr-2 recognises viral dsRNA in a similar manner to RIG-I and Mda-5 in mammals and initiates a signalling cascade leading to the expression and secretion of Vago (Paradkar et al., 2012), a small cytokine with a function similar to interferon in the mammalian system. Secreted Vago binds to an unknown receptor on neighbouring cells leading to the signalling cascade shown in Fig 1.9 and resulting in activation and translocation of STAT. Activated STAT acts as a transcription factor inducing expression of antimicrobial peptides (AMPs) such as two DENV restriction factors (Souza-Neto et al., 2009) and vir-1 (Paradkar et al., 2012). However, treatment with poly I:C (a synthetic analogue of dsRNA) or BTV dsRNA did not lead to *vago* upregulation and STAT activation in *Culex tarsalis* cells (Paradkar et al., 2012) and infection of U4.4 cells with the alphavirus SFV did not lead to activation of STAT (Fragkoudis et al., 2008). Taken together these findings suggest that activation of

STAT may be a specific anti-flaviviral response. However, when STAT was activated prior to SFV infection by treatment with heat-inactivated *Escherichia coli* bacteria, replication of SFV was reduced (Fragkoudis et al., 2008). Due to the concurrent activation of the Imd pathway, it was not clear if this was a specific consequence of JAK/STAT activation. However, alphavirus replication does appear to induce activation of STAT in *D. melanogaster*. Replication of SINV in *D. melanogaster* resulted in increased expression of *vago* and *attacin-C* (*attC*), among other STAT-regulated genes. Furthermore, *attC* was shown to have an antiviral function against SINV in this system (Huang et al., 2013). In another study the effect of SINV infection on gene expression levels of *stat* in Aag2 cells was investigated. While there was no direct evidence of STAT activation, *stat* expression levels increased approximately 1.5-fold upon SINV infection (Barletta et al., 2012).

In other arbovirus vectors such as ticks and midges there is only limited information on JAK/STAT. In *I. scapularis* ticks it was shown that there is a functional JAK/STAT pathway which controls infection with the intracellular tick-borne bacterium *Anaplasma phagocytophilum* (Liu et al., 2012), but some of the key players of the pathway remain unknown and there is no information on whether JAK/STAT may also have an antiviral function. New insights into the role of JAK/STAT in the antiviral response of midges may be gained in the future through analysis of the *Culicoides* genome.

The Toll pathway

Unlike the mammalian Toll-like receptors (TLRs), Toll in arthropods is not a pattern recognition receptor (PRR), but pattern recognition is mediated by extracellular PRRs (Kurata et al., 2006; Li and Xiang, 2013). Upon recognition of PAMPs, for example lipoteichoic acid of gram-positive bacteria, peptidoglycan of fungi and possibly virus debris, the cytokine spaetzle is cleaved into its active form and binds to the Toll receptor (Arnot et al., 2010). A downstream signalling cascade (Fig 1.9) similar to those of mammalian TLRs results in degradation of the IκB orthologue Cactus and activation of the transcription factor REL1 (isoforms A/B in *Ae. aegypti*) (Shin et al., 2005), an orthologue of NFκB, which translocates to the nucleus and initiates transcription of AMPs such as defensins. During DENV infection of *Ae.*

aegypti mosquitoes the Toll pathway is activated in the midgut and plays an important role in controlling DENV infection (Xi et al., 2008). In contrast to DENV, evidence so far suggests that alphaviruses are not controlled by Toll in insects. In U4.4 cells SFV replication was not reduced by expression of a constitutively active Toll receptor, in fact there was a small increase in replication (Fragkoudis et al., 2008). Furthermore, in *Drosophila* SINV was unaffected by mutations in the Toll pathway (Avadhanula et al., 2009). However, both systems used in these experiments on alphaviruses were not natural whole mosquito infections. While U4.4 cells are derived from a relevant species of mosquito (*Ae. albopictus*), a cell line cannot represent everything that happens in the complex midgut as investigated for DENV. The study performed with SINV in *Drosophila* used live flies, however, *Drosophila* is not a haematophagous vector of arboviruses and thus may lack mechanisms evolved specifically against vector-borne alphaviruses. In *Anopheles gambiae* the concurrent injection of dsRNA against Cactus and ONNV resulted in an increased viral load 7 days post-injection compared to controls without dsRNA targeting Cactus (Waldock et al., 2012). As knockdown of the negative regulator Cactus should result in increased activation of REL1, this result provides further evidence that the Toll pathway is not involved in controlling alphavirus replication. Further studies on other viruses using live mosquitoes could define whether the antiviral role of the Toll pathway is indeed specific to flaviviruses.

In ticks and midges the Toll pathway has not been characterised and components are mostly unknown. However, for the tick *I. scapularis* there are a number of putative Toll receptors in the published genome (Hill and Wikel, 2005) and also orthologues of REL1 and Cactus (Kopacek et al., 2010). Their role in immune defences against bacterial or viral infection remains unknown.

The Imd pathway

The Imd pathway in mosquitoes is classically activated by gram-negative bacteria. A downstream signalling cascade (Kingsolver et al., 2013; Merkling and van Rij, 2013) (Fig 1.9) results in activation of REL2 (Shin et al., 2002), another orthologue of NFκB. The Imd pathway in *Drosophila* has been implicated in the antiviral response to insect viruses such as Cricket paralysis virus (Costa et al., 2009), Sigma virus

(Tsai et al., 2008) and Nora virus (Cordes et al., 2013), however the only arboviruses associated with an Imd immune response in insects are alphaviruses. SINV replication in *D. melanogaster* resulted in increased expression of components of the Imd pathway and the downstream gene *diptericin-B* has antiviral activity against SINV (Huang et al., 2013). Pre-activation of the Imd pathway by heat-inactivated *E. coli* also increased SFV replication in U4.4 cells (Fragkoudis et al., 2008). In the mosquito *A. gambiae*, ONNV infection led to changes in expression of Imd pathway components, possibly activating the Imd pathway, but knockdown of REL2 gene expression did not affect virus production, so that the role of Imd in ONNV infection remains unclear (Waldock et al., 2012). The Imd pathway in mosquitoes has not been implicated in an antiviral response against arboviruses other than alphaviruses.

While some components of the Imd pathway such as REL2 and Caspar can be found in the *I. scapularis* genome, an orthologue of Imd itself could not be identified by basic local alignment search (tblastn). NF-κB orthologues named RelA and RelB were characterised in nuclear extracts of the *I. scapularis* cell line ISE6 and were found to act as transcription factors with similar binding sites compared to other organisms (Naranjo et al., 2013). The authors also showed that binding activity of this NF-κB orthologue was increased in infection with *A. phagocytophilum*, indicating activation of an Imd-related pathway by this intracellular bacterium. Whether this pathway plays a role in virus infection remains unknown, but tools made available by research on bacterial pathogens may lead to new insights into antiviral responses. In addition, a relatively large number of AMPs have been found in ticks, and some of them, such as defensins, have been well characterised, but regulation of these remains unclear and in particular antiviral effects of the discovered AMPs are unknown (reviewed in Kopacek et al., 2010).

1.4.3 Other antiviral defences of arthropods

Besides RNAi and the JAK/STAT, Toll and IMD signalling pathways there are other responses of arthropods to virus infection including autophagy, heat shock proteins (reviewed in Kingsolver et al., 2013; Merkling and van Rij, 2013) and melanisation (Rodriguez-Andres et al., 2012).

Melanisation is a wound healing process which is also used to defend against bacteria by insects. It is a humoral response mediated by a cascade of molecules and enzymes in the haemolymph, involving the key enzyme phenoloxidase (PO), and it is often referred to as the PO cascade (Cerenius et al., 2008; Christensen et al., 2005). The melanisation pathway of insects is summarised in Fig 1.10.

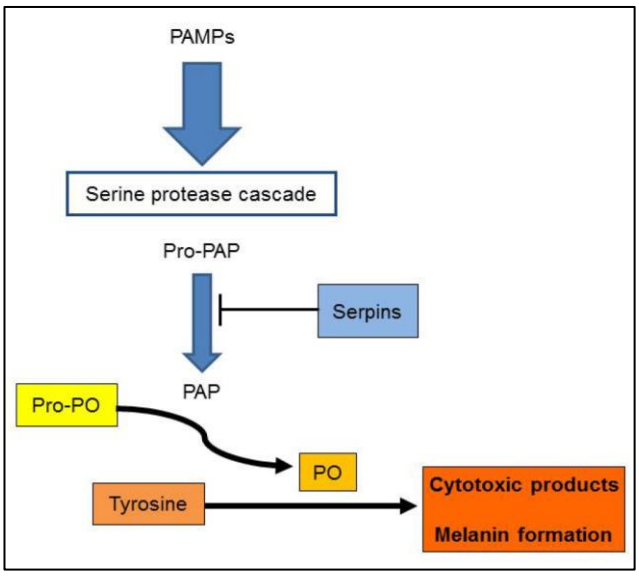

Figure 1.10: Melanisation in insects. PAMPs of microorganisms induce a serine protease cascade which results in the cleavage and activation of PO activating proteins (PAPs), which convert PPO into PO. Activated PO mediates oxidation of tyrosine into dopamine which is then further converted into cytotoxic products, reactive oxygen species or melanin. (Image kindly provided by Dr Julio Rodriguez-Andres)

Ten years ago it was shown that expression of dsRNA targeting a precursor of PO (pro-phenoloxidase I) by SINV lowered PO activity in the mosquito *Armigeres subalbatus* and increased SINV replication (Tamang et al., 2004). However, this observation was followed up only recently when PO activity was shown to act as an antiviral response to SFV in *Aedes* mosquitoes (Rodriguez-Andres et al., 2012). SFV was able to activate PO with efficiency similar to *E. coli* in U4.4 conditioned medium and when a suppressor of the PO pathway was inserted into the SFV genome, replication was increased in *Ae. aegypti* mosquitoes (Rodriguez-Andres et al., 2012). Another study showed that ONNV infection of *A. gambiae* reduced expression of components of the melanisation cascade and in co-infection studies ONNV infection inhibited melanisation of *Plasmodium* ookinetes (Waldock et al.,

2012). It is possible that *A. gambiae* PO also has antiviral activity and ONNV has evolved to counteract this mechanism.

In ticks melanisation is a controversial topic. It is still unclear whether there is a PO cascade in ticks. PO activity has been identified in horseshoe crabs (Nagai and Kawabata, 2000; Nellaiappan and Sugumaran, 1996), which as ancient arachnids are more closely related to ticks than insects. There has been one report of PO activity in a nymph stage of the soft tick *Ornithodoros moubata* (Kadota et al., 2002). Another study found no evidence of PO activity in three hard tick species of different genera, however, this may have been due to small amounts of haemolymph used or a PO inhibitory factor present in the samples (Zhioua et al., 1997).

1.5 AIM OF THE PROJECT

The aim of this PhD project was to extend knowledge on tick antiviral responses. In particular, the aim was to investigate whether antiviral responses observed in insects, such as the model organism *D. melanogaster* and mosquito vectors, are also present in tick cells and, if so, to determine whether they are involved in controlling virus replication.

1.5.1 Objectives:

- To characterise virus infection in selected tick cell lines
- To identify tick orthologues of genes involved in insect antiviral immunity
- To investigate the role of these orthologues in antiviral immunity in tick cells
- To investigate the role of the *Aedes* and *Ixodes* orthologues of *Drosophila* CG4572 on virus replication

2. Materials and Methods

[Due to the laboratory move from the Roslin Institute to the Pirbright Institute in September 2012, some methods were performed differently after the move – this is indicated in the sections concerned.]

2.1 CELL CULTURE

2.1.1 Tick cell culture

For this project the *I. ricinus*-derived cell line IRE11 (Simser et al., 2002) and the *I. scapularis*-derived cell lines ISE6 (Kurtti et al., 1996), ISE18 and IDE8 (Munderloh et al., 1994) were maintained in culture. IRE11 and ISE18 cells were adapted to maintenance in Leibovitz's L-15 medium (GE Healthcare Life Sciences) supplemented with 20% foetal bovine serum (FBS), 10% tryptose phosphate broth (TPB), 2 mM L-glutamine and 100 U/ml penicillin and 100 µg/ml streptomycin (P/S). IDE8 cells were maintained in L-15B medium (see appendix, 8.1.1) (Munderloh and Kurtti, 1989) supplemented with 5% FBS, 10% TPB, 0.1% bovine lipoprotein concentrate (MP Biomedicals), 2 mM L-glutamine and P/S. ISE6 were kept in L-15B300 medium, which consists of L-15B diluted with water (1 part MilliQ water to 3 parts L15B) before addition of supplements (5% FBS, 10% TPB, 0.1% bovine lipoprotein concentrate, 2mM L-glutamine and P/S). Cells were incubated at 32°C in 2.2 ml complete medium in tightly closed flat-sided culture tubes (Nunclon™Δ) and subcultured every 2-4 weeks. Three quarters of culture medium was changed weekly. For subculture 2.2 ml of fresh medium was added to the culture, cells were detached by pipetting and 2.2 ml of the cell suspension was transferred into a new tube. Whenever tick cells were seeded into 24-well plates, an air-tight bag was placed around the plates and a wet tissue was added to the bag to create a humid chamber around the plates to prevent drying out.

2.1.2 Mammalian cell culture

The baby hamster kidney cell line BHK-21 was used for propagation of SFV and plaque assays of both SFV and LGTV. BHK-21 cells were kept in Glasgow Minimum Essential Medium (GMEM) supplemented with 5% newborn calf serum (NBCS), 10% TPB and P/S (from here on referred to as 5% GMEM). Cells were

maintained at 37°C in a humidified atmosphere of 5% CO_2 in air. The African green monkey cell line Vero was used for propagation of LGTV. Vero cells were kept in Dulbecco's Minimum Essential Medium (DMEM) supplemented with 10% FBS and P/S (from here on referred to as 10% DMEM).

2.1.3 Mosquito cell culture

In this study the *Ae. Aegypti*-derived cell line Aag2 (Peleg, 1968) and the *Ae. Albopictus*-derived cell line U4.4 were used (Singh, 1967). Aag2 and U4.4 cells were both maintained in Leibovitz's L-15 medium supplemented with 10% FBS and 10% TPB. Cells were incubated in Nunc™ cell culture treated flasks with filter caps at 28°C in a non-humidified atmosphere. Whenever cells were seeded into 24-well plates a humid chamber was created around the plates to prevent drying out.

2.2 VIRUS PROPAGATION

2.2.1 SFV reporter viruses

SFV reporter constructs used in this project are all based on the full length SFV clone pSP6-SFV4 (Liljestrom et al., 1991) and were provided by Dr Andres Merits (University of Tartu, Estonia), except for SFV4-steGFP which was provided by Dr Rennos Fragkoudis (The Pirbright Institute). The following SFV reporter constructs were used in the present study (Figure 1.4):

- SFV4(3H)-*Rluc* (Kiiver et al., 2008)
  Rluc is inserted into the non-structural ORF between nsP3 and nsP4.
- SFV4(3F)-ZsGreen (based on SFV4(3F)-eGFP (Tamberg et al., 2007)
  ZsGreen is inserted into the non-structural ORF and is expressed as a fusion protein with nsP3. Thus, ZsGreen signal indicates the localisation of nsP3 in an infected cell.
- SFV4-steGFP (Fragkoudis et al., 2007)
  eGFP is inserted into the structural ORF and is released into the cytosol of an infected cell.

- SFV1-*Rluc* VRPs using single helper plasmid (Liljestrom and Garoff, 1991)
  This is an SFV replicon expressing *Rluc* under the subgenomic promoter. Packaging of the replicon to generate VRPs was achieved by co-transfection of mRNA derived from a single helper plasmid expressing the structural proteins of SFV.

The SFV4-steGFP plasmid encodes for the viral genome under the control of a CMV promoter. All other plasmids encode the SFV genome or structural proteins (in case of the helper plasmid) under the control of the promoter for bacteriophage SP6 RNA Polymerase.

Transformation of Sure2 competent *E. coli*

Plasmids containing viral cDNA were grown in Sure2 competent *E. coli* (Stratagene). Sure2 competent *E.coli* were thawed on ice and gently mixed. To each aliquot of bacteria 2 µl of β-mercaptoethanol (provided with the competent *E. coli*) were added. The tubes containing competent bacteria and β-mercaptoethanol were shaken gently and incubated on ice for 10 min, while shaking gently every 2 min. Then, 0.1-50 ng of the plasmid DNA was added to one aliquot of bacteria in a 1 µl volume for maximum efficiency. The tubes were gently shaken and incubated on ice for 30 minutes. The bacteria were heat shocked in a 42°C water bath for 30 s. Subsequently, the bacteria were incubated for 2 min on ice. SOC Medium (Sigma-Aldrich®) was preheated to 37°C and 900 µl were added to the bacteria. The bacteria were then incubated at 37°C for 1 h while shaking at 190-250 rpm. After 1 h, 100 µl of the transformation mixture was plated on Luria Bertani (LB) agar plates containing 50 µg/ml ampicillin. The rest of the bacteria suspension was centrifuged at 2,000 x g for 2 minutes and plated in 100 µl medium on LB agar plates containing 50 µg/ml ampicillin. The plates were incubated for 12-16h at 37°C and then moved to short-term storage at 4°C.

Preparation of plasmid DNA

Plasmid DNA was isolated using a QIAGEN® EndoFree Plasmid Maxi Kit according to the protocol supplied by the manufacturer. Briefly, starter cultures were made by picking a colony from the agar plates (see last section), inoculating it into 5

ml LB-broth and incubating it for ~6 h at 37°C while shaking at 190-250 rpm. 500 µl of the starter culture were then transferred to a large volume of LB-broth (200-250 ml) for overnight incubation (37°C; 190-250 rpm). After 12-16 h bacteria cultures were centrifuged at 4,000 x g for 15 min at 4ºC and then resuspended, lysed for 5 min and the lysis reaction stopped using the provided QIAGEN® buffers P1, P2 and P3, respectively. The bacterial lysate was then filtered through a provided cartridge as described by the manufacturer and added to a DNA-binding column. After two wash steps, plasmid DNA was eluted with the provided elution buffer and precipitated with isopropanol during centrifugation (1 h, 4,000 x g, 4°C). The resulting DNA pellet was washed once with 70% ethanol and after 20 min of centrifugation (4,000 x g, 4°C) was air dried and then dissolved in RNase/DNase-free water (Sigma-Aldrich®). DNA concentration was determined using a NanoDrop 2000 spectrophotometer (Thermo Scientific™).

Linearisation of plasmid DNA

10 µg of the plasmids containing SFV cDNA were linearised using SpeI restriction endonucleases. 10 µg DNA were mixed with 5µl NEB® buffer 4, 5 µl 10x bovine serum albumin (BSA, Sigma-Aldrich®), 1 µl SpeI endonuclease (NEB®) and RNase/DNase-free water up to a volume of 50 µl. The reaction was incubated for 2-4 h at 37°C. The linearised product was then loaded onto a 1% agarose gel and run at 100V for 40 min. The band representing linearised plasmid DNA was cut from the gel and DNA purified using the NucleoSpin® Gel and PCR Clean-up kit (Macherey-Nagel) according to the manufacturer's instructions.

In vitro transcription of infectious viral RNA

The linearised plasmid was transcribed *in vitro* to synthesise capped transcripts using the MEGAscript® SP6 *in vitro* transcription kit (Ambion®) resulting in infectious viral RNA.

Transfection of BHK-21 cells by electroporation

The *in vitro* transcript (or 10 µg of plasmid DNA for SFV4-steGFP) was electroporated into BHK-21 cells using a Bio-Rad Gene Pulser Xcell™ electroporator. Briefly, cells were detached from an approximately 80% confluent

175 cm^2 tissue culture flask and 1.8 x 10^6 cells were resuspended in 800 µl ice-cold phosphate-buffered saline (PBS) to achieve the optimum cell density for efficient electroporation. The resultant cell suspension was added to the *in vitro*-transcribed RNA (or plasmid DNA), mixed by pipetting and incubated for 2 min on ice. 400 µl of the cell/nucleic acid suspension were added to a 0.4 cm electroporation cuvette (Bio-Rad). The cells were pulsed twice using a square wave of 850 V for 0.4 milliseconds and the procedure was repeated with the other half of the cells/nucleic acid. Electroporated cells were added to a new 175 cm^2 flask with 20 ml of warm GMEM supplemented with 10% NBCS, 10% TPB and P/S and incubated at 37°C in a humidified atmosphere of 5% CO_2 in air.

Virus purification

24 h and 48 h after transfection the supernatant containing virus was collected and centrifuged at 3,000 x g for 30 min at 4°C to remove any cell debris. To concentrate the virus the supernatant was ultracentrifuged as follows. The supernatant was added to an ultracentrifugation tube (38.5 ml, Beckman Ultra-Clear™) and approximately 10 ml of 20% (w/v) sucrose (Sigma-Aldrich®) in TNE buffer (50 mM Tris HCl, 100 mM NaCl and 0.1 mM EDTA, pH 7.4) was added by pipetting under the supernatant to create a sucrose cushion. Each tube was then placed in a holder specific to the rotor and balanced by weight. The tubes in the holders were carefully attached to the rotor (SW28), which was then placed in the Beckman L8-70M ultracentrifuge and the virus particles were sedimented through the sucrose cushion for 90 min at 25,000 rpm (125,000 x g) and 4ºC. After ultracentrifugation, supernatants were decanted and the virus was resuspended in 100 µl of TNE buffer while rocking for at least 2 h or overnight on ice. The virus suspensions from each tube were then pooled and the tubes were rinsed with a further 50 µl of TNE buffer which was added to the pool. Virus was distributed into 50 µl aliquots stored at -80°C. Virus titre was determined by plaque assay (see 2.2.3).

2.2.2 LGTV

The LGTV strain TP21 (Smith, 1956) was kindly provided by Dr Sonja Best (Rocky Mountain Laboratories, Hamilton, Montana) and Dr Esther Schnettler (MRC-Centre for Virus Research, University of Glasgow). To grow virus stocks, Vero cells were

seeded into T175cm^2 flasks (10^7 cells per flask) and infected at a multiplicity of infection (MOI) of 0.01. Supernatant was harvested approximately 5-7 days p.i. (upon visible CPE), clarified by centrifugation (4000 x g, 30 min, 4ºC), aliquoted (1-10 ml aliquots) and frozen at -80ºC. Aliquots of virus stock were never re-frozen after thawing. Virus stock titre was determined by plaque assay as described in (see 2.2.3).

2.2.3 Determination of virus titre by plaque assay

SFV

A standard plaque assay was used to detect and quantify infectious plaque-forming units (PFU) in virus stocks or supernatant of infected cells. BHK-21 cells were seeded into 6-well or 12-well plates at a density of 3 x 10^5 or 1.5 x 10^5 cells per well in 2 ml or 1 ml of 5% GMEM, respectively. The next day, ten-fold dilutions of virus stock or supernatant were prepared using PBS containing 0.75% BSA (PBSA). When the cells were approximately 80% confluent the medium was removed and 400 µl of virus dilution were added to duplicate wells for each dilution. The plates were placed within a humid box on a rocker for 1 h at room temperature (RT) to rock gently. The rocker was set to a slow gentle movement, fast enough to avoid drying out of the cells and slow enough to avoid disruption of the cell monolayer (this applies to all infections). After 1 h a semi-solid overlay was added that would inhibit movement of viral particles through the medium and only allow spread of virus from infected to neighbouring cells. In this study two different overlay methods were used for SFV plaque assays.

At Roslin, BD Bacto™ Agar was used. After infection for 1 h, 2% GMEM was mixed with 4% liquid agar in PBS (10 volumes GMEM and 3 volumes liquid agar) and 3 ml or 1.5ml of the mixture were added to each well of a 6- or 12-well plate.

At Pirbright, Avicel was used (FMC biopolymer, Avicel RC-591 NF). After infection for 1 h, 2xMEM (Invitrogen, 21935-028) with 4% FBS was mixed 1:1 with 1.2% Avicel in water and 3 ml or 1.5ml of the mixture were added to each well of a 6- or 12-well plate.

The plates were incubated at 37°C in a humidified atmosphere of 5% CO_2 in air for 2-3 days and then fixed in 4% paraformaldehyde (PFA) for at least 1 h. The fixative

and the agar/Avicel were removed and the cells stained with 0.1% toluidine blue for 30 min. Finally, plates were washed with water and clear areas in the stained monolayer (plaques) due to the CPE of the virus could be seen. These plaques were counted and the virus titre was calculated as PFU per ml:

$$\left(\frac{\textit{mean number of plaques}}{\textit{volume of inoculum in ml}} \right) \textit{ x dilution factor}$$

Both overlays gave similar plaque numbers when compared directly; however, plaque size with Avicel was larger compared to agar and plaque assays performed with Avicel were always fixed 2 days p.i.. Within experiments the same overlay was used.

LGTV

LGTV plaque assays were performed as described above for SFV with the following differences. LGTV samples were diluted in 5% GMEM and assays were always performed with Avicel overlay. Carboxymethyl cellulose (CMC) and BD Bacto™ Agar were also tested as overlays but did not result in visible plaques with CMC and only gave poorly visible plaques with agar. Cells were fixed 4 days p.i. due to the slower onset of CPE in LGTV-infected cells compared to SFV-infected cells. Among all tested combinations of medium, overlay and time-point, only 2xMEM with Avicel fixed 4 days p.i. resulted in easily countable plaques.

2.3 INFECTION OF TICK CELLS

2.3.1 Infection with SFV

For most experiments IDE8, IRE11 or ISE18 cells were seeded at a density of $5x10^5$ cells per ml in either a 24-well plate (1 ml cell suspension) or flat-sided culture tubes (2.2 ml cell suspension). For some experiments IDE8 cells were seeded at a higher density, namely $1x10^6$ cells per ml. SFV stocks were diluted in PBSA as necessary to obtain the desired MOI[3]. For infection of tick cells, 50 µl of virus suspension was

[3] The MOI is an indicator of the ratio of infectious particles to cells in the inoculum; i.e. in theory an MOI of 1 indicates that for each cell there is one infectious virus particle. However, since the titre of SFV was measured in BHK-21 cells, an accurate MOI can only be determined for BHK-21 cells, but not for tick cells or any other cell line, due to potential differences in susceptibility to infection.

added to each well or tube. Unless otherwise indicated medium was not changed before or after inoculation with virus.

2.3.2 Infection with LGTV

IDE8 cells were seeded either at $1x10^6$ or $5x10^5$ cells/well of a 24-well plate. LGTV stock was diluted as necessary in 5% DMEM. For low MOI infection, 50 µl of diluted virus suspension was added to each well; due to the low titre of the LGTV stock, it was necessary to add up to 500 µl of undiluted virus stock to infect at MOI 1. Plates were placed on a rocker at RT for 30 min and then incubated at 32ºC for 1 h. Medium was changed 1.5 h after addition of LGTV.

2.4 INFECTION OF MOSQUITO CELLS

Aag2 or U4.4 mosquito cells were seeded into 24-well or 6-well plates at 1.7×10^5 cells per ml in 1 ml or 4 ml, respectively. SFV was diluted in PBSA as necessary to achieve the desired MOI and 200 µl of virus dilution were added to a well of a 24-well plate (400 µl for a 6-well plate) and incubated at RT on a rocker. After 1 h appropriate complete L-15 medium was added (1 ml/well for 24-well plate or 2 ml/well for 6-well plate).

2.5 FLUORESCENCE MICROSCOPY

For live cell fluorescence microscopy of tick cells infected with virus expressing GFP or ZsGreen, an inverted fluorescence microscope (Zeiss Axio D2 Observer) was used. Cells fixed on coverslips were visualised by confocal fluorescent microscopy with a Zeiss LSM 710 (Roslin) or a Leica SP2 (Pirbright) confocal microscope.

2.6 ELECTRON MICROSCOPY

For EM, cells were harvested by gentle detachment and centrifuged at 200 x g for 5 min; the supernatant medium was discarded, the cell pellet was resuspended gently in 1 ml PBS and centrifuged as before. The supernatant PBS was discarded and the cell pellet was gently resuspended in 3% glutaraldehyde in cacodylate buffer and held on ice for 2-24 h. At this stage, samples were transferred to Steve Mitchell who completed the processing at the Electron Microscope Unit in the School of Biological Sciences, King's Buildings. The cells were post-fixed in 1% osmium tetroxide in cacodylate buffer, dehydrated in acetone and embedded in Araldite resin. Sections were cut on a Reichert OMU4 ultramicrotome (Leica), stained in uranyl acetate and lead citrate and viewed in a Phillips CM120 transmission electron microscope. Images were taken using a Gatan Orius CCD camera.

2.7 LUCIFERASE ASSAY

For the luciferase assay detecting *Renilla* or Firefly luciferase, cells were either harvested by pipetting, centrifuged (500 x g, 5 min) and the cell pellet lysed in 100 µl 1x Passive Lysis Buffer (Promega) or lysed directly in wells by removal of culture supernatant and addition of 100 µl 1x Passive Lysis Buffer. For lysis, mosquito cells were incubated at RT for 15 min on a rocker as instructed by the manufacturer (Promega). Tick cells were incubated for efficient lysis for 60 min on a rocker. Lysates were stored at -20°C. After collection of samples at all time points within an experiment, the frozen samples were thawed at RT on a rocker for 30 min. Firefly luciferase and *Rluc* activity were then measured using a Dual Luciferase assay kit (Promega). Briefly, 5-10 µl mosquito cell lysate or 20 µl tick cell lysate per sample were added to a 96-well microplate. First, lyophilised Luciferase Assay Substrate was dissolved in Luciferase Assay Buffer II, and 50x Stop & Glo® Substrate was diluted 1:50 using Stop & Glo® Buffer. 50 µl Luciferase Assay solution were added to the lysate to measure firefly luciferase with a GloMax®-Multi Microplate Multimode Reader. Then 50 µl 1x Stop & Glo® solution were added and *Rluc* activity measured with the same reader. The readings were transferred to an Excel

spreadsheet using the provided Instinct™ software (Promega) and further analysed using GraphPad Prism.

2.8 FLOW CYTOMETRY

2.8.1 Flow cytometry experiments carried out at Roslin (Chapters 3, 4)

For flow cytometry tick cells were harvested from the tube or well by pipetting and transferred into a 1.5 ml microcentrifuge tube. Cells were centrifuged for 5 min at 300 x g and supernatant was discarded. Cells were then resuspended in 200 µl of 4% PFA and incubated for fixation for 30 min. Afterwards cells were pelleted by centrifugation (5 min, 300 x g) and resuspended in 150 µl PBS, transferred into a 5 ml round-bottom tube and depending on the number of cells more PBS was added (at least up to a final volume of 500 µl). Cells were then analysed for green fluorescence by flow cytometry on a Becton Dickinson (BD) FACScalibur. For acquisition and analysis of data the BD software CellQuest™ Pro was used. During acquisition, the main population of cells was gated for (Gate 1) by size, using forward scatter (FSC), and granularity, using side scatter (SSC) (see Figure 3.12). Uninfected control samples were used to set up the laser for green fluorescence (FL1) to adjust background levels. FL1 was plotted against a far red laser (FL4) and a gate determined to exclude most uninfected cells (Gate 2). During acquisition 20000 gated events (Gate 1) were acquired per sample. During analysis, gates were optimised for exclusion of uninfected cells and maximised detection of infected cells, and then the same gate was used for the data collected from each sample to determine the proportion of ZsGreen-positive cells in all samples. Data was transferred into an Excel spreadsheet and further analysed using GraphPad Prism.

2.8.2 Flow cytometry experiments carried out at Pirbright (Chapter 5)

Cells were harvested and fixed as described above; however 10 min prior to fixation LIVE/DEAD® stain (Invitrogen; Near-IR Dead Cell Stain, 633/635; Cat# L10119) was added to assess whether analysed cells were viable at the time of fixation. Dead or damaged cells would allow the dye to enter the cell and result in a far red fluorescent signal. For set-up of the lasers of the flow cytometer and as control

conditions, parallel cultures were not treated with LIVE/DEAD® stain and otherwise harvested and fixed identically.

Cells were analysed for green fluorescence (488nm laser, see appendix Figure 8.1) and far red fluorescence (633nm laser; see appendix Figure 8.1) by flow cytometry on a Becton Dickinson LSRFortessa using the BD software FACSDiva™. Initially samples with only ZsGreen (SFV4(3F)-ZsGreen infected cells) and only LIVE/DEAD® stain were used to allow the software to calculate compensation settings between the two signals. The compensation was 4.98 for LiveDead780 against GFP and 0.01 for GFP against LiveDead780. During acquisition, the main cell population was gated for using FSC and SSC (see Fig 2.1). Doublets were excluded by gating for the linear cell population on FSC/FSC and SSC/SSC plots. Cells were then gated for the cells which were viable before fixation using the signal of the LIVE/DEAD® staining (viable cells should have intact PM and not allow the dye to enter the cell). The resulting cell population was analysed for ZsGreen-positivity and green signal intensity was plotted against FSC. Analysis of acquired data was performed using FCS express version 3 (De Novo software) and gates were determined as described for the acquisition. The same gates were then used for each sample to determine the proportion of ZsGreen-positive cells. Data was transferred into an Excel spreadsheet and further analysed using GraphPad Prism.

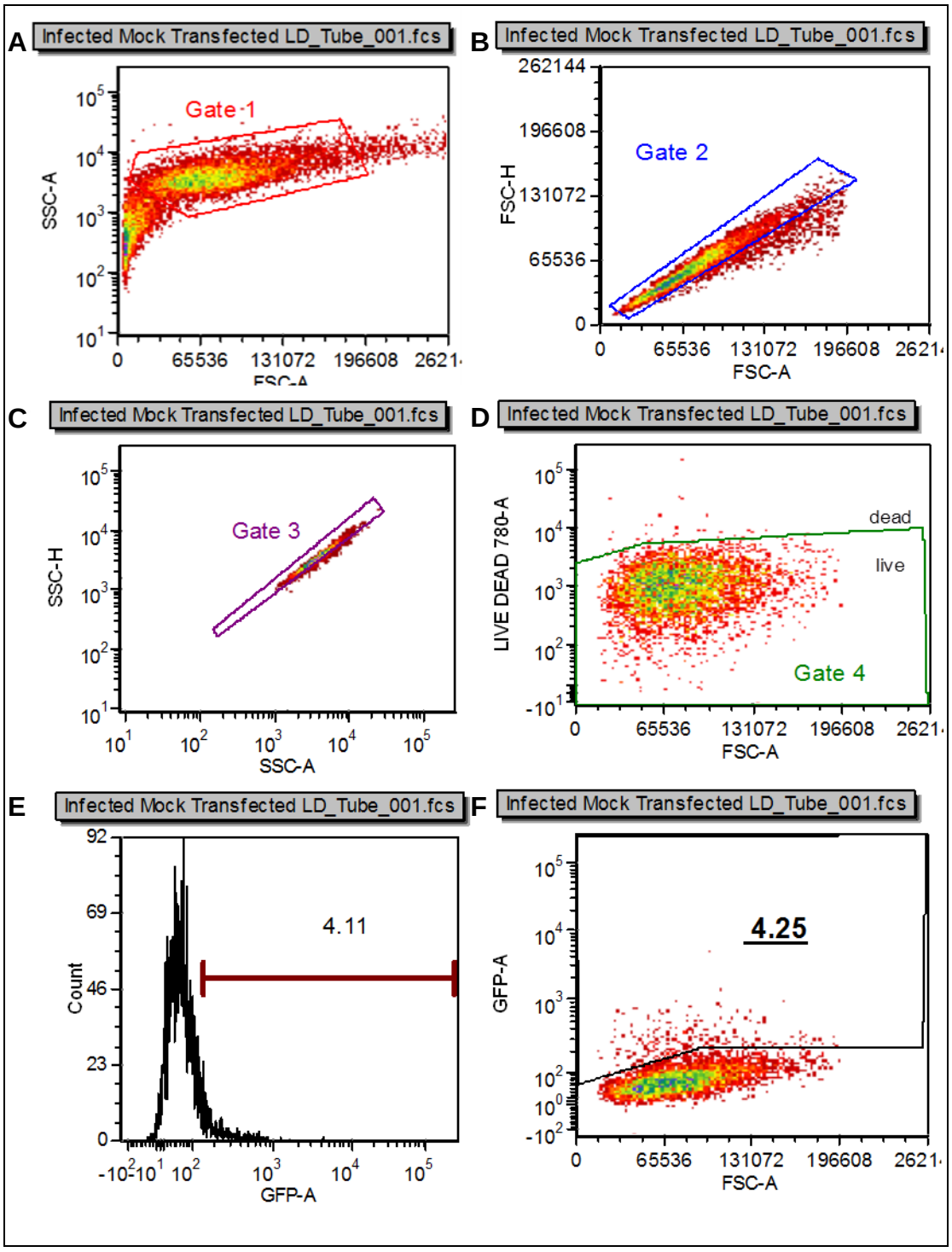

Figure 2.1: Gating of samples obtained by flow cytometric analysis using the BD LSRFortessa. The main cell population was gated for (A), cell doublets were excluded from analysis (B,C) and analysed for LIVE/DEAD staining (D). The population of cells negative for LIVE/DEAD stain was gated for and analysed for green fluorescence by histogram (E) and dot plot (F). Gating the number of positive cells in the dot plot was considered more accurate and the proportion of green cells (here 4.25%) was acquired from all samples and used for the generation of graphs and for statistical analysis (see Figure 5.14).

2.9 RNA EXTRACTION

Total RNA was extracted using the QIAGEN RNeasy® Mini kit according to the manufacturer's instructions. The optional DNase digestion step was always performed during the extraction. Briefly, cells were lysed in the provided buffer RLT containing 1 % (v/v) β-mercaptoethanol for 30 min on a rocker at RT and then frozen at -20ºC (freeze/thaw will increase efficiency of lysis). For extraction, cells were thawed on a rocker for 30-60 min and an equal volume of 70% (v/v) ethanol was added and the lysate was transferred onto an RNeasy spin column. After centrifugation (1 min, 11,000 x g, RT), supernatant was discarded and 350 µl wash buffer RW (provided) were added and the columns centrifuged (30 s, 11,000 x g, RT). RNase-free DNase was prepared as instructed by the manufacturer (QIAGEN, RNase-free DNase set) and 80 µl of the solution were added to the column and incubated for 15 min at RT for digestion of remaining genomic DNA. Subsequently, another wash step with 350 µl buffer RW was performed as above and supernatant discarded. Two wash steps with buffer RPE (with ethanol added as instructed) were performed using 700 µl (first wash) and 500 µl (second wash) and centrifugation (30 s, 11,000 x g, RT). Supernatants were discarded and to dry the membrane by removing remaining buffer, another centrifugation step was performed (2 min, 11,000 x g, RT). Finally, 30-50 µl RNase/DNase-free water were added directly onto the membrane of the column, incubated for 1 min and then centrifuged for elution (1 min, 11,000 x g, RT). RNA concentration was measured using a NanoDrop 2000 spectrophotometer.

2.10 cDNA SYNTHESIS BY REVERSE TRANSCRIPTION

Reverse transcription was performed in 0.2 ml thin-walled PCR tubes using an Applied Biosystems® Veriti® 96-Well Thermal Cycler (Life Technologies™). 500 or 1000 ng extracted RNA were used per reaction.

2.10.1 Reverse transcription using Super Script III (Roslin)

For RT-PCR the SuperScript™ III reverse transcriptase enzyme kit (Invitrogen™, UK) was used. Oligo $(dt)_{15}$ primer, dNTPs and RNaseIn® inhibitor were purchased

from Promega, UK. Nuclease-free water was purchased from Sigma-Aldrich®, UK. The reaction mixture had a final volume of 20 µl and was prepared as follows:

1 µl of Oligo $(dt)_{15}$ primer
500/1000 ng RNA
1 µl of 10 mM dNTPs
DNase/RNase-free water to a total volume of 12 µl

The mixture was heated for 5 min at 65°C and then chilled on ice for 1 min for primer annealing. The tubes were kept on ice and 4 µl of 5x First-Strand buffer, 1 µl of 0.1 M DTT and 1 µl of RNaseIn™ recombinant ribonuclease inhibitor were added. The reaction was then incubated at 50°C and after 2 min 1µl of SuperScript™ III reverse transcriptase (from Moloney murine leukaemia virus) was added. The reaction was incubated for 1 h at 50°C. A final incubation of 15 min at 70°C was performed and the cDNA was stored at -20°C.

2.10.2 Reverse transcription using high capacity cDNA synthesis kit (Pirbright)

Due to the large numbers of samples generated during experiments, the more affordable and efficient High Capacity cDNA Reverse Transcription Kit (Life Technologies) was used. Random hexamer primers, dNTPs and RNase inhibitor were provided with the kit. Where necessary, oligo $(dt)_{15}$ primer was purchased from Promega, UK. Nuclease-free water was purchased from Sigma-Aldrich®, UK. The reaction mixture had a final volume of 20 µl and was prepared as follows:

500/1000 ng RNA
DNase/RNase-free water to a total volume of 10 µl

To the template RNA, 10 µl of a 2x reaction master mix were added:

2 µl 10x RT buffer
2 µl 10x RT random primers
0.6 µl 25x dNTP mix (100 mM)
1 µl RNase inhibitor
1 µl MultiScribe™ Reverse Transcriptase
3.2 µl nuclease-free water

The reactions were then incubated in the thermal cycler for 10 min at 25°C, 2 h at 37°C and 5 min at 85°C to stop the reaction. cDNA was stored at -20°C.

2.11 POLYMERASE CHAIN REACTION (PCR)

PCR reactions were performed in 0.2 ml thin-walled PCR tubes using GoTaq® DNA polymerase (Promega). Whenever proof-reading activity was desired KOD DNA polymerase (Novagen®, Merck Millipore) was used (mainly for amplification of T7-PCR products for generation of dsRNA, see 2.14).

Reactions for PCRs using Taq polymerase were as follows:

5 µl 5x GoTaq® buffer
1 µl dNTP mix (10 mM)
1 µl $MgCl_2$ (25mM)
1 µl Forward primer (10 µM)
1 µl Reverse primer (10 µM)
0.5 µl GoTaq® polymerase
2-5 µl template DNA
nuclease-free water for a final volume of 25 µl

Reactions for PCRs using KOD polymerase were as follows:

5 µl 10X Buffer #1 for KOD DNA Polymerase (pH 8.0)
2.5 µl dNTP mix (10 mM)
2.5 µl $MgCL_2$ (25mM)
2.5 µl Forward primer (10 µM)
2.5 µl Reverse primer (10 µM)
1 µl KOD polymerase
2-5 µl template DNA
nuclease-free water for a final volume of 50 µl

PCR reactions were performed in an Veriti® 96-Well Thermal Cycler with the following reaction times and temperatures:

2 min 95°C
20 s 95°C
20 s 55-60°C } 25-35 cycles
30 s 72°C
7 min 72°C

Extension time at 72°C was increased for PCR products over 1 kb. PCR products were stored at 4ºC (-20ºC for long-term storage) or analysed directly by gel electrophoresis on agarose gels, composed of 1-2 % (w/v) agarose in 1x TAE (Severn Biotech Ltd®). Agarose gels were supplemented with 3 µl ethidium bromide per 100 ml of gel, and were run at 100V for approximately 30-50 min. Primer sequences were either designed using the online software Primer3 (Koressaar and Remm, 2007; Untergasser et al., 2012), or used as published or as provided by colleagues (Table 2.1). Other primers used during this study which did not result in PCR products can be found in the appendix (Table 8.4).

Table 2.1: List of primers used for PCR in the present study.

primer name	sequence (5' to 3')	T_a	gene (origin)
putative Rel_RS_forw	ACCGCTACAAGAGCGAGAGT	55°C	IxRel (Renata Strouhalová, unpublished)
putative Rel_RS_rev	GTAGCAGCAGTCCTCCTCGT	55°C	
putative Toll_T7_forw2485	TAATACGACTCACTATAGGGAACCGGCAGACTATCATTGC	58°C	IxToll (this study)
putative Toll_T7_rev2778	TAATACGACTCACTATAGGGGAGGAAGTCCTTGGACACCA	58°C	
Ixodes_Toll4_F	TAATACGACTCACTATAGGGGGACTACGCATTCAGGCAAT	58°C	IxToll-4 (this study)
Ixodes_Toll4_R	TAATACGACTCACTATAGGGTGGTCAGCAACAGGAGAGTG	58°C	
Ixodes_Toll7_F	TAATACGACTCACTATAGGGATGATTTCTGTGCCCAGGTC	58°C	IxToll-7 (this study)
Ixodes_Toll7_R	TAATACGACTCACTATAGGGCGAATAAGATCGGCGAATGT	58°C	
putative Cactus2_forw186	CGAGACCGACATCTCCAAGT	55°C	IxCactus (this study)
putative Cactus2_rev483	GAACAGGAGCTGCTTCCATC	55°C	
putative Dif1_forw110	AGCAGCCCTATGTGGTCATC	55°C	IxDif (this study)
putative Dif1_rev402	TGTGAAGCTGCAGGTCATGT	55°C	
statF	AGGTCAAGGTGTCCATCATC	58°C	STAT (Liu et al 2012)
statR	GATACTCCATTGTTCCTGTGTTG	58°C	
putative PIAS_forw978	CACCAGCCTACGAGGTTCTC	58°C	IxPIAS (this study)
putative PIAS_rev1269	GGTTTCCTTCTTTGCCACAA	58°C	
JAKF	GAGTACCTGGAAGAGAAG	58°C	JAK (Liu et al 2012)
JAKR	TGTGGATGTAGTAGTAGTG	58°C	
STAT-full-14_bases-F	GCGGCTTCAAGAGCTTCC	55°C	STAT (this study)
STAT-full-F	ATGGCGCTGTGGGGGCGGCTTCAAGAGCTTCC	55°C	
STAT-full-R	TCACTGCATGGCTTGGTC	55°C	
IxVago-1_F1	ATGAGAACTCCGACAAACGT	58°C	IxVago-1 (+IxVago- 3, IxVago-5) (this study)
IxVago-1_R1	TCATTTTCCTGGGTACCGGTAA	58°C	
Ixodes_CG4572_3_F	TAATACGACTCACTATAGGGCCAGGGTACCTTGATCTCCA	58°C	IxCG4572_3 (this study)
Ixodes_CG4572_3_R	TAATACGACTCACTATAGGGTGGCATAGAAGTCGTTGCTG	58°C	
egghead_T7_F	TAATACGACTCACTATAGGGTCTACCTGATGCGTCTGCTG	58°C	IxEgghead (this study)
egghead_T7_R	TAATACGACTCACTATAGGGGTTCGTTGGCGTATGTGATG	58°C	
Ago-30_F	GTAATACGACTCACTATAGGGACATACGAGCACTGACGG	58°C	Ago-30 (Schnettler, unpublished)
Ago-30_R	GTAATACGACTCACTATAGGGTGGTGCAACATTTTATCGA	58°C	
Ago-16_valid_F	GTAATACGACTCACTATAGGGCGTTATGAAGGGTGATCAGAAG	58°C	Ago-16 (Schnettler, unpublished)
Ago-16_valid_R	GTAATACGACTCACTATAGGGGACTGGTACTGATTCTCCCA	58°C	
Aag2_egghead_T7_F	TAATACGACTCACTATAGGGATCTGCATTCGGGTCGTAAC	58°C	AeEgghead (this study)
Aag2_egghead_T7_R	TAATACGACTCACTATAGGGCTCAGCGTGGACGTGAGTAA	58°C	
Aag2_cg4572_05.1_T7_F	TAATACGACTCACTATAGGGAAGCCGTTCCACGACAATAC	58°C	CG4572_05.1 (this study)
Aag2_cg4572_05.1_T7_R	TAATACGACTCACTATAGGGGTAGGTGTTGAACCCGGAGA	58°C	
Aag2_cg4572_56.1_T7_F	TAATACGACTCACTATAGGGATAACGACAACGCCAAGGTC	58°C	CG4572_56.1 (this study)
Aag2_cg4572_56.1_T7_R	TAATACGACTCACTATAGGGGCCACAATGATGTCCAACTG	58°C	
Aag2_cg4572_06.1_T7_F	TAATACGACTCACTATAGGGAACCGCCTTATCCAAGGTCT	58°C	CG4572_06.1 (this study)
Aag2_cg4572_06.1_T7_R	TAATACGACTCACTATAGGGGATCATGTCGAAAGCCCACT	58°C	

2.12 QUANTITATIVE REAL TIME PCR (QPCR)

For quantitative real time PCR (qPCR) cDNA made from RNA from tick or mosquito cells was used as a template. All qPCRs were performed on a ViiA™ 7 Real-Time PCR System (Life Technologies™) using the FastStart Universal SYBR Master (Rox) supplied by Roche Applied Science (product no. 04913850001).

A master mix was prepared containing the following volumes per reaction:

3.8 µl RNAse/DNase-free water
0.6 µl forward primer
0.6 µl reverse primer
10 µl FastStart Universal SYBR Master (Rox)

15 µl of master mix per reaction were pipetted into wells of MicroAmp® 96-well plates (Applied Biosystems®, Cat# 4349606) and 5 µl template cDNA were added per reaction. The plates were sealed with a clear adhesive lid (Applied Biosystems®, Cat# 4360954) and centrifuged briefly (~30 s) at 200 x g. The following cycling conditions were used:

10 min 95°C
20 s 95°C ┐
20 s 60°C ├ 40 cycles
20 s 72°C ┘

Primer sequences used for qPCR are shown in table 2.2. For quantification of SCRV a qPCR was established by Joana Ferrolho with the help of Houssam Attoui (The Pirbright Institute). The necessary information was kindly provided by Joana Ferrolho. LGTV NS5 primer sequences were kindly provided by Esther Schnettler. SFV nsp3 primers were kindly provided by Rennos Fragkoudis (Fragkoudis et al., 2008). STAT and Gene9 primer sequences were published by Liu et *al*. (2012).

For all experiments in tick cells, including infection experiments, *I. scapularis* β-actin was used as a housekeeping gene. Samples were normalised against total RNA, by using equal amounts of total RNA for cDNA synthesis and equal volumes of cDNA for qPCR. There was no significant change in β-actin levels observed in either SFV- or LGTV-infected cells during the performed experiments (with the exception of SFV infection with MOI 50, see 3.2.9). It was thus concluded that β-actin was suitable to serve as a housekeeping gene and RNA levels of other genes were

normalised against it using cycle threshold (ct) values. Relative gene expression was determined using the ΔCT method described by (Livak and Schmittgen, 2001):

Calculation: Relative target copy numbers normalised to β-actin = $2^{CT(target)-CT(\beta\text{-actin})}$

Table 2.2: List of primers used for qPCR in the present study. Primer sequences were designed using Primer3, used as published or as provided by colleagues.

primer name	sequence (5' to 3')	gene (origin)
RTPCR_SCRV_F	CAGCAGTACCTGGTCACGAA	Seg1 - VP1 gene Genbank133431.1 (J. Ferrolho)
RTPCR_SCRV_R	AACACATCCGATCCATCCAT	
SFVnsP3-for	GCAAGAGGCAAACGAACAGA	SFV nsp3 gene DQ189086.1 (Fragkoudis et *al*. 2008)
SFVnsP3-rev	GGGAAAAGATGAGCAAACCA	
LGTV_qPCR_F	ACCCAAGACTGCTACGTGTGGAAA	LGTV NS5 gene EU790644.1 (E. Schnettler)
LGTV_qPCR_R	TGAGGAAGTAAAGGGCCTTGCTGA	
actin_ixodes_qPCR_F	AAGGACCTGTACGCCAACAC	*I. scapularis* actin XM_002408066.1 (this study)
actin_ixodes_qPCR_R	ACATCTGCTGGAAGGTGGAC	
statF	AGGTCAAGGTGTCCATCATC	*I. scapularis* STAT HQ710832.1 (Liu et *al*. 2012)
statR	GATACTCCATTGTTCCTGTGTTG	
IxVago1-qPCR_3'_F	GTGCGGTCTCATCGGAAACC	*I. scapularis* IxVAgo1 XM_002415485.1 (this study)
IxVago1-qPCR_3'_R	ACCAGCTTTATTCCTGATACAGC	
gene-9F	AAAGCCCGAACCAGGACCCGC	Gene9 (Liu et *al* 2012)
gene-9R	TGGCAATAGTGTCGCCCCAC	

2.13 IDENTIFICATION OF GENE ORTHOLOGUES IN THE *I. SCAPULARIS* GENOME

2.13.1 Basic Local Alignment Search Tool

Using the Basic Local Alignment Search Tool (BLAST) (Altschul et al., 1990) on the National Center for Biotechnology Information (NCBI) website, tick orthologues of genes known for *D. melanogaster* and other insect species were identified. Sequences used are listed in Table 2.3.

Table 2.3: List of proteins and accession numbers used for BLAST searches of protein orthologues in the *I. scapularis* genome.

Type of animal	Species	Protein	NCBI accession number
Insect	***D. melanogaster***	prophenoloxidase	BAB17671.1
Insect	***D. melanogaster***	prophenoloxidase	AAF57775.1
Insect	***Ae. aegypti***	prophenoloxidase	XP_001663691.1
Crustacean	***Litopenaeus vannamei***	prophenoloxidase	ABL10871.1
Arachnid	***Limulus polyphemus***	hemocyanin	1NOL_A
Insect	***D. melanogaster***	Imd	NP_573394.1
Insect	***Ae. aegypti***	Imd	XP_001660624.1
Crustacean	***L. vannamei***	Imd	ACL37048.1
Insect	***D. melanogaster***	Relish	AAF54333.2
Arachnid	***Carcinoscorpius rotundicauda***	Relish	ABC75034.1
Arachnid	***C. rotundicauda***	NF-κB	AAZ40333.1
Insect	***D. melanogaster***	Caspar	NP_611080.1
Insect	***D. melanogaster***	Toll	AAQ64935.1
Insect	***D. melanogaster***	MyD88	AAF58953.1
Insect	***D. melanogaster***	Cactus	AAA85908.1
Insect	***D. melanogaster***	Dif	AAA28465.1
Insect	***D. melanogaster***	Dorsal	AAF53611.1
Insect	***Ae. aegypti***	Dorsal	AAW67215.1
Insect	***D. melanogaster***	STAT	AAC46984.1
Insect	***D. melanogaster***	JAK (Hopscotch)	AAF48035.1
Insect	***D. melanogaster***	PIAS	AAF58984.1
Insect	***D. melanogaster***	SOCS16D	AAF48765.4
Insect	***D. melanogaster***	SOCS44A	AAF59129.1
Insect	***D. melanogaster***	SOCS36E	AAF53652.2
Insect	***C. quinquefasciatus***	CxVago	XP_001842264
Insect	***D. melanogaster***	Drosha	AAF59169.1
Insect	***D. melanogaster***	Pasha	AAF57175.1
Insect	***D. melanogaster***	PIWI	AGA18880.1
Insect	***D. melanogaster***	NinaC	AAF52505.1
Insect	***D. melanogaster***	Egghead	AAF43419.1
Insect	***D. melanogaster***	CG4572	AAF55705.1

2.13.2 Alignment of sequences

Coding DNA sequence (cds) or mRNA sequences were saved as FASTA files and imported into the freeware Bioedit (Tom Hall, Ibis Biosciences, http://www.mbio.ncsu.edu/bioedit/bioedit.html). Sequences were analysed in Bioedit and sequence alignments made with the integrated accessory application ClustalW (Thompson et al., 1994).

2.13.3 Phylogeny of *I. scapularis* STAT

A phylogenetic tree for STAT, including tick STAT was made with the help of Darren Obbard (University of Edinburgh) to establish which other STAT proteins are most closely related to tick STAT (based on sequence alignments). A large selection of available STAT sequences was used (Table 2.4) and if necessary 5' and 3' untranslated regions of the mRNA sequences were deleted to obtain the cds.

Selected STAT sequences were aligned at the protein level using the software MUSCLE at the default parameters with 8 rounds of improvement (Edgar, 2004a, b) and sequences were then converted back to DNA coding sequences for tree-building. Regions with very low similarity were deleted as they provide little phylogenetic information and could be actively misleading (because they are difficult to align). The sequence alignment was then analysed using the software MRBAYES (Ronquist et al., 2012) which is based on Bayesian inference of phylogenetic trees. 1st/2nd/3rd-position partitions were used, each position-partition with independent rates, base composition, General Time Reversible (GTR) substitution and 4-category Gamma-distributed rate variation (MUSCLE and MRBAYES runs were performed by Darren Obbard). The phylogenetic tree was visualised using the free software TreeView (Page, 1996).

Table 2.4: List of genes used to create phylogenetic tree of STAT.

Species	common name or taxonomic group	gene	NCBI cds or mRNA accession number
Acyrthosiphon pisum	pea aphid	predicted *stat*	XM_003247914.1
Aedes aegypti	yellow fever mosquito	*stat*	EF175868.1
Amphimedon queenslandica	sponge	predicted *stat*	XM_003385230.1
Anopheles gambiae	malaria mosquito	*stat*	AJ010299.1
Apis mellifera	western honey bee	predicted *stat*	XM_397181.4
Biomphalaria glabrata	freshwater snail	*stat*1	FJ804763.1
Biomphalaria glabrata	freshwater snail	*stat*2	FJ804764.1
Bombyx mori	silkmoth	*stat*	NM_001163916.1
Culex quinquefasciatus	southern house mosquito	*stat*	XM_001866572.1
*Daphnia pulex**	water flea	predicted *stat*	DappuDraft_97641*
Drosophila melanogaster	common fruit fly	*stat*92E	NM_169899.3
Homo sapiens	human	*stat*1	NM_007315.3
Homo sapiens	human	*stat*2	NM_198332.1
Homo sapiens	human	*stat*3	NM_139276.2
Homo sapiens	human	*stat*4	NM_003151.3
Homo sapiens	human	*stat*5A	NM_001288718.1
Homo sapiens	human	*stat*5B	NM_012448.3
Homo sapiens	human	*stat*6	NM_001178078.1
Hyphantria cunea	fall webworm	*stat*	EF114290.1
Ixodes scapularis	deer tick	*stat*	HQ710832.1
Monosiga brevicollis	choanoflagellate	*stat*	XM_001749687.1
Nematostella vectensis	starlet sea anemone	*stat*	XM_001634986.1
Pediculus humanus corporis	body louse	predicted *stat*	XM_002427628.1
Penaeus monodon	tiger prawn	*stat*, long isoform	EU367985.1
Saccoglossus kowalevskii	acorn worm (hemichordate)	predicted *stat*	XM_002733478.1
Strongylocentrotus purpuratus	sea urchin	predicted *stat*	XM_001179176.1
Takifugu rubripes	pufferfish	predicted *stat*	XM_003962146.1
Tribolium castaneum	red flour beetle	predicted *stat*	XM_964384.2
Trichinella spiralis	pork worm (nematode)	*stat*	XM_003368981.1
Trichoplax adhaerens	*Placozoa*	hypothetical protein	XM_002110148.1

*sequence from wfleabase.org

2.14 KNOCKDOWN OF GENE EXPRESSION IN TICK CELLS

For knockdown of gene expression, tick cells were treated with long dsRNA (approximately 300-600 bp) complementary to a fragment of the target gene. The tick cell line IDE8 was used for knockdown experiments in this study. IDE8 cells can

take up dsRNA from the medium without a transfection reagent, which can result in effective knockdown of gene expression (Barry et al., 2013). Long dsRNA was made using the Megascript® RNAi kit (Ambion®) which is based on an *in vitro* transcription using T7 polymerase transcribing from both ends of a PCR product to produce complementary RNA strands. Briefly, target-specific primers were designed (Table 2.5) with 5' T7 promoter overhangs (T7 promoter sequence = TAATACGACTCACTATAGGG). Using these primers and tick cell cDNA as a template, 300-600 bp fragments of the genes of interest were amplified by PCR. For the control dsRNAs targeting eGFP and *Rluc,* the plasmids pIB-eGFP and pSP6-SFV4(3H)-*Rluc* were used, respectively, to generate T7-PCR products as templates for synthesis of dsRNA. The amplified fragments were purified from an agarose gel using NucleoSpin® Gel and PCR Clean-up kit (Macherey-Nagel), and most of them cloned into pJET (CloneJet™ PCR Cloning kit, Thermo Scientific) and sequenced; alternatively fragments were used directly to make dsRNA.

The kit consists of 3 steps:

1) T7 RNA transcription performed overnight (or for at least 4 h) at 37ºC
2) RNase/DNase digest for 1 h at 37ºC to remove template DNA and any ssRNA
3) purification of dsRNA using provided columns

The concentration of purified dsRNA was measured by NanoDrop 2000 spectrophotometer and dsRNA was analysed by agarose gel electrophoresis to determine purity and product size.

The presence of dsRNA itself may activate signalling pathways in the cells or result in upregulation of components of the RNAi system and could influence virus replication. Thus as a negative control dsRNA targeting eGFP was generated and used as a non-specific dsRNA control. In experiments where the dsRNA specific to the gene of interest was <400 bp in size, dsRNA against eGFP of 298 bp was used (primer set: eGFP_T7_forw374/ eGFP_T7_rev672); for experiments where the fragment to knock down the gene of interest was ≥ 400 bp a larger dsRNA fragment of 615bp targeting eGFP was used (primer set: dsT7eGFPFD/dsT7eGFPRE). As a positive control for efficient dsRNA uptake and processing, dsRNA against *Rluc* was used in some experiments. This dsRNA targeting *Rluc* will target *Rluc* reporter virus and/or *Rluc* plasmids. This dsRNA was also used as a negative control in

experiments using GFP or ZsGreen reporter virus. Primers used to generate these control dsRNAs are also shown in Table 2.5.

Table 2.5: List of T7-primers used for generation of dsRNA for knockdown of gene expression in tick cells.

primer name	gene name	Sequence
eGFP_T7_forw374	eGFP	TAATACGACTCACTATAGGGAGCTGAAGGGCATCGACTT
eGFP_T7_rev672	eGFP	TAATACGACTCACTATAGGGGAACTCCAGCAGGACCATGT
dsT7eGFPFD	eGFP#	TAATACGACTCACTATAGGGATGGTGAGCAAGGGCGAGGAGCTGTTC
dsT7eGFPRE	eGFP#	TAATACGACTCACTATAGGGCTGGGTGCTCAGGTAGTGGTTGTCGGGC
T7dsRenFD	*Rluc#*	TAATACGACTCACTATAGGGATGACTTCGAAAGTTTATGATCCAG
T7dsRenRE	*Rluc#*	TAATACGACTCACTATAGGGCTGCAAATTCTTCTGGTTCTAACTTTC
putative Toll_T7_forw2485	IxToll-1	TAATACGACTCACTATAGGGAACCGGCAGACTATCATTGC
putative Toll_T7_rev2778	IxToll-1	TAATACGACTCACTATAGGGGAGGAAGTCCTTGGACACCA
Ixodes_Toll4_F	IxToll-4	TAATACGACTCACTATAGGGGGACTACGCATTCAGGCAAT
Ixodes_Toll4_R	IxToll-4	TAATACGACTCACTATAGGGTGGTCAGCAACAGGAGAGTG
Ixodes_Toll7_F	IxToll-7	TAATACGACTCACTATAGGGATGATTTCTGTGCCCAGGTC
Ixodes_Toll7_R	IxToll-7	TAATACGACTCACTATAGGGCGAATAAGATCGGCGAATGT
putative Cactus_T7_forw186	IxCactus	TAATACGACTCACTATAGGGCGAGACCGACATCTCCAAGT
putative Cactus_T7_rev483	IxCactus	TAATACGACTCACTATAGGGGAACAGGAGCTGCTTCCATC
putative Dif_T7_forw110	IxDif	TAATACGACTCACTATAGGGAGCAGCCCTATGTGGTCATC
putative Dif_T7_rev402	IxDif	TAATACGACTCACTATAGGGTGTGAAGCTGCAGGTCATGT
putative STAT_T7_forw1024	STAT	TAATACGACTCACTATAGGGATGAAGACCAACACGCGATT
putative STAT_T7_rev1318	STAT	TAATACGACTCACTATAGGGCCATCACAGACTCCGTTCCT
putative PIAS_T7_forw978	IxPIAS	TAATACGACTCACTATAGGGCACCAGCCTACGAGGTTCTC
putative PIAS_T7_rev1269	IxPIAS	TAATACGACTCACTATAGGGGGTTTCCTTCTTTGCCACAA
IxVago-1_T7_F1	IxVago-1	TAATACGACTCACTATAGGGATGAGAACTCCGACAAACGT
IxVago-1_T7_R1	IxVago-1	TAATACGACTCACTATAGGGTCATTTTCCTGGGTACCGGTAA
Ago-16_F	Ago-16*	GTAATACGACTCACTATAGGGAAGATCACGAGGGTATCGGTAGT
Ago-16_R	Ago-16*	GTAATACGACTCACTATAGGGACTTTTCTGCACCACGTCTTG
Ago-30_F	Ago-30*	GTAATACGACTCACTATAGGGACATACGAGCACTGACGG
Ago-30_R	Ago-30*	GTAATACGACTCACTATAGGGTGGTGCAACATTTTATCGA
Ixodes_CG4572_3_F	IxCG4572_3	TAATACGACTCACTATAGGGCCAGGGTACCTTGATCTCCA
Ixodes_CG4572_3_R	IxCG4572_3	TAATACGACTCACTATAGGGTGGCATAGAAGTCGTTGCTG

#*sequence provided by Rennos Fragkoudis (#) or Esther Schnettler (*)

For knockdown experiments, 5 x 10^5 IDE8 cells were seeded per well of a 24-well plate and 24 h later 400 ng dsRNA were added to the cultures. Cells were infected with SFV or LGTV 72 h after addition of dsRNA unless otherwise indicated.

2.15 KNOCKDOWN OF GENE EXPRESSION IN MOSQUITO CELLS

As for tick cells, mosquito cells were treated with gene-specific long dsRNA (300-600 bp) to knock down target gene expression. Long dsRNA was generated as described above (see 2.14) using the primers in Table 2.6. However, mosquito cells do not take up dsRNA from the medium efficiently without a transfection reagent. Thus dsRNA was transfected into cells using Lipofectamine® 2000 transfection reagent (Life Technologies™). 24 h before transfection, Aag2 or U4.4 cells were seeded at a density of 1.7 x 10^5 cells per well of a 24-well plate in 1 ml of complete L-15 medium. Before transfection, cell supernatant was removed and 500 µl of fresh medium were added to each well.

Table 2.6: List of T7-primers used for generation of dsRNA for knockdown of gene expression in mosquito cells.

primer name	gene	Sequence
Aag2_egghead_T7_F	AeEgghead	TAATACGACTCACTATAGGGATCTGCATTCGGGTCGTAAC
Aag2_egghead_T7_R	AeEgghead	TAATACGACTCACTATAGGGCTCAGCGTGGACGTGAGTAA
Aag2_cg4572_05.1_T7_F	CG4572_05.1	TAATACGACTCACTATAGGGAAGCCGTTCCACGACAATAC
Aag2_cg4572_05.1_T7_R	CG4572_05.1	TAATACGACTCACTATAGGGGTAGGTGTTGAACCCGGAGA
Aag2_cg4572_56.1_T7_F	CG4572_56.1	TAATACGACTCACTATAGGGATAACGACAACGCCAAGGTC
Aag2_cg4572_56.1_T7_R	CG4572_56.1	TAATACGACTCACTATAGGGGCCACAATGATGTCCAACTG
Aag2_cg4572_06.1_T7_F	CG4572_06.1	TAATACGACTCACTATAGGGAACCGCCTTATCCAAGGTCT
Aag2_cg4572_06.1_T7_R	CG4572_06.1	TAATACGACTCACTATAGGGGATCATGTCGAAAGCCCACT

In one microfuge tube, 50 µl Opti-MEM® (Life Technologies™) were added to 50 ng dsRNA and in another 1µl Kipofectamine® 2000 was added to 50 µl Opti-MEM®. For multiple wells, the amounts were multiplied as necessary and 5 ml round bottom reaction tubes (Falcon, Cat# 352052) were used for larger volumes. After 5 min incubation at RT, the dsRNA mix was added to the lipofectamine solution and incubated at RT for 20 min. It was then added to the cells and the cells were incubated at 28°C. After 5 h the medium was removed and 1 ml of fresh medium were added per well. Cells were infected 24 or 48 h post transfection.

2.16 KNOCKDOWN VALIDATIONS

Knockdown validation was performed either by Western blot (see 2.18), qPCR (see 2.12) or semi-quantitative RT-PCR. For semi-quantitative RT-PCR, a PCR reaction (see 2.11) was performed with a reduced cycle number (25-32 cycles) to result in low levels of PCR product, which were then run on a 1% agarose gel and visualised using either a self-built gel documentation system using a Nikon camera (built by Houssam Attoui) or with a Bio-Rad ChemiDoc™ XRS+ System. The signal intensity of the bands was quantified using ImageJ (for images acquired with self-built system) or the Bio-Rad Image Lab™ Software (for images acquired with Bio-Rad ChemiDoc™ XRS+ System). Knockdown samples were then normalised to the GFP or *Rluc* dsRNA control samples.

2.17 INHIBITORS OF STAT PHOSPHORYLATION

Two inhibitors of human STAT5 phosphorylation were used in tick cells in an attempt to inhibit *I. scapularis* STAT phosphorylation. The two inhibitors were the STAT5 inhibitor N′-((4-Oxo-4H-chromen-3-yl)methylene)nicotinohydrazide (Calbiochem®) and piceatannol (Sigma-Aldrich®), both of which were dissolved from powder in DMSO to a stock concentration of 80 nmol/µl and 10 nmol/µl, respectively. Cells were treated with DMSO as a control, 800 µM Calbiochem STAT5 inhibitor or 100 µM piceatannol.

2.18 WESTERN BLOT

2.18.1 Sample preparation

Culture supernatant was removed and cells grown in 24-well plates were lysed in 100 µl Nonidet-P40 lysis buffer per well while rocking for 20 min on ice. Subsequently, 100 µl of 2x Laemmli sample buffer (Bio-Rad) supplemented with 1% (v/v) β-mercaptoethanol (Sigma-Aldrich®) were added and the samples were incubated for 10 min at 95ºC for denaturation of proteins. Samples were then stored at -20ºC.

Nonidet-P40 lysis buffer
20 mM Tris-HCl (pH 8)
137 mM NaCl
10% glycerol
1 % Nonidet-P40
2 mM EDTA
1x Phosphatase inhibitor cocktail set II (Calbiochem)
1x HALT Protease Inhibitor cocktail (Thermo Scientific)

2.18.2 Sodium dodecyl sulphate – polyacrylamide gel electrophoresis (SDS-PAGE)

Polyacrylamide gel preparation

Polyacrylamide gels were either purchased from Bio-Rad (MiniProtean® TGX™ gels) or prepared manually using the Bio-Rad Mini-PROTEAN® system and the buffers listed below. Just before use, 10 µl of tetramethylethylenediamine (TEMED, Sigma-Aldrich®) and 70 µl of ammonium persulphate (APS, Sigma-Aldrich®) were added to 5 ml of the resolving gel solution and it was poured between two glass plates. A space of approximately 2 cm was left at the top of the gel and this was filled with isopropanol (Sigma-Aldrich®) to level the gel. Once the resolving gel had set, the isopropanol was discarded and the top of the gel was gently washed with distilled water. The stacking gel (4% acrylamide) was prepared, by addition of 5 µl of TEMED and 50 µl APS to 2 ml of the stacking gel solution. After pouring the stacking gel on top of the resolving gel, a 0.75 mm comb was immediately inserted into the stacking gel to create wells for loading samples. The gel was left to set and then used for gel electrophoresis.

0.5 M Tris-Base pH6.8
30 g Tris-Base
500 ml dH_2O
pH to 6.8

1.5 M Tris-Base pH8.8
98.6 g Tris-Base
500 ml dH_2O
pH to 8.8

Resolving Gel (12% Acrylamide)
30 ml 40% acrylamide
43 ml dH_2O
25 ml 1.5 M Tris-Base pH8.8
1 ml 10% (w/v) SDS

Stacking Gel (4% Acrylamide)
10ml 40% acrylamide
64ml dH_2O
25ml 0.5M Tris-Base pH6.8
1ml 10% (w/v) SDS

Gel solutions were stored at 4^{o}C in the dark and kept for a maximum of 1 month.

Used per resolving gel:
5 ml 12% acrylamide
10 µl TEMED
70 µl 10% APS

Used per stacking gel:
2 ml 4% acrylamide
4 µl TEMED
30 µl 10% APS

Gel electrophoresis

Gels were assembled into an electrophoresis tank (Bio-Rad) and 1x running buffer (see below) was added until the gel was covered. The combs were removed and 10 µl of HyperPAGE prestained protein marker (Bioline) was added to one well and up to 25 µl of cell lysate were added to each of the other wells. If less than 10 samples were run per gel, empty wells were filled with 10 µl 2x Laemmli sample buffer (Bio-Rad). The gel was then run at 100-140 V until the dye of the loading buffer reached the bottom of the gel.

10 x Running Buffer
30.5 g Tris Base
94 g glycine
50 ml of 20% SDS (w/v)
H_2O to a total of 1000 ml
→ dilute 1:10 for 1x running buffer

2.18.3 Transfer of proteins to nitrocellulose membranes

Proteins were transferred from the gel onto a nitrocellulose membrane by wet blotting using the Bio-Rad Mini-PROTEAN® system. Hybond ECL nitrocellulose membrane (GE Healthcare), extra thick Western blot filter paper (Thermo Scientific) and foam pads were soaked in transfer buffer (see below). A foam pad was placed inside the transfer cassette, followed by a piece of filter paper, the protein gel, the nitrocellulose membrane and another piece of filter paper. On some occasions thinner filter paper was used and the number of filter papers adjusted accordingly to achieve similar thickness. A plastic pipette was rolled over the cassette to remove any bubbles after each step of assembly. Another wet foam pad was added on top and the cassette was closed. The cassette was placed into an electrophoresis tank with the nitrocellulose membrane facing towards the positive pole to allow transfer of the negatively charged proteins from the gel to the membrane. The tank was filled with transfer buffer, an ice pack was inserted in the tank and the transfer was run at 100 V for 60 minutes. Finally, the nitrocellulose membrane was removed from the cassette and placed in Tris-buffered saline with Tween-20 (TBS-T) until probed.

Transfer Buffer
100 ml 10 x running buffer (see above)
700 ml dH_2O
200 ml Methanol

TBS-T (pH 7.4)
8.8 g NaCl
0.2 g KCl
3 g Tris
500 µl Tween-20

2.18.4 Immunolabelling

The membrane was blocked for 30 min in 5% (w/v) milk powder (Marvel) in TBS-T, to reduce nonspecific antibody binding. It was then probed with the primary antibody (see table 2.7) diluted in 5% (w/v) milk powder and incubated overnight at 4°C and for an additional 1 h at RT while rocking gently. The membrane was washed in TBS-T (3 x 10 min) and then secondary antibody (Table 2.7) diluted in MilliQ water was added for 30-60 min while rocking gently. The membrane was washed another three times for 10 min with TBS-T and once in MilliQ water. Fluorescence intensity of the secondary antibody was detected using the Licor® Odyssey CLx scanning system. The membrane was discarded or washed in TBS-T (3 x 15 min) then re-used for re-probing for a loading control (β-actin) or for other target proteins.

At Pirbright, Western blots were performed using horseradish peroxidase (HRP)-conjugated secondary antibodies (or HRP-conjugated primary antibody) and enhanced chemi-luminescence (ECL) reaction (Pierce™, Thermo Scientific). Chemi-luminescence of blots was visualised using a Bio-Rad ChemiDoc™ XRS+ System. However, none of the blots were presented in the results section of this thesis. For the attempted detection of tick and mosquito Vago, different blocking solutions (BSA, milk powder of different brands, Cas-Block) were used and different concentrations of primary (1:500-1:5000) and secondary antibody (1:500-1:1000) were tested, but no blot with clear Vago signal and clear background was achieved.

Table 2.7: List of antibodies used for Western blot analysis.

Antibody	Source		Targeting	raised in	dilution
Phospho-Stat5 (Tyr694) (C71E5) Rabbit mAb	Cell Signalling	#9314	STAT5-P	rabbit	1:750
β-Actin (13E5) Rabbit mAb	Cell Signalling	#4970	β-actin	rabbit	1:750
Anti-Vago antibody (GenScript)	Peter Walker	-	CxVago	rabbit	1:200 - 1:5000
V5 Mouse Monoclonal Antibody, HRP Conjugate	Life Technologies	R961-25	V5-tag	mouse	1:200 - 1:1000
Anti-SUMO1	Ron Hay	-	SUMO1	sheep	1:750
Anti-SUMO2/3	Ron Hay	-	SUMO1	sheep	1:750
Goat anti-Rabbit IgG H&L (HRP-conjugated)	Abcam	ab6721	rabbit IgG	goat	1:1000
IRDye 800CW Donkey anti-Goat IgG (H + L)*	Licor®	926-32214	goat IgG	donkey	1:10000
IRDye 800CW Donkey anti-Rabbit IgG (H + L)	Licor®	926-32213	rabbit IgG	goat	1:10000

*crossreacts with primary antibody derived from sheep

Antibodies against mosquito Vago and human SUMO were kindly provided by Peter Walker (CSIRO, AAHL, Geelong) and Susan Jacobs (The Pirbright Institute), respectively. The SUMO antibodies were originally a kind gift from Ron Hay (University of Dundee).

2.19 CLONING OF IXVAGO

IxVago-1 was cloned into pIB/V5-His (Life Technologies™), an insect vector driving expression using the promoter OpIE2 derived from the baculovirus *Orgyia pseudotsugata* multicapsid nuclear polyhedrosis virus. Primers amplifying the entire cds were used and restriction sites for NotI added to the forward primer and the restriction site for XbaI to the reverse primer (see Table 2.8, restriction sites in red). The reverse primer was designed in a way that the stop codon of the cds would be deleted and the V5-His-tag encoded by the pIB/V5-His plasmid would be fused to IxVago-1. The full length sequence was then amplified by PCR from IDE8 cDNA and plasmid and PCR product were digested using NotI and XbaI restriction enzymes. Both plasmid and PCR product were purified from an agarose gel after restriction digest using the NucleoSpin® Gel and PCR Clean-up kit (Macherey-Nagel). Vector and insect were then mixed at equal amounts and ligated with T4-ligase overnight on ice (the ice melted overnight). The whole ligation reaction was then transformed into competent Dh5α bacteria (Life Technologies™) as described above (see 2.2.1) and plated on LB-agar plates. Six colonies were picked and grown in 5 ml LB-broth overnight and purified using the ISOLATE II Plasmid Mini kit (Bioline) according to the manufacturer's instructions. Sequencing of the six clones indicated correct cloning and the expected sequence for all of them, but expression after transfection could not be shown in IDE8, U4.4 or Aag2 cells and no further experiments were performed using the generated plasmid.

Table 2.8: Primers used for cloning of IxVago1 into pIB-V5/His plasmid.

Primer name	primer sequence	T_a
IxVago-1_cloning_F	TATA**GCGGCCGC**cATGAGAACTCCGACAAACGT	58°C
IxVago-1_cloning-fusion_R	CGCG**TCTAGA**ggTTTTCCTGGGTACCGGTAATC	58°C
pIB_seq_OpIE2_F*	CGCAACGATCTGGTAAACAC	(seq*)
pIB_seq_OpIE2_R*	GACAATACAAACTAAGATTTAGTCAG	(seq*)

*used for sequencing reaction.

2.20 IMMUNOFLUORESCENCE STAINING

For immunostaining experiments, tick cells were seeded on coverslips and fixed with 4 % PFA for at least 30 min. The coverslips were then washed with PBS (3 x 5 min) and either kept at 4ºC for up to 4 weeks or used straight away for immunofluorescence staining. All steps were performed at RT. For permeabilisation, cells were incubated for 30 min in 0.3 % (v/v) TritonX100/PBS and then washed (3 x 5 min). Since tick cells are difficult to permeabilise, further incubation with 0.1 % (w/v) SDS/PBS for 10 min and another wash with PBS (3 x 5 min) were performed. To reduce nonspecific antibody binding, a blocking step was performed: cells were incubated for 60 min in CAS-BLOCK™ (Life Technologies™). Then cells were incubated with primary antibody for 90 min (see Table 2.9) and washed with PBS (3 x 5 min). The secondary antibody was added (see Table 2.9) and incubated again for 60 min, followed by a wash with PBS (3 x 5 min). To stain nuclei, 4',6-diamidino-2-phenylindole, dihydrochloride (DAPI) was added for 15 min at a concentration of 5 µg/ml. Finally cells were washed again with PBS (2 x 5 min) and the coverslips were mounted onto a slide using VECTASHIELD® mounting medium for fluorescence (Vector Laboratories, Cat# H-1000).

Table 2.9: Antibodies used for immunofluorescence staining.

Antibody	Source	Targeting	raised in	dilution
Primary LGTV NS5 antibody	Sonja Best	LGTV NS5	chicken	1:800
Primary LGTV NS3 antibody	Sonja Best	LGTV NS3	chicken	1:500
Alexa Fluor® 488 Goat Anti-Chicken IgG	Life Technologies	Chicken	goat	1:1000

2.21 HEAT-INACTIVATION OF *E. COLI*

For experiments reported in Chapter 4 (see Figure 4.3), E. *coli* (Dh5α, Invitrogen) were grown overnight in 5 ml of LB broth. Bacteria were then centrifuged for 5 min at 3000 x g and resuspended in 3 ml appropriate complete L-15 medium. Bacteria were transferred into 3 microcentrifuge tubes and incubated at 85°C for 15 min for heat-inactivation. The suspension was then cooled briefly on ice. 100 µl heat-

inactivated bacteria were added per well (24-well plate) of U4.4 or IDE8 cells prior to infection with SFV4(3H)-*Rluc*.

2.22 MODELLING OF PROTEIN STRUCTURE

3D modelling for the prediction of the *Ixodes* Vago structure was performed using the online platform Phyre (Kelley and Sternberg, 2009). Three dimensional (3D) protein structures were predicted using Phyre2 (www.rcsb.org), which predicts secondary structure of amino acid sequences and generates 3D models by comparing the query protein to homologous crystallised proteins in the online Protein Data Base (Bennett-Lovsey et al., 2008). Phyre-generated structure predictions were visualised using the open-source molecular visualisation software PyMOL (Schrödiner LLC).

2.23 SIGNAL PEPTIDE PREDICTION

The putative cytokine-like mode of action of Vago is based on secretion from the cell. Secretion of proteins requires the presence of a signal peptide sequence targeting proteins for secretion during translation at the ER (Briggs and Gierasch, 1986). Presence of signal peptide sequences and location of cleavage sites in the different IxVago sequences were predicted using the free web based SignalP 4.0 server (Petersen et al., 2011). Upon entry and submission of an amino acid sequence, SignalP 4.0 predicts the presence and location of signal peptide cleavage sites in these sequences.

2.24 STATISTICAL ANALYSIS

All statistical analysis was performed using GraphPad Prism 6. Depending on the individual experiments different statistical analyses were performed.

2.24.1 Knockdown experiments

To compare different dsRNA treatments at one specific time point, One-way ANOVA with multiple comparisons, without correction for multiple comparisons (Fisher's LSD test) was performed. In knockdown experiments, each condition was compared to the GFP dsRNA control or as indicated.

2.24.2 Timecourse experiments

For differences between two conditions over time, Two-way ANOVA with multiple comparisons was performed with correction for multiple comparisons (Sidak).

3. Characterisation of SFV and LGTV infection of three ixodid tick cell lines

3.1 INTRODUCTION

There are over 50 different tick cell lines available in the Tick Cell Biobank, including 9 cell lines derived from *Ixodes spp.* ticks (Lesley Bell-Sakyi, personal communication). Many of these cell lines have not been studied extensively with regard to virus replication and production. Understanding the kinetics of virus replication was considered to be an essential prerequisite for planning experiments to examine antiviral mechanisms. Especially for tick cell lines, which are heterogeneous cultures (Bell-Sakyi et al., 2007), it is important to know how many cells can actually be infected as different cell types may differ in virus susceptibility. The kinetics of virus replication and production need to be established to inform future studies on the responses of infected cells.

In the first part of this study arbovirus infection of three tick cell lines was characterised in detail to get a better understanding of virus replication and virus production dynamics in these cell lines. The list of cell lines was narrowed down to the genus *Ixodes*, with *I. ricinus* being the tick vector of TBEV in Europe and *I. scapularis* being the vector of a number of pathogens in the United States. Another reason for choosing these related tick species was that *I. scapularis* is to date the only tick species with a sequenced genome. Initially, a cell line from each of these species was chosen for characterisation: ISE18 derived from *I. scapularis* and IRE11 derived from *I. ricinus*. In a parallel study undertaken by a fellow PhD student, Ms Sabine Weisheit, two other cell lines from these two tick species were characterised, ISE6 (*I. scapularis*) and IRE/CTVM19 (*I. ricinus*). The aim was to identify one cell line which was suitable and well-characterised for use in future experiments. The *I. scapularis* cell line IDE8 was also characterised in collaboration with Sabine Weisheit (The Pirbright Institute) and Esther Schnettler since IDE8 was identified as a cell line that is very convenient to work with due to its relatively rapid growth and ability to grow in multiwell plates (Esther Schnettler, personal communication).

The two arboviruses SFV and LGTV were chosen for the present study. SFV is a very useful model virus and can infect many tick cell lines but is not known to be naturally transmitted by ticks (see 1.2.1). LGTV is a tick-borne arbovirus of low

pathogenicity, making it a useful model virus for more pathogenic tick-borne viruses such as TBEV (see 1.2.2). The two viruses represent two important arbovirus groups, alphaviruses and flaviviruses. Since alphaviruses are not known to be transmitted by ticks whereas several flaviviruses including LGTV are, comparison of the responses of tick cells to these viruses could contribute to an understanding of this difference.

3.1.1 Objectives

- Identify a suitable cell line to use in subsequent experiments on the response of tick cells to virus infection
- Establish experimental conditions for virus infection of selected tick cell lines
- Determine whether the selected *Ixodes* spp cell lines are susceptible to SFV infection
- Characterise virus infection of selected *Ixodes* spp tick cell lines
- Determine suitable time-points and MOIs for future experiments with SFV and LGTV

3.1.2 Materials and Methods

General methods used for experiments in this chapter are described in the Materials and Methods section of this thesis (Chapter 2) and information on experimental design is provided in the text and figure legends. SFV reporter virus constructs used in this chapter are described in detail previously (see 1.2.1 and 2.2.1). *Renilla* luciferase (*Rluc*) activity of SFV4(3H)-*Rluc* infected cells was used as a substitute measure for non-structural viral gene expression and an indication of virus replication (see page 23).

3.2 RESULTS

3.2.1 Initial experiments

The tick cell lines ISE18, IRE11, ISE6 and IRE/CTVM19 were tested for their ability to be infected with SFV4-steGFP. GFP expression was determined by fluorescence microscopy. The cell lines could all be infected with SFV4-steGFP at an MOI of 5, but the number of GFP-positive cells varied greatly. Approximately

80% of ISE18 cells were GFP-positive 24 h post-infection (p.i.), but at the same time-point only 1.5% of IRE11 cells expressed GFP (data not shown). Roughly 70% of cells expressed GFP in IRE/CTVM19 cells 48h p.i. and approximately 50% of cells were GFP-positive in the *I. scapularis* cell line ISE6 after infection with SFV4(3F)-ZsGreen at MOI 5 (Sabine Weisheit, personal communication).
IRE11 and ISE18 were selected for further study. The number of GFP-positive cells in IRE11 was low, but it was considered that it could be beneficial to compare the response to infection of cell lines with high and low numbers of GFP-positive cells. Infection with a flavivirus such as TBEV or LGTV could be more efficient than infection with SFV.

3.2.2 Visualisation of virus replication in tick cells

In mammalian and mosquito cells, alphaviruses replicate in association with cellular membranes (Friedman et al., 1972; Frolova et al., 2010; Spuul et al., 2007). In mammalian cells these membranes are of endosomal origin or part of the plasma membrane and form specific virus replication compartments termed 'spherules' (Spuul et al., 2011). Flaviviruses such as TBEV have been shown to form similar structures during replication in mammalian (Senigl et al., 2006) and tick cells (Offerdahl et al., 2012).

In order to find out whether alphavirus replication in tick cells occurs on membranes as described for mammalian cells, an attempt was made to visualise virus replication in selected tick cell lines. To visualise SFV replication by fluorescence microscopy the reporter virus SFV4(3F)-ZsGreen was used to infect the two cell lines ISE18 and IRE11 at MOI 5, both in flat-sided tubes (Fig 3.1A) and on coverslips in 24-well plates (Fig 3.1B). SFV4(3F)-ZsGreen has ZsGreen fused to the non-structural protein 3 (nsP3) which localises to the site of virus replication in an infected cell (Tamberg et al., 2007). Images were acquired 48 hours p.i. by fluorescence microscopy of live cells in flat-sided tubes (Fig 3.1) and in a separate experiment cells were fixed 24 h p.i. on coverslips and imaged by confocal microscopy. In mammalian and mosquito cells, infection with SFV4(3F)-ZsGreen generates a punctate signal distribution indicating the localisation of SFV replication complexes. Both ISE18 and IRE11

cells infected with SFV4(3F)-ZsGreen showed the punctate ZsGreen distribution typically seen in mammalian and mosquito cells. These fluorescence microscopy results are consistent with the presence of SFV replication complexes in these tick cell lines similar to those observed previously in mammalian and mosquito cells.

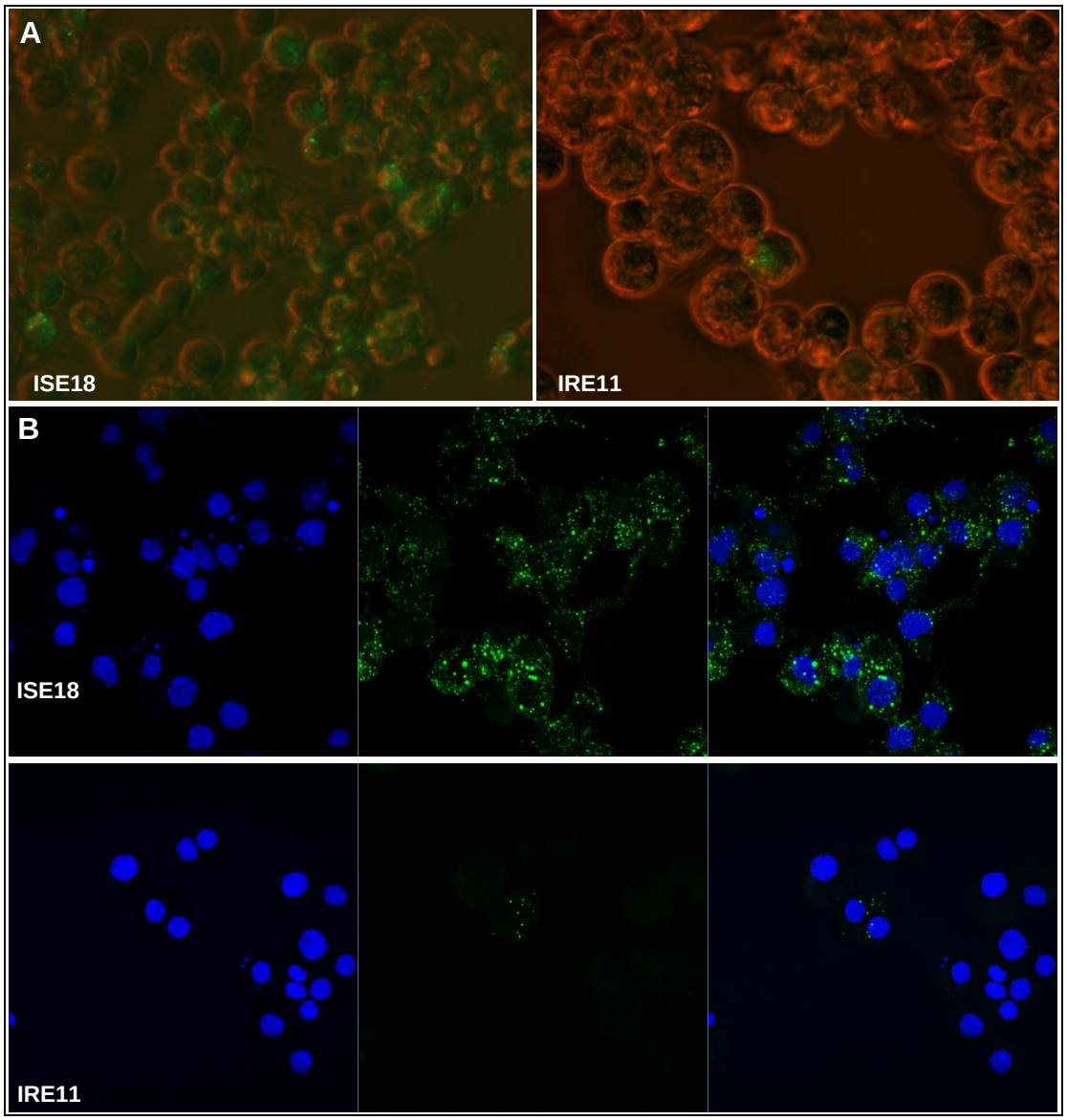

Figure 3.1: Tick cell lines ISE18 and IRE11 were infected at an MOI of 5 with SFV4(3F)-ZsGreen which has ZsGreen fused to the non-structural protein 3 (nsP3). A) Live cell imaging of infected cells 48 h post-infection. The images shown are an overlay of brightfield and fluorescent microscopy. Cells show a punctate distribution of green signal indicating the localisation of nsP3 to replication complexes. B) Maximum projection of a Z-stack image series taken by confocal microscopy at 24 h p.i.. Cell nuclei are shown in blue (DAPI stain) and punctate distribution of green signal indicates the localisation of nsP3 to replication complexes.

More detailed investigation was undertaken by EM. ISE18 cells were infected with SFV4(3F)-ZsGreen at MOI 50 and 24 h p.i. efficient infection (>70% of cells infected) was confirmed by fluorescence microscopy. Cells were then fixed and processed for EM (see 0). Examination by EM of control, mock-infected ISE18 cells and SFV-infected ISE18 cells both showed an icosahedral virus of approximately 70-80 nm diameter in the cytosol of most cells (Fig 3.2). These virus particles were predominantly located around cytoplasmic vacuoles and were of orbivirus-like morphology (Pat Nuttall and Houssam Attoui, personal communication). Due to the high abundance of the observed orbivirus-like endogenous viruses, it was not possible to identify structures which appeared to be specific to SFV replication in ISE18 cells (approximately 100 cells were investigated), especially since it was not known whether SFV replication in tick cells appears similar to mammalian cells. Unidentified endogenous viruses have also been observed in other tick cell lines (Alberdi et al., 2012; Bell-Sakyi and Attoui, 2013). In order to see if IRE11 cells are infected with endogenous viruses, untreated IRE11 cells were fixed and processed for EM. In most IRE11 cells, virus particles of approximately 70-80 nm diameter were also observed (Fig 3.2). However, virus distribution and electron density of virus particles differed between IRE11 and ISE18 cells.

In samples of SFV-infected ISE18 cells no viruses resembling SFV could be seen and no replication complexes as described in mammalian cells could be found in this experiment. In future an attempt could be made to sort cells by flow cytometry for ZsGreen-positive cells, so that effectively all cells viewed by EM would be SFV-infected, in an attempt to increase the chance of finding SFV replication complexes in these tick cells.

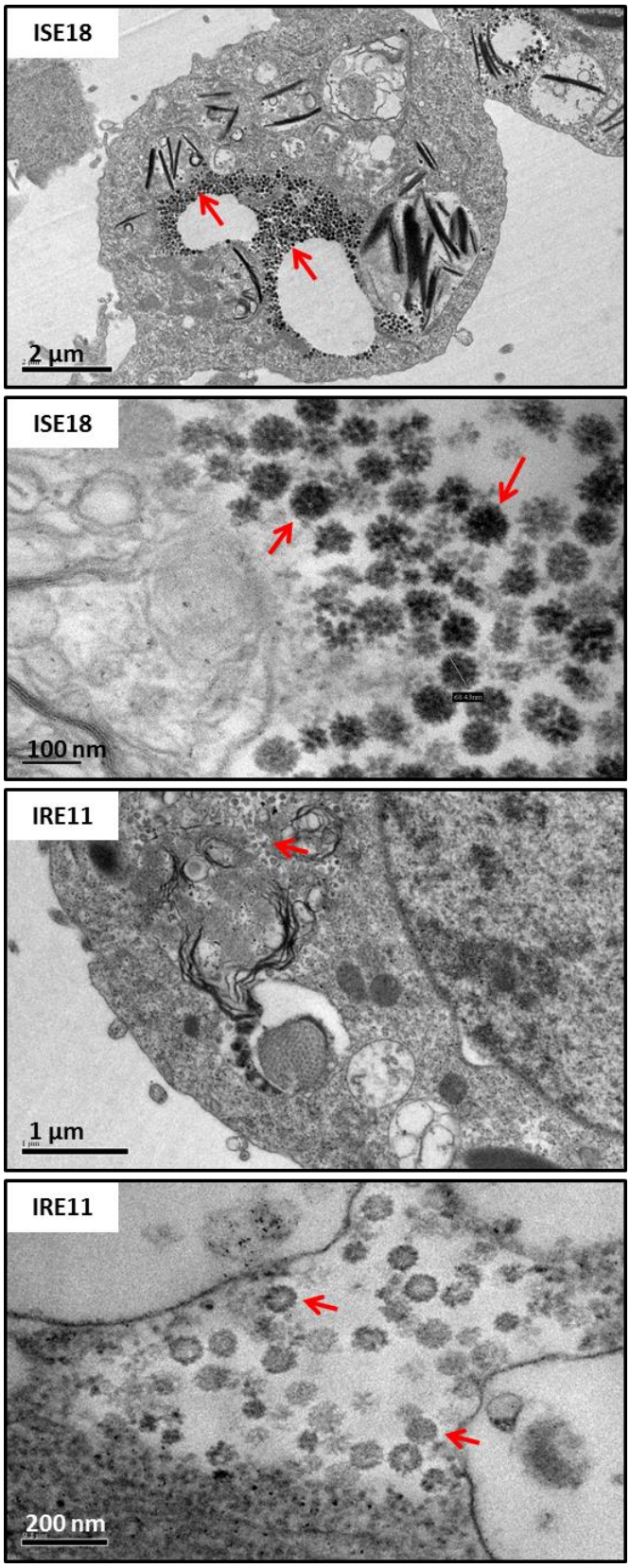

Figure 3.2: EM of ISE18 and IRE11 cells shows that cultures are infected by an unknown virus with Orbivirus-like morphology (indicated by the arrows).

In a combined effort with Dr Lesley Bell-Sakyi, Dr Rennos Fragkoudis and Ms Sabine Weisheit (all Pirbright Institute), a further attempt to visualise SFV replication in tick and mosquito cells was made. BDE/CTVM16 cells derived from eggs of the tick *R. decoloratus* (Bell-Sakyi, 2004), C6/36 cells derived from larvae of the mosquito *Aedes albopictus* (Singh, 1967) and mammalian BHK-21 cells were chosen for this experiment because of the very high levels of SFV infection achievable in these cells and the resulting increased likelihood of visualising SFV replication. Cells were infected with SFV4(3F)-ZsGreen at an MOI of 10 and high levels of infection (>70% of cells infected) were validated by fluorescence microscopy (data not shown) before cells were fixed and processed for EM. BHK-21 cells were fixed at 6 and 10 h p.i., while C6/36 cells were fixed at 10 and 24 h p.i. and tick cells were fixed 24 and 48 h p.i. due to the observed slower replication of SFV in arthropod cells.

In BHK-21 cells it was not possible to visualise CPV-I but CPV-II were observed at 6 h and 10 h p.i. (Fig 3.3A). CPV-II are usually observed in a later stage of infection, have a different morphology to CPV-I and contain glycoproteins suggesting a role in packaging of viral genomes (Soonsawad et al. 2010). While untreated C6/36 cells were also already infected by at least one apparently endogenous virus (data not shown), SFV could be easily distinguished by its morphology. However, replication complexes similar to CPV-I or CPV-II could not be visualised, only budding viruses which were abundant on the PM of the cells (Fig 3.3B). The observed structures show some similarity to CPV-I replication complexes, but while replication complexes usually are of low electron density with just an electron dense centre, these structures appear electron dense throughout, suggesting they were budding virus particles. Untreated BDE/CTVM16 cells were also infected with at least one unknown virus (Lesley Bell-Sakyi, personal communication). In SFV-infected BDE/CTVM16 cells, structures consistent with budding SFV were observed at the cell surface (Fig 3.3C). Similar structures were not observed in mock-infected cells. It was not possible to acquire convincing images of SFV replication complexes in BDE/CTVM16 cells; however, structures with morphology similar to CPV-I were observed (see Appendix, Figure 8.2).

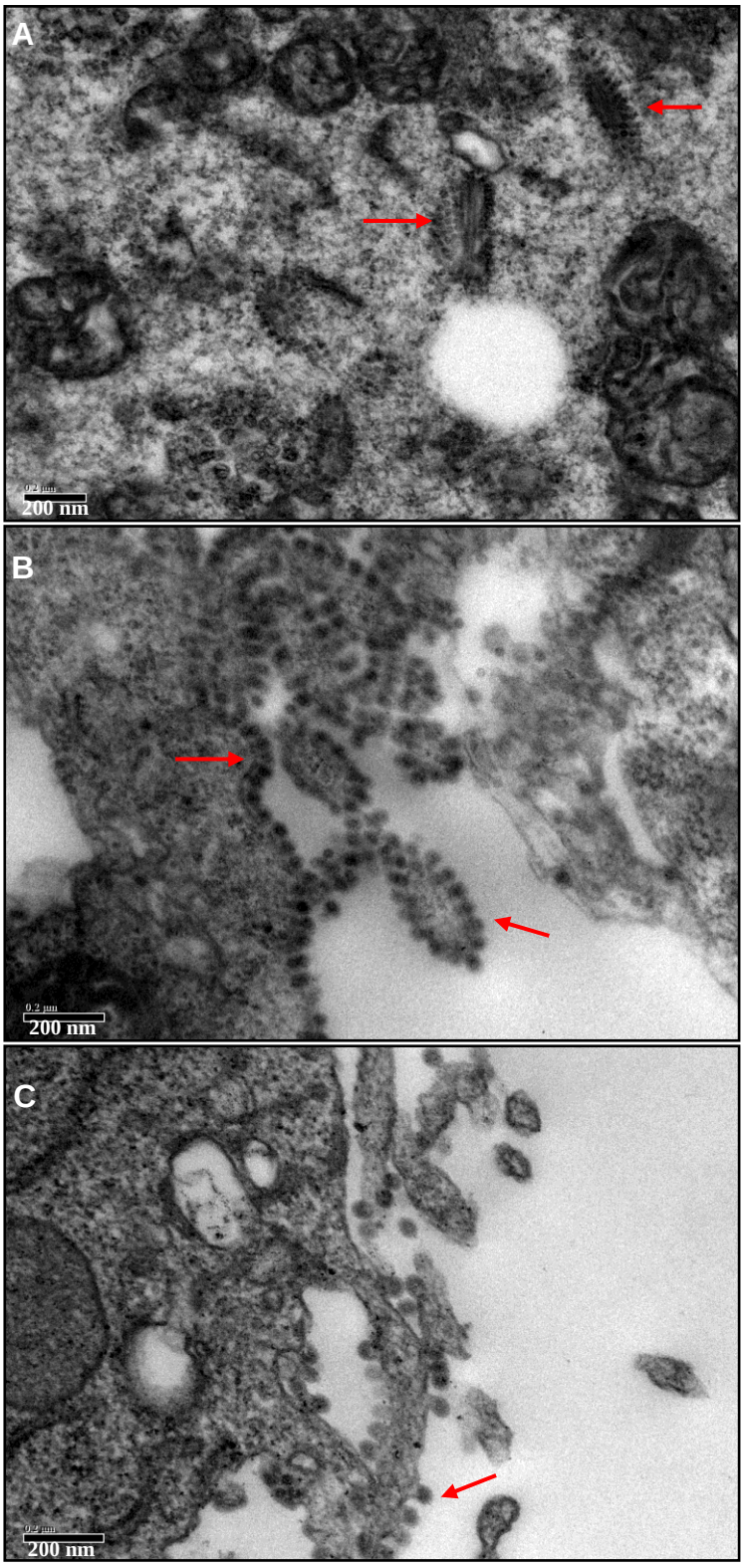

Figure 3.3: Mammalian BHK-21 (A), mosquito C6/36 (B) and tick BDE/CTVM16 (C) cells were infected with SFV4(3F)-ZsGreen and visualised EM (experiment performed together with Sabine Weisheit, Dr Rennos Fragkoudis and Dr Lesley Bell-Sakyi). Arrows indicate CPV-II (A) and budding virus particles (B, C).

The differences seen for the different cell lines could be either incidental due to inadequate sample processing or due to the differences in time-points chosen and speed of replication. Overall, higher quality images and different time-points may show whether SFV forms replication complexes in tick cells as observed in mammalian cells.

3.2.3 Establishing experimental conditions for IRE11 and ISE18 cells

For general culture, both IRE11 and ISE18 cells were maintained in tightly closed flat-sided culture tubes. Tick cell lines can have difficulty maintaining their medium at an acid pH if they are not grown in a sealed vessel where the medium is in contact with only a relatively small volume of air. For large-scale experiments the use of these tubes is not ideal since 1.1 x 10^6 cells are needed per tube - more than twice as many cells as for one well of a 24-well plate (and in an infection experiment twice as much virus). Since tick cells multiply much slower than for example mammalian BHK-21 or mosquito cells, this poses a real problem for any large-scale experiments.

To determine if 24-well plates could be used for experiments with ISE18 and IRE11, cells were seeded in dilutions ranging from 1x10^5 to 6x10^5 cells per well into 24-well plates. The plates were placed inside a plastic bag which contained a piece of wet tissue and was tightly closed to maintain humidity and minimise air exchange. By visual assessment of cell morphology over a seven-day period it was concluded that cells seeded at a density ranging from 2 x 10^5 to 5 x 10^5 cells per well looked healthy and viable after one week; however, the pH indicator phenol red, which is part of the L-15 medium, indicated a change to a more alkaline pH 24 h after seeding by a change in colour of cell culture medium. This can be an indication of reduced cell metabolism.

In an initial experiment to determine kinetics of virus replication, cells were seeded in 24-well plates at a density of 2x10^5 cells per well and infected 24 h later with SFV4(3H)-*Rluc* (see 2.2.1) at an MOI of 0.28. Samples for luciferase assay were taken from triplicate wells at 12, 24, 36, 60 and 72 h p.i. and every day after that up to day 7 p.i. to identify virus replication kinetics. The cells were counted every 24 h (Fig 3.4). Luciferase assay of the collected samples showed no measurable *Rluc*

activity in any of the samples (data not shown). One possible reason for this is that more than 2 x 10^5 cells might have to be lysed per sample to detect a signal, because *Rluc* activity in *Ixodes* spp tick cells is considerably lower than in mammalian, mosquito and other tick cell lines (Rennos Fragkoudis and Gerald Barry, personal communication). Moreover, the MOI that was used (0.28) was comparatively low and may have been insufficient to infect all cells susceptible to SFV infection.

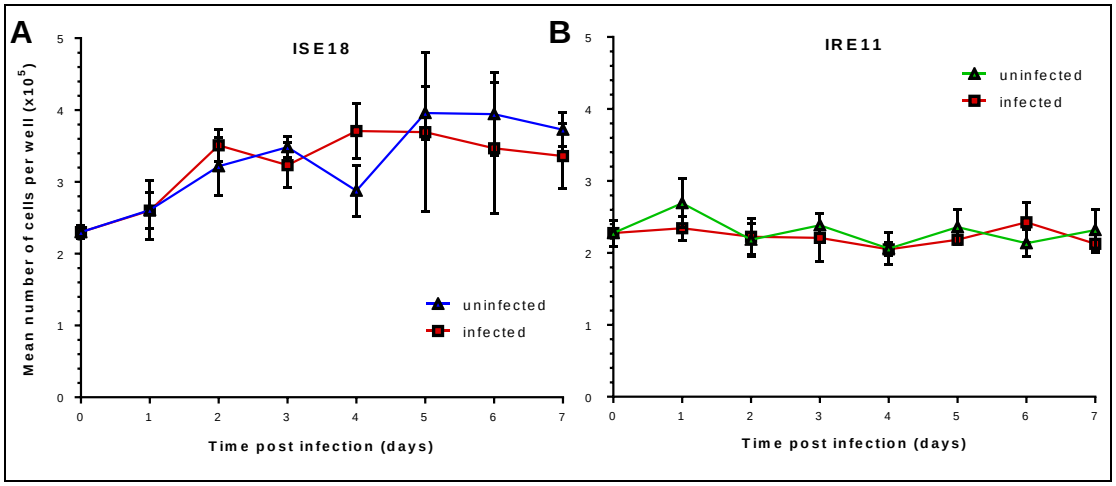

Figure 3.4: Growth of ISE18 (A) and IRE11 (B) cells after infection with SFV4(3H)-*Rluc* at an MOI of 0.28. Cells were seeded in 24-well plates 24 h prior to infection. Each data point represents the mean of three replicate cultures; the error bars represent the standard deviation (SD).

Furthermore, the cell counts showed that IRE11 cells did not grow at all during the course of this experiment (Fig 3.4B) and, while ISE18 cells showed an increase in cell numbers (Fig 3.4A), growth was inconsistent. Given the disappointing results in 24-well plates, the growth rate of the two cell lines under optimum conditions in flat-sided culture tubes was determined (Fig 3.5). 1.1 x 10^6 cells were seeded in flat-sided culture tubes and cells in duplicate tubes were counted at 1-3 day intervals. Both cell lines grew at a similar rate within the first 10 days after seeding. IRE11 cell numbers doubled within 5-6 days and ISE18 cells doubled after 6 days. However, while IRE11 cells exhibited a sigmoid growth curve in the first 10 days after seeding, ISE18 cells showed almost linear growth and did not reach saturation and reduction of cell growth within 11 days. After comparison of growth in 24-well plates and flat-

sided culture tubes it was decided to perform experiments in flat-sided tubes, due to the reduction and inconsistency of growth in 24-well plates. Some experiments with ISE18 over short periods of time (≤ 3 days) were performed in 24-well plates since growth of ISE18 in wells was comparable to growth in tubes for the first three days. In the following text unless indicated otherwise, experiments using ISE18 and IRE11 were performed in flat-sided tubes and cells were seeded at the beginning of an experiment at $1.1x10^6$ cells per tube.

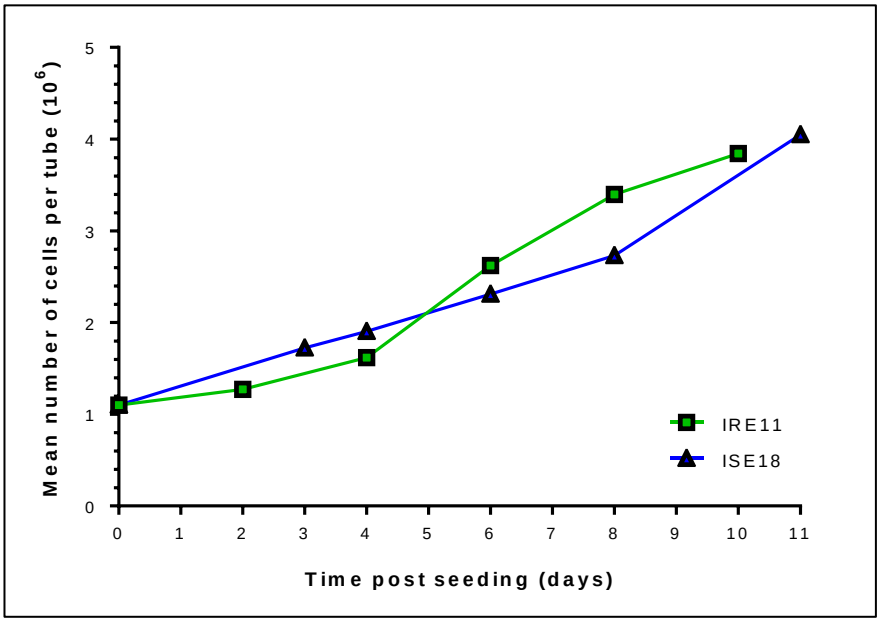

Figure 3.5: Growth of the cell lines ISE18 and IRE11 in flat-sided culture tubes monitored over 11 and 10 days, respectively. Cells were seeded at a density of 5 x 10^5 cells per ml in 2.2 ml complete L-15 medium and counted at 1-3 day intervals. Each data point represents the mean of two replicate cultures.

3.2.4 Kinetics of SFV non-structural gene expression in ISE18 and IRE11

In order to investigate innate defences of tick cells against arbovirus infection, the aim of this thesis, it was essential to first identify the kinetics of virus replication and production in the tick cell lines to be studied. Knowledge of the dynamics of virus replication would inform about the time-points at which to investigate cell responses. Many different reporter virus constructs are available for SFV (Fragkoudis et al.,

2007; Kiiver et al., 2008; Tamberg et al., 2007), which makes it useful as a model virus to study virus gene expression and innate defences in arthropod cells.

For determination of SFV gene expression kinetics, the *Rluc* reporter virus SFV4(3H)-*Rluc* was used. SFV4(3H)-*Rluc* expresses *Rluc* within the non-structural ORF; *Rluc* is cleaved from nsP3 with high efficiency. Early in replication *Rluc* expression serves as a measure for virus replication, while later in infection RNA is still replicated but expression of non-structural proteins decreases (Kiiver et al., 2008). The two tick cell lines ISE18 and IRE11 were infected at an MOI of 5, with the aim of infecting all cells susceptible to SFV infection. Three replicate tubes per time-point were seeded, infected, and then counted and lysed every 24 h for seven days following infection. *Rluc* activity in the cell lysate was measured (Fig 3.6).

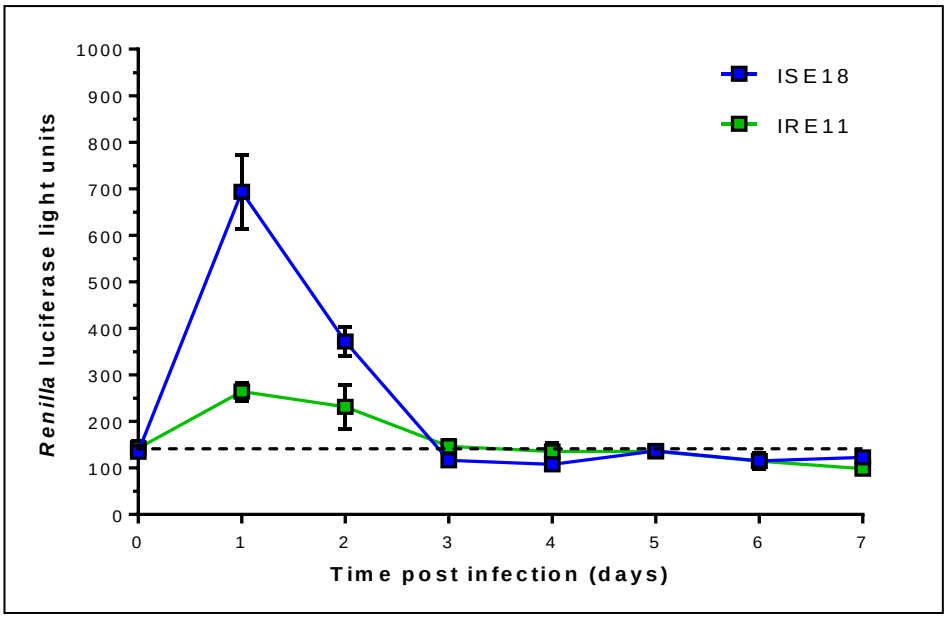

Figure 3.6: *Rluc* activity in ISE18 and IRE11 cells after infection with SFV4(3H)-*Rluc* at MOI 5. Experiment was performed in flat-sided tubes. Each data point represents the mean of three replicate cultures; the error bars represent the SD. The dotted line represents the limit of detection as determined by background *Rluc* levels of mock-infected controls.

The kinetics of viral gene expression were similar for both cell lines. After an initial peak of *Rluc* activity at 24 h post-infection, activity dropped and quickly reached the background level at 72 h post-infection and then stayed at this background level. *Rluc* activity was higher in ISE18 cells than in IRE11 cells which correlates with

similar experiments performed in 24-well plates (data not shown) and is consistent with the lower proportion of IRE11 cells infected with SFV4(3F)-ZsGreen compared to ISE18 cells (see Figure 3.1).

Growth of uninfected cells was comparable to previous growth curves (Figure 3.5) and while infection with SFV did not affect growth of IRE11, SFV-infected ISE18 grew at a similar rate to uninfected ISE18 cells during the first 3 days p.i., but thereafter growth rate was decreased compared to uninfected cultures (Fig 3.7). There was also a decrease in ISE18 cell adherence between 3 and 5 days p.i. (visual assessment). The decrease in the growth rate of infected ISE18 cultures was surprising since it had previously been observed that some other tick cell line cultures showed an unaffected or even increased growth rate following infection with SFV (Sharmin Haideri, personal communication). Further experiments to determine the fate of infected cells could be undertaken to determine whether this reduced culture growth rate was caused by cell death or by slower growth of SFV-infected ISE18 cells. It is possible that individual IRE11 were similarly affected by SFV, but death or reduced growth of infected cells may have gone unnoticed due to the small proportion of infected cells in the culture.

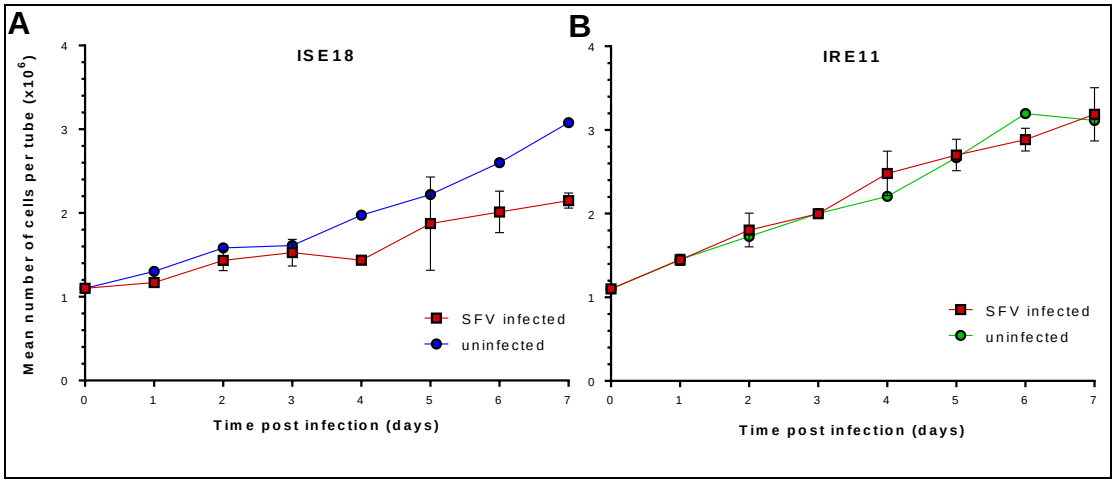

Figure 3.7: Growth of ISE18 (A) and IRE11 (B) cells after infection with SFV4(3H)-*Rluc* at MOI 5. Experiment was performed in flat-sided tubes. Each data point represents the mean of three replicate cultures; the error bars represent the SD.

Knowing that the highest *Rluc* activity was observed at 24 h p.i., this time-point was chosen for a trial infection with different MOIs ranging from 0.1 to 100. Due to the limited number of cells available at this stage of the project, the experiment was performed in 24-well plates. 5 x 10^5 ISE18 or IRE11 cells were seeded per well and infected 24 h later. Infection of ISE18 with SFV4(3H)-*Rluc* resulted in detectable levels of *Rluc* in cell lysates for each MOI used (Fig 3.8A). Increase in MOI resulted in increased *Rluc* activity, even for high MOIs. *Rluc* activity ranged from 431 (±85.9) light units (MOI 0.1) to 38,280 (±5,246) *Rluc* light units (MOI 100). These levels were much lower than observed for mammalian BHK-21, mosquito U4.4 cells or tick BDE/CTVM16 cells, which can have *Rluc* activity of over 10^5 or even 10^6 24 h p.i. with SFV4(3H)-*Rluc*.

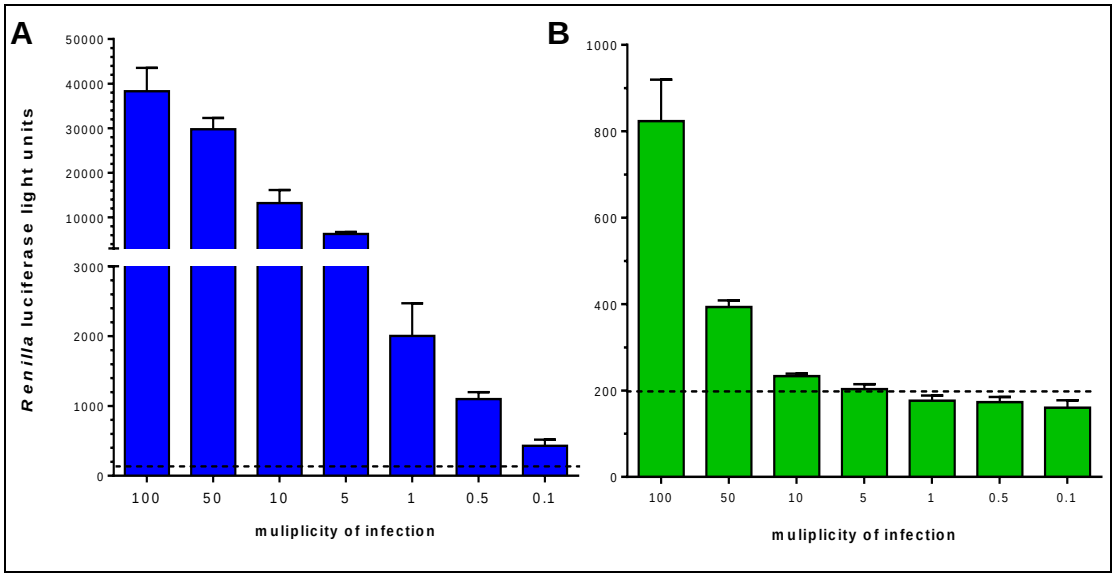

Figure 3.8: *Rluc* activity levels in ISE18 (A) and IRE11 (B) infected with different MOI of SFV4(3H)-*Rluc.* Experiment was performed in 24-well plates. The dotted line indicates the limit of detection as determined by background *Rluc* levels of mock-infected controls. Each data point represents the mean of three replicate cultures; the error bars represent the SD.

In IRE11 cells, *Rluc* activity was only detectable in lysates of cells infected at MOI 10 or higher (Fig 3.8B). This result may have been related to the use of 24-well plates, since *Rluc* activity was detectable in the previous experiment at 24 h p.i. in IRE11 cells infected at MOI 5 in flat-sided tubes (Figure 3.6).

For ISE18 a similar experiment was performed using a ZsGreen reporter virus and analysis by flow cytometry. ISE18 cells were infected with SFV4(3F)-ZsGreen at different MOIs ranging from 0.5 to 50, harvested 24 h and 48 h p.i., fixed with 4% PFA and analysed by flow cytometry (Fig 3.9). The maximum number of cells expressing detectable amounts of ZsGreen was approximately 80%. At 24 h p.i. 80% ZsGreen-positivity was only detected in cells infected at an MOI of 50, but at 48 h p.i. cells infected with all tested MOIs had reached the maximum infection rate, indicating a rapid spread of virus through the culture. The increase in luciferase levels (Fig 3.8) and percentage of ZsGreen-positive cells (Fig 3.9) with increasing MOIs from 1 to 100 indicates that the dynamics of SFV infection are different to those in BHK-21 cells. As described in Chapter 2 (see 2.2.3) the MOI is defined by BHK-infectious units and susceptibility of BHK-21 cells may be different to that of tick cells.

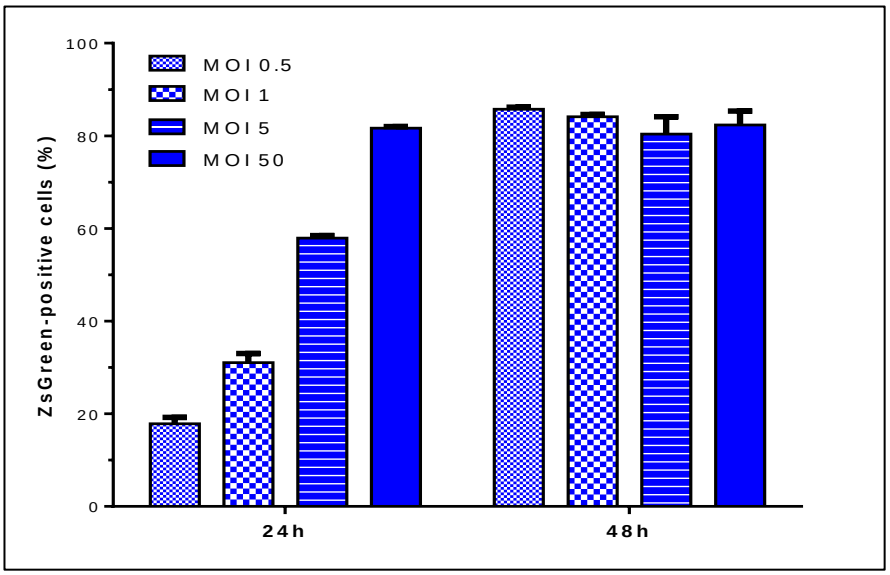

Figure 3.9: Percentage of ZsGreen-positive ISE18 cells following infection with different MOI of SFV4(3F)-ZsGreen. Experiment was performed in flat-sided tubes. Each data point represents the mean of three replicate cultures; the error bars represent the SD.

One of the planned experiments was a virus production curve, which requires a medium change soon after infection. In other experiments SFV was simply added to the culture supernatant for infection. It was thus important to establish prior to a virus

production experiment, whether completely changing the medium of the cells 4 h p.i. would affect either the cells or the efficiency of infection. For this purpose, ISE18 and IRE11 cells were seeded into flat-sided tubes and inoculated with SFV4(3F)-ZsGreen or SFV4(3H)-*Rluc* at MOI 5 for 4 h and then all medium was changed to fresh complete L-15. 24 h p.i. cells infected with SFV4(3F)-ZsGreen were harvested, fixed and analysed by flow cytometry (Fig 3.10 A/C) and cells infected with SFV4(3H)-*Rluc* were lysed and analysed by luciferase assay (Fig 3.10 B/D).

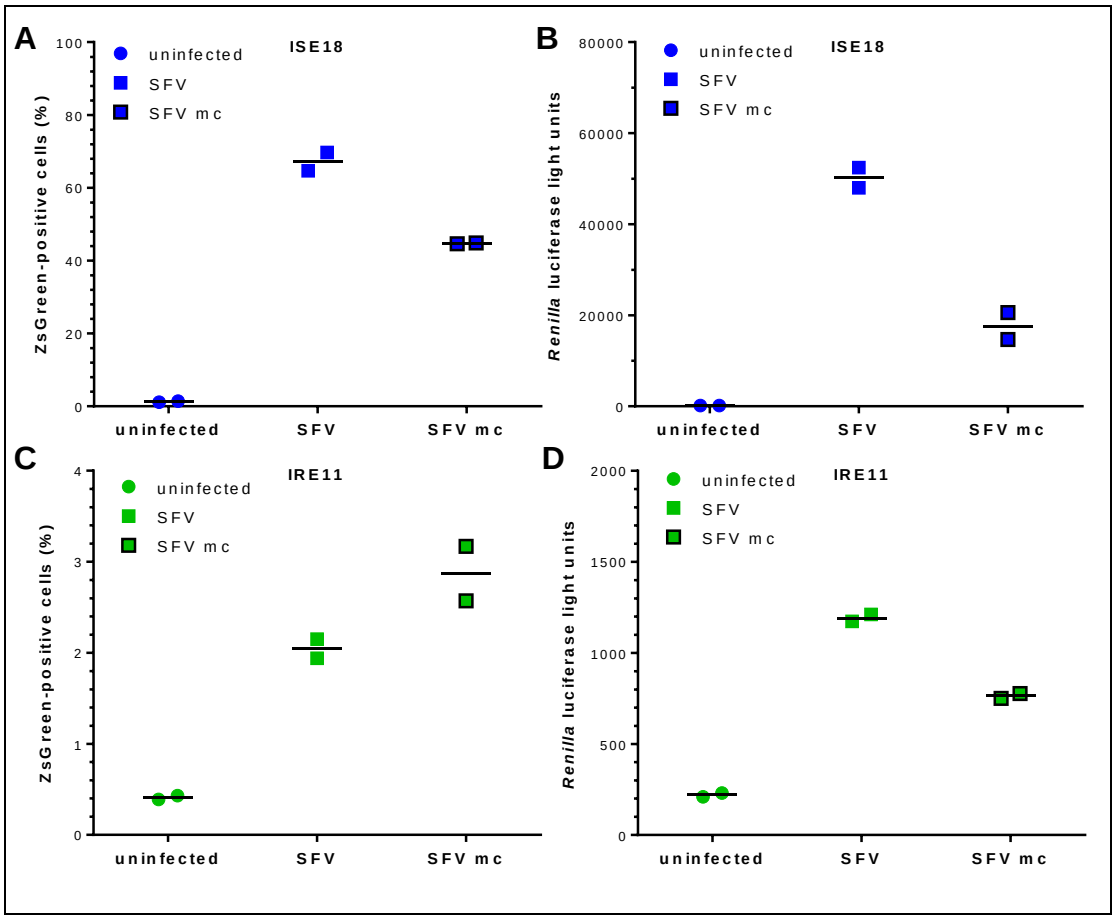

Figure 3.10: Effects of a medium change (mc) 4 h p.i. with SFV. Number of ZsGreen-positive ISE18 (A) and IRE11 (C) cells 24 h p.i. with SFV4(3F)-ZsGreen (MOI 5) was reduced in ISE18 and increased in IRE11 compared to cells without medium change. Expression of non-structural virus genes as measured by Rluc activity was reduced in SFV4(3H)-*Rluc* infected ISE18 (B) and IRE11 (D) cells when medium was changed 4 h p.i.. Experiment was performed in flat-sided tubes.

Both ISE18 and IRE11 cells appeared unaffected by the medium change as determined by visual assessment of cell morphology, cell adherence and colour of culture medium as an indicator of pH. However, efficiency of virus infection was reduced in ISE18 cells. Approximately 20% fewer ISE18 cells were ZsGreen-positive 24 h p.i. with SFV4(3F)-ZsGreen at MOI 5 when medium was changed 4 h p.i. compared to control infection without medium change (Fig 3.10A). In lysates of ISE18 cells infected with SFV4(3H)-*Rluc*, *Rluc* activity was also reduced (~2.8 fold) if medium was changed 4 h p.i. (Fig 3.10B).

In contrast, slightly more IRE11 cells were ZsGreen-positive in tubes where medium was changed 4 h p.i. than in tubes without medium change (Fig 3.10C). However, *Rluc* activity was also reduced in IRE11 cells with medium change 4 h p.i. with SFV4(3H)-*Rluc* compared to cells that had not undergone medium change (Fig 3.10D). It was concluded that while a change of medium does affect efficiency of SFV infection, there were still high levels of infection and replication. In flat-sided tubes the ratio of medium volume to area of adherent cells is large and it may thus take more than 4 h for all infectious virus particles to attach to cells. To increase infection levels, a 2-fold higher MOI (MOI 10) was chosen for the following experiment.

In order to determine the kinetics of virus spread through the culture, how soon after infection ZsGreen can be detected and how long the nsp3-ZsGreen fusion protein is present in infected cells, ISE18 and IRE11 cells were infected with SFV4(3F)-ZsGreen at high and low MOI and sampled for flow cytometry over three weeks (ISE18) or one week (IRE11) (Fig 3.11). Culture supernatant from this experiment was also collected for plaque assay to generate a virus production curve (see 3.2.5).

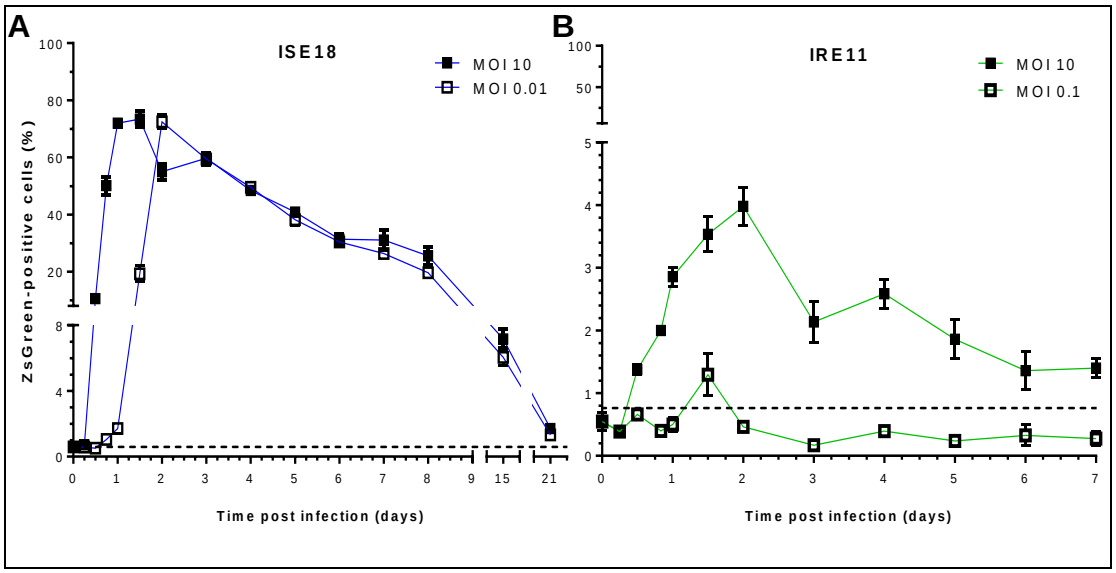

Figure 3.11: Flow cytometry analysis of ISE18 (A) and IRE11 (B) cells infected with SFV4(3F)-ZsGreen at a low and a high MOI as indicated. Experiment was performed in flat-sided tubes. Each data point represents the mean of three individual samples; the error bars represent the SD and the dotted line represents the limit of detection.

ISE18 and IRE11 cells were seeded in triplicate for each time-point in tubes (1.1 x 10^6 cells/tube) and inoculated with SFV4(3F)-ZsGreen 24 h later, to infect at MOI 10 and MOI 0.01 (ISE18) or MOI 0.1 (IRE11). Due to the poor susceptibility of IRE11 to SFV infection, a 10-fold higher MOI than that used for ISE18 was chosen as the low MOI. At 4 h p.i. the medium of all tubes was changed to fresh complete L15 medium. Culture supernatant was collected and cells were harvested and fixed at 6 h, 12 h, 18 h, 24 h, 36 h, 48 h p.i. and thereafter every day up to days 7 and 8 p.i. for IRE11 and ISE18, respectively. At each time-point, medium of the cultures used for the subsequent sampling time-point was changed to obtain a virus production curve as opposed to measuring accumulated virus over time. For ISE18, samples were also harvested 15 and 21 days p.i. and medium for these time-points was changed 24 h prior to sampling. Cells were analysed by flow cytometry for numbers of ZsGreen-positive cells (Fig 3.11 and Fig 3.12).

Consistent with observations by microscopy and previous flow cytometry experiments, the maximum proportion of ZsGreen-positive ISE18 cells was approximately 80% while only about 4% of IRE11 cells became ZsGreen-positive. At MOI 10, ZsGreen-positive cells could be detected in both cell lines from 12 h p.i.

onwards. The maximum number of infected cells was reached at 24 h p.i. in ISE18 and at 48 h p.i. in IRE11 cells. The number of green ISE18 cells decreased slowly and there were still ZsGreen-positive ISE18 cells two and three weeks p.i. (7.2% and 1.7%, respectively). In IRE11 there was a drop in ZsGreen-positive cells between two and three days p.i. followed by a steady decline. After one week a small percentage (1.4%) of IRE11 cells was still ZsGreen-positive.

At MOI 0.01, the maximum number of ZsGreen-positive ISE18 cells was also approximately 80% but this was not reached until 48 h p.i. (compared to 24 h at MOI 10). Numbers of ZsGreen-positive ISE18 cells then gradually decreased at a similar rate to cells infected at MOI 10. In IRE11 cells infected at MOI 0.1 ZsGreen-positive cells could only be detected at 36 h p.i. and the percentage of infected cells was approximately 3-fold lower compared to IRE11 infected at MOI 10.

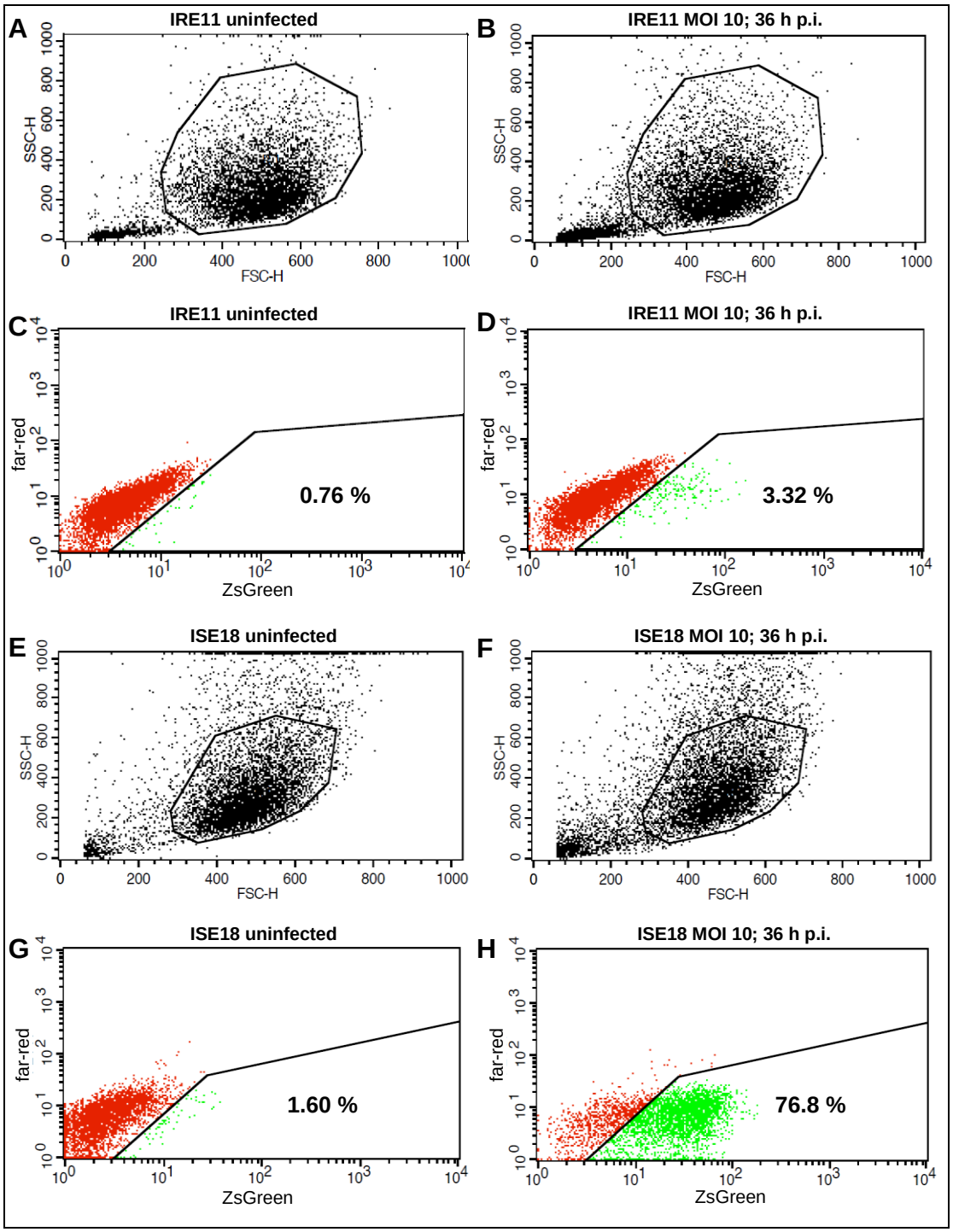

Figure 3.12: Representative examples of flow cytometry raw data for IRE11 and ISE18 cells infected with SFV4(3F)-ZsGreen at MOI 10 (36 h p.i.). Forward scatter (FSC-H) and side scatter (SSC-H) indicate cell size and granularity, respectively (A, B, E, F). The main cell population was gated for as indicated by the polygonal gate. Gated cells were then analysed for ZsGreen expression (C, D, G, H). The far-red channel was chosen as the constant on the Y-axis which was not affected by infection with SFV4(3F)-Zsgreen. ZsGreen positive cells are represented in green.

3.2.5 Kinetics of SFV production in ISE18 and IRE11

As described in the previous section (experiment shown in Figure 3.11), supernatant was collected from cells infected with SFV4(3F)-ZsGreen and virus titre was measured by plaque assay on BHK-21 cells. Virus was produced as early as 12 h p.i. in ISE18 cells and peaked at 18 h p.i. for MOI 10 and 36 h p.i. for MOI 0.01 and then decreased at a slow rate which was comparable between the two MOIs (Fig 3.13A). However, virus production remained at a high level (~10^6 PFU/ml) over the 8 day experimental period. Other experiments showed that virus was still produced two weeks p.i. in ISE18 at a high level of approximately $1.8x10^5$ PFU/ml (data not shown).

For IRE11 interpretation of data is more difficult. Infectious particles observed at 6 h p.i. could have been remaining virus particles which were not removed by the change of medium 4 h p.i.. To infect 10^6 cells at an MOI of 10, 10^7 PFU were added. If the medium change at 4 h p.i. was 95% effective in removing input virus, the amount of remaining virus would be in the order of $5x10^5$ PFU. Given the volume of cell culture medium was 2.2 ml, this equates to $2.3x10^5$ PFU/ml, which is similar to the titre measured at 6 h p.i.. In IRE11 infected at MOI 10 viral titres did not exceed the titres measured at 6 h p.i. at any later time-point, leaving it unclear whether virus was produced or whether the measured viral titres were infectious particles remaining from the original inoculum (Fig 3.13B). However, since medium was changed twice for all other samples taken (4h p.i. and at the time-point prior to the one measured) it is likely that virus was produced by IRE11 cells. Another indicator that IRE11 cells probably produced infectious SFV particles was that supernatant of cells infected at MOI 0.1 showed an increase in virus titre at 18 h p.i. compared to 6 h p.i.; the virus titre was approximately 50-fold higher than that of the remaining virus inoculum at 6 h p.i.. These results suggest that while infected IRE11 cells produce infectious SFV particles, the amount of virus produced by IRE11 cell cultures is low.

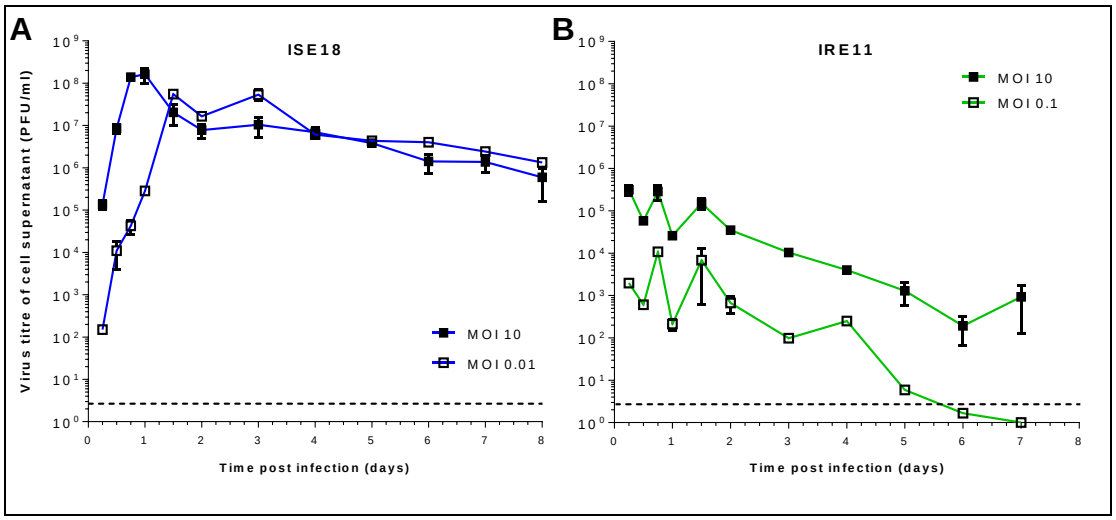

Figure 3.13: SFV4(3F)-ZsGreen virus production in ISE18 (A) and IRE11 (B) cell cultures infected with a low and high MOI as indicated. BHK-21-infectious units were measured by plaque assay (see 2.2.3). Experiment was performed in flat-sided tubes. Each data point represents the mean of three replicate cultures; the error bars represent the SD.

3.2.6 Transfection of expression plasmids into tick cells

For many experiments it is beneficial to be able to transfect expression plasmids into cells, for example to overexpress a protein of interest and investigate its effect on virus replication. In tick cells efficient transfection and expression of plasmid DNA can be very difficult. Several attempts were made by colleagues to determine which transfection reagent and which promoter are best for use in tick cells but there has been little success with the reagents tested (Esther Schnettler & Sabine Weisheit, personal communication). During their experiments to transfect different plasmids expressing luciferase, the highest levels of luciferase activity were measured in samples transfected with plasmids under the OpIE2 promoter, a baculovirus promoter known to result in high level transcription in insect cells (Theilmann and Stewart, 1992).

In ISE18 and IRE11 little or no expression of transfected plasmids was observed (data not shown). To investigate in a pilot experiment whether it was the uptake of plasmid DNA or the expression of transfected DNA that was causing the problem, ISE18 cells were seeded in a 24-well plate and transfected with 500 ng of a fluorescein-labelled plasmid or a plasmid expressing eGFP under the OpIE2

promoter (pIB-eGFP) using two different transfection reagents, GeneJammer (Agilent Technologies) and Lipofectamine®2000 (Life Technologies™). Cells were harvested, washed twice with PBS and fixed with 4% PFA 24 h post-transfection and analysed by flow cytometry.

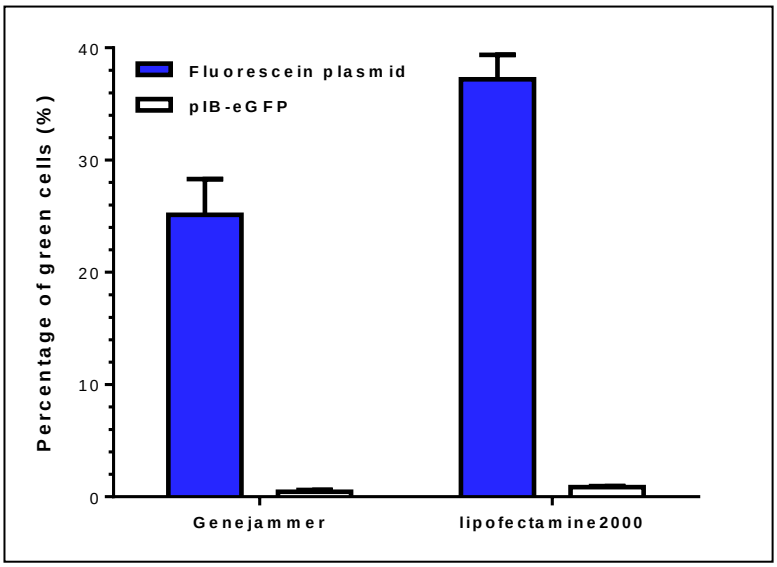

Figure 3.14: Transfection efficiency in ISE18 cells measured by uptake of a fluorescein-labelled plasmid and expression of an eGFP-encoding plasmid (pIB-eGFP). Experiment was performed in a 24-well plate. Each data point represents the mean of three individual samples; the error bars represent the SD.

While there was almost no detectable expression of eGFP after transfection of pIB-eGFP, green fluorescence in 25% (GeneJammer) or 35% (Lipofectamine®2000) of cells transfected with the fluorescein-labelled plasmid indicated detectable uptake of plasmid DNA by cells (Fig 3.14). Uptake was slightly higher using Lipofectamine®2000 compared to GeneJammer, however the presented data was from a single experiment. The observation that DNA is taken up (with varying efficiency) but reporter genes are not expressed at high levels was also observed for other *Ixodes* spp tick cell lines by Sabine Weisheit and Esther Schnettler. Unfortunately, an attempt to clone the promoter region of tick tubulin for use as a promoter of gene expression in tick cells as part of the present study failed (data not shown). Many problems were encountered such as very GC-rich areas adjacent to

sites of transcription and also high divergence of published genome sequence data on NCBI from sequences actually amplified from tick cells.

3.2.7 Selection of the *I. scapularis* cell line IDE8 for further study

The characterisation of the two cell lines ISE18 and IRE11 revealed a number of potential problems for future experiments. While approximately 80% of ISE18 cells could be infected with SFV4(3F)-ZsGreen, only up to 4% of IRE11 cells could be infected (Figure 3.11). IRE11 were also difficult to work with in general as they could not be used in 24-well plates and were difficult to grow to very high densities in tubes; thus more tubes were needed per experiment than for ISE18. In experiments using ISE18, IRE11 or IDE8 cell lysates for Western blot analysis, β-actin was repeatedly not detected in ISE18 cell lysates using an antibody against human β-actin (see 2.12), even though the antibody cross-reacted with tick actin of all other cell lines tested (data not shown). A large proportion of experiments planned for this PhD project would involve the use of dsRNA for reducing expression of specific tick genes (referred to as knockdown experiments) and subsequent virus infection. In a preliminary experiment, addition of dsRNA against *Rluc* 24 h prior to infection with SFV4(3H)-*Rluc* resulted in a 95% knockdown of *Rluc* activity in ISE18, while in IRE11 cells no reduction of *Rluc* activity was observed (data not shown). The *I. scapularis*-derived cell line IDE8 is relatively consistent in knockdown experiments, easy to grow to large numbers and it is well-suited for use in 24-well plates (Barry et al., 2013; Esther Schnettler, personal communication). The original disadvantage of IDE8 cells was the presence of a persistent infection with the orbivirus SCRV (Alberdi et al., 2012; Attoui et al., 2001), which could interfere with experiments investigating responses to SFV or LGTV. However, during the initial characterisation of ISE18 and IRE11, it was shown that both cell lines are also persistently infected with at least one unknown virus. With IDE8 being generally better suited for large scale and knockdown experiments it was decided to change to IDE8 for the experiments described in chapters 4 and 5. Knowing that IDE8 cells are persistently infected with SCRV has one advantage; it enables investigation of the effects of SFV and LGTV infection on SCRV replication.

In parallel to this project, my colleague Sabine Weisheit investigated transcriptomic and proteomic changes after infection of IDE8 cells with TBEV at two and six days p.i.. The use of IDE8 cells for both projects had the further advantage that it would allow future comparison of the two independent studies. All experiments using IDE8 cells were performed in 24-well plates and cells were seeded at densities of either $5x10^5$ or $1x10^6$ cells per well as indicated.

In an attempt to determine the number of SFV-infected IDE8 cells by flow cytometry, both ISE18 and IDE8 cells were infected with SFV4(3F)-ZsGreen at an MOI of 50. As previously shown (Figure 3.11), approximately 80% of ISE18 cells were positive for ZsGreen. ZsGreen could only be detected in 40% of IDE8 cells by flow cytometric analysis (data not shown). This lower number of ZsGreen-positive IDE8 cells could at least in part be explained by the limitations of flow cytometry. IDE8 cells had a higher background autofluorescence than ISE18 so that the difference in mean intensity between infected and uninfected cells was less. Instead of a clear second positive population there was only a minor shift of the mean intensity of the whole population. It was thus not possible to set a gate which would include all ZsGreen-positive cells. In a microscopy-based experiment performed by Sabine Weisheit, the maximum number of IDE8 cells infected with SFV4(3F)-ZsGreen was determined by manual counting as 50% at 24 h p.i. at MOI 10. SFV4(3F)-ZsGreen results in a punctate signal distribution (see Figure 3.1) which makes it easier to distinguish between infected and uninfected cells than a virus construct which results in GFP distributed evenly across the highly autofluorescent cell. However, it is still possible to miss infected cells with low numbers of replication complexes which may not have been exactly in the focal plane of the image acquired.

To further compare the cell lines ISE18 and IDE8, cells were infected with SFV4(3H)-*Rluc* at different MOIs ranging from 0.1 to 50 and *Rluc* activity was measured in cells lysed 24 h p.i. (Fig 3.15). *Rluc* activity of lysates from the two cell lines was comparable with almost identical levels for cells infected at a high MOI (50, 10 and 5). At MOI 1 and MOI 0.5, *Rluc* activity was slightly higher in IDE8 than in ISE18.

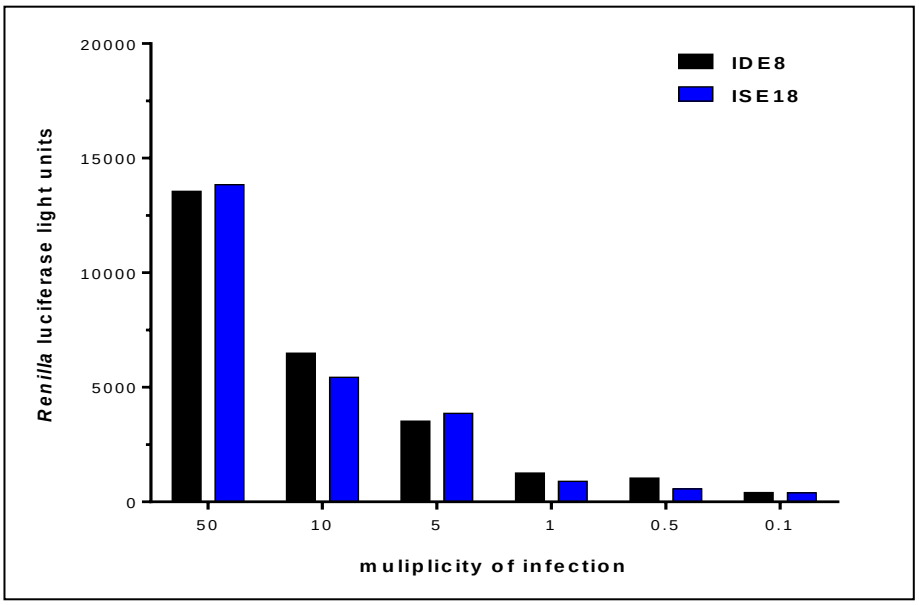

Figure 3.15: *Rluc* activity in ISE18 and IDE8 cells infected with different MOIs of SFV4(3H)-*Rluc*. Experiment was performed in a 24-well plate ($1x10^6$ cells/well). Each data point represents the mean of two replicate cultures.

After showing that the susceptibility of IDE8 to SFV infection was probably not very different to that of ISE18 cells, replication dynamics were investigated. First IDE8 cells were infected with SFV4(3H)-*Rluc* at four different MOIs (0.01, 0.1, 1 and 5) and lysed for luciferase assay every 24 h up to 5 days p.i. (Fig 3.16). In cells lysed 24 h p.i. *Rluc* activity was detectable for all tested MOIs; activity was highest at 24 h p.i. and then decreased. The observed decrease in *Rluc* activity after 24 h p.i. was slower compared to the kinetics measured in ISE18 cells (Figure 3.6). In IDE8 cells infected at MOI 5 *Rluc* activity was low but still detectable 5 days p.i. (Fig 3.16).

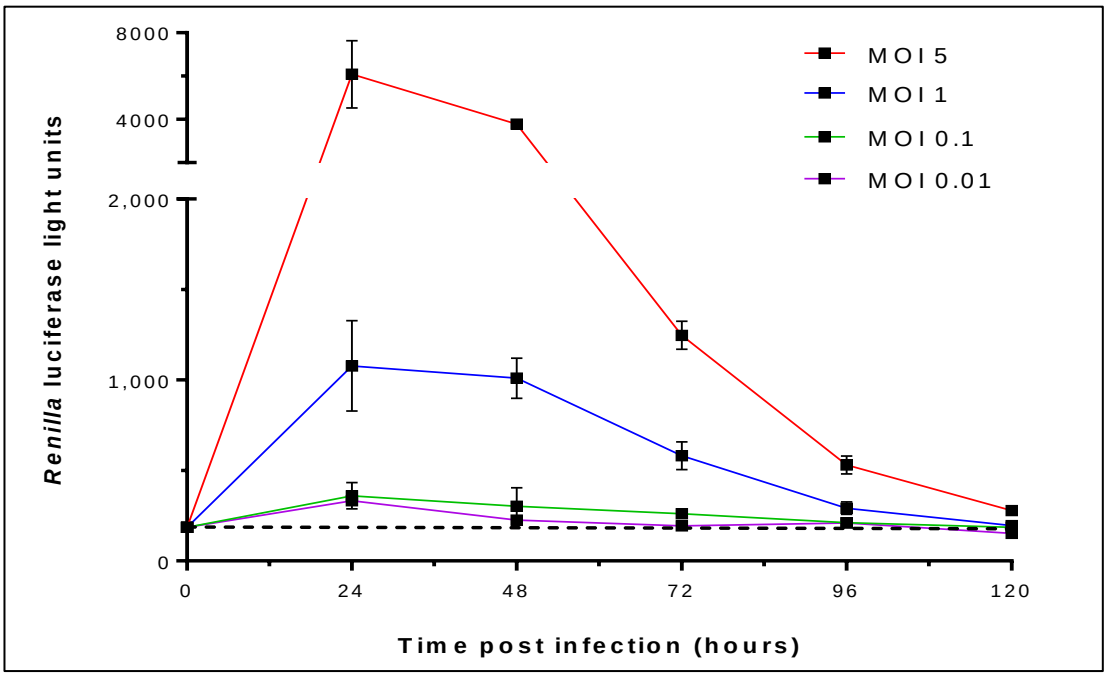

Figure 3.16: *Rluc* activity over five days in IDE8 cells infected with SFV4(3H)-*Rluc* at four different MOIs. Experiment was performed in 24-well plates ($5x10^5$ cells/well). Each data point represents the mean of three replicate cultures. The error bars represent the SD.

As *Rluc* activity of SFV4(3H)-*Rluc* infected cells is a substitute for measuring viral non-structural gene expression, but does not necessarily correlate with viral RNA copy numbers, a second experiment was performed where viral genome and mRNA copies were detected by qPCR. IDE8 cells were infected at MOI 1 and lysed every 24 h over one week for RNA extraction, cDNA synthesis and qPCR (Fig. 3.17). In contrast to *Rluc* activity, viral RNA levels were highest at 48 h p.i. and then decreased approximately 40-fold by 7 days p.i..

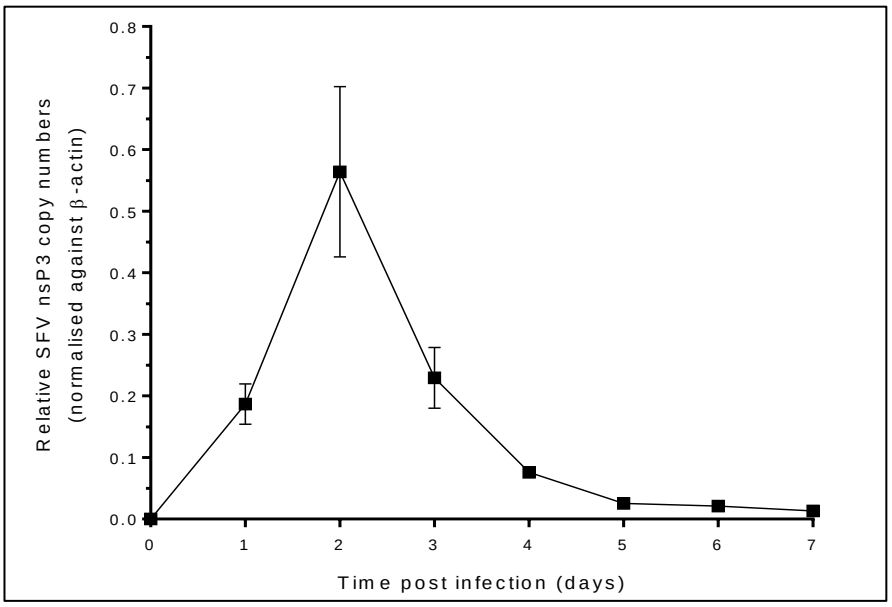

Figure 3.17: SFV nsP3 RNA levels over seven days in IDE8 cells infected with SFV4(3H)-*Rluc* at MOI 1. Experiment was performed in 24-well plates ($1x10^6$ cells/well). Each data point represents the mean of four replicate cultures. The error bars represent the SD.

3.2.8 LGTV infection of IDE8 tick cells

While SFV is a useful tool for many experiments, it is mosquito-borne and has not been shown to be transmitted by ticks. The objective of this study was to compare the response of tick cells to a non tick-transmitted virus and to a tick-transmitted virus. The flavivirus LGTV was chosen as the latter. LGTV is closely related to TBEV and has been isolated from ticks of the species *Ixodes granulatus* (Smith, 1956). LGTV infection was only characterised in IDE8 cells as it was planned to continue working with this cell line only.

Firstly, susceptibility of IDE8 cells to LGTV infection was determined by infection and subsequent immunostaining for LGTV NS5 (Fig 3.18) and NS3 (data not shown). For this IDE8 cells were seeded on coverslips, infected at MOI 1 and fixed with 4% PFA 48 h p.i.. Immunostaining for LGTV NS3 and NS5 was used to visualise infected IDE8 cells by confocal microscopy. While it was possible to conclude that LGTV-infected cells were NS3-positive, background levels of non-specific staining in uninfected cells were high and made visualisation for accurate

counting difficult. Images for counting were thus acquired for cells stained with anti-NS5 antibody (Fig 3.18).

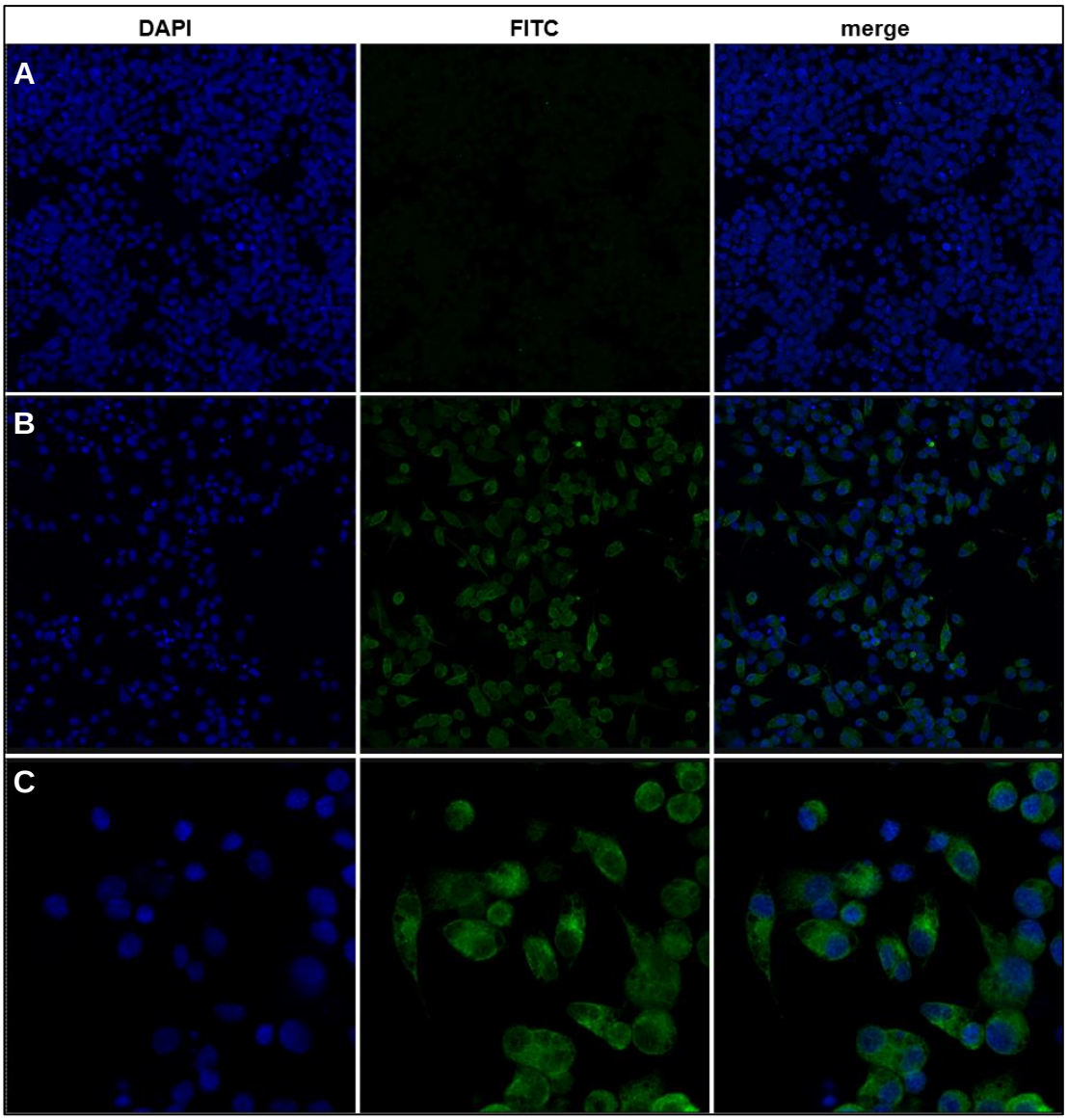

Figure 3.18: LGTV can infect almost all IDE8 cells in a culture. IDE8 cells were seeded on coverslips ($5x10^5$ cells/well) and infected at an MOI of 1 with LGTV. Cells were fixed 48 h p.i., stained for LGTV NS5 and analysed by confocal microscopy. Images show maximum projections of Z-stacks of uninfected IDE8 (A) and infected IDE8 (B) taken with a 10x objective and infected IDE8 taken a 40x objective (C).

Images of three different areas were acquired with a 10x objective of three replicate cultures for each condition. Both total cells and green cells were measured by

counting using the software ImageJ (Table 3.1). On average 97% (±0.83) of cells in IDE8 cultures infected with LGTV were positive for NS5. It could thus be concluded that nearly all cells in an IDE8 culture are susceptible to infection with LGTV.

Table 3.1. Numbers and percentages of green cells in LGTV NS5 immunostaining of IDE8.

	Area 1			Area 2			Area 3		
	No. of green cells	Total no. of cells	%	No. of green cells	Total no. of cells	%	No. of green cells	Total no. of cells	%
Replicate 1	424	440	**96**	145	149	**97**	247	259	**95**
Replicate 2	253	267	**95**	321	331	**97**	94	98	**96**
Replicate 3	518	532	**97**	554	571	**97**	530	540	**98**

In order to determine kinetics of LGTV replication and production, IDE8 cells were infected at MOI 1 or MOI 0.005 and sampled every 24 h p.i. for RNA extraction, cDNA synthesis and qPCR. Cell supernatants were harvested to measure LGTV production by plaque assay. 24 h prior to each time-point, culture supernatant was changed to obtain a virus production curve for the specified 24 h intervals. In addition, supernatant after the first medium change at 1.5 h p.i. was titrated to quantify remaining infectious virus (Fig 3.19B). In parallel, IDE8 cells were also infected at MOI 1 and MOI 0.005 and fixed in suspension every 24 h p.i. for immunostaining to determine the changes in proportion of infected cells over time; however, staining in suspension could not be achieved without a high background signal in uninfected cells so that evaluation of the percentage of infected cells was not possible in the collected samples.

LGTV RNA levels measured by qPCR for a region of NS5 were highest at 2 days p.i. for MOI 1 and 4 days p.i. for MOI 0.005 (Fig 3.19A). LGTV RNA levels in cells infected at MOI 1 increased quickly up to 2 days and then decreased but stayed at a high level over the remaining experimental period. LGTV RNA levels in cells infected at MOI 0.005 were low at 24 h p.i., increased rapidly by 2 days p.i. and then remained at a high level for the rest of the experiment. Virus production peaked for both MOIs at 2 days p.i. and then decreased slightly, but remained around 10^4 PFU/well throughout the experiment. These results are consistent with establishment

of a high-level persistent infection without visible CPE, as shown for LGTV infection of ISE6 cells (Offerdahl et al., 2012); however, no cell viability studies beyond visual assessment were undertaken as part of this study.

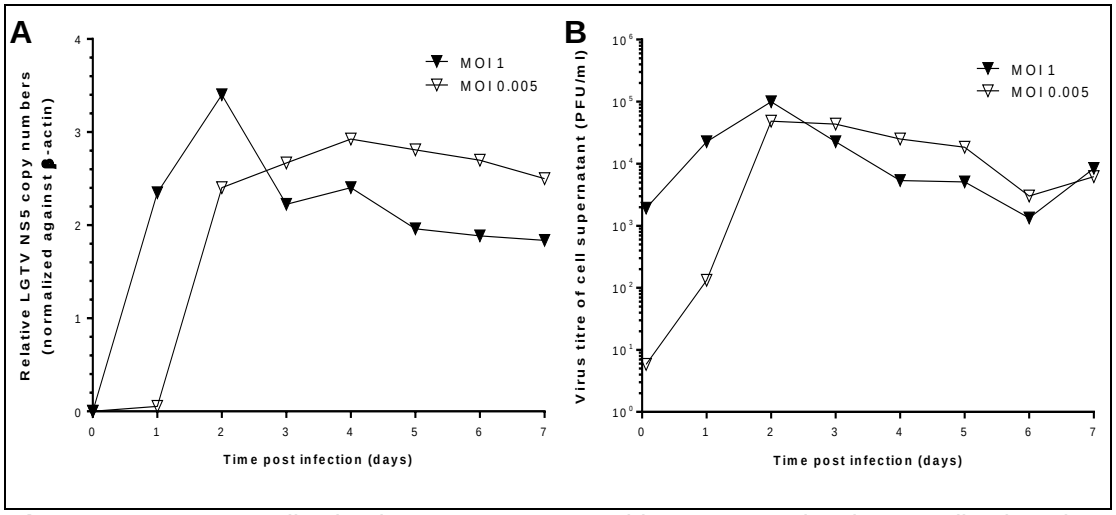

Figure 3.19: LGTV replication in IDE8 as measured by NS5 RNA levels normalised against β-actin (A) and LGTV production in IDE8 measured by plaque assay on BHK-21 cells. Each data point represents the mean of two replicate cultures.

3.2.9 Effects of arbovirus infection on SCRV in IDE8 cells

Persistent infection of IDE8 cells with the orbivirus SCRV virus complicates interpretation of data retrieved from infection experiments with arboviruses, as it is not known how innate immunity controls SCRV and how this may affect subsequent SFV or LGTV replication. However, it also allows investigation of the complex interaction between different viruses in tick cells. Therefore an attempt was made to investigate the effects of SFV and LGTV infection of IDE8 cells on SCRV.

In an initial experiment IDE8 cells were infected with SFV4(3H)-*Rluc* at MOI 1 and MOI 50, RNA was isolated 24 h p.i., cDNA was made by RT-PCR and SCRV RNA levels were determined by qPCR (copy numbers relative to β-actin, normalised using ct values). While there was an increase in relative SCRV RNA compared to β–actin, this increase was not statistically significant at MOI 1. In IDE8 cells infected with SFV at MOI 50 the increase (~2.5-fold) in relative SCRV RNA levels was significant, but this should be interpreted with caution. MOI 50 is a very high MOI

and while β–actin served as a consistent housekeeping gene in other experiments (see 2.12), β–actin ct values were not comparable between conditions in this experiment (β–actin mean ct values: uninfected = 18.4; SFV MOI 50 = 19.4). The observed increase in relative SCRV RNA levels after infection with SFV at MOI 50 could be attributed to a decrease in β–actin RNA levels rather than higher SCRV RNA levels.

For an initial indication of whether LGTV infection of IDE8 cells could have an impact on SCRV replication, samples obtained from the LGTV time course of infection with MOI 1 (Figure 3.19) were used for qPCR to quantify SCRV RNA levels (Fig 3.20A). Up to day 4 p.i. SCRV levels stayed consistent, but at 5 days p.i. there was a 5.5-fold increase in relative SCRV copy numbers which persisted to day 7 p.i.. The limitation of this experiment was the lack of an uninfected control over all time-points, to see whether SCRV levels would change over the course of one week independent of LGTV infection. In addition the changing of medium 24 h before sampling may have affected results, as adding fresh medium may have affected for example cell proliferation or pH of the medium indirectly influencing SCRV replication.

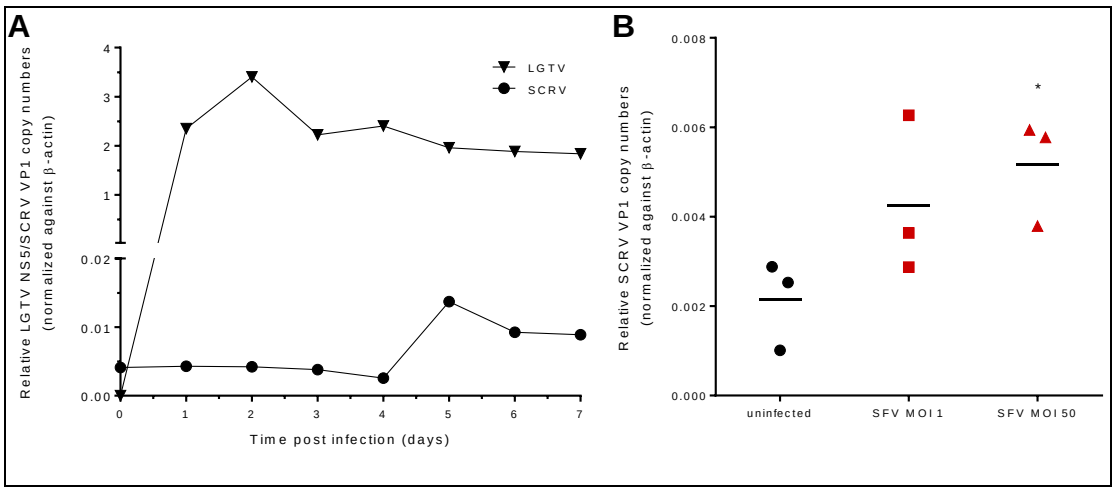

Figure 3.20: LGTV and SCRV RNA levels after infection with LGTV at MOI 1 (A) and SCRV RNA levels 24 h p.i. with SFV4(3H)-*Rluc* (B). Each data point represents the mean of two (A) or three (B) individual replicates. Statistical significance (B) was determined by Student's t-test and is indicated as follows: * p<0.05.

Considering the limitations of both initial experiments, another time course of SFV and LGTV infection with 4 replicates per time-point was performed. IDE8 cells were mock-infected, infected with SFV (MOI 1) or infected with LGTV (MOI 1). Cells were harvested on days 1-5 and 7 p.i., RNA was extracted, cDNA synthesised and analysed by qPCR for SFV, LGTV and SCRV RNA levels (Fig 3.21). LGTV RNA levels were higher than SFV levels throughout the experiment (Fig 3.21A). Replication of both SFV and LGTV peaked at 48 h p.i. and then decreased.

In the uninfected control samples, relative SCRV RNA levels (normalised to β-actin) showed only little variation over the 7 day experimental period (Fig 3.21B). Following SFV or LGTV infection, there was a significant increase in SCRV RNA levels 4 days later. The increase in SCRV RNA levels was greatest at 5 days p.i. and higher in LGTV infected cells (up to 6.8-fold) than in SFV infected cells (up to 2.3-fold). In conclusion, infection of IDE8 cells with SFV or LGTV affected SCRV replication from 4 days p.i., while there was no significant difference during the first 3 days p.i..

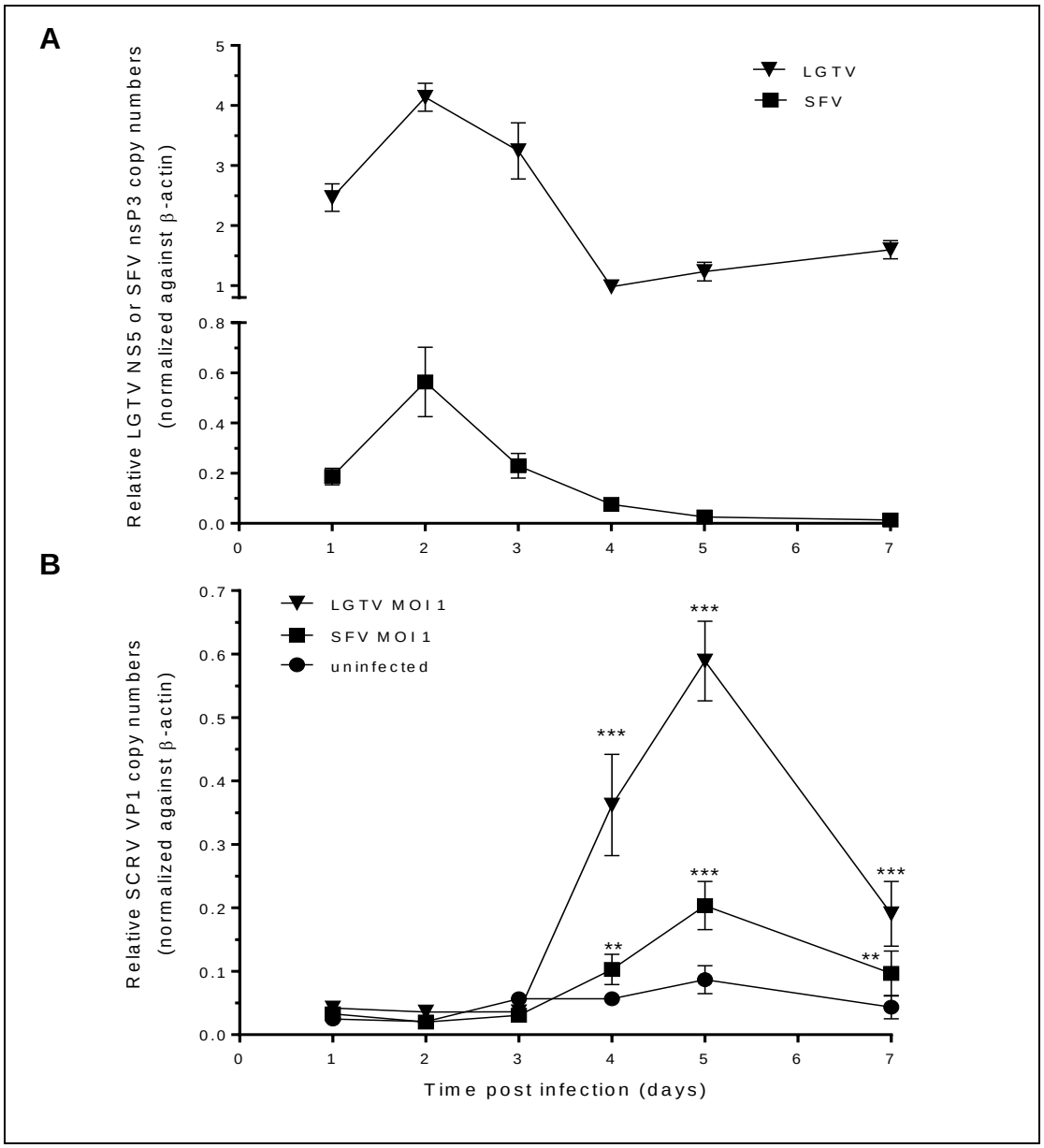

Figure 3.21: SCRV replication in IDE8 cells infected with LGTV or SFV. (A) LGTV NS5 and SFV nsP3 levels over 7 days p.i. as indication of virus replication. (B) SCRV levels during infection with SFV and LGTV compared to uninfected control cultures. Each data point represents the mean of four replicate cultures. Error bars indicate SD. Statistical significance was determined by two-way ANOVA with multiple comparisons between SFV or LGTV infected samples and uninfected control samples; it is indicated as follows: ***p≤0.0001; **p<0.01; *p<0.05.

3.2.10 Summary of results

- SFV4(3F)-ZsGreen infection of IRE11 and ISE18 results in a punctate ZsGreen distribution, similar to that seen in mammalian or mosquito cells
- Like IDE8 cells, both ISE18 and IRE11 cells harbour endogenous viruses
- Approximately 80% of ISE18, 4% of IRE11 and 50% of IDE8 cells expressed detectable levels of ZsGreen after infection with SFV4(3F)-ZsGreen (MOI 10) as measured by flow cytometry for ISE18 and IRE11, and microscopy for IDE8
- *Rluc* activity in ISE18, IRE11 and IDE8 cells infected with SFV4(3H)-*Rluc* was highest at 24 h p.i. and decreased thereafter; *Rluc* activity was comparable between ISE18 and IDE8 cells, but generally lower in IRE11 cells
- Both ISE18 and IRE11 expressed ZsGreen by 12 h p.i. with SFV4(3F)-ZsGreen
- ISE18 produced infectious SFV particles by 12 h p.i. with SFV4(3F)-ZsGreen; whether or not IRE11 produce infectious SFV particles remains unclear
- 97% of IDE8 cells were susceptible to infection with LGTV and virus replication was high with a peak in RNA levels at 48 h p.i. for cells infected at MOI 1 and 96 h p.i. for cells infected at MOI 0.005; LGTV was produced in IDE8 by at least 24 h p.i. (no earlier time-points were investigated) and peaked at 48 h p.i. for both MOI 1 and MOI 0.005
- SCRV RNA levels increased from 4 days p.i. with SFV and LGTV compared to uninfected controls; the increase in SCRV RNA levels was higher in LGTV-infected compared to SFV-infected cells

3.3 DISCUSSION

In the first part of this PhD study, experimental conditions for working with tick cells were established. Learning to work with tick cells took time and patience as growth of tick cells is much slower than that of mammalian cells and frequent subculture (more than every two weeks) can be problematic depending on the cell line and may

result in loss of the culture. IDE8 could be subcultured quite frequently; on occasion weekly subculture was possible without affecting health and growth of the cells (visual assessment). For large scale experiments the use of 24-well plates as opposed to flat-sided culture tubes is preferable, yet use of 24-well plates had to be established and despite the use of plastic bags to reduce air exchange and a wet tissue to create a humid environment, 24-well plates remained unsuitable for use with the tick cell line IRE11. Other difficulties included for example the high autofluorescence of some cell lines, which made fluorescence microscopy experiments more challenging. While autofluorescence in ISE18 could be considered negligible, IRE11 and IDE8 cells had high levels of autofluorescence. The cause of these high levels of autofluorescence remains unknown, but could also be observed in other arthropod cells, such as the mosquito cell line Aag2 (data not shown). Furthermore, ISE18 often grow three-dimensionally into large clumps, which also affected for example the ability to easily assess ZsGreen-positive cells by fluorescent microscopy. However, flow cytometry proved to be a good solution to this problem, since cell clumps were mostly broken up by pipetting the cells off the tubes prior to fixation. For ISE18 flow cytometry allowed a fairly accurate quantification of infected cells. For IDE8 neither flow cytometry nor fluorescence microscopy were ideal to determine the percentage of infected cells, but it was possible to get a rough idea of susceptibility to SFV infection.

It was also observed that, compared to most other cells, the tick cell lines used in this study were more resistant to many lysis buffers, including passive lysis buffer for luciferase samples and Nonidet™ P40 lysis buffer, used to lyse samples for SDS-PAGE. To achieve efficient lysis for luciferase assay, the incubation time on a shaker was increased 4-fold from 15 min for mammalian and mosquito cells (manufacturer's instructions) to 1 h for tick cells (see 2.7).

These first experiments were essential to establish experimental conditions and gain experience in performing virus infections of tick cells. Investigating SFV infection of three different cell lines revealed many similarities and differences. While all cell lines were susceptible to virus infection, infection efficiency varied greatly between IRE11 and the two *I. scapularis* cell lines. Both percentage of infected cells and *Rluc*

activity were lower in infected IRE11 cultures than in ISE18 and IDE8 cells, which were comparable in infection levels and kinetics of *Rluc* activity. One reason for this variation could be a difference in species susceptibility. However, in another *I. ricinus* cell line, IRE/CTVM19, up to 70% of cells can be infected with SFV (Sabine Weisheit, personal communication), indicating that it is not a simple species-specific difference. More likely it is due to the heterogeneity of the cells in culture – it is possible that certain cell types are not susceptible to SFV infection and that in IRE11 these cells are in the majority. Unfortunately, very few antibodies are available for ticks; otherwise cell type-specific antibodies could have been used to identify the tissue origin of the susceptible and the non-susceptible cells. Another possible reason for the low infection levels in IRE11 could be a very strong antiviral immune response. It is possible that antiviral responses are pre-activated in IRE11 due to the presence of at least two endogenous viruses (see Figure 3.2 and Lesley Bell-Sakyi, personal communication). While it would have been interesting to investigate why only few IRE11 cells can be infected with SFV, it was concluded that IRE11 were unsuitable for the purpose of this study due to the difficulties described in 3.2.7.

The cell line selected for further studies, IDE8, supported growth of both SFV and LGTV. The kinetics of LGTV production in IDE8 were comparable to kinetics previously shown for LGTV infection of the *Rhipicephalus appendiculatus* cell line RA-243 (Leake et al., 1980) and the *I. scapularis* cell line ISE6 (Offerdahl et al., 2012). LGTV infection levels in IDE8 were higher than those of SFV. LGTV is a tick-borne virus which naturally infects, and has therefore been selected to replicate in, *Ixodes* spp ticks as opposed to SFV which is naturally mosquito-borne; however, much higher SFV infection levels can be achieved in other tick cell lines such as BDE/CTVM16 (Barry et al., 2013). Both viruses were titrated on BHK-21 cells and the MOI was calculated based on BHK-21-infectious units. Differences in susceptibility of BHK-21 cells to SFV and LGTV may result in variations in the number of viruses capable of infecting IDE8 cells when using the same BHK cell-derived MOI.

Unlike the cell lines ISE18 and IRE11 which are persistently infected with unknown viruses, use of IDE8 at least allowed quantification of its known endogenous

orbivirus SCRV to determine whether subsequent infection with an alphavirus or a flavivirus affects the persistent SCRV infection. Interestingly, infection with both SFV and LGTV did affect replication of SCRV, leading to an increase in SCRV RNA levels 4 days later. While it is possible that this increase in SCRV RNA was caused by nonspecific responses to arbovirus infection, such as differences in cell proliferation, cell cycle and cell stress responses, it is also possible that the increased replication was caused specifically by the modulation of ongoing antiviral responses as a result of the second virus infection. That SCRV RNA levels increased as SFV and LGTV RNA were brought under control (Figure 3.21) is consistent with a competitive control response not an additive one. That is, whatever is controlling the SCRV RNA levels is not augmented by the second virus but is diverted to controlling the second virus allowing SCRV some escape from the controlling cellular responses. One likely candidate for such a response is the RNAi system (Garcia et al., 2005; Garcia et al., 2006). If the persistent SCRV infection is generally controlled by the RNAi response, adding a new virus that is also controlled by antiviral RNAi may result in a saturation of the RNAi machinery allowing SCRV to replicate to higher levels. An alternative is that SFV and/or LGTV encode a suppressor of an antiviral response such as RNAi, which controls SCRV replication (Fragkoudis et al., 2009; Kakumani et al., 2013; Schnettler et al., 2012). A third possibility is that SCRV benefits from certain cellular mechanisms triggered by SFV and LGTV and that these mechanisms indirectly assist SCRV replication.

Important for this project, however, was the fact that SCRV RNA levels were not significantly affected during the first three days p.i. with LGTV and SFV. Thus it is unlikely that changes in SCRV RNA levels could affect LGTV and SFV replication and production early in infection. However, the possibility remains that the presence of SCRV in these cells affects arbovirus infections and that ‘sterile’ uninfected tick cells, if these exist, could have different kinetics of SFV and LGTV replication and production.

In conclusion, the cell line IDE8 was chosen for use in subsequent studies. IDE8 cells were susceptible to SFV and LGTV infection, with at least 50% of cells susceptible to infection with SFV and approximately 97% of cells susceptible to

infection with LGTV. Suitable sampling time-points and MOIs were determined for the two viruses in IDE8 cells. For infection with SFV, sampling at 24 h p.i. was suitable for most experiments using *Rluc* activity as a read-out and 24 or 48 h p.i. for experiments using qPCR as a read-out. For infection with LGTV, sampling at 48 h p.i. was suitable for most experiments. When looking at antiviral defences, a very high MOI can hide effects due to the inability of the cells to control a very high level infection. Thus for most experiments MOI 1 was chosen as a high MOI since multiple infections per cell should be at a minimum compared to MOI ≥5. Subsequent experiments using SFV4(3H)-*Rluc* and *Rluc* activity as a read-out were mostly performed using MOI 1 since *Rluc* activity in cells infected at a lower MOI could be difficult to detect. For infection with LGTV MOI 1 was chosen for high MOI experiments and, in most experiments, MOI 0.005 for infection at a low MOI.

4. Identification of innate immunity signalling pathways in tick cells

4.1 INTRODUCTION

Antiviral responses of arthropods were described in the introduction to this thesis (see 1.4). The aim of this chapter was firstly to identify putative tick orthologues of proteins involved in the innate immunity signalling pathways of insects, and secondly to investigate whether these proteins play a role in controlling virus replication in tick cells. Ticks belong to the *Chelicerata* and are quite basal in the phylum *Arthropoda*. Dipteran insects including mosquitoes and *D. melanogaster* are higher insects (Fig 4.1). Insects and ticks are therefore considerably distant in evolution and may have evolved different responses to virus infections.

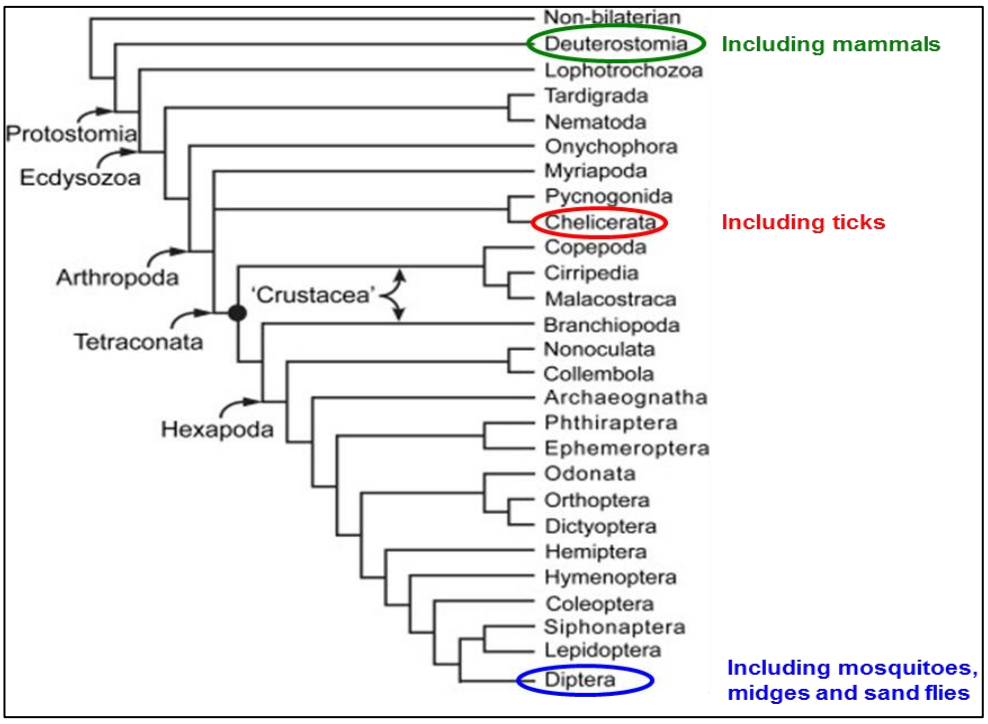

Figure 4.1: Phylogenetic tree of major animal lineages inferred from maximum likelihood analysis based on highly conserved regions from genes of the nervous system (adapted from Andrew, 2011). Ticks as members of the *Chelicerata* are considered basal in the phylum Arthropoda. Most other arthropod vectors, such as mosquitoes, midges and sand flies belong to the order *Diptera* within the class *Hexapoda/Insecta* and are considered 'higher insects' which have evolved rapidly.

Many proteins have evolved rapidly in dipteran insects and may differ substantially from those in ticks. Furthermore, it cannot be concluded that sequence and function

of orthologues have been conserved between ticks and insects. However, it is likely that the general composition of the immune system in arthropods is conserved and that ticks, as haematophagous ectoparasites, come across immune challenges similar to those experienced by mosquitoes and midges. Thus the starting hypothesis of this project is that most immunity pathways of insects also exist in ticks. As it has already been shown that ticks have an antiviral RNAi response (Garcia et al., 2005; Garcia et al., 2006; Kurscheid et al., 2009; Schnettler et al. 2014, submitted), the focus of this chapter was to determine whether other innate immunity pathways identified in insects exist and have an antiviral function in tick cells. As many signalling pathways in insects are activated by bacterial PAMPs, initial experiments were performed to see whether pre-exposure of tick cells to Gram-negative bacteria affected subsequent SFV replication. Furthermore, the components of a variety of putative immunity pathways were identified and, for selected pathways, their potential antiviral role was investigated.

4.1.1 Objectives

- Investigate the effect of pre-exposure or pre-infection of tick cells with Gram-negative bacteria on subsequent SFV replication
- Determine whether there is antiviral PO activity in tick cells
- Identify components of innate immunity signalling pathways in *I. scapularis*
- Determine whether these are expressed in selected *Ixodes* spp. tick cell lines
- Determine their role in SFV, LGTV and SCRV replication

4.1.2 Experimental design

Initial experiments

For the initial experiments investigating the effect of pre-exposure or pre-infection with Gram-negative bacteria on SFV replication, IDE8 and ISE6 cells were used. Heat-inactivated *E. coli* were used to pre-treat cells as described in the Materials and Methods chapter (see 2.21) and the respective Results section of this chapter. Experiments investigating pre-infection with the intracellular bacterium *Ehrlichia*

ruminantium were performed as described in the respective Results section and Moniuszko et *al*. (2014) which is attached at the end of this thesis.

Melanisation experiments

Experiments investigating the existence and putative antiviral role of PO in tick cells were performed with guidance from Julio Rodriguez-Andres (University of Edinburgh; now AAHL, CSIRO, Geelong) and methods were adopted from his publication on the antiviral role of mosquito PO (Rodriguez-Andres et al., 2012). He kindly provided the necessary buffers and aliquots of viruses described in the respective results section.

Identification of innate immunity signalling pathways

Orthologues of known microbial response pathway components were first identified using the online BLAST as provided by the NCBI on their website (http://blast.ncbi.nlm.nih.gov/Blast.cgi). BLAST identifies regions of local similarity between a nucleotide or protein query sequence and sequences within a given database. It calculates the statistical significance between matches and provides a table format ranking of the closest matches (i.e. in this study, the most likely orthologues). BLAST was used in an attempt to identify functional and evolutionary relationships using insect and other arthropod query sequences to search the *I. scapularis* nucleotide and protein databases.

There are five types of BLAST searches (http://blast.ncbi.nlm.nih.gov/Blast.cgi):

- blastn: nucleotide blast; searches a nucleotide database using a nucleotide query
- blastp: protein blast; searches a protein database using a protein query sequence
- blastx: searches a protein database using a translated nucleotide query
- tblastn: searches a translated nucleotide database using a protein query
- tblastx: searches a translated nucleotide database using a translated nucleotide query

The BLAST searches used in this project were mainly blastp and tblastn. Blastp was used to identify similarity between query sequences and putative *I. scapularis* orthologues, while tblastn was used for higher sensitivity, as it could identify nucleotide sequences without a matching protein sequence. Protein sequences were used for BLAST search instead of nucleotide sequences, as codon usage may vary between different species and using nucleotide queries (blastn) may significantly lower the likelihood of finding orthologues. All protein sequences used for BLAST searches can be found in the Materials and Methods section of this thesis (Table 2.3).

Upon identification of putative orthologues, gene expression was investigated in *I. scapularis* and *I. ricinus* tick cell lines by RT-PCR using sequence-specific primers (Table 2.1 and Table 2.5) and RNA extracted from the cell lines (see 2.9-2.11). When orthologues were found to be expressed, dsRNA was generated using cDNA from IDE8 cells (see 2.14) and used for knockdown experiments (Fig 4.2).

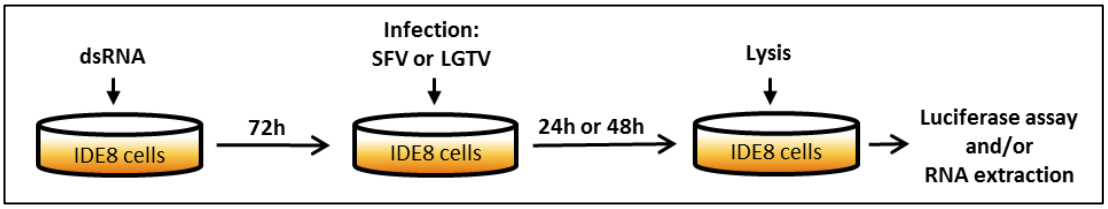

Figure 4.2: General experimental design for knockdown experiments. Cells were seeded at $5x10^5$ cells/well in 24-well plates and, 24 h after seeding, 400 ng dsRNA were added per well (see also 2.14). Different MOIs were used as specified in the Results sections for each experiment.

Due to the many different immunity pathways that the present study covered and time limitations, only selected pathways and components were investigated in knockdown experiments.

4.2 RESULTS

4.2.1 Effect of pre-treatment or pre-infection with Gram-negative bacteria on SFV replication

Many of the signalling pathways which also have an antiviral role are primarily antibacterial in insects. Activating these defences in U4.4 mosquito cells using heat-inactivated bacteria has been shown to affect SFV replication (Fragkoudis et al., 2008). Heat-inactivated *E. coli* expose the cells and any cell-derived molecules in the cell supernatant to bacterial PAMPs including for example lipopolysaccharide (LPS). In insect cells these PAMPs have been shown to activate immunity pathways such as JAK/STAT and Imd (Fragkoudis et al., 2008; Wang et al., 2006). In U4.4 cells it has also been shown that secreted PPO in the cell culture supernatant can be activated by SFV or heat-inactivated *E. coli* and that PO has antiviral activity against SFV (Rodriguez-Andres et al., 2012).

In an attempt to see whether a similar effect can be observed in tick cells, IDE8 cells were pre-treated with heat-inactivated *E. coli* either 2 h or 10 min before infection with SFV (see 2.21). Cells were infected at MOI 1 either by addition of 50 µl SFV4(3H)-*Rluc* suspension directly into the cell supernatant (Fig 4.3 medium) or by removal of cell supernatant and addition of 300 µl PBSA containing SFV4(3H)-*Rluc* (Fig 4.3 PBSA). Cells were lysed 24 h p.i. and *Rluc* activity was measured. As a positive control U4.4 cells were treated identically in a parallel experiment.

In U4.4 cells, significantly higher ($p<0.0001$) *Rluc* activity was observed in cells infected by removing the medium and replacing it with PBSA containing SFV4(3H)*Rluc*, compared to cells infected by adding SFV directly to the medium (data not shown). PPO and any other antiviral agents present in the cell supernatant would have been removed with the medium prior to infection in PBSA. The increase could be partially caused by the more efficient infection in a smaller volume used during infection with PBSA. Pre-treatment of U4.4 cells with heat-inactivated *E. coli* resulted in a significant reduction in *Rluc* activity compared to the non-treated control (NTC) both in cells infected by virus addition to the medium (78% reduced)

and in cells infected with virus in PBSA (74% reduced) (Fig 4.3A). Adding the bacteria 2 h or 10 min before infection made no difference (Fig 4.3A). These results were consistent between two independent experiments and with previously published results (Fragkoudis et al., 2008).

In IDE8 cells, the results varied between the two experiments performed. Higher *Rluc* activity was observed in non-treated IDE8 control cells infected by addition of SFV to the medium compared to cells infected by incubation with PBSA in one out of the two experiments. In the other experiment, infection in medium or PBSA resulted in similar levels of *Rluc* activity (data not shown). In cells treated with heat-inactivated *E. coli* and infected by addition of SFV into the medium, there was a significant reduction in *Rluc* activity compared to the NTC cells (Fig 4.3B). *Rluc* activity was reduced by 39% in cells treated for 10 min and by 24% in cells treated for 2 h prior to infection. In IDE8 cells infected in PBSA, pre-treatment with *E. coli* did not have a significant effect on *Rluc* activity.

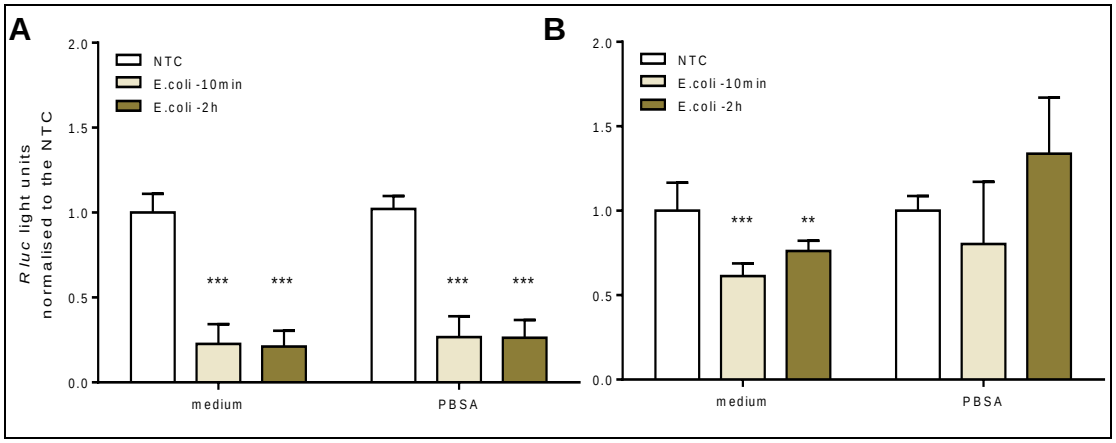

Figure 4.3: Effects on SFV-driven *Rluc* activity of pre-treatment with heat-inactivated *E. coli* in mosquito and tick cells. U4.4 mosquito cells (A) and IDE8 tick cells (B) were not treated (NTC) or treated with heat-inactivated *E. coli* 10 min or 2 h prior to SFV infection. Cells were then infected with SFV4(3H)-*Rluc* at MOI 1, either by adding 50 µl virus dilution directly into the cell culture medium (no removal of *E. coli* containing medium) or by removing the medium and adding 300 µl of virus diluted in PBSA for 1 h before adding 1 ml of fresh medium. Cells were lysed 24 h p.i. and *Rluc* activity was measured and normalised to the NTC. Each data point represents the mean of seven individual samples derived from two individual experiments; error bars represent the standard deviation (SD). Statistical significance was determined by one-way ANOVA with multiple comparisons each to the NTC (Fisher's LSD) as indicated (***p≤0.0001; **p<0.01).

Another experiment was performed with IDE8 cells as described above, except that the effects of treatment with bacteria on SFV, LGTV and the endogenous orbivirus SCRV were investigated in parallel. Cells were pre-treated with heat-inactivated *E. coli* as described above and parallel cultures were either not infected, or infected at MOI 0.1 with either SFV4(3F)-ZsGreen or LGTV by addition of 50 µl virus suspension directly into the culture medium. 24 h p.i. cells were lysed, RNA was extracted, cDNA was prepared and levels of RNA transcripts of SCRV segment 1 (VP1 gene), SFV nsP3 and LGTV NS5 were analysed by qPCR. Pre-treatment with *E. coli* did not have a significant effect on SCRV, SFV or LGTV replication in IDE8 cells (Fig 4.4). The previous experiments (Figure 4.3) were performed with *Rluc* activity as a measure for virus replication. However, having shown that RNA levels, a more accurate measure of virus replication, are unaffected (Fig 4.4), it is possible that the previously observed effect on *Rluc* activity was due to differences in viral gene expression rather than RNA replication.

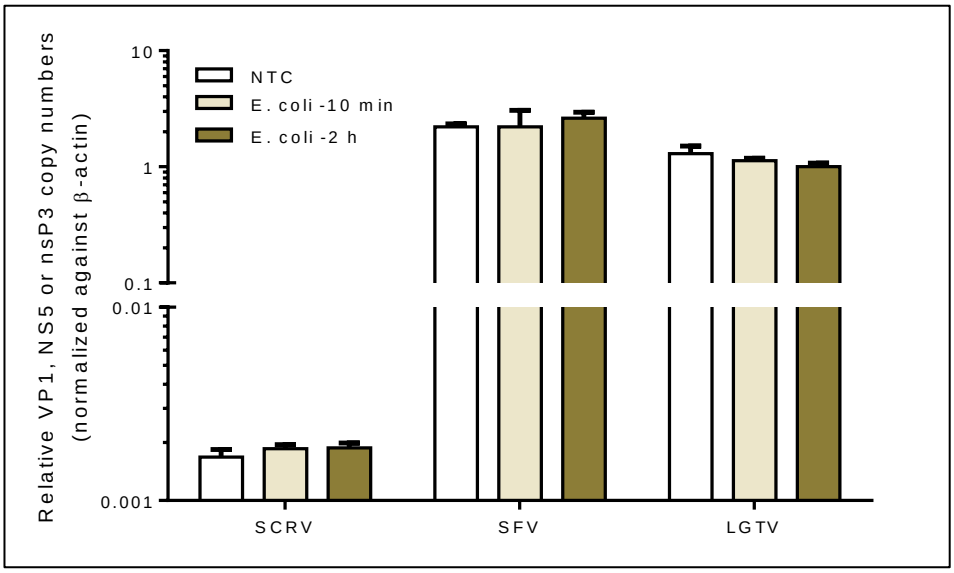

Figure 4.4: Effects of pre-treatment with heat-inactivated *E. coli* prior to infection on SCRV, SFV and LGTV replication in IDE8 cells. IDE8 cells were not infected (SCRV), infected with SFV4(3F)-ZsGreen (SFV) or infected with LGTV at MOI 0.1, by adding 50 µl virus dilution directly into the cell culture medium. Prior to infection cells were not treated (NTC) or treated with heat-inactivated *E. coli* 10 min or 2 h prior to infection. Each data point represents the mean of three individual samples; the error bars represent the standard deviation (SD).

An interesting observation was made in an experiment performed as part of a separate study (Moniuszko et al., 2014). Cells of the *I. scapularis* cell line ISE6 were infected with the obligate intracellular tick-borne bacterium *E. ruminantium* and SFV separately and as a co-infection to investigate whether co-infection of these two pathogens affected replication of either of them. This experiment was performed with assistance from Lesley Bell-Sakyi who infected (or mock-infected) ISE6 cells with semi-purified *E. ruminantium* 7 days prior to infection with SFV4(3H)-*Rluc* and Pilar Alberdi who extracted DNA and measured replication of *E. ruminantium* by qPCR. Cells were infected with SFV4(3H)-*Rluc* at MOI 5 and lysed 24, 48 and 72 h p.i. with SFV for luciferase assay (Fig 4.5). Pre-infection with *E. ruminantium* resulted in a significant increase in *Rluc* activity across all time-points ($p \leq 0.01$, two-way ANOVA), and individually at 24 h ($p \leq 0.0001$) and 48 h ($p \leq 0.01$) p.i. as determined by multiple comparisons (Fisher's LSD). In a second experiment, cells were first infected with SFV4(3H)-*Rluc* at MOI 5 and 48 h later with *E. ruminantium*. However, neither of the two microorganisms was significantly affected by co-infection compared to individual infections in this experiment (Moniuszko et al., 2014).

Overall, these two initial experiments indicate that pathways activated by bacteria can also affect SFV replication in tick cells. Priming of IDE8 tick cells with inactivated bacteria had no effect on virus replication, but reduced viral non-structural gene expression as measured by luciferase activity. Established active intracellular bacterial replication increased virus driven luciferase levels in ISE6 cells.

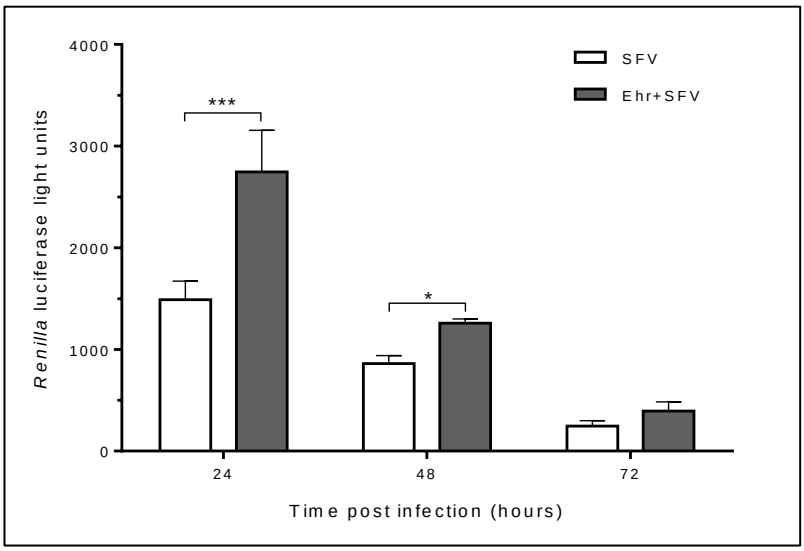

Figure 4.5: ISE6 cells infected with *E. ruminantium* (Ehr) or mock-infected 7 days prior to infection with SFV4(3H)-*Rluc* at MOI 5. Cells were lysed 24, 48 and 72 h p.i. with SFV. Each data point represents the mean of three individual samples; the bars represent the standard deviation (SD). Representative of two independent experiments. Statistical significance was determined by two-way ANOVA with multiple comparisons and is indicated as follows: ***p≤0.0001; *p<0.05.

4.2.2 Is there melanisation in tick cells?

The role of PO, a key enzyme of the melanisation cascade, in controlling alphavirus infection in mosquitoes was described in the Introduction (see 1.4.3). In ticks the existence of the precursor protein pro-phenoloxidase (PPO) and the melanisation pathway is still undetermined. In an attempt to identify a putative orthologue with PO activity in ticks, BLAST searches of proteins with PO activity from different organisms were performed. From insects, two different *D. melanogaster* and one *Ae. aegypti* PPO sequences were used for BLAST search against the *I. scapularis* protein and nucleotide databases (blastp & tblastn), but no orthologues were found. In horseshoe crabs, hemocyanin has PO activity (Coates et al., 2011), so the hemocyanin sequence of the horseshoe crab *Limulus polyphemus* was also used for BLAST search of the *I. scapularis* protein database, but again no orthologues were found.

Pilot experiments were performed to investigate whether tick cell culture supernatant contains an enzyme similar to PPO and to see whether it would be worth pursuing

investigations on tick melanisation. The experiments were performed using the cell line ISE18. Supernatant of ISE18 tick cell cultures was collected, treated with live *E. coli* (Dh5α) or SFV for 5 min and a PO activity assay was performed as described previously (Rodriguez-Andres et al., 2012). The experiment was performed three times. The results were inconclusive, due to high levels of variation in the controls, and it was not possible to determine whether *E. coli* or SFV caused any increase in PO activity in tick cell culture supernatant (data not shown).

In another set of pilot experiments, ISE18 tick cells were infected with SFV4 constructs encoding either ZsGreen or firefly luciferase (*FFluc*) and expressing either the forward (Egf1.0F) or the reverse (Egf1.0R) sequence encoding the protein Egf1.0 under a second subgenomic promoter (Rodriguez-Andres et al., 2012). The forward sequence drives expression of Egf1.0, whereas the reverse sequence was cloned as a control and should not result in protein expression. Egf1.0 is an inhibitor of PO activity expressed by the insect pathogen *Microplitis demolitor* bracovirus (Lu et al., 2008). The virus constructs were generated by Julio Rodriguez-Andres based on SFV4(3F)-Zsgreen or SFV4(3H)-*FFluc* (Fig 4.6A/B). The virus stocks, which were kindly provided by Julio Rodriguez-Andres, were re-titrated on BHK21-cells prior to use, to enable use of accurate BHK21-infective units comparable between the viruses encoding the forward and reverse Egf1.0 sequences.

First, ISE18 cells were infected with either SFV4(3F)-ZsGreen-Egf1.0F or SFV4(3F)-ZsGreen-Egf1.0R at either MOI 0.5 or MOI 0.05 in triplicate, fixed 24 h p.i. and analysed for green fluorescence by flow cytometry (see 2.8.1). Infection with SFV4(3F)-ZsGreen-Egf1.0R, encoding the reverse sequence of Egf1.0, resulted in a small increase in the proportion of infected cells compared to infection with SFV4(3F)-ZsGreen-Egf1.0F, encoding the forward sequence of Egf1.0 (Fig 4.6C). This result was comparable to infection of BHK-21 cells (Julio Rodriguez-Andres, personal communication). Similarly, infection of ISE18 cells with SFV4(3H)-*FFluc*-Egf1.0R resulted in increased levels of *FFluc* activity in cell lysates compared to lysates of cells infected with SFV4(3H)-*FFluc*-Egf1.0F both for MOI 10 (Fig 4.6D) and MOI 1 (Fig 4.6E). This is again in accordance with what was observed after infection of BHK21-cells with the two viruses (Julio Rodriguez-Andres, personal

communication), indicating a small replicative disadvantage of the virus expressing functional Egf1.0. Importantly, expression of Egf1.0 had no benefit for virus replication or spread in ISE18 tick cells, suggesting that if the melanisation system exists, it is not effective against SFV or Egf1.0 is not an effective inhibitor of this system in ISE18 tick cells. While it may be worth investigating other tick cell lines, studies on melanisation were discontinued after the initial experiments to allow greater focus on other putative immunity pathways.

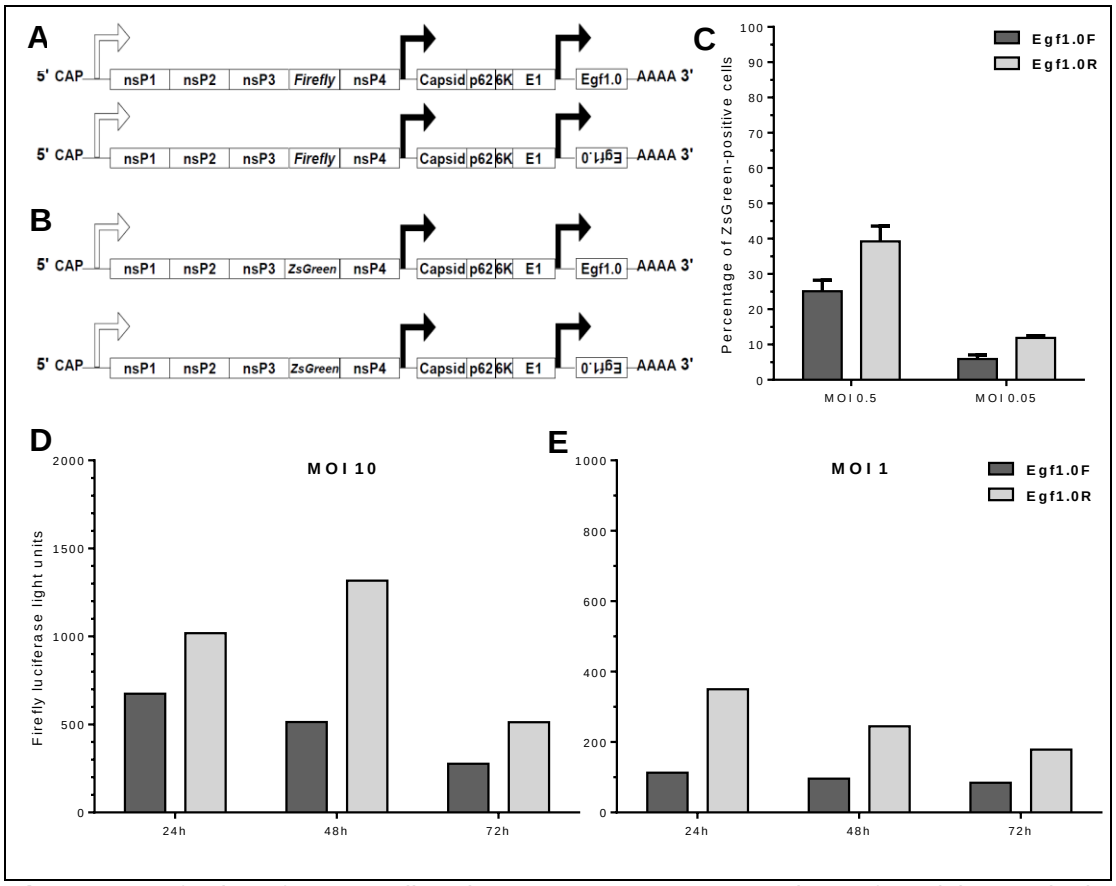

Figure 4.6: Infection of ISE18 cells using SFV constructs expressing Egf1.0. (A) SFV4(3H)-*FFluc*-Egf1.0F (top) and SFV4(3H)-*FFluc*-Egf1.0R (bottom) encoding the reporter gene *FFluc* and Egf1.0 either in forward or reverse orientation. (B) SFV4(3F)-ZsGreen-Egf1.0F (top) and SFV4(3F)-ZsGreen-Egf1.0R (bottom) encoding the reporter gene ZsGreen and Egf1.0 either in forward or reverse orientation (from Rodriguez-Andres et al. 2012). (C) Percentage of ZsGreen-positive cells 24 h p.i. with SFV4(3F)-ZsGreen-Egf1.0F/R at MOI 0.5 and MOI 0.05. Each data point represents mean values of triplicate cultures. Error bars represent standard deviation. (D) *FFluc* activity 24 h p.i. with SFV4(3H)-*FFluc*-Egf1.0F/R at MOI 10. Each data point represents mean values of duplicate cultures. (E) *FFluc* activity 24 h p.i. with SFV4(3H)-*FFluc*-Egf1.0F/R at MOI 1. Each data point represents mean values of duplicate cultures.

4.2.3 The Imd pathway appears to be incomplete in the *I. scapularis* genome

D. melanogaster Imd is a small protein of 273 aa length with a death domain (DD) towards its C-terminus for protein-protein interactions. Imd protein sequences from two different insect species (*D. melanogaster*, *Ae. aegypti*) and a crustacean species (*Litopenaeus vannamei*) were used for a BLAST search against the *I. scapularis* protein and nucleotide database, but no orthologue was found (blastp and tblastn).

Other components of the Imd and related pathways were investigated. The downstream effect of Imd activation in insects is activation of the NFκ-B-related transcription factor Relish (Rel). Using the *D. melanogaster* Rel sequence (DmRel) a putative orthologue was sought using BLAST. Two putative Rel/NFκ-B orthologues were identified (Table 4.1). However, one of the orthologues had more similarity with the NFκ-B-like transcription factor Dorsal, which is activated by the Toll pathway. No further orthologues were identified by BLAST search using the NFκ-B (Wang et al., 2006) or Rel (Fan et al., 2008) sequences of the horseshoe crab *Carcinoscorpius rotundicauda*, which is more closely related to ticks than *D. melanogaster*. As with Rel in other arthropods, CrNFκ-B is also activated upon infection with gram-negative bacteria, yet no Imd has been identified in horseshoe crabs (Wang et al., 2006).

Table 4.1: Putative orthologues of Imd pathway components identified by BLAST search of the *I. scapularis* protein database using *D. melanogaster* protein sequences.

Query sequence	*Ixodes* orthologue	Query Coverage	Max. Identity	Length (aa)	mRNA accession no.	Protein accession no.
DmRel	IxRel	26%	32%	349	XM_002434459.1	XP_002434504.1
DmRel	IxDorsal	31%	31%	370	XM_002399338.1	XP_002399379.1
DmCaspar	Caspar	96%	34%	586	XM_002405982.1	XP_002406026.1

Ixodes Rel (IxRel) has an annotated Rel homology domain (RHD) and a DNA binding site; two publications have previously identified this protein as a Rel/ NFκ-B orthologue and studied its role as a transcription factor (Galindo et al., 2009; Naranjo et al., 2013). However, DmRel and Rel proteins of other arthropod species are

generally larger than 900 aa, whereas the identified IxRel sequence only consists of 349 aa. It should thus be considered that this sequence is only a subunit of Rel or only a partial sequence. Gene expression of *IxRel* in IDE8 cells was detected using RT-PCR; ISE6 cells, which have previously been shown to express *IxRel* (Naranjo et al., 2013) were included as a positive control. PCR products of the expected size were amplified from both IDE8 and ISE6 cDNA (Fig 4.7).

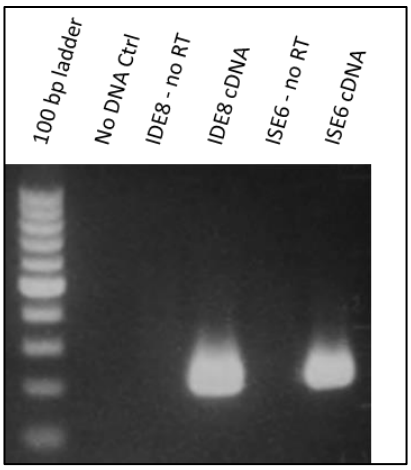

Figure 4.7: *IxRel* is expressed in the *I. scapularis* cell lines IDE8 and ISE6. RT-PCR was performed using IDE8 and ISE6 RNA. During cDNA synthesis parallel reactions were performed without addition of reverse transcriptase (no RT) to show that samples were not contaminated with DNA and the amplified bands were derived from cDNA. (Performed together with visiting PhD student Renata Strouhalová of the Institute of Parasitology in České Budějovice)

The negative regulator of Rel in *D. melanogaster* is Caspar (Kim et al., 2006). By Blast search a putative orthologue of DmCaspar was identified in the *I. scapularis* protein database (Table 4.1), but when the identified sequence was used to blast against the entire non-redundant (nr) protein database, the sequence most closely related was Fas-associated factor 1 (FAF-1) of the migratory locust *Locusta migratoria manilensis*, the jumping ant *Harpegnathos saltator* and mammalian species including human and chimpanzee. In humans FAF-1 (Ryu et al., 1999) is involved in apoptosis for which its ubiquitin homologous domain is required (Ryu and Kim, 2001). Whether it is involved in inhibition of Rel or in apoptosis remains unknown. The potential antiviral effect of the identified orthologues was not

investigated as part of this study to allow more detailed investigation of other pathways.

During the search for Imd orthologues an interesting side observation was made. When a domain-enhanced BLAST search was performed (blastp using DELTA-BLAST algorithm) as another attempt to find an Imd orthologue, a putative orthologue of the death-associated protein kinase-1 (DAPK-1) was found (XP_002434008.1). While it is not an orthologue of Imd, and probably not involved in the Imd pathway, DAPK-1 in mammalian cells is a mediator of interferon-γ induced cell death (Deiss et al., 1995) and may play a role in antiviral immunity mediated via apoptosis. It is present in many mammalian cells and in the model organism *C. elegans* (Bialik and Kimchi, 2006), but has not been found in *D. melanogaster*. Chuang and Chisholm showed the phylogenetic relationship between DAPK-1 orthologues and related kinases (Chuang and Chisholm, 2014). A putative orthologue of DAPK-1 could also be found in the mite *Metaseiulus occidentalis* (XP_003740547.1), which is an arachnid and closely related to ticks. Both the mite and tick DAPK as annotated on NCBI lack a kinase region, but annotation and assembly of genes is not very reliable in the *I. scapularis* genome at this stage, so it is possible that the first part of the protein sequence is missing in the annotation, particularly since the region in front of the predicted start codon for this protein is mainly unidentified nucleotides (observed in genomic data on NCBI). The putative *I. scapularis* orthologue of DAPK contains the other necessary domains, namely ankyrin repeats, a Ras-like domain and a DD. It is quite similar to mammalian DAPK-1 (similarity to human DAPK-1: 66% coverage and 27% identity). It is also similar to DAPK-1 of the nematode *Ascaris suum* (64% coverage, 31% identity). While this finding is apparently unrelated to the Imd pathway it was considered of interest as DAPKs are important in mammalian cells, but not present in insects revealing a potentially important difference between the two arthropod classes (*Insecta* and *Arachnida*). It may be of value to investigate the function of *I. scapularis* DAPK in future studies.

4.2.4 The Toll pathway in *Ixodes scapularis* cells

Orthologues

D. melanogaster encodes nine Toll receptors, most of which are only known to be important for embryonic development. Toll(-1) has been associated with innate defences against fungi and Gram-positive bacteria (Lemaitre et al., 1996; Valanne et al., 2011) and Toll-9 is also involved in antimicrobial defences (Ooi et al., 2002). In addition, it has been shown recently that vesicular stomatitis virus (VSV) experimentally activates DmToll-7 resulting in induction of antiviral autophagy (Nakamoto et al., 2012). Other Tolls have only been vaguely implicated in *Drosophila* immunity. The two key domains of Toll receptors are the leucine rich repeat (LRR), usually located towards the N-terminus, and the Toll-interleukin 1-receptor homologous (TIR) domain. Blast search of the *I. scapularis* protein database, using the DmToll protein sequence as a query, yielded a number of putative IxToll proteins, most of which were annotated as putative Toll receptors, which I have termed IxToll-1 to 7 (Table 4.2). No obvious direct orthologues for each of the DmTolls were found and the numbering was assigned based on the closest sequence similarity to *Drosophila* Toll-1 (IxToll-1 closest to IxToll-7 furthest hit during BLAST search).

Table 4.2: Putative orthologues of the Toll pathway components identified by BLAST search of the *I. scapularis* protein database using *D. melanogaster* protein sequences.

Query sequence	*Ixodes* protein	Query Coverage	Max. Identity	Length (aa)	mRNA accession no.	Protein accession no.
DmToll	IxToll-1	91%	30%	1086	XM_002399538.1	XP_002399580.1
DmToll	IxToll-2	57%	41%	436	XM_002406760.1	XP_002406804.1
DmToll	IxToll-3	56%	26%	818	XM_002407997.1	XP_002408041.1
DmToll	IxToll-4	35%	31%	421	XM_002406758.1	XP_002406802.1
DmToll	IxToll-5	86%	26%	1344	XM_002400584.1	XP_002400628.1
DmToll	IxToll-6	21%	37%	250	XM_002406759.1	XP_002406803.1
DmToll	IxToll-7	87%	25%	1226	XM_002402185.1	XP_002402229.1
DmMyD88	IxMyD88	48%	26%	364	XM_002407328.1	XP_002407372.1
DmDif	IxDorsal*	44%	44%	370	XM_002399338.1	XP_002399379.1
DmDorsal	IxDorsal*	43%	57%	370	XM_002399338.1	XP_002399379.1
DmCactus	IxCactus	46%	32%	454	XM_002409625.1	XP_002409669.1
DmCactus	IxCactus-2	42%	30%	363	XM_002405079.1	XP_002405123.1

* the same gene was identified by BLAST search using DmDif and DmDorsal; it was considered a Dorsal orthologue

IxToll-3 consists of LRR domains but no TIR domain, while IxToll-6 has a TIR domain but no LRR domain. *Drosophila* Toll receptors are generally large proteins of around 1000 aa, yet the sequences of IxToll-2, IxToll-4 and IxToll-6 were less than 500 aa long, indicating that these could be partial or poorly-assembled sequences. More LRR-containing proteins were found but no other proteins with both LRR and TIR domains.

Expression of the putative *IxToll-1*, *IxToll-4* and *IxToll-7* in IDE8 cells was detected by RT-PCR (Fig 4.8). Sequencing of the PCR products showed the expected sequences. *IxToll-7* primers resulted in a double band; the smaller fragment was concluded to be a PCR bi-product derived from the larger fragment, since even after gel purification of the larger fragment, PCR using the *IxToll-7* primers amplified the two PCR products. The larger band had the expected size, was sequenced and used to generate dsRNA for future studies. Expression of other *IxTolls* (2, 3, 5 and 6) could not be detected by RT-PCR in IDE8 cells using two different sets of primers.

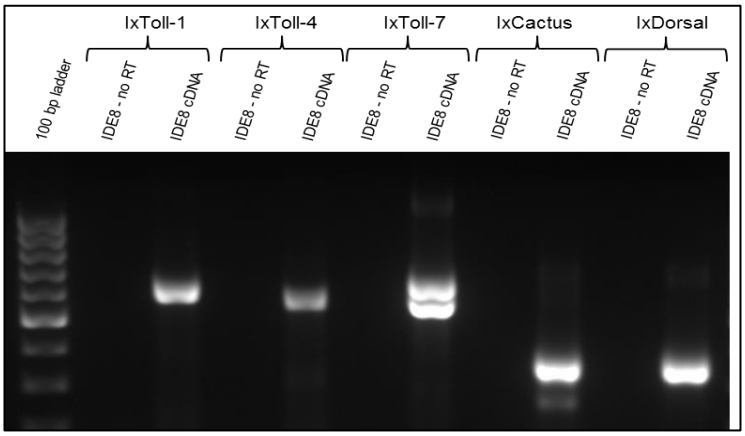

Figure 4.8: *IxToll-1*, *IxToll-4*, *IxToll-7*, *IxCactus* and *IxDorsal* are expressed in IDE8 cells. RT-PCR was performed using IDE8 RNA. During cDNA synthesis parallel reactions were performed without addition of reverse transcriptase (no RT) to show that samples were not contaminated with DNA and the amplified bands were derived from cDNA.

MyD88 is an intracellular adaptor protein involved in Toll signalling. In *Drosophila* and mammals, activated Toll binds MyD88 via the TIR domains of both proteins and initiates the downstream signalling cascade. An IxMyD88 orthologue with relatively low coverage (48%) and maximum identity of 26% was identified (Table 4.2). This,

like DmMyD88, had an annotated DD and a TIR domain and was of similar size to DmMyD88. However, expression of *IxMyD88* could not be shown in IDE8 cells.

Activation of the Toll pathway in *Drosophila* results in activation of the Rel-homologues Dif and/or Dorsal which translocate to the nucleus and act as transcription factors. A putative *I. scapularis* Dorsal orthologue was identified (Table 4.2) but no Dif orthologue was found. Similarly, mosquitoes do not appear to encode Dif, but have a Dorsal orthologue, namely REL1 (Shin et al., 2005). The putative IxDorsal contains a RHD and when compared with DmDif, DmDorsal, AaeREL1 and CrNFκ-B, it has closest sequence similarity to CrNFκ-B and is more closely related to AaeREL1 than DmDorsal. Expression of the putative *IxDorsal* was detected in IDE8 cells by RT-PCR (Fig 4.8) and dsRNA was generated for knockdown experiments.

In *Drosophila*, Cactus is a negative regulator of the Toll pathway and is bound to Dif and Dorsal in non-signalling conditions. For translocation of Dif/Dorsal to the nucleus, degradation of Cactus is required (Wu and Anderson, 1998). The DmCactus sequence was used to blast against the *I. scapularis* protein database and two putative Cactus orthologues were identified (Table 4.2). Expression of putative *IxCactus* was detected in IDE8 cells by RT-PCR (Fig 4.8) and dsRNA was generated for knockdown experiments. IxCactus-2 was identified during later analysis and not investigated, but has been added to Table 4.2 for completeness.

Silencing of gene expression of Toll pathway orthologues

Once putative pathway components were identified and expression in IDE8 cells was shown for some of the pathway components, knockdown experiments were performed as shown in Figure 4.2. IDE8 cells were seeded into 24-well plates and dsRNA targeting either GFP as a control or IxToll-1, IxToll-4, IxToll-7, IxCactus or IxDorsal was added to the wells. In addition, dsRNA against each of the three Tolls was added in combination. 72 h after addition of dsRNA, cells were infected with SFV4(3H)-*Rluc* at MOI 1 and lysed 24 h p.i. for luciferase assay. Knockdown efficiency at the time of infection was determined by semi-quantitative RT-PCR from parallel wells.

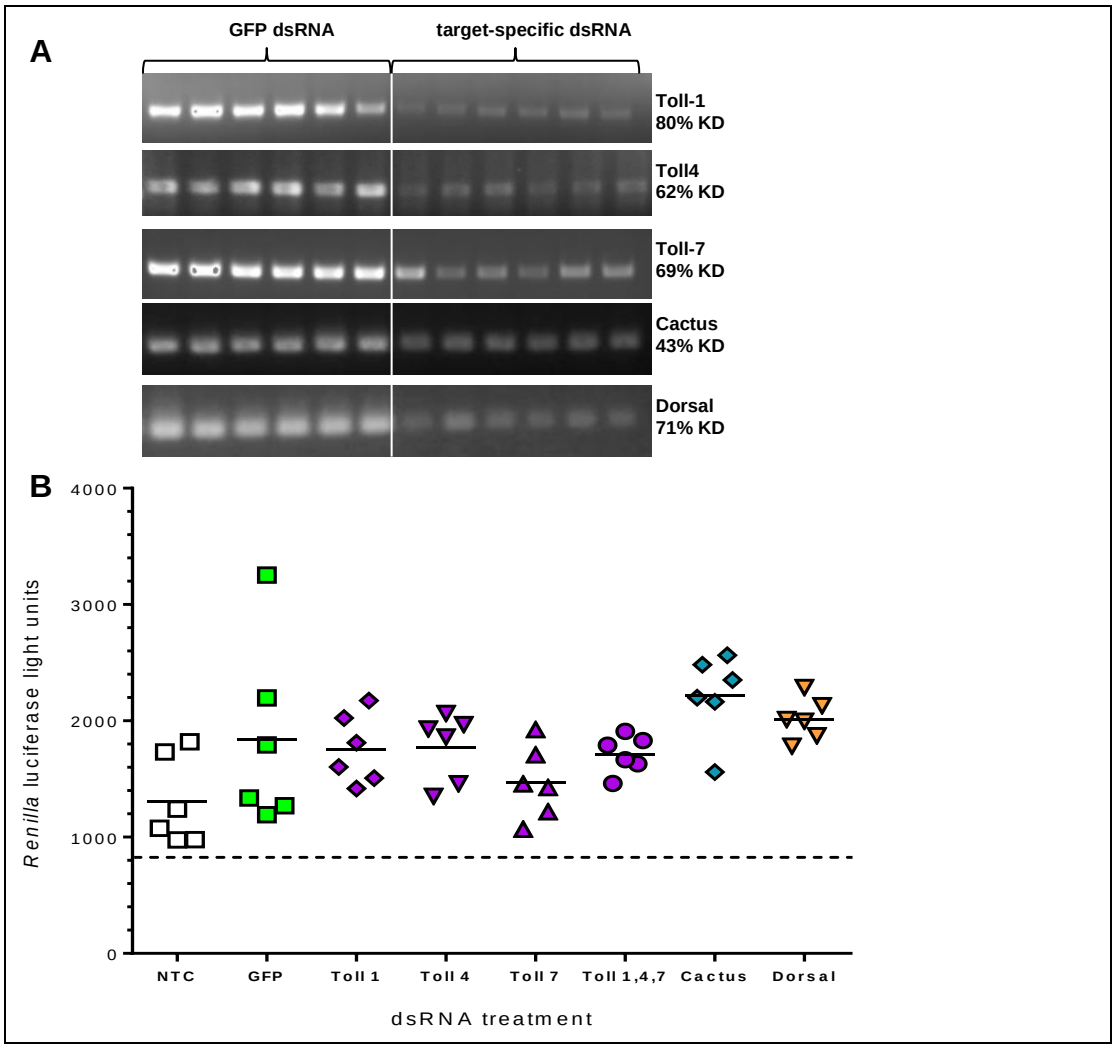

Figure 4.9: Knockdown of gene expression of putative Toll pathway components in IDE8 cells has little effect on SFV replication. (A) Semi-quantitative RT-PCR was performed as a measure of knockdown efficiency. Signal intensity of PCR products from cells treated with a target-specific dsRNA was compared to that of cells treated with dsRNA targeting GFP as a control. (B) *Rluc* activity of non-treated control (NTC) cells and cells treated control (GFP) or target-specific dsRNA 72 h prior to infection with SFV4(3H)-*Rluc* at MOI 1.

Treatment of cells with dsRNA resulted in a significant but variable decrease in target mRNA levels with a reduction of 43-80% (Fig 4.9A), but no significant difference in *Rluc* activity was detected for any of the targeted genes ($p>0.05$, ANOVA) (Fig 4.9B). However, an outlier was observed in the GFP control samples and when it was removed, a significant increase in *Rluc* activity could be shown by One-way ANOVA following targeting of *IxCactus* (1.4-fold increase; $p<0.01$) and *IxDorsal* (1.3-fold increase; $p<0.05$) gene expression. The increase in *Rluc* activity

was not large, and while a small (non-significant) increase was also observed in one repeat experiment, no difference was seen in another repeat experiment. Overall, these results indicate that the selected proteins do not play a significant role in controlling SFV in IDE8 tick cells.

4.2.5 The JAK/STAT pathway in *Ixodes scapularis* cells

JAK/STAT downstream signalling components

An important signalling pathway in insect and mammalian innate immunity is the JAK/STAT pathway (see 1.4.2). This pathway has been implicated in antiviral defences in both *D. melanogaster* (Deddouche et al., 2008; Dostert et al., 2005) and mosquitoes (Paradkar et al., 2012; Souza-Neto et al., 2009). Both a JAK and a STAT orthologue have been described previously in *I. scapularis* ticks (Liu et al., 2012). The same putative orthologues as published were identified in *I. scapularis* by BLAST search using *D. melanogaster* sequences of STAT and JAK (named Hopscotch in *Drosophila*) (Table 4.3). One of the negative regulators of the JAK/STAT pathway in *D. melanogaster* is the protein inhibitor of activated STAT (PIAS) (Betz et al., 2001; Dostert et al., 2005). An *I. scapularis* orthologue of PIAS was identified by BLAST search (Table 4.3). While PIAS is a direct inhibitor of activated STAT, it is also a small ubiquitin-like modifier (SUMO) E3 ligase. Sumoylation is a regulatory post-translational protein modification which can influence stability and function of proteins (reviewed by Flotho and Melchior, 2013). Viruses can interact with SUMO-related pathways (reviewed by Everett et al., 2013); thus IxPIAS was not only considered a putative negative regulator of STAT but also a putative component of the sumoylation system.

Suppressor of cytokine signalling (SOCS) proteins are negative regulators of the JAK/STAT pathway in both *Drosophila* and mammalian systems. Using the three *D. melanogaster* SOCS sequences (SOCS16D, SOCS44A and SOCS36E), four putative SOCS orthologues were identified in the *I. scapularis* genome (Table 4.3). All four sequences had a Scr homology 2 (SH2) domain which is typically found in SOCS proteins. Apart from IxSOCS-2, all orthologues contain a C-terminal SOCS superfamily domain. Interestingly, a DDE superfamily endonuclease domain was

annotated in the sequence of IxSOCS-4, which is generally associated with DNA transposition and may thus indicate a more complex function for this orthologue.

Table 4.3: Putative orthologues of the JAK/STAT pathway components identified by BLAST search of the *I. scapularis* protein database using *D. melanogaster* protein sequences.

Query sequence	*Ixodes* protein	Query Coverage	Max. Identity	Length (aa)	mRNA accession no.	Protein accession no.
DmSTAT92E	STAT	94%	37%	752	HQ710832.1	ADU86241.1
DmHopscotch	JAK	80%	45%	1097	XM_002406395.1	XP_002406439.1
DmPIAS	IxPIAS	85%	40%	480	XM_002434620.1	XP_002434665.1
DmSOCS44A	IxSOCS-1	29%	33%	293	ISCW019435 *	EEC10036.1
DmSOCS36E	IxSOCS-2	13%	32%	171	XM_002404534.1	XP_002404578.1
DmSOCS36E	IxSOCS-3	21%	65%	229	XM_002403457.1	XP_002403501.1
DmSOCS36E	IxSOCS-4	14%	37%	883	XM_002415548.1	XP_002415593.1

* Gene ID

Expression of JAK, STAT and IxPIAS was detected by RT-PCR using tick cell RNA. STAT and IxPIAS were expressed in the four tick cell lines ISE18, IDE8, IRE11 and IRE/CTVM19 (Figure 4.10A/B), but JAK expression was only investigated in IDE8 cells where it was found to be expressed (Figure 4.10C). Expression of the identified SOCS proteins in tick cells was not determined as part of the present study.

The STAT PCR products amplified from the four cell lines were sequenced and aligned with the corresponding region of STAT provided in the NCBI nucleotide database (Fig 4.10 D). In the *I. ricinus* cell lines a silent mutation (G>C at position 38) was observed compared to *I. scapularis* sequences. Sequences from all cell lines were significantly different compared to the published sequence between position 50 and 100 of the sequenced fragment. A number of other nucleotide changes were observed in the cell line sequences compared to the published sequence, all of which were consistent between the four cell lines. The differences between position 50 and 100, may be a result of incorrect exon assembly of the NCBI sequence. While the STAT sequence in cell lines may vary from live ticks, it is unlikely that the sequence has evolved in the same manner in four separate cell lines from two different species. For future studies it could be of value to amplify the full-length STAT sequence to

obtain the correct sequence. While a band of the correct size (~2200 nt) could be amplified (data not shown), attempts to clone the full length STAT into a sequencing vector (pJET) and an expression vector (pIB/V5-His) failed.

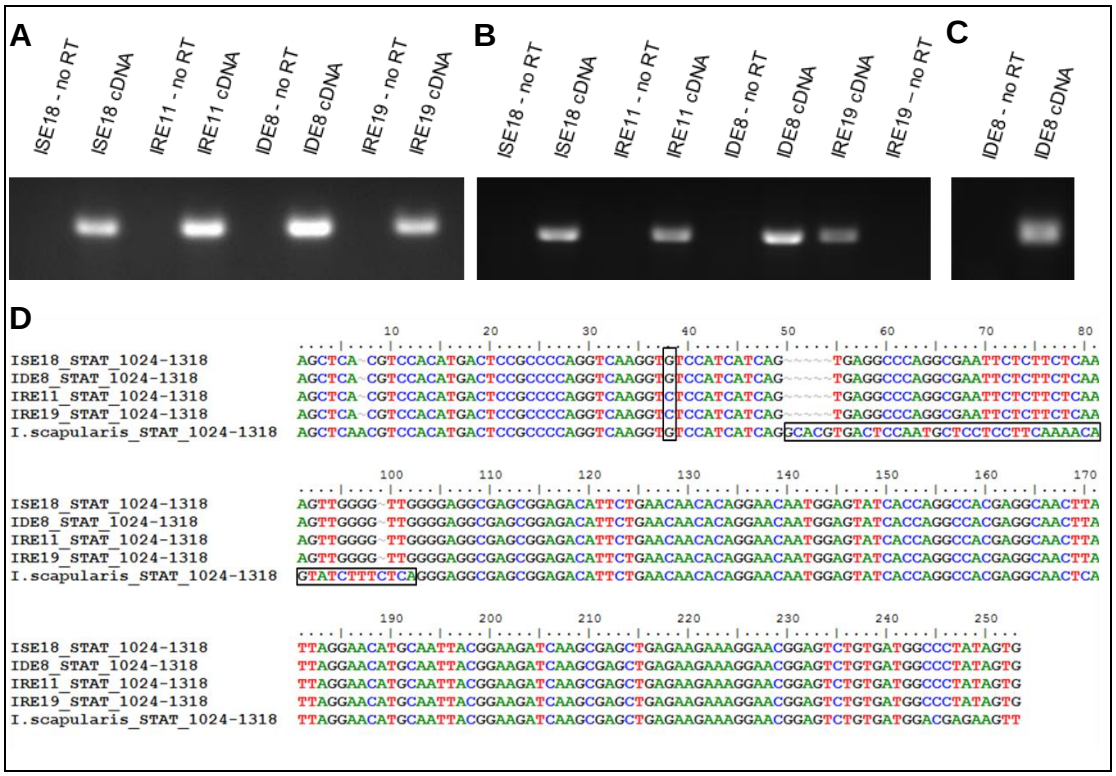

Figure 4.10: Expression of JAK/STAT pathway orthologues in tick cells. (A) STAT and (B) PIAS are expressed in the four different tick cell lines ISE18, IRE11, IDE8 and IRE/CTVM19. (C) JAK is expressed in IDE8 cells. RT-PCR was performed using tick cell RNA. During cDNA synthesis parallel reactions were performed without addition of reverse transcriptase (no RT) to show that samples were not contaminated with DNA and the amplified bands were derived from cDNA. (D) The amplified STAT fragments were sequenced and aligned with the *I. scapularis* sequence on NCBI.

The phylogeny of STAT was inferred (Figure 4.11) in order to see the sequence relationship of IxSTAT to STAT sequences of other species. The placozoan *Trichoplax adhaerens* as the simplest of all multicellular animals encodes a putative STAT situated on a long branch with little relation to other STATs. While the majority of STATs of bilaterian animals form a cluster, the STAT of the nematode *Trichinella spiralis* and the human STATs 1-4 are not included in this cluster. Nematodes often destabilise phylogenetic trees and it is unsurprising that *T. spiralis*

STAT falls into the cluster of non-bilaterian STATs (Darren Obbard, personal communication). The human STATs 1-4 appear to share a common ancestor, but they are on a long branch indicating rapid evolution, making it quite difficult to model. It is possible that the inclusion of more vertebrate/mammalian STAT sequences could have further elucidated the relationship of human STAT1-4 with human STAT5-6 and arthropod STATs. It thus remains unclear whether this is a problem of modelling or whether there were two copies in the ancestral bilaterians with different losses in the descendants. The IxSTAT sequence is at the base of the arthropod phylum, which correlates with overall species phylogeny. *Drosophila* and mosquito STATs have evolved rapidly, but human STAT5 and STAT6 appear closely related to IxSTAT.

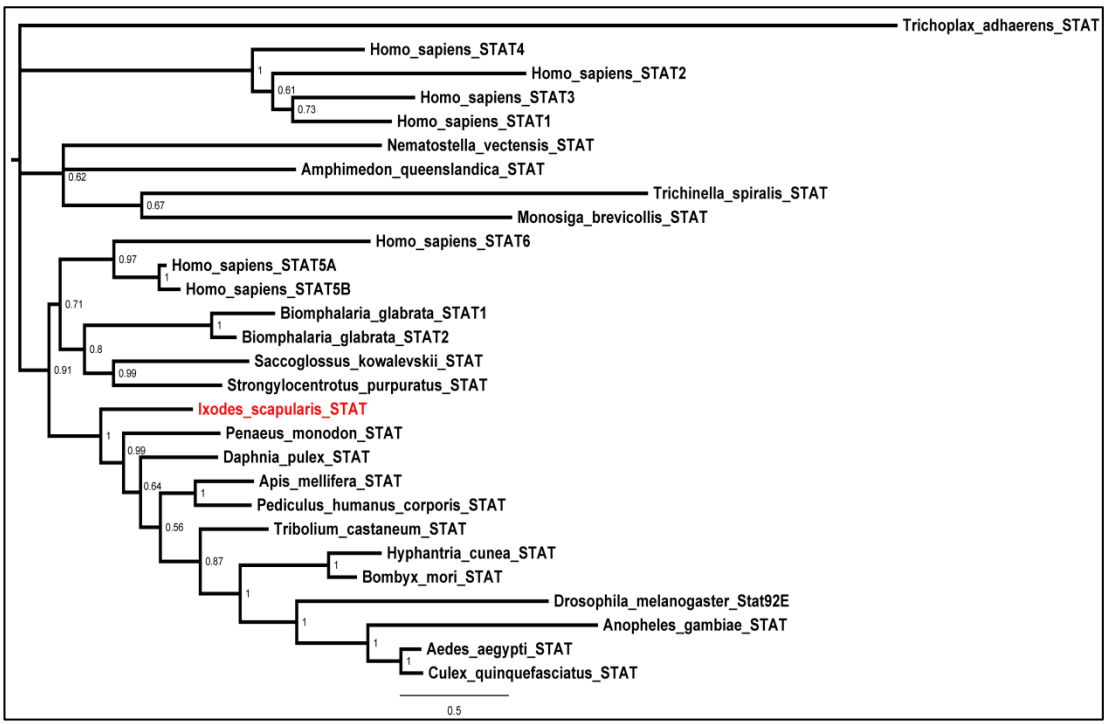

Figure 4.11: Bayesian inference of STAT phylogeny of selected STAT sequences. A list of the species, common names and accession numbers is provided in Chapter 2 (Table 2.4).

At the beginning of the present study, no genes were known to be regulated by STAT in ticks. An orthologue of the gene *vir-1*, which is up-regulated by STAT in insects, could not be found in the *I. scapularis* genome. Another option to show STAT

activation is to examine STAT phosphorylation. The close sequence similarity of IxSTAT to human STAT5 suggested that cross-reacting antibodies might be available commercially. The phosphorylation site of IxSTAT and human STAT5A is largely conserved, specifically with the tyrosine that is phosphorylated in human STAT5 being conserved (Fig 4.12, arrow).

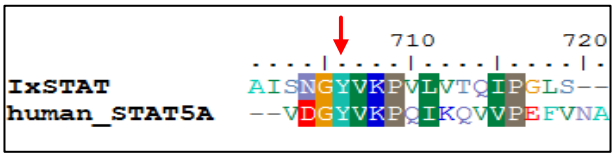

Figure 4.12: Alignment of the STAT5A phosphorylation site and the corresponding region of IxSTAT. The sequence in this region is quite conserved indicating that the conserved tyrosine (arrow) could be a site of phosphorylation in IxSTAT.

While no antibody targeting unmodified human STAT was found that cross-reacted with IxSTAT, an antibody targeting phosphorylated human STAT5A cross-reacted with IxSTAT, presumably in its phosphorylated state, though this cannot be concluded for certain. Using this antibody, IxSTAT could be detected in IDE8 cells by Western blot (as described in 2.18) and the specificity of the antibody was demonstrated by knockdown of STAT expression using long dsRNA with subsequent loss of signal (Fig 4.13). In all blots performed with lysates of untreated tick cells (IRE11 and IDE8 cells), IxSTAT could be detected (Fig 4.13, Fig 4.14).

This was surprising, as the antibody was expected to detect only phosphorylated STAT (p-STAT). This could be due to a number of reasons: either the antibody detects non-phosphorylated IxSTAT, or IxSTAT is phosphorylated at this site even in its inactivated state, or IxSTAT is constantly activated in tick cells perhaps due to a role in cellular maintenance or the presence of endogenous microorganisms in the cell lines IDE8 and IRE11, as discussed in the introduction and Chapter 3 of this study.

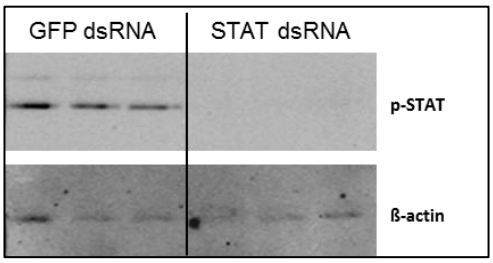

Figure 4.13: p-STAT can be detected in IDE8 cells using antibody raised against phosphorylated human STAT-5. Triplicate wells of IDE8 cells were treated for 72 h with dsRNA targeting either STAT or GFP as a control. Cells were lysed and and analysed by Western Blot.

In order to investigate whether STAT is activated by infection with SFV, IRE11 cells were infected with SFV4(3H)-*Rluc* at MOI 60, cells were lysed at 0, 30, 60, 90, 120 min p.i. and p-STAT levels were measured by semi-quantitative Western blot (LI-COR®, see 2.18). While there were wide variations between samples in p-STAT signal intensity, no consistent increase or decrease in signal intensity was observed (Fig 4.14 and data not shown). Parallel cultures were treated with heat-inactivated *E. coli* as another putative stimulus of STAT activation, but no increase in p-STAT was detected over a 3 h period after addition of the bacteria (data not shown).

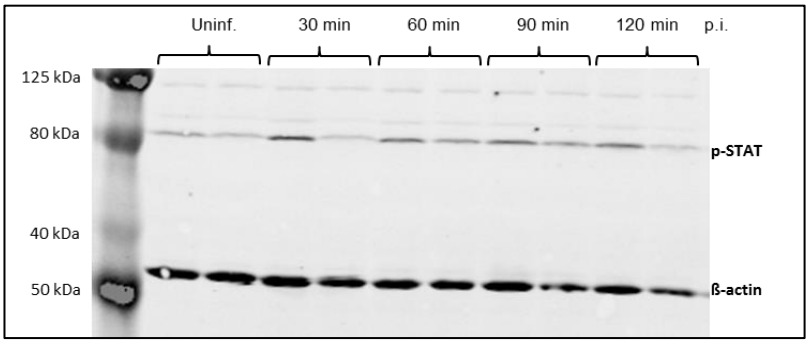

Figure 4.14: STAT phosphorylation in IRE11 cells after SFV infection of duplicate cultures. While there was some variation in levels of p-STAT, no consistent increase or decrease after SFV infection was observed.

Inhibition of STAT phosphorylation might allow reduction of p-STAT background levels in uninfected cells, enabling detection of any increase in p-STAT resulting from infection with SFV. Two inhibitors of STAT5 phosphorylation were tested as

inhibitors of IxSTAT phosphorylation: the tyrosine kinase inhibitor piceatannol (Sigma-Aldrich®), which has been shown to inhibit human STAT3 and STAT5 phosphorylation (Su and David, 2000), and the STAT5 inhibitor N′-((4-Oxo-4H-chromen-3-yl)methylene)nicotinohydrazide (Muller et al., 2008; Calbiochem®). IDE8 cells were treated with one or other of the two drugs for 30 min and subsequently infected (or mock-infected) with $1.5x10^8$ PFU of SFV4(3H)-*Rluc* and lysed 2 h p.i. for Western blot analysis (Fig 4.15).

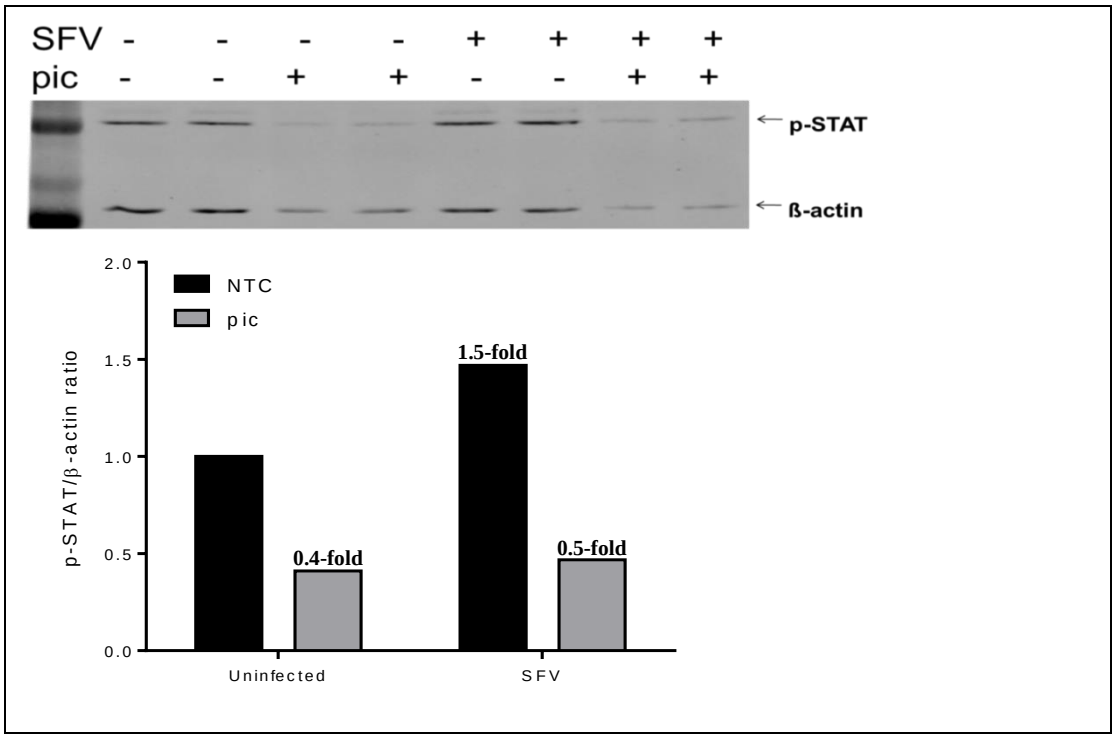

Figure 4.15: STAT phosphorylation in IDE8 cells after SFV infection. (A) Western Blot of IDE8 cell lysates detecting p-STAT. Cells were mock-treated (NTC) or treated with the drug piceatannol (pic), an inhibitor of STAT5 phosphorylation in mammalian cells. After 30 min cells were infected (or mock-infected) with $1.5x10^8$ PFU of SFV4(3H)-*Rluc* and lysed 2 h p.i.. (B) Ratio of p-STAT/ß-actin determined by semi-quantitative LI-COR® Western Blot.

Piceatannol did not result in any CPE by visual assessment of cells using microscopy, but when cell lysates were analysed by Western blot, there was not only a reduction in p-STAT, but also in ß-actin levels compared to NTC cells (Fig 4.15) indicating at least some cytotoxicity. Quantification of the p-STAT/ß-actin ratio demonstrated a 0.4-fold decrease in p-STAT in uninfected cells and a 0.5-fold

decrease in infected cells after treatment with piceatannol compared to uninfected NTC cells. The p-STAT/ß-actin ratio in SFV-infected non-treated cells was increased by 1.5-fold compared to uninfected NTC cells. Treatment of IDE8 cells with the Calbiochem® STAT5 inhibitor resulted in almost instant death of the culture at the concentration recommended for mammalian cells (800 µM). Lower concentrations (≥200 µM) were also detrimental (data not shown).

The publication of three *I. scapularis* STAT regulated genes, namely gene7 (DQ065996.1), gene9 (DQ066155.1) and gene15 (XM_002399691.1) (Liu et al., 2012), provided another potential way to detect STAT activation. If these genes were expressed in IDE8 cells and regulated by activated STAT, knockdown of STAT expression should result in a reduction and activation of STAT in an increase of gene7, gene9 and gene15 mRNA levels. Quantification of these genes by qPCR after virus infection might allow the detection of STAT activation. Using the published qPCR primer sequences, gene7 and gene15 could not be detected in cDNA derived from IDE8 cells. Using the gene9 primers a fragment of approximately 300 bp was amplified. Usually, short fragment sizes smaller than 200 bp are preferred for qPCR, but the primers were used for qPCR despite the rather large fragment observed. However, qPCR of cells with 95% knockdown of STAT expression (mRNA level as validated by qPCR), showed no difference in RNA levels of the amplified fragment (data not shown). To verify the primer sequences, a BLAST search of the *I. scapularis* nr nucleotide database using the gene9 primers was performed. The search did not result in any hits with 100% identity. The primers were then aligned with the cds of gene9, but did not match the gene9 sequence provided on NCBI. Considering a possible mix-up between forward and reverse primers, the reverse complement of the forward primer was made, but could not be found in the gene9 sequence either. The same was observed for the primer sequences for gene15. The primer sequences for gene7 aligned to the gene7 cds, but expression of gene7 was not detected in IDE8 cells. The qPCR primers for JAK and STAT published by Liu et *al*. 2012 worked in IDE8 cells.

I. scapularis expresses orthologues of Vago (IxVago)

As described in the introduction to this thesis (see 1.4.2), a recently discovered important component of the antiviral STAT pathway in insects is Vago (Deddouche et al., 2008; Paradkar et al., 2012). As a potentially important component of the JAK/STAT pathway in ticks, *I. scapularis* orthologues of *Culex* Vago (CxVago) were identified by BLAST search and sequence analysis. Sequence similarity between *D. melanogaster* and *C. quinquefasciatus* Vago is not highly conserved, however eight specific cysteine residues are conserved and form a Von Willebrandt factor type C (VWC) domain when their 3D structure is modelled. Seven potential orthologues of CxVago were found and named IxVago-1 to IxVago-7 (Table 4.4). Due to the very low sequence similarity, it is possible that other *I. scapularis* Vago-like proteins were missed during the analysis.

Table 4.4: Putative orthologues of CxVago (XP_001842264.1) in the *I. scapularis* genome.

Ixodes protein	Query Coverage	Max. Identity	Length (aa)	mRNA accession no.	Protein accession no.
IxVago-1	62%	28%	120	AY775815.1	AAV80782.1
IxVago-2	53%	25%	106	XM_002411599.1	XP_002411644.1
IxVago-3	62%	28%	120	XM_002415485.1	XP_002415530.1
IxVago-4	41%	32%	103	XM_002434522.1	XP_002434567.1
IxVago-5	61%	28%	120	DQ066130.1	AAY66767.1
IxVago-6	61%	31%	101	XM_002401964.1	XP_002402008.1
IxVago-7	18%	36%	122	XM_002412280.1	XP_002412325.1

All putative IxVago orthologues were of a similar size to CxVago and when the amino acid sequences were aligned using ClustalW the eight conserved cysteine residues were identified in six of the seven putative orthologues (Fig 4.16). IxVago-7 had only four of the conserved cysteines towards the C-terminus. In CxVago these cysteine residues are crucial for the formation of a VWC domain (Paradkar et al., 2012). When aligned it was observed that the nucleotide sequences of IxVago-1 and IxVago-3 were identical except for an A>G nucleotide change on position 314 in the IxVago-3 sequence, resulting in an amino acid change of Q>R at position 105. Similarly IxVago-5 is almost identical in sequence to IxVago-3, except for a C>T

nucleotide change at position 302, resulting in an amino acid change of R>C at position 101 of the IxVago-5 sequence (position 107 of the alignment in Fig 4.16).

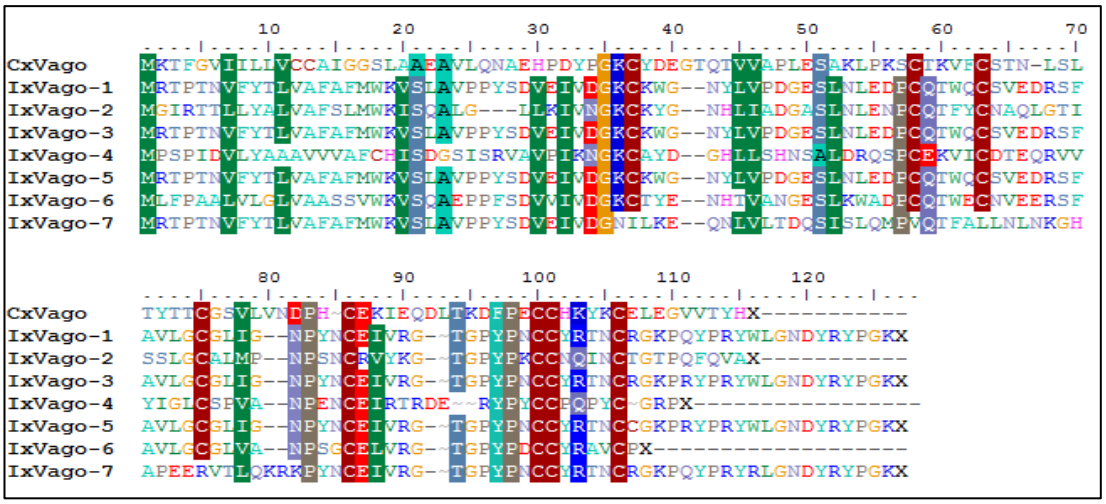

Figure 4.16: ClustalW alignment of CxVago and IxVago sequences. The amino acid abbreviations suggested by the IUPAC-IUB Joint Commission on Biochemical Nomenclature (1984) were used.

By 3D modelling using the free webserver Phyre (Kelley and Sternberg, 2009) a predicted VWC domain was predicted in all putative IxVago sequences, including IxVago-7 despite having only four cysteines as opposed to eight. The 3D models of the *Ixodes* orthologues were similar in structure to the CxVago model with the exception of IxVago-6 which lacked the defined beta hairpin structure (see Appendix, Figure 8.4). All orthologues have a variable α-helix structure at the C-terminus and IxVago-4 has a beta sheet structure starting closer to the N-terminus compared to the other proteins.

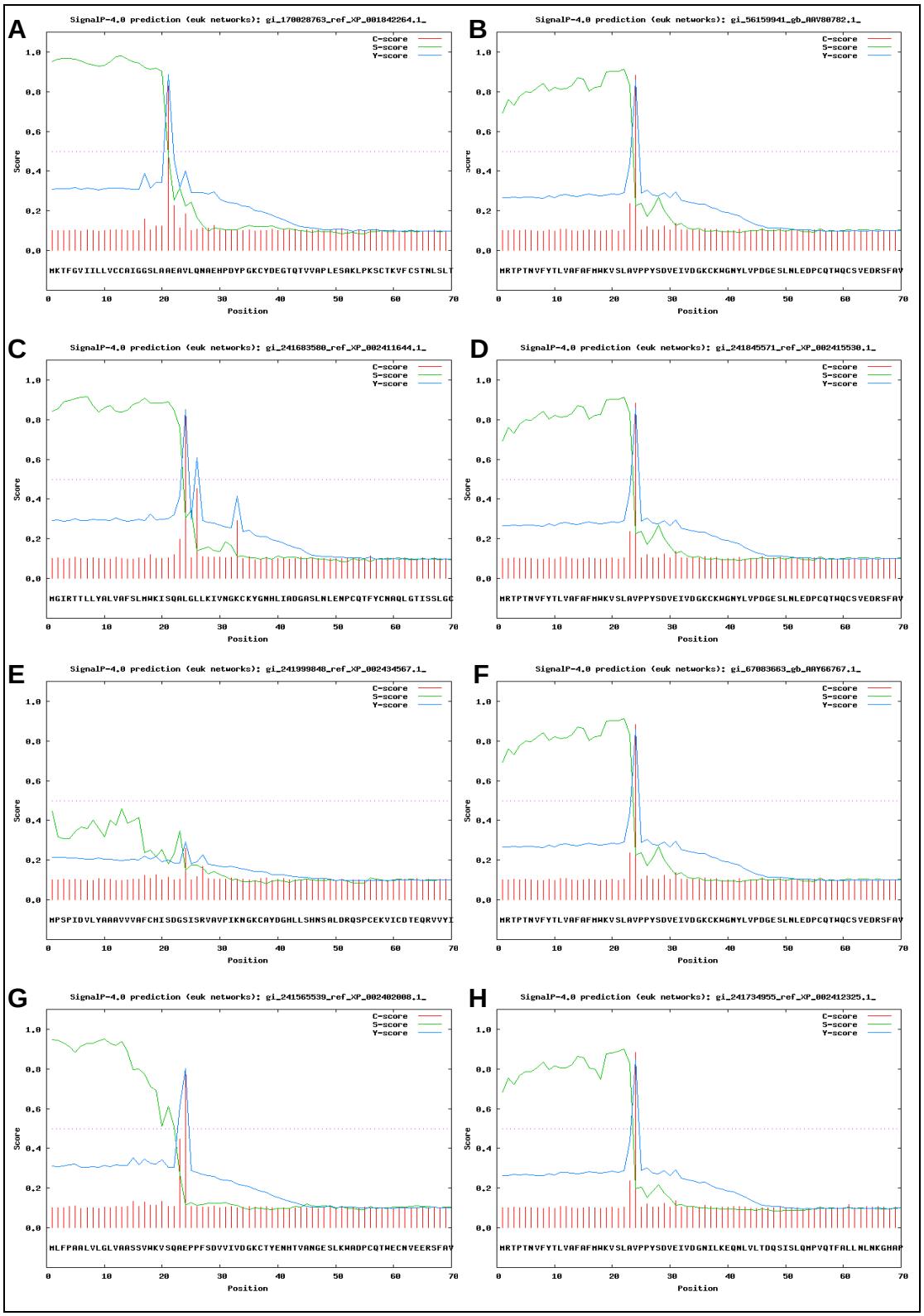

Figure 4.17: Signal peptide prediction for CxVago (A), IxVago-1 (B), IxVago-2 (C), IxVago-3 (D), IxVago-4 (E), IxVago-5 (F), IxVago-6 (G) and IxVago-7 (H) using SignalP 4.0. The peaks of the S-score (green) and the C-score (red) indicate the site of a predicted N-terminal signal peptide sequence and the site of cleavage. The Y-score (blue) is a combination of the C-score and the slope of the S-score and indicates the most likely site of cleavage.

Since Vago has to be secreted from the cell to act as an IFN-like cytokine, all IxVago sequences were analysed for signal peptide sequences necessary for protein secretion using the free webserver SignalP 4.0 (Petersen et al., 2011). As in CxVago, all IxVago aa sequences had a signal peptide sequence for secretion around position 26, with the exception of IxVago-4, which showed only a very weak putative signal peptide sequence (Fig 4.17). During secretion, the N-terminus is cleaved off at the signal peptide sequence resulting in a shortened version of the protein. Extracellularly, Vago will thus be missing part of the N-terminal sequence and may have a different conformation. Putative conformation of the secreted Vago sequences was thus modelled again using Phyre2 (Fig 4.18). Interestingly, the structure of IxVago-6 is more comparable to the other Vago sequences in its cleaved state.

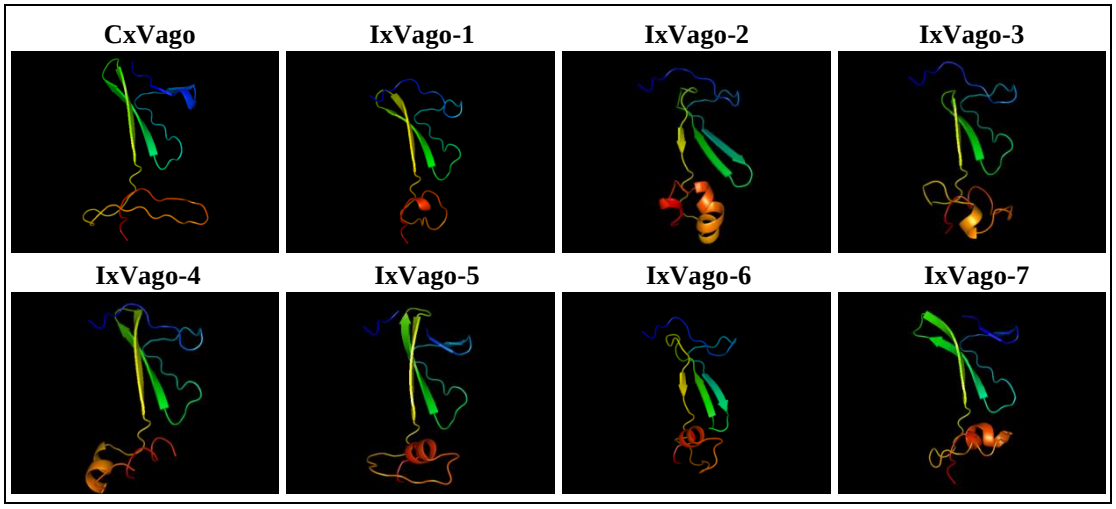

Figure 4.18: 3D-modelling of CxVago and IxVago structures after putative cleavage at the N-terminus for protein secretion.

Expression of IxVago-1 and IxVago-2 was detected by RT-PCR in IDE8 cells (data not shown). IxVago-4 and IxVago-6 were not detected. IxVago-3 and IxVago-5 could not be differentiated from IxVago-1 by PCR due to the high sequence similarity. The full-length cds of putative IxVago-1 was amplified and cloned into the vector pJET1.2 (CloneJET kit, Thermo Scientific) and six clones were sequenced. A silent mutation (T>C) was found at position 297 of IxVago-1 amplified

from IDE8 cells in all six sequenced clones. None of the amplified sequences were IxVago-3 or IxVago-5, which may still be expressed at lower quantities.

The full-length IxVago-1 cds was then cloned into the insect expression vector pIB/V5-His as a fusion protein with the V5-His-tag and sequenced (see 2.19). While the cloned sequence was correct, expression in tick cells after transfection could not be detected by Western Blot (anti-V5 and anti-His-tag), possibly due to the very low levels of expression after transfection as observed for other genes (see 3.2.6). The effect of overexpression of IxVago on virus infection could not be determined due to the time limitations of this study. With additional time, other approaches could have been used to overexpress IxVago in tick cells. One suitable, straightforward approach to investigate the effect of IxVago on virus infection would have been to clone IxVago into the SFV sequence under the control of a second subgenomic promoter. High levels of *Rluc* activity have been observed in tick cells infected with SFV1-*Rluc* VRPs which express *Rluc* under the subgenomic promoter (see Figure 5.17); thus SFV encoding IxVago under the control of a second subgenomic promoter would probably express high levels of IxVago. If the putative IxVago activates STAT and JAK/STAT signalling is involved in an antiviral defence, the virus encoding IxVago should have a disadvantage compared to a control virus (with for example the reverse sequence). By cloning the IxVago sequence into a replicon, supernatant of tick cells infected with the VRPs could be used to pre-treat other cultures prior to infection, to investigate whether this has any antiviral effect.

In an attempt to directly show non-tagged IxVago, antibody targeting mosquito Vago, kindly provided by Peter Walker (AAHL, CSIRO, Geelong), was used for Western blot analysis of tick cell lysates. The sequence used to generate the antibody was aligned with the corresponding IxVago-1 sequence (Fig 4.19), but showed little sequence conservation. The antibody was tested using different dilutions and membrane blocking agents (see 2.18.4), but IxVago could not be detected in IDE8 cell lysate using the antibody to cxVago. An antibody detecting IxVago would have been useful to validate knockdown of gene expression or to detect whether IxVago is upregulated after virus infection.

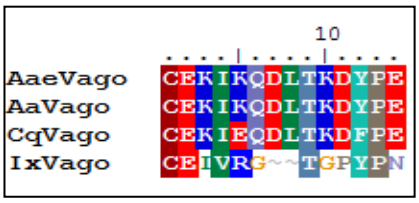

Figure 4.19: Alignment of the peptide sequence used to generate the mosquito Vago antibody (provided by Peter Walker) in AaeVago, AaVago, CqVago and IxVago-1. The three mosquito sequences from *Ae. aegypti*, *Ae. albopictus* and *C. quinquefasciatus* were highly conserved, while the IxVago sequence is highly diverse in this region of the protein.

Knockdown of STAT and IxVago-1 expression in IDE8 cells

In order to investigate whether the JAK/STAT pathway is involved in controlling virus replication in IDE8 cells, expression of JAK/STAT pathway components was knocked down using long dsRNA. Knockdown of components of the immune system may affect replication of the endogenous SCRV which persistently infects IDE8 cells. Thus it was first determined whether knockdown of STAT or IxVago-1 affects SCRV RNA levels. IDE8 cells were seeded into 24-well plates and 24 h after seeding inoculated with dsRNA targeting GFP or *Rluc* (controls), STAT or IxVago-1. Parallel wells were left as NTC. Knockdown of STAT and IxVago-1 expression was quantified by qPCR and STAT mRNA levels were reduced by 65% 24 h after addition of dsRNA and by 94% at 90 h after addition of dsRNA (Fig 4.20A); however, while there were minor differences in IxVago-1 mRNA levels between conditions, IxVago-1 RNA levels were not significantly reduced by addition of dsRNA targeting IxVago-1 (Fig 4.20B). 24 h after addition of dsRNA, IxVago-1 RNA levels were significantly increased compared to the GFP control, but not compared to the *Rluc* control (Fig 4.20B). Thus the increase in IxVago-1 RNA levels appears to be the result of general variation between experimental conditions. SCRV RNA levels (normalised to ß-actin) were not significantly different in cells treated with dsRNA targeting STAT, compared to cells treated with non-specific (GFP and *Rluc*) dsRNA controls (Fig 4.20C). Treatment with dsRNA targeting IxVago-1 resulted in a small but statistically significant increase ($p<0.05$) in SCRV RNA levels 120 h after addition of dsRNA (Fig 4.20C).

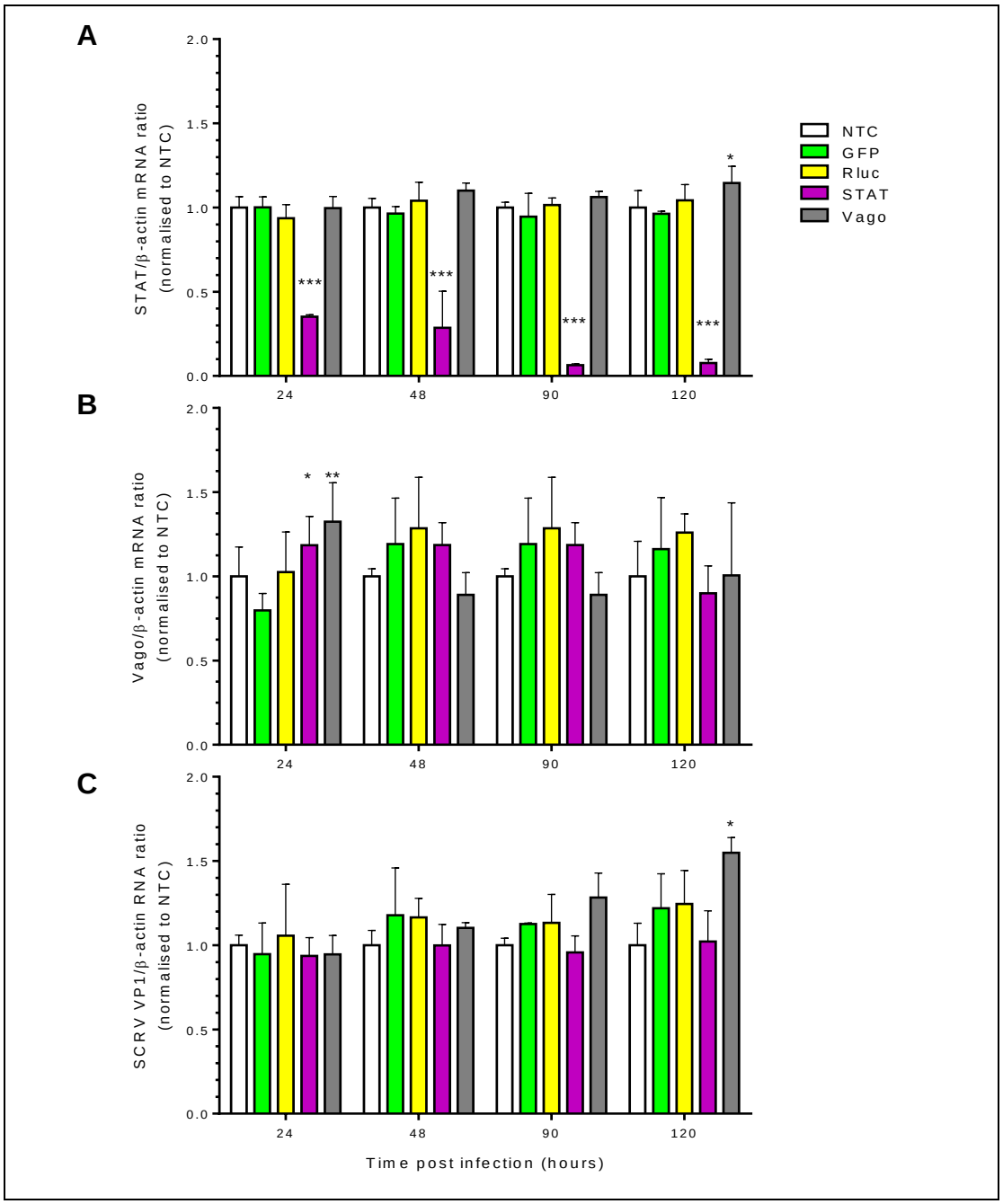

Figure 4.20: Knockdown of STAT expression does not affect SCRV RNA levels up to 5 days after addition of dsRNA. IDE8 cells treated with dsRNA and lysed 24, 48, 90 and 120 h after addition of dsRNA for RNA extraction and cDNA synthesis. Levels of STAT (A), IxVago-1 (B) and SCRV VP1 (C) RNA were measured by qPCR. RNA levels were normalised to ß-actin and the ratio was then normalised to the non-treated control (NTC). The legend indicates dsRNA treatment. Bars represent triplicate cultures and error bars indicate SD. Statistical significance as indicated (***p≤0.0001; **p<0.01; *p<0.05) was determined by One-way ANOVA with multiple comparisons (Fisher's LSD).

The dsRNA used to knock down IxVago-1 expression targets the entire IxVago-1 sequence and should be cleaved by tick Dcr into a pool of siRNAs targeting the whole IxVago-1 sequence. Additionally, if IxVago-3 and IxVago-5 are expressed, the dsRNA will target those as well, due to the high sequence similarity. Since IxVago-1 expression was quantified over five days and a large amount of dsRNA was added to the cells, it remains unclear why no knockdown could be established for IxVago-1. In an initial attempt to validate knockdown of IxVago-1 expression, the primers used to generate the dsRNA were used for RT-PCR, but residual, unprocessed IxVago-1 dsRNA could be detected (data not shown). This has been observed on occasion during knockdown validation of other genes (the present study) and new primers were designed with the reverse primer binding in the 3' UTR of the IxVago-1 mRNA to avoid amplification of cDNA derived from residual dsRNA. These were used for IxVago-1 mRNA amplification by qPCR as shown in Fig 4.20C, but it is possible that the large amounts of residual dsRNA still affected accuracy of knockdown validation. Due to time limitations of this study, no solution for this problem was found. One possible solution could be the use of oligo(dT) primers during cDNA synthesis, to ensure amplification of only mRNA, and a subsequent RNase digest to remove any residual RNA which could still serve as a template for PCR. However, SCRV and LGTV do not generate polyadenylated RNA and would thus not be reverse transcribed using oligo(dT) primers. Thus separate reactions would have to be prepared for quantification of SCRV or LGTV and validation of IxVago-1 knockdown, which is associated with a considerable additional cost for large scale experiments. Another possible solution would be to generate a smaller fragment of dsRNA targeting only the 5' end of IxVago-1.

Knockdown of STAT expression had no effect on SCRV levels. Next, the effect of knocking down components of the JAK/STAT pathway on SFV was investigated. IDE8 cells were treated with dsRNA against GFP, STAT or IxPIAS and 72 h later infected with SFV4(3H)-*Rluc* at MOI 5 and lysed 24 h p.i. for luciferase assay. Three individual experiments were performed; the first two experiments were normalised to the NTC and the combined results are presented (Fig 4.21A). The knockdown efficiency was not validated for reasons of time and economy. Treatment of IDE8

cells with dsRNA targeting STAT resulted in no significant increase or decrease in *Rluc* activity compared to the GFP control. Treatment with dsRNA targeting IxPIAS, however, resulted in a significant increase in *Rluc* activity compared to the GFP control ($p \leq 0.0001$).

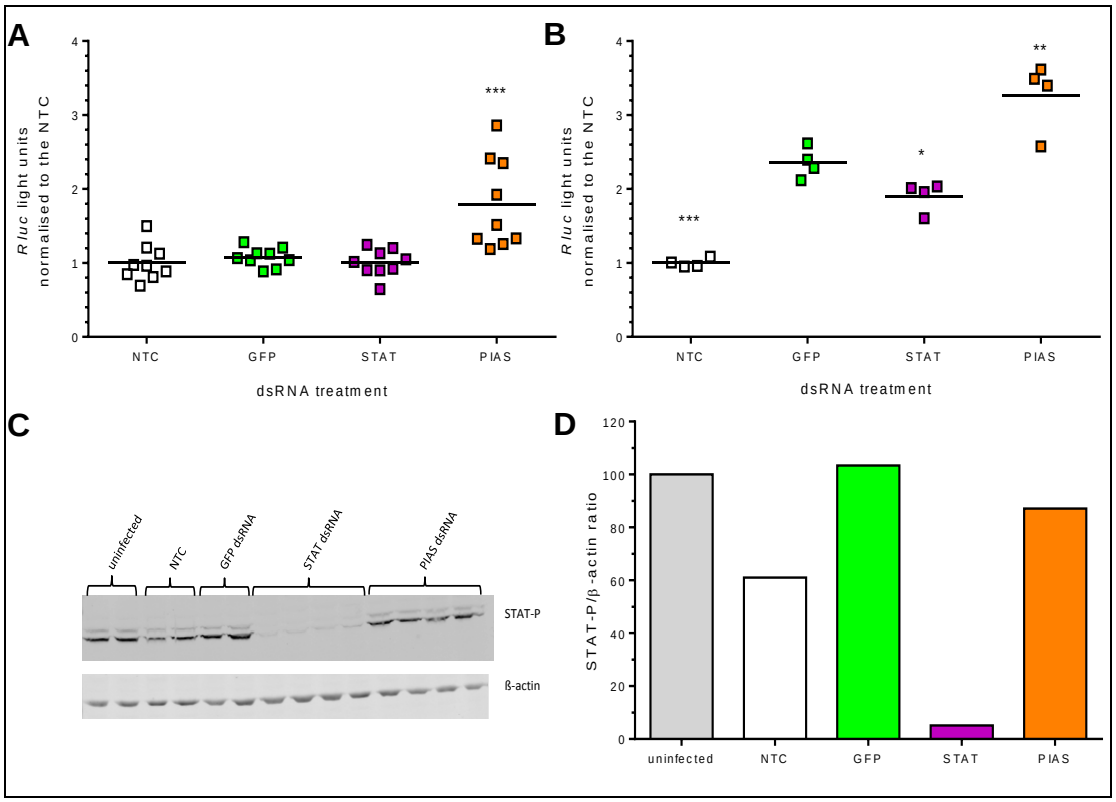

Figure 4.21: Effect of STAT and PIAS knockdown in IDE8 cells on SFV replication. IDE8 cells were treated with dsRNA targeting GFP, STAT or IxPIAS and infected 72 h later with SFV4(3H)-*Rluc* at MOI 5 and lysed 24 h p.i. for luciferase assay. (A) Data from two separate experiments was combined. *Rluc* activity was normalised to the NTC. In a third experiment half of the cells were lysed for luciferase assay (B), the other half were lysed for Western blot (C). Signal intensity of p-STAT and ß-actin were measured by semi-quantitative Western blot (LI-COR®) and the p-STAT/ß-actin was determined (D) to validate efficiency of STAT knockdown. Statistical significance as indicated (***$p \leq 0.0001$; **$p < 0.01$; *$p < 0.05$) was determined by One-way ANOVA with multiple comparisons compared to the GFP control (Fisher's LSD).

In the third experiment only half of each cell sample was lysed for luciferase assay, while the other half was lysed for Western blot analysis. *Rluc* activity was measured (Fig 4.21B) and knockdown of STAT was validated by Western blot (Fig 4.21C/D). *Rluc* activity was more than 2-fold increased in lysates from cells treated with

dsRNA against GFP prior to SFV infection compared to NTC cells. While this increase was not observed in the two experiments presented in Fig 4.21A it has been observed in many other experiments during this study and may depend on factors such as cell cycle/passaging, cell density or MOI used. Compared to the GFP control, *Rluc* activity was significantly decreased ($p<0.05$) in cells where STAT expression was knocked down (Fig 4.21B). However, the difference between the two conditions was only small (20% reduction). In contrast, treatment with dsRNA targeting IxPIAS, resulted in a significant increase ($p<0.01$) in *Rluc* activity compared to the GFP control (Fig 4.21B), as was also observed in the previous two experiments (Fig 4.21A). Knockdown of STAT was validated by Western blot (Fig 4.21C) and signal intensity of p-STAT and ß-actin was quantified. The ratio of p-STAT/ß-actin was plotted for the different conditions (Fig 4.21D) demonstrating approximately 95% reduction in p-STAT compared to the GFP control. If the antibody used indeed recognises activated STAT and if IxPIAS acts as a negative regulator of activated STAT, knockdown of IxPIAS expression should result in an increase in p-STAT. However, p-STAT levels were similar to the GFP control. The effect of IxPIAS knockdown on SFV may be unrelated to levels of activated STAT, but related to another function of IxPIAS during virus replication. In mammalian cells, PIAS interacts with transcription factors such as STAT by inhibiting their interaction with DNA and may thus not generally affect the amount of p-STAT (reviewed by Shuai, 2006). However, PIAS is also predicted to be an E3 SUMO ligase and knockdown may disrupt the regulation of cellular or viral proteins. However, since it remains unclear whether the p-STAT-5 antibody used detects activated STAT or *I. scapularis* STAT generally, it is difficult to draw conclusions from the presented data. Western blots using antibodies against the highly conserved SUMO proteins were performed (for sequence alignments and more information see Appendix, Figure 8.3) and while it was possible to detect many different bands as expected for a SUMO blot (Susan Jacobs, personal communication), no specific differences were observed between any of the controls and the STAT and IxPIAS knockdown samples (data not shown). Another potential problem was that knockdown of PIAS was not validated in these experiments, which would be important for the conclusion that the observed effect

was due to knockdown of IxPIAS gene expression. A commercial antibody against human PIAS-1/3 (Santa Cruz®, sc-8153) targeting a partially conserved region of the proteins was tested for knockdown validation by Western blot, but did not detect IxPIAS.

Next, the effect of knocking down STAT expression on LGTV replication and production was investigated. In the presented experiments, IxVago-1 expression was also knocked down in parallel, but no effect on LGTV was observed and knockdown efficiency could not be validated due to the technical difficulties described above. IDE8 cells were treated with dsRNA targeting STAT, or GFP as a control, and infected with LGTV at MOI 0.1 72 h later. Cell supernatant was collected 48 h p.i., cells were lysed for RNA extraction and cDNA was made. LGTV NS5 levels were determined by qPCR and normalised to ß-actin (Fig 4.22A). No significant difference between NTC, GFP- and STAT-treated cells was observed. Infectious virus titre was determined by plaque assay, but no significant difference between the three conditions was observed (Fig 4.22B). STAT knockdown was validated by qPCR and STAT levels were reduced by 95% in samples treated with dsRNA targeting STAT compared to the GFP control (data not shown).

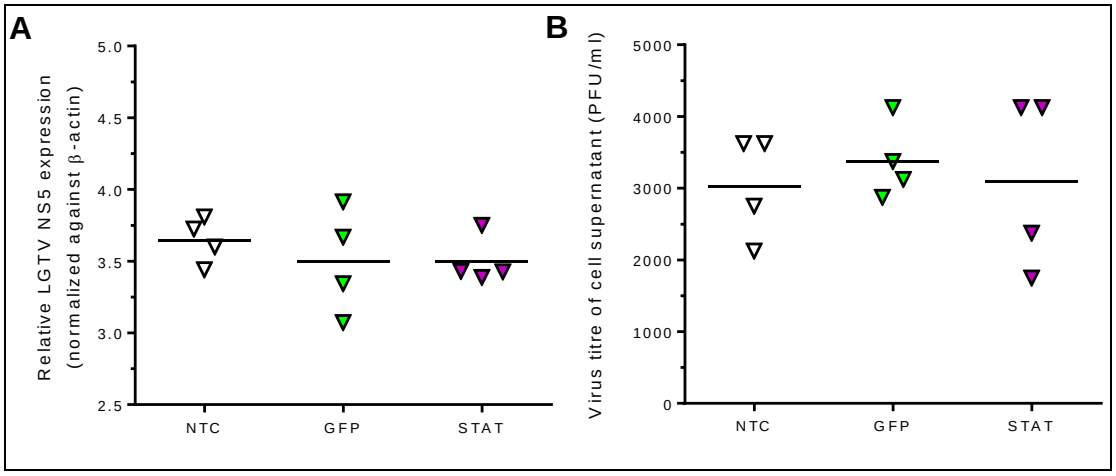

Figure 4.22: Knockdown of STAT expression in IDE8 cells does not affect LGTV replication (A) or production (B). IDE8 cells were treated with dsRNA targeting GFP or STAT and infected with LGTV-TP21 at MOI 0.1 72 h after addition of dsRNA. 48 h p.i., supernatant was harvested for plaque assay and cells lysed for RNA extraction. Statistical significance was tested for using One-way ANOVA with multiple comparisons compared to the GFP control (Fisher's LSD test).

4.2.6 Summary of results

- Pre-treatment of IDE8 cells with heat-inactivated *E. coli* resulted in a decrease in *Rluc* activity after subsequent infection with SFV4(3H)-*Rluc*, but viral RNA levels for SFV, SCRV and LGTV were unaffected by treatment with the bacteria
- Pre-infection of ISE6 cells with the intracellular bacterium *E. ruminantium* resulted in an increase in subsequent SFV replication
- No evidence for a tick orthologue of Imd or for melanisation in tick cells was found
- Putative components of the Toll pathway were identified, but no antiviral role could be demonstrated
- Components of the JAK/STAT pathway including an orthologue of the cytokine Vago were identified and an antibody suitable for the detection of *Ixodes* STAT was identified
- Knockdown of STAT expression did not result in an increase in the endogenous SCRV over 5 days after addition of dsRNA
- Knockdown of STAT expression had no effect on the acute phase of infection with either of the two arboviruses SFV or LGTV, suggesting that it may not be involved in cellular antiviral defences in IDE8 cells
- Knockdown of PIAS resulted in increased replication of SFV

4.3 DISCUSSION

The aim of this study was to determine if innate immunity pathways known from insects are also present in ticks and, if present, whether these pathways play a role in controlling virus replication. The results are summarised in Fig 4.23. The findings of Liu et *al*. (2012) regarding the orthologues of JAK and STAT in *I. scapularis* were confirmed and other components, such as PIAS and SOCS proteins, were identified by BLAST search. Orthologues of Toll pathway components were also identified, but no orthologue of Imd was found. While the Imd pathway is present in insects and crustaceans (Lemaitre and Hoffmann, 2007; Wang et al., 2009; Wang et al., 2011), no reports were found of Imd orthologues in lower bilaterians such as *C. elegans* or in other arachnids such as horseshoe crabs. One predicted protein from the cnidarian *Nematostella vectensis* (XP_001618286) has been hypothesised to be an Imd orthologue (Wang et al., 2009), but sequence coverage is low and no functional analysis was performed. Thus it remains unknown whether or not there is an Imd pathway in ticks. Melanisation is an important wound healing and antimicrobial mechanism in insects (Cerenius and Soderhall, 2004; Lemaitre and Hoffmann, 2007; Zou et al., 2010), which has been shown to have antiviral activity against SFV (Rodriguez-Andres et al., 2012). However, no orthologue of PO and no evidence for an antiviral PO cascade in tick cell supernatant was found, which is not entirely unexpected as melanisation in ticks has been discussed in the past, but no conclusive evidence for its presence in hard ticks has been found (Hajdusek et al., 2013; Zhioua et al., 1997). There has been only one report of PO activity in a nymph stage of the soft tick *O. moubata* (Kadota et al., 2002) suggesting that either hard ticks have lost the enzyme responsible for PO activity, or that further studies are necessary to demonstrate PO activity in hard ticks. Humoral processes similar to melanisation and also mediated by serine proteases and their inhibitors include, for example, coagulation, which can mediate wound healing and antimicrobial responses independent of PO (Cerenius and Soderhall, 2011; Lemaitre and Hoffmann, 2007; Muta and Iwanaga, 1996). There is some indication that haemolymph coagulation occurs in ticks, which may be sufficient to mediate wound healing and antimicrobial

defences together with other humoral responses present in ticks such as nodulation, encapsulation and the complement system (Hajdusek et al., 2013).

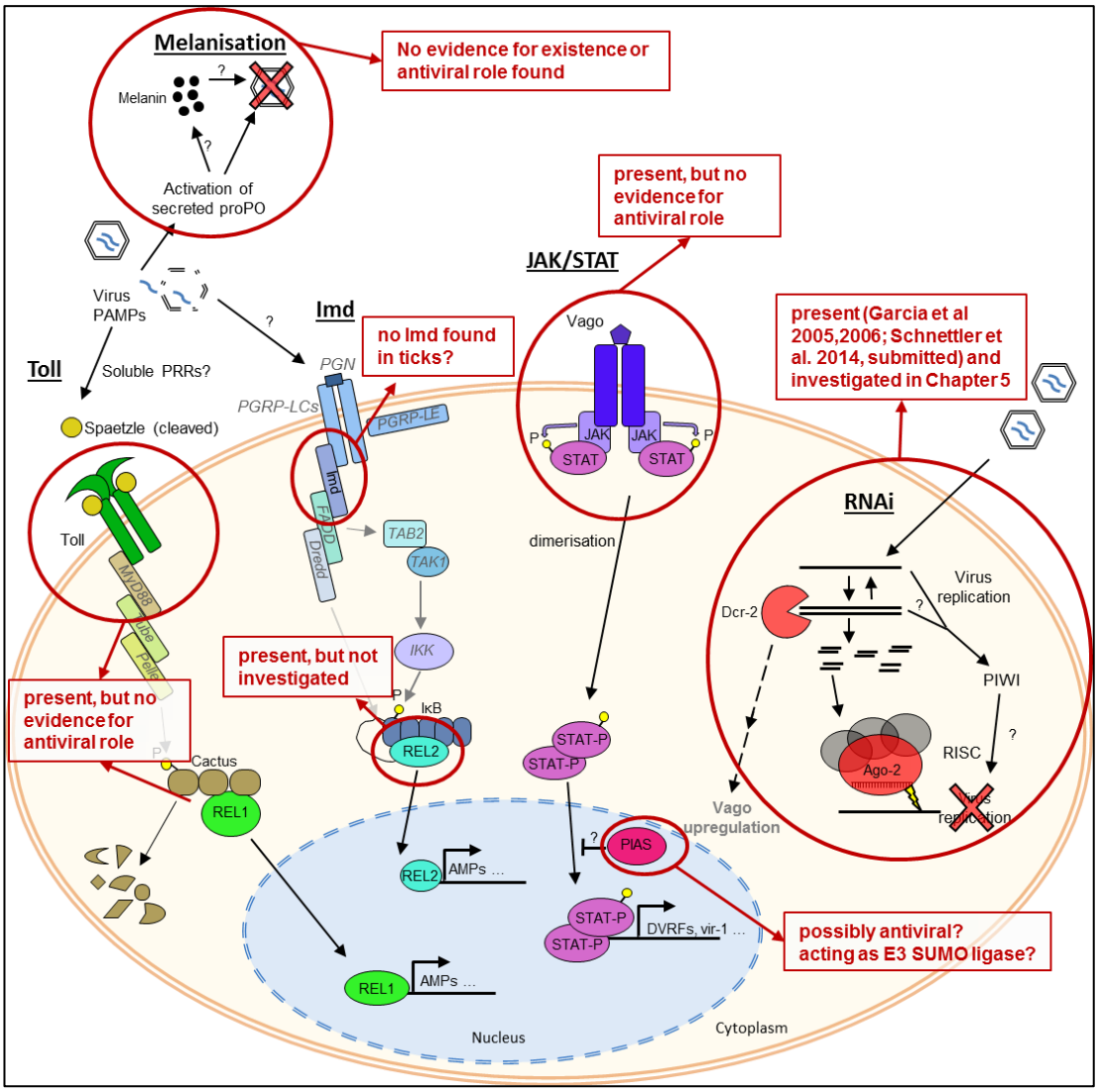

Figure 4.23: Graphic summary of Chapter 4 findings. (Modified from Rückert et al. 2014, in press)

Overall no conclusive evidence was found for an involvement of signalling pathways in the antiviral defence mechanisms of tick cells (Fig 4.23). There are many possible explanations – for example the lack of antiviral effects observed could be due to the cell lines being an inadequate system to represent tick immunity or the presence of an efficient RNAi system in ticks may preclude the necessity for additional antiviral

pathways. Many studies demonstrating the involvement of signalling pathways in antiviral responses of mosquitoes focus on events in the midgut (Rider et al., 2013; Xi et al., 2008). The complex midgut environment cannot be imitated by a cell line system, thus signalling pathways may still play a role in tick antiviral immunity *in vivo*. Furthermore, the heterogeneity of tick cell lines is a potential confounding factor in the studies performed. Only up to ~50% of IDE8 cells are susceptible to SFV infection (see 3.2.7), so if there were differences between dsRNA uptake and processing among cell types, it would be possible that those cells with the least efficient knockdown could be the only ones susceptible to SFV infection. While this particular scenario is unlikely it could be one of the potential drawbacks of using heterogenous cell lines. Another factor which may influence signalling pathways is the persistent infection of host cells with endogenous viruses (Alberdi et al., 2012; Attoui et al., 2001; Bell-Sakyi and Attoui, 2013). The endogenous orbivirus SCRV may be antagonising the antiviral immune response in untreated cells; thus knocking down pathway components may provide no further benefit to the infecting arbovirus. In order to answer this question, IDE8 cells would have to be cured of the persistent SCRV infection, which may be achievable by RNAi-mediated silencing of SCRV (discussed by (Bell-Sakyi and Attoui, 2013), or else it might be helpful to perform experiments to overexpress pathway components. Overexpression of antiviral proteins could overwhelm the putative inhibition of antiviral pathways by SCRV and provide a means of investigating their effect on SCRV or arboviruses. However, this approach is associated with another difficulty of working with tick cell lines, that is the inefficient expression of proteins from plasmids transfected into tick cells (discussed in 3.2.6). A way around this problem could be the use of lentiviral constructs to insert the genes stably into the tick cell genome to result in constitutive expression as previously described (Kurtti et al., 2008). Another possible solution is the generation of SFV VRPs encoding the desired genes of interest, but this may interfere with studies of virus infection, due to the expression of viral non-structural proteins.

Another possible explanation for the lack of evidence for antiviral roles of the proteins investigated is that the RNAi response in ticks represents such a strong

antiviral response that little involvement of other immune responses is necessary. Furthermore, effects of immune responses may differ between different viruses and for example a bunyavirus may be affected by JAK/STAT even if SFV and LGTV appeared not to be. The investigations into the different signalling pathways correlate with the initial experiment using heat-inactivated *E. coli* to pre-treat tick cells, which had no consistent effect on virus replication. However, the question why infection with the intracellular bacterium *E. ruminantium* (Moniuszko et al., 2014) resulted in an increase in virus replication remains unanswered. One explanation is that infection with *E. ruminantium* results in an inhibition of innate immunity pathways by the bacteria to enhance replication, and SFV may indirectly benefit from this. Furthermore, there may be a difference between extracellular and intracellular bacteria and their activation of different immune responses. The intracellular *E. ruminantium* may activate cellular responses inside the cell which somehow benefit the virus. Finally, infection of ISE6 tick cells with *E. ruminantium* will ultimately result in death of the culture and may have harmed the cells significantly by day 7 p.i. rendering the unhealthy cells unable to efficiently defend themselves against SFV infection.

Another protein probably involved in regulation of tick immunity is subolesin. It is an orthologue of insect Akirin and involved in regulation of NFκ-B (Naranjo et al., 2013) but also regulates other genes (de la Fuente et al., 2008). Two experiments were performed to knockdown expression of subolesin in ISE18 cells and subsequently infect them with SFV. While knockdown of subolesin consistently resulted in a decrease in *Rluc* activity as a measure for SFV replication (data not shown), it is difficult to draw any conclusions from this. The cells appeared to be less healthy 3 days after treatment with dsRNA against subolesin as assessed visually by microscopy, which is in contrast to previous studies, where knockdown of subolesin did not affect the tick cell lines IDE8 (Blouin et al., 2008) or ISE6 (Gerald Barry, Lesley Bell-Sakyi, personal communication). Furthermore, subolesin may regulate a large number of genes involved in general cell cycle events, which could indirectly affect SFV replication. Subolesin has been implicated in tick innate immune

responses to bacterial infection, but also in tick physiology and development (reviewed by de la Fuente et al., 2008; de la Fuente et al., 2011).

Due to the extent of research still necessary to unveil mechanisms of tick immunity, the present study could only scratch the surface of tick innate immunity signalling pathways. It was necessary to first establish the majority of methods, and a lack of reagents for work with tick cells was a constant limitation in experimental design. The study revealed the necessity for future projects focusing on the cellular mechanisms of signalling pathways in ticks. A first step should be to decipher the specific interactions between the identified putative orthologues to verify their roles in signalling. Despite the lack of evidence for an antiviral role of signalling pathways in this study it would be worth investigating their role in tick cellular biology and their putative antiviral role *in vivo*. In addition, a number of other immune responses and cell stress responses including the complement system, sumoylation, apoptosis and autophagy may be worth investigating in the future.

However, the lack of evidence for an antiviral role of the investigated signalling pathways suggested that RNAi may be the most important antiviral mechanism in ticks. Thus a putative component of the tick RNAi response was investigated as part of studies reported in the following chapter.

5. The antiviral role of CG4572 and selected RNAi components in tick and mosquito cells

5.1 INTRODUCTION

Antiviral RNAi is considered to be the most important antiviral mechanism known in mosquitoes and other insects (Blair, 2011). Arguably the most important components of the RNAi machinery are Ago and Dcr proteins. *I. scapularis* Ago and Dcr orthologues have been identified and characterised by Esther Schnettler who kindly provided her unpublished manuscript for information (Schnettler et *al*. 2014, submitted). Her study suggested that five Ago and two Dcr orthologues are encoded in the *I. scapularis* genome and are expressed in IDE8 cells (Fig 5.1). Inference of the phylogeny of metazoan Ago proteins suggested that four of the *I. scapularis* Ago orthologues (Ago-16, Ago-30, Ago-68 and Ago-96) are related to Ago-2, which is involved in the exogenous antiviral RNAi pathway, and one orthologue (Ago-78) is more closely related to Ago-1, which is involved in the miRNA pathway in other arthropods (Fig 5.1).

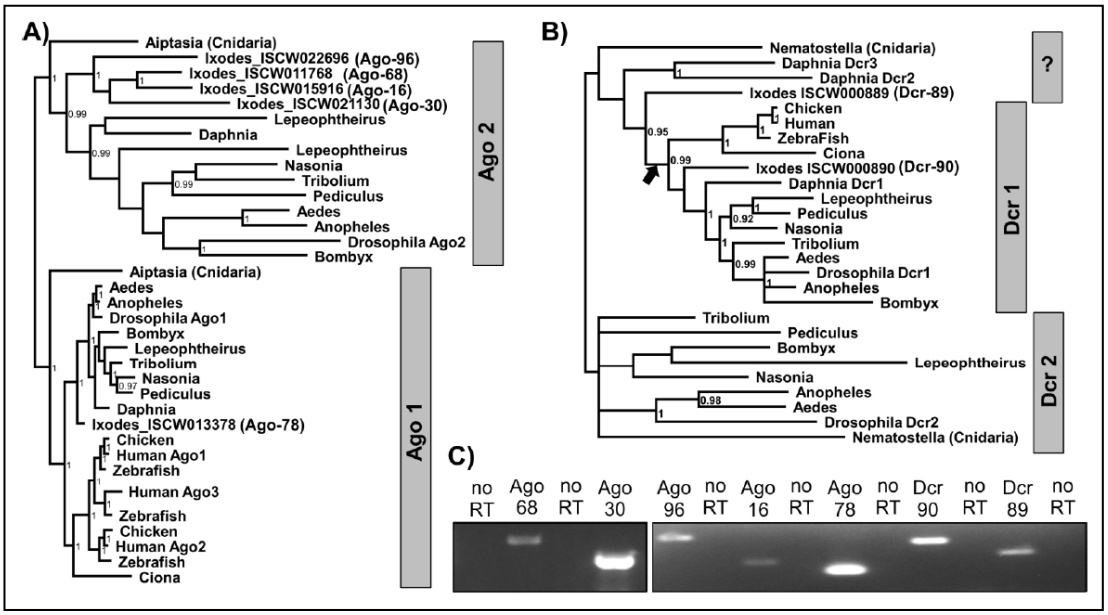

Figure 5.1: Ago and Dcr orthologues in *I. scapularis*. Gene trees of metazoan (A) Ago-subfamily genes and (B) Dcr genes. (C) Expression of the identified Ago and Dcr proteins was shown in IDE8 cells by RT-PCR (taken from Schnettler et al. 2014, submitted).

Knockdown of the identified Ago and Dcr proteins had variable effects on LGTV replication. Knockdown of Ago-16, Ago-30 and Ago-68 resulted in an increase in LGTV replication (approx. 1.6-1.8-fold), but none of the other knockdowns affected LGTV. In knockdown experiments with subsequent transfection of a LGTV replicon expressing *Rluc*, only Ago-16, Ago-30 and Dcr-90 knockdown increased *Rluc* activity. Since the effects on replication of LGTV were quite small (<2-fold increase), the authors investigated a putative role of the 3'UTRs of LGTV and TBEV as suppressors of the RNAi response. If LGTV had a mechanism to counteract antiviral RNAi, knocking down components of the RNAi machinery would not be of much additional benefit to the virus. The authors found evidence that the 3'UTRs of both LGTV and TBEV have RNAi suppressor activity in IDE8 tick cells.

Two of the aims of this part of the present study were to investigate whether the endogenous orbivirus SCRV is controlled by the IDE8 RNAi system and what effect knockdown of the two Ago proteins Ago-16 and Ago-30 has on SFV replication in IDE8 cells. The presence of components of the miRNA and piRNA pathways in *I. scapularis* was also investigated by BLAST search but due to time limitations no further studies were performed with the identified genes as part of this project.

However, the main objective of this part of the study was to focus on selected putative components of the dsRNA uptake machinery which would be required for systemic RNAi. Systemic spread of the RNAi response is an important aspect of antiviral RNAi in many organisms. While plants and the model organism *C. elegans* (*Nematoda*) use RdRPs to amplify dsRNA (Voinnet, 2005), no protein with RdRP activity has been conclusively identified in arthropods. Using a computational approach a putative RdRP has been identified in ticks, but no experimental evidence in support of this has been reported (Kurscheid et al., 2009). Furthermore, it has been shown that long (≥ 31 bp) dsRNA in the medium can be internalised by *D. melanogaster* cells (Saleh et al., 2006; Ulvila et al., 2006) and that systemic spread of the RNAi response is essential for efficient antiviral RNAi in *D. melanogaster* (Saleh et al., 2009). Uptake was most efficient for dsRNA >200 bp in length. Furthermore, in U4.4 mosquito cell culture, it has been shown that siRNA molecules produced in infected cells can spread through the culture in a contact-dependent manner

(Attarzadeh-Yazdi et al., 2009), but dsRNA uptake in mosquito cell culture is inefficient and transfection is necessary (Rennos Fragkoudis, personal communication). The mechanisms by which siRNA and/or dsRNA spread through the body of an insect are not well understood, but a number of components of the dsRNA uptake machinery have been identified in *D. melanogaster* (Saleh et al., 2006). Three of the identified components, namely the genes *ninaC*, *egghead* and *CG4572*, were selected for a follow-up study demonstrating the importance of RNAi spread for an efficient antiviral response (Saleh et al., 2009). In *Drosophila*, *egghead* encodes a seven-transmembrane-domain glycosyltransferease, *ninaC* encodes a protein involved in vesicle transport and *CG4572* encodes a serine carboxypeptidase of unknown cellular function. Saleh et al. (2009) showed that homozygous knockout of the three genes significantly decreased fly survival after infection with SINV and DCV, while viability and fertility in uninfected knockout flies were not significantly different to wild type flies. The strongest effect was observed in CG4572$^{-/-}$ flies. Some evidence was provided that the observed effect is due to a deficiency in spread of the RNAi response. However, when expression of orthologues of the three genes was knocked down in *C. elegans* only knockdown of *ninaC* expression resulted in a loss of systemic RNAi, whereas knockdown of *CG4572* expression did not affect systemic RNAi and the effect of *egghead* knockdown on systemic RNAi was limited (Saleh et al., 2009). Another study demonstrated the role of CG4572 in the RNAi-mediated control of persistent flock house virus (FHV) infection in *Drosophila* cell culture (Goic et al., 2013).

It has been shown that many tick cell lines can take up dsRNA from the culture medium (Barry et al., 2013) and tick orthologues were previously identified for *ninaC*, *egghead* and *CG4572* among other components of the dsRNA uptake machinery (Kurscheid et al., 2009). No reports were found of mosquito orthologues of the three proteins. Thus, the aims of the present study were to confirm the findings of Kurscheid et *al*. (2009) regarding the presence of *ninaC*, *egghead* and *CG4572* in *I. scapularis*, to identify *Ae. aegypti* orthologues, to investigate expression of these genes in tick and mosquito cells and to determine whether they are required for RNAi responses to virus infection.

5.1.1 Objectives

- Identify *I. scapularis* orthologues of components of the miRNA and piRNA pathways
- Identify *I. scapularis* and *Ae. aegypti* orthologues of the genes *ninaC*, *egghead* and *CG4572* which may be important for uptake and spread of dsRNA.
- Investigate whether SCRV is controlled by antiviral RNAi in IDE8 cells
- Determine the effect of Ago-16 and Ago-30 knockdown on SFV and LGTV replication in IDE8 cells
- If present, investigate the role of NinaC, egghead and CG4572 in SFV, SCRV and LGTV replication in IDE8 tick cells, and in SFV replication in mosquito cells
- Determine whether there is spread of siRNAs through IDE8 tick and Aag2 mosquito cell cultures

5.1.2 Methods and experimental design

BLAST searches and knockdown experiments were performed as described previously in Chapter 4 (see 4.1.2). Accession numbers of protein sequences used for BLAST search are provided in Chapter 2 (see Table 2.3) and knockdown of gene expression was performed as described for tick (2.14) and mosquito (2.15) cells. Experiments performed to determine whether there is spread of the siRNA response in IDE8 and Aag2 cells were conducted as described below in the respective Results sections. Transfections of mosquito cells were performed as described in 2.15.

5.2 RESULTS

5.2.1 Orthologues of the RNAi system in *I. scapularis*

Arguably the most important components of siRNA and miRNA processing are Ago and Dcr proteins. Furthermore, for miRNA processing, the proteins Drosha and Pasha are essential for the initial processing of transcribed pri-miRNA into pre-

miRNA which is then transported out of the nucleus for processing by Dcr-1. A putative orthologue of the enzyme Drosha was found in *I. scapularis* by BLAST search (Table 5.1). While the sequence only covered 57% of the *D. melanogaster* sequence and the orthologue is much smaller (778 aa as opposed to 1327 aa), sequence identity of the similar region was 61% and no other *Drosophila* protein was closer in sequence similarity (as determined using the putative *I. scapularis* Drosha sequence for blastp against *D. melanogaster* nr protein sequences). According to the annotation on NCBI, this sequence spans sequencing gaps and may be missing exons. The putative *I. scapularis* Drosha (annotated as putative ribonuclease III) contains two ribonuclease III domains in close proximity to each other, as seen in *Drosophila* and human Drosha. Furthermore, a putative Pasha orthologue was also identified by BLAST search (Table 5.1). It is shorter than DmPasha (373 aa instead of 642 aa) and lacks annotated dsRNA-binding and RNaseIII domains, but when the identified protein was used to BLAST back against the *D. melanogaster* nr protein database, Pasha was the only hit. As observed before for Drosha, the annotated Pasha sequence appears to span sequencing gaps and may be missing exons.

Table 5.1: Putative orthologues of proteins involved in RNAi identified by BLAST search of the *I. scapularis* genome using *D. melanogaster* protein sequences.

orthologue of	Ixodes gene	Query Coverage	Max. Identity	Length (aa)	mRNA accession no.	Protein accession no.
Drosha	ribonuclease III	57%	61%	778	XM_002416087.1	XP_002416132.1
Pasha	IxPasha	45%	43%	373	XM_002409066.1	XP_002409110.1
PIWI	PIWI-like protein 1*	91%	39%	849	XM_002399349.1	XP_002399390.1
PIWI	PIWI-like protein 2*	89%	34%	755	XM_002411725.1	XP_002411770.1
PIWI	PIWI-like protein 3*	40%	37%	375	XM_002413940.1	XP_002413985.1

* On NCBI these genes were annotated as putative Cniwi proteins, which is the cnidarian orthologue of *Drosophila* PIWI.

The third major component of RNAi is the piRNA system. Its role in antiviral defences in mosquitoes is becoming more and more evident and was discussed in the introduction of this thesis (see 1.4.1). Schnettler et *al*. (submitted) have shown that, besides the major group of 22 nt small RNAs, a class of small RNAs of 27-29 nt is found in tick cells, with a peak at 28 nt. There is an unproven possibility that these

longer small RNAs represent piRNAs. In other arthropods, piRNA molecules are processed by PIWI-like proteins. BLAST search of the *I. scapularis* nr protein database using DmPIWI provided three putative *I. scapularis* PIWI orthologues (Table 5.1) which were annotated as Cniwi proteins on NCBI (the cnidarian orthologue of PIWI). The proteins have annotated PIWI and PAZ domains, and include a nucleotide binding site. When the *I. scapularis* PIWI-like protein 1 was used for a BLAST search (blastp) against the non-redundant (nr) protein database, good coverage (89%) and sequence identity (45%) to the human PIWI orthologue HIWI (accession no. AAK92281.1) were found. These observations indicate the presence of a piRNA pathway in ticks which could be investigated for its putative antiviral role in the future. Components of the PIWI pathway have also been identified in *R. microplus* and *I. scapularis* by Kurscheid et *al*. (2009).

5.2.2 Orthologues of dsRNA uptake proteins in *I. scapularis* and *Ae. aegypti*

The three *D. melanogaster* protein sequences for NinaC, egghead and CG4572 were used to BLAST against the *I. scapularis* and *Ae. aegypti* nr protein databases. Putative orthologues for egghead and CG4572 with good sequence similarity and coverage were found in both *I. scapularis* and *Ae. aegypti*. The putative *I. scapularis* egghead orthologue covered 98% of the *D. melanogaster* egghead sequence, was almost identical in length (two amino acids longer) and had 68% maximum identity (Table 5.2). Expression of egghead mRNA in IDE8 cells was confirmed by RT-PCR (Fig 5.1). Ten putative orthologues of CG4572 were found in *I. scapularis* with over 74% sequence coverage and of similar length (361-476 aa) to DmCG4572 (482 aa) (Table 5.2). Using RT-PCR, expression was detected for one of the orthologues, namely IxCG4572_3 (Fig 5.2), but none of the other orthologues could be detected using two different primer sets for each gene.

Table 5.2: Putative orthologues of egghead, CG4572 and NinaC in *I.scapularis*.

	Coverage	Max. Identity	Length (aa)	mRNA accession no.	Protein accession no.
IxEgghead	98%	68%	459	XM_002405816.1	XP_002405860.1
IxCG4572_1	87%	46%	468	XM_002409079.1	XP_002409123.1
IxCG4572_2	87%	45%	465	XM_002403990.1	XP_002404034.1
IxCG4572_3	87%	45%	473	XM_002405400.1	XP_002405444.1
IxCG4572_4	89%	44%	471	XM_002404245.1	XP_002404289.1
IxCG4572_5	90%	42%	447	XM_002415828.1	XP_002415873.1
IxCG4572_6	77%	44%	374	XM_002435219.1	XP_002435264.1
IxCG4572_7	74%	42%	361	XM_002402597.1	XP_002402641.1
IxCG4572_8	89%	32%	435	XM_002399922.1	XP_002399966.1
IxCG4572_9	87%	33%	476	XM_002402819.1	XP_002402863.1
IxCG4572_10	88%	30%	443	XM_002414145.1	XP_002414190.1
IxNinaC	70%	33%	818	XM_002401095.1	XP_002401139.1

When the gene published as a NinaC orthologue (ABJB011087029.1, Kurscheid et *al*. 2009) was compared to the *D. melanogaster* NinaC sequence, only a small proportion (10%) was covered. Since it was such a short overlapping region, it was not investigated further as part of this study. In a later analysis and BLAST search using the *D. melanogaster* NinaC sequence, a putative myosin orthologue was identified as close in sequence similarity to DmNinaC in *I. scapularis* (70% coverage and 33% max. identity). Since DmNinaC is also a myosin orthologue, the identified protein may be an *I. scapularis* orthologue of NinaC and was included in Table 5.2 for completeness.

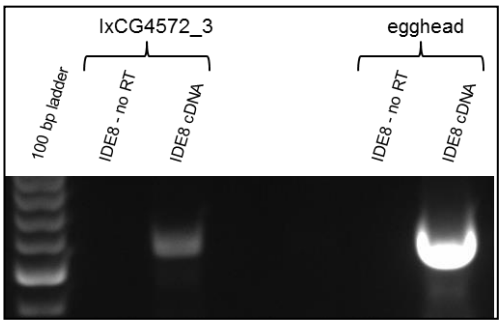

Figure 5.2: mRNA expression of IxCg4572_3 and egghead in IDE8 cells detected by RT-PCR.

The putative *Ae. aegypti* egghead orthologue covers the whole query sequence and has 86% maximum identity with *Drosophila* egghead (Table 5.3). It is of almost identical length as *Drosophila* egghead (457 aa) and mRNA expression was detected by RT-PCR in Aag2 cells (data not shown).

Furthermore, three *Ae. aegypti* orthologues of CG4572 were identified by BLAST search (Table 5.3) and expression of all three was detected by RT-PCR in Aag2 cells. PCR products of the expected size were also amplified from the *Ae. albopictus* cell line U4.4 using primers targeting *Ae. aegypti* CG4572_05.1 and CG4572_56.1, but not for CG4572_06.1. Further sequence information was gained from a personal communication with Julio Rodriguez-Andres (AAHL, CSIRO, Geelong), who screened his transcriptomic database derived from SFV-infected and control U4.4 cells. He identified contigs from two CG4572 orthologues which had close sequence similarity to CG4572_05.1 and CG4572_56.1. Neither of the genes was differentially expressed after SFV infection in his transcriptomic study. The contig sequences are included in the appendix (see 8.4.1).

A NinaC/Myosin orthologue was also identified (blastp), which covered 95% of the DmNinaC sequence and had quite a high maximum similarity (53%), but the putative orthologues of NinaC in *I. scapularis* and *Ae. aegypti* were not further investigated as part of the present study.

Table 5.3: Orthologues of egghead, CG4572 and NinaC in *Ae. aegypti*.

	Coverage	Max. Identity	Length (aa)	mRNA accession no.	Protein accession no.
AaeEgghead	100%	86%	458	XM_001649545.1	XP_001649595.1
CG4572_56.1	98%	54%	481	XM_001659856.1	XP_001659906.1
CG4572_05.1	92%	54%	484	XM_001652005.1	XP_001652055.1
CG4572_06.1	89%	48%	471	XM_001652006.1	XP_001652056.1
Myosin (NinaC)	95%	53%	1561	XM_001649142.1	XP_001649192

The *D. melanogaster*, *Ae. aegypti* and *I. scapularis* sequences of the identified egghead and CG4572 orthologues were aligned using ClustalW. In particular, the protein sequence of egghead was highly conserved between the three species (Fig

5.3). When the egghead sequences were used to BLAST against the vertebrate nr protein database, no orthologues were found, indicating that egghead may be a highly conserved arthropod protein which is not present in vertebrates.

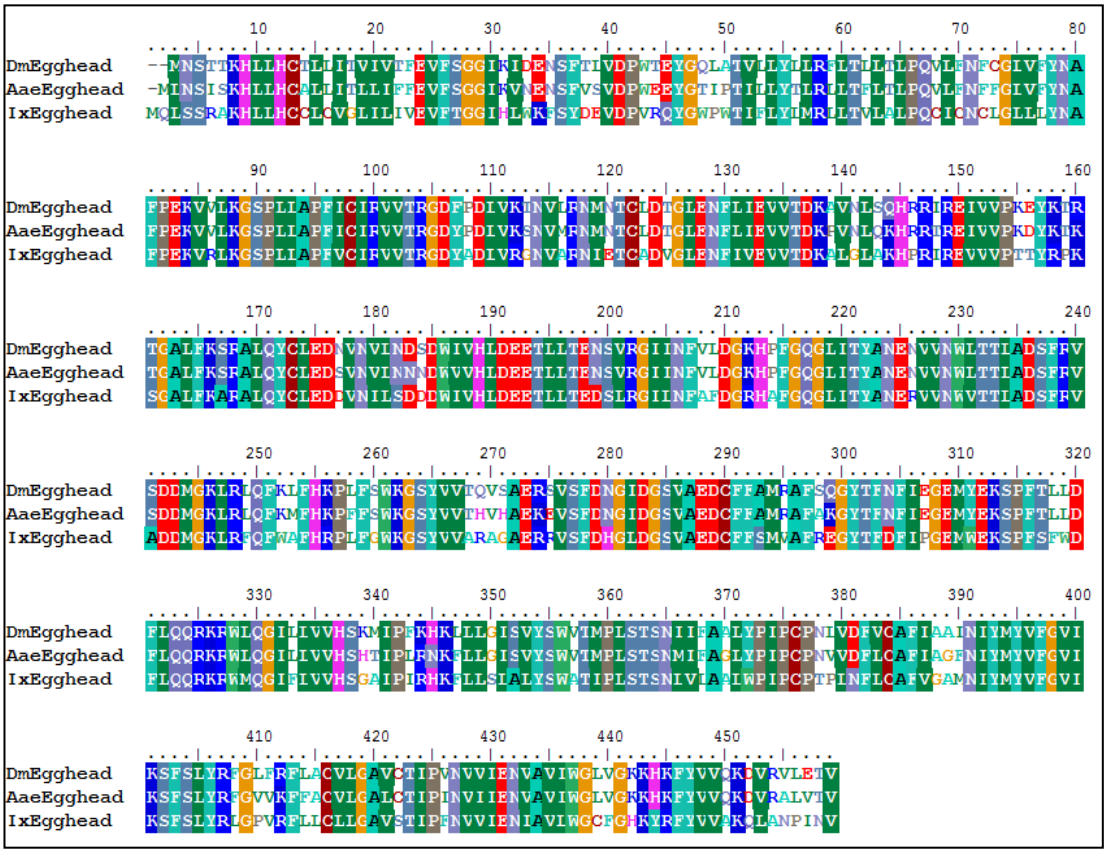

Figure 5.3: Alignment of *D. melanogaster (*Dm*)*, *Ae. aegypti* (Aae) and *I. scapularis* (Ix) egghead sequences using ClustalW.

Alignment of DmCg4572, the three identified mosquito CG4572 and IxCG4572_3 showed that some regions of the sequence are highly conserved, while other regions diverge between the five sequences (Figure 5.4). As expected there is a high level of conservation between the four insect sequences and more differences between these and the tick sequence.

Following this analysis, dsRNA was generated from IDE8 cDNA targeting egghead and IxCG4572_3, and from Aag2 cells targeting egghead and the three mosquito Cg4572 orthologues. dsRNA was also generated from U4.4 cDNA for the two *Aedes*

CG4572 orthologues CG4572_05.1 and CG4572_56.1. The *Ae. albopictus* genome is not published and it cannot be guaranteed that the sequences amplified from U4.4 cDNA are in fact the same CG4572 orthologues as identified in the *Ae. aegypti* genome. While the results obtained were included in this study, for future studies or publication the full length sequences of the *Ae. albopictus* genes should be determined.

Figure 5.4: Alignment of *D. melanogaster* (Dm), *Ae. aegypti* (Aae) and *I. scapularis* (Ix) CG4572 sequences using ClustalW.

5.2.3 The role of tick RNAi in SCRV, SFV and LGTV replication

As potentially the most important antiviral mechanism in arthropods, RNAi is likely to be involved in controlling the persistent infection of IDE8 cells with SCRV. In order to investigate this possibility, components of the RNAi machinery were knocked down in IDE8 cells and SCRV levels were measured 72 h after addition of dsRNA. Three independent experiments were performed in which IDE8 cells were seeded at $5x10^5$ cells per well, treated with dsRNA targeting GFP, CG4572, Ago16, Ago30 or no dsRNA as a control (NTC). In two of the experiments (Expts 1 and 2), dsRNA was simply added to the cultures. In the third experiment (Expt 3), dsRNA was transfected as described for mosquito cells (see 2.15), using 200 ng dsRNA per well, in an attempt to maximise knockdown efficiency. Knockdown efficiency for Ago16 and Ago30 was validated by semi-quantitative RT-PCR (see 2.16). For Ago30 the primers used to generate dsRNA were used, but for Ago16 a second primer set was used to validate knockdown efficiency, as established previously (Sabine Weisheit and Esther Schnettler, personal communication). Levels of Ago16 mRNA were significantly reduced by 52%, 41% and 69% in Expts 1, 2 and 3 respectively, suggesting that transfection of dsRNA resulted in more efficient Ago16 knockdown at the selected time-point, compared to adding the dsRNA to the medium (Fig 5.5). Ago30 levels were also significantly reduced in all experiments. Efficiency of Ago30 knockdown was generally higher than for Ago16, with 83%, 92% and 78% knockdown efficiency in Expts 1-3 (Fig 5.5). Interestingly, Expt 3 had the lowest Ago30 knockdown efficiency, suggesting that transfection of dsRNA resulted in less efficient knockdown of Ago30 at the selected time-point, compared to adding the dsRNA to the medium.

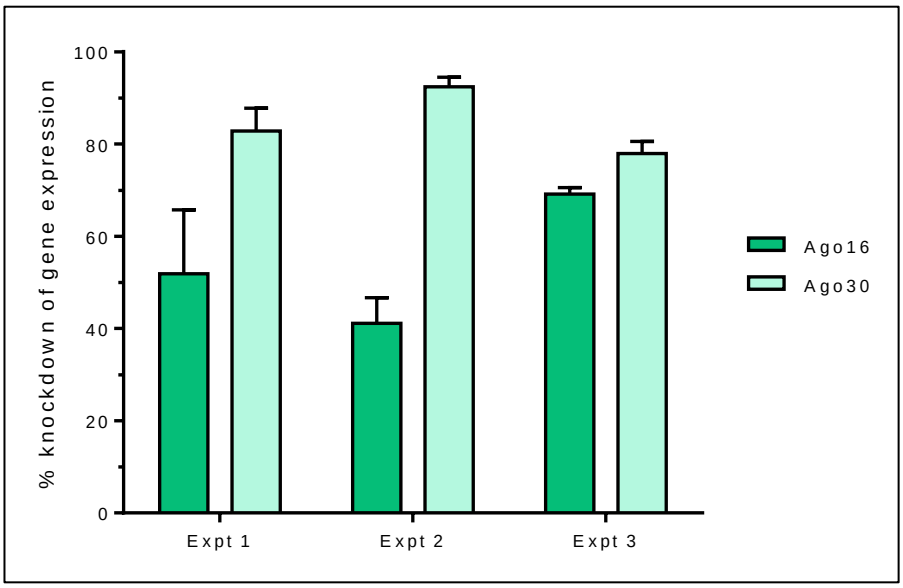

Figure 5.5: Knockdown of Ago16 and Ago30 expression in IDE8 cells as detected by semi-quantitative PCR relative to the GFP dsRNA control. Each data point represents four replicate cultures and error bars indicate SD.

CG4572 knockdown validation proved difficult, mainly due to the very low level of expression detected by RT-PCR, which in some cases was undetectable. Furthermore, RT-PCR using the primers used to generate dsRNA resulted in amplification of (probably) remaining dsRNA, thus showing an increase in CG4572_3 instead of a decrease. Two other primer sets amplifying a different region of the cds were designed, but did not allow conclusive validation of knockdown, largely due to the very low levels obtained by PCR.

SCRV RNA levels were determined in the three experiments and are presented separately for individual experiments due to the different trend in Expt 1 (Fig 5.6 A-C) and normalised and combined to visualise the overall trend (Fig 5.6D). In all experiments, addition of the non-specific dsRNA control targeting GFP resulted in a significant increase in SCRV levels 72 h after addition, indicating that dsRNA may activate responses beneficial to SCRV replication or divert responses away from controlling virus replication. Addition of IxCG4572_3 dsRNA had no effect on SCRV replication. The hypothesis is that CG4572 is involved in spread of the antiviral RNAi response through the culture, which protects uninfected cells against impending virus infection. Thus, it is not surprising that a virus persistently infecting

these cells was not affected by knockdown of IxCG4572_3 as it is likely to have infected all susceptible cells in the culture already. However, as it was not possible to validate knockdown of IxCG4572_3, it is possible that there was no significant reduction in IxCG4572_3 mRNA levels.

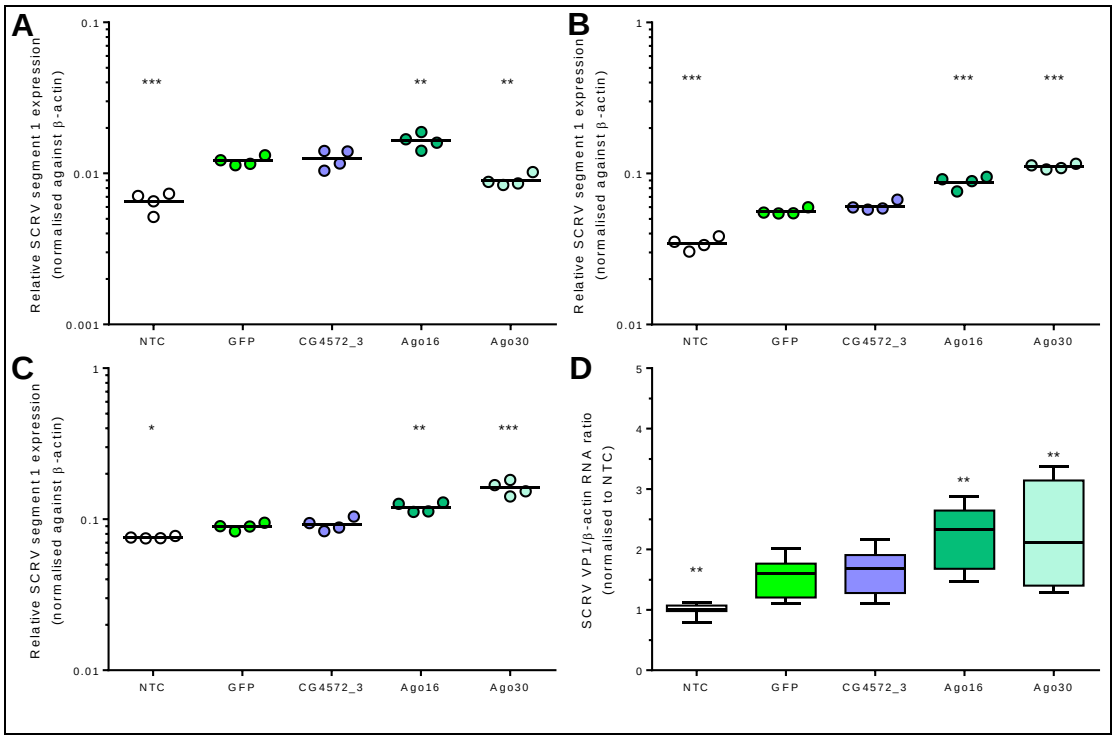

Figure 5.6: Knockdown of Ago-16 or Ago-30 expression in IDE8 cells affects SCRV replication. IDE8 cells were treated for 72 h with dsRNA targeting GFP, CG4572_3, Ago16, Ago30 or no dsRNA (NTC) and lysed for RNA extraction and qRT-PCR to quantify SCRV RNA levels. Three experiments were performed with four replicates per experiment. Results for each experiment are presented individually (A, B, C) and combined after normalisation to the NTC (D). Statistical significance as indicated (***p≤0.0001; **p<0.01) was determined by One-way ANOVA with multiple comparisons to the GFP control (Fisher's LSD).

In all three experiments, knockdown of Ago16 expression resulted in a small (1.3-1.6-fold) but significant increase in SCRV replication, which was also significant after normalisation and combination of the three experiments ($p<0.01$) (Fig 5.6D). After knockdown of Ago30, SCRV RNA levels were significantly decreased (0.7-fold) in Expt 1 (Fig 5.6A), but significantly increased in Expt 2 (2.0-fold) and Expt 3 (1.8-fold) and overall when the three experiments were combined (Fig 5.6D). The reason for the difference observed between the three experiments remains unknown,

but it was observed that SCRV RNA levels in NTC cells were generally 5.3-fold and 11.6-fold higher in Expts 2 and 3 respectively, compared to Expt 1. Overall, these results indicate that replication of SCRV is at least partially controlled by the RNAi machinery.

Next, the effect of egghead and CG4572 on arbovirus replication was investigated. IxEgghead knockdown had no effect on SFV replication in two pilot experiments in IDE8 cells and was thus not further investigated in this study. In order to investigate the effect of CG4572_3 knockdown on SFV replication, IDE8 cells were treated with dsRNA targeting GFP, IxCG4572_3 or no dsRNA (NTC), infected with SFV4(3H)-*Rluc* at MOI 1 and lysed 24 h p.i. (Fig 5.7A). *Rluc* activity as a measure of SFV replication was significantly increased (2.3-fold) in IDE8 cells treated with dsRNA targeting IxCG4572_3 (Fig 5.7A). A similar increase was observed in two further experiments performed as described above (data not shown).

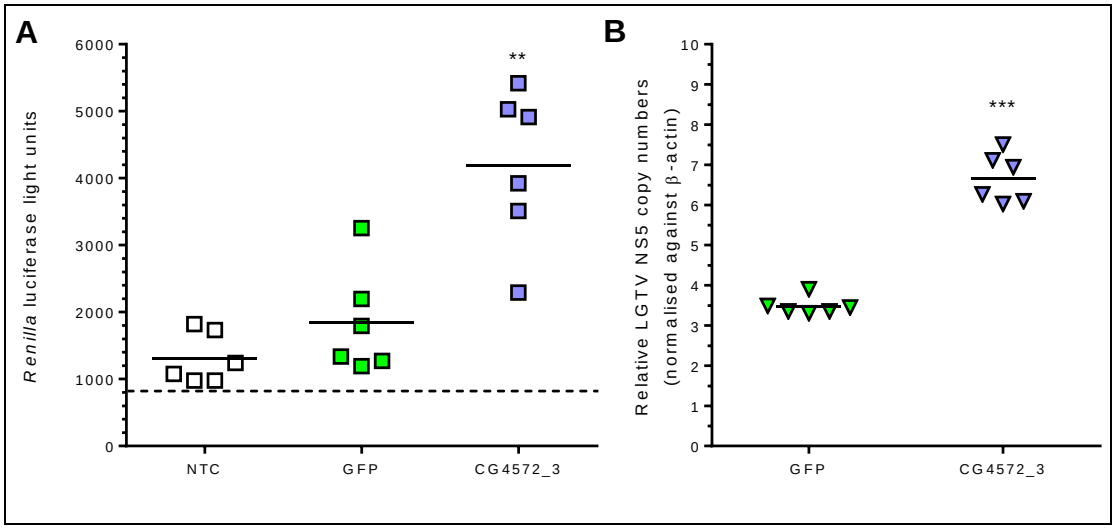

Figure 5.7: Knockdown of CG4572_3 expression in IDE8 cells results in an increase in SFV and LGTV replication. IDE8 cells were treated for 72 h with dsRNA targeting GFP, CG4572_3 or no dsRNA (NTC), infected with (A) SFV4(3H)-*Rluc* at MOI 1 or (B) LGTV at MOI 0.1 and lysed for (A) *Rluc* assay as a measure for SFV replication or (B) RNA extraction and qRT-PCR to quantify LGTV RNA levels. Statistical significance as indicated (**p<0.01) was determined by (A) One-way ANOVA with multiple comparisons (Fisher's LSD) or (B) Student's t-test. The dotted line indicates the limit of detection.

In order to investigate the effect of CG4572_3 knockdown on LGTV replication, IDE8 cells were treated with dsRNA targeting GFP, IxCG4572_3 or no dsRNA (NTC), infected with LGTV at MOI 0.1 and lysed 48 h p.i. (Fig 5.7B). LGTV replication as measured by qPCR was significantly increased (1.9-fold) in IDE8 cells treated with dsRNA targeting IxCG4572_3 compared to the GFP control. IxCG4572_3 knockdown in these experiments could not be validated due to the technical difficulties discussed above.

In order to further investigate the role of components of the RNAi system, expression of two of the *I. scapularis* Ago proteins, Ago16 and Ago30, was also knocked down in a subsequent experiment. IDE8 cells were treated for 72 h with dsRNA targeting GFP, IxCG4572_3, Ago16, Ago30 or no dsRNA (NTC), and cells were then infected with either SFV4(3H)-*Rluc* (MOI 1 or MOI 0.01) or with LGTV (MOI 1 or MOI 0.005). 48 h p.i. with SFV or LGTV, culture supernatants were harvested and cells lysed. Knockdown of Ago16 and Ago30 was validated by semi-quantitative PCR (Fig 5.8). In all cultures treated with Ago16 dsRNA, Ago16 expression was significantly reduced by 40-60%, and in cultures treated with Ago30 dsRNA the levels of Ago30 mRNA were significantly reduced by 69-91%. As described previously, IxCG4572_3 knockdown efficiency could not be determined.

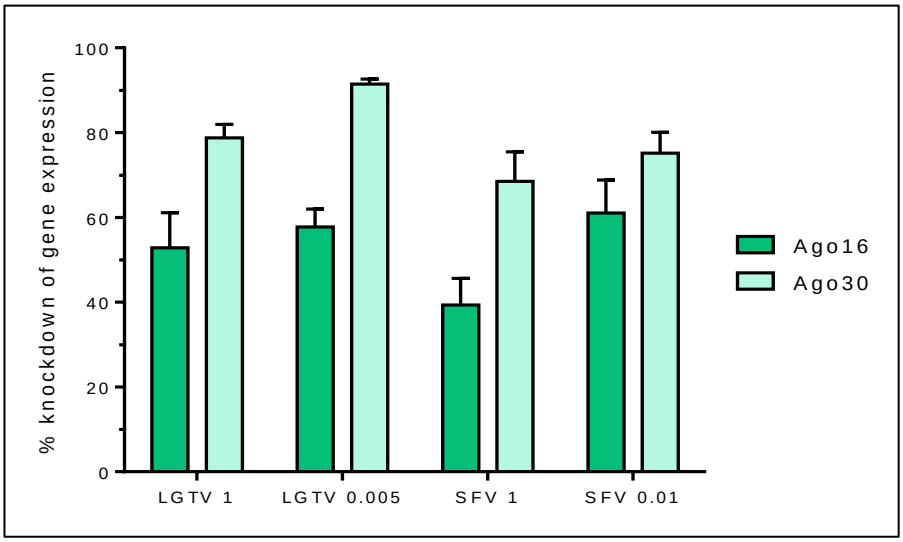

Figure 5.8: Knockdown of Ago16 and Ago30 expression in IDE8 cells as detected by semi-quantitative PCR relative to the GFP dsRNA control. Each data point represents four replicate cultures and error bars indicate SD.

Knockdown of Ago30 had a dramatic effect on SFV replication. In IDE8 cells infected with SFV at MOI 1, both SFV RNA levels and infectious virus titre were increased significantly by approximately 10-fold compared to the GFP control (Fig 5.9A,B). Surprisingly, knockdown of Ago16 resulted in a decrease in SFV RNA and titre, after infection with MOI 1, but the observed decrease was not statistically significant (Fig 5.9A,B). Upon infection with SFV at MOI 1, knockdown of IxCG4572_3 had no effect on infectious virus titre and resulted only in a small increase (1.4-fold) in SFV RNA levels, which was not statistically significant. Infection of IDE8 cells with SFV at MOI 0.01, resulted in high standard deviation and outliers in almost every condition. This might be caused by the increased effect that confounding factors can have during a low MOI infection, such as minor differences in amount of virus added to each sample, the cell type which is first infected, if knockdown was efficient in the cells first infected and how many cells become infected with multiple infectious particles. Despite the high variability, SFV RNA levels and infectious virus titre were significantly increased (>100-fold) in cultures with reduced Ago30 expression (Fig 5.9C,D).

The data obtained was difficult to interpret due to the outliers – one sample of the NTC cells was over 39-fold increased compared to the other three NTC samples both in viral RNA and titre (Fig 5.9C,D). Furthermore, in cells treated with dsRNA targeting IxCG4572_3, SFV RNA levels and titres were increased by 6.1-fold and 7.6-fold, respectively, but due to the high variability among samples the effect was not statistically significant. Similarly, knockdown of Ago16 resulted in an increase in SFV RNA and virus titre after infection with MOI 0.01 compared to the GFP control, but the increase was not statistically significant (Fig 5.9C,D). Overall, SFV replication and virus production was were only significantly affected by knockdown of Ago30 expression, which appears to play an important role in controlling SFV replication in IDE8 cells.

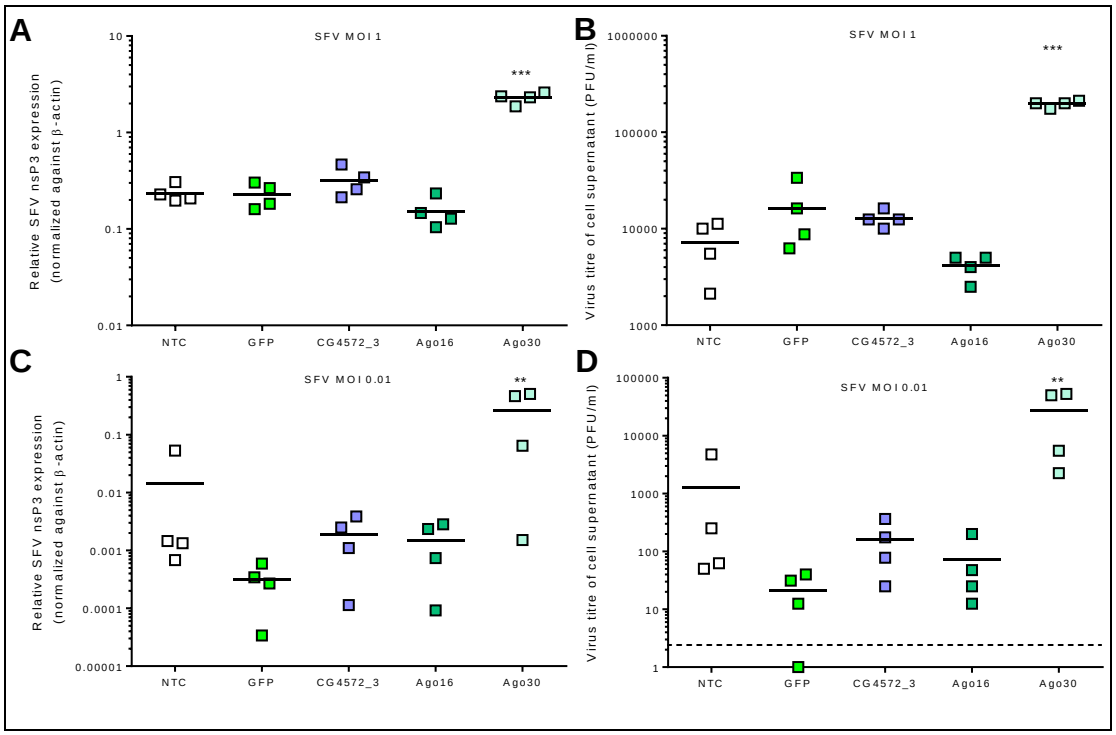

Figure 5.9: Knockdown of CG4572_3 or Ago-30 expression increases SFV replication in IDE8 cells compared to the GFP control. IDE8 cells were treated for 72 h with dsRNA targeting GFP, CG4572_3, Ago16, Ago30 or no dsRNA (NTC). Cells were infected with SFV4(3H)-*Rluc* at MOI 1 (A, B) or MOI 0.01 (C, D) and lysed 48 h p.i. for RNA extraction and supernatant was collected for plaque assay. Viral RNA levels were measured by qPCR (A, C) and infectious virus produced by the cells was titrated by plaque assay (B, D). Statistical significance as indicated (***p≤0.0001; **p<0.01) was determined by One-way ANOVA with multiple comparisons to the GFP control (Fisher's LSD).

None of the dsRNA treatments had an effect on LGTV replication or production in cells infected with MOI 1 (Fig 5.10A,B). In cells infected with MOI 0.005, LGTV replication was slightly increased in cells with reduced Ago16 and Ago30 expression, but the effect was only significant for Ago30 knockdown (Fig 5.10C,D). No difference was observed when cells were treated with dsRNA targeting IxCG4572_3 in this experiment, but since knockdown efficiency could not be validated, this could have been due to failure to silence IxCg4572_3 expression. These results, together with the results of the study performed by Esther Schnettler and colleagues indicate that Ago16 and Ago30 may not play an important role in controlling LGTV replication, whereas Ago30 in particular appears to be heavily involved in antiviral RNAi against SFV.

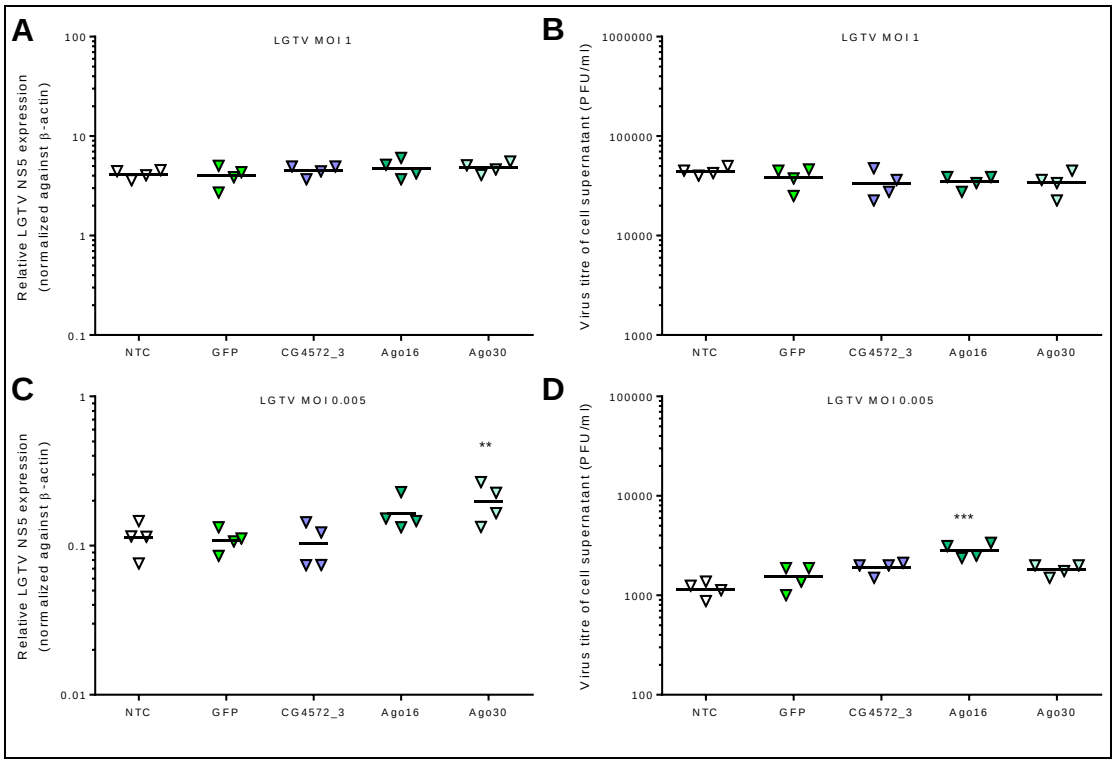

Figure 5.10: Knockdown of Ago16 or Ago-30 expression increases LGTV replication in IDE8 cells infected at a low MOI. IDE8 cells were treated for 72 h with dsRNA targeting GFP, CG4572_3, Ago16, Ago30 or no dsRNA (NTC). Cells were infected with LGTV at MOI 1 (A, B) or MOI 0.005 (C, D) and lysed 48 h p.i. for RNA extraction and supernatant was collected for plaque assay. Viral RNA levels were measured by qPCR (A, C) and infectious virus produced by the cells was titered by plaque assay (B, D). Statistical significance as indicated (***p≤0.0001; **p<0.01) was determined by One-way ANOVA with multiple comparisons to the GFP control (Fisher's LSD).

5.2.4 The role of CG4572 in antiviral defences of Aag2 cells

In addition to tick CG4572, the roles of mosquito egghead and CG4572 in the cellular antiviral response were investigated using knockdown experiments. Initially, CG4572_05.1 and CG4572_56.1 were amplified from Aag2 cells to generate dsRNA. In a pilot experiment, triplicate cultures of Aag2 cells were either mock-transfected or transfected with dsRNA targeting GFP, *Rluc*, egghead, CG4572_05.1, CG4572_56.1, or mixtures of dsRNA targeting both CG4572 orthologues or targeting both CG4572s and egghead. 24 h after transfection, cells were infected with SFV4(3H)-*Rluc* at MOI 0.01 and 48 h p.i. cells were harvested and split in two equal volumes; one half was lysed for luciferase assay, while the other half was lysed for RNA extraction and RT-PCR to validate knockdown efficiency. Knockdown of

egghead expression was significantly reduced by approximately 60-80% after transfection of dsRNA targeting egghead and a mixture of dsRNA targeting both CG4572 and egghead (Fig 5.11A). Expression of CG4572_56.1 was reduced to variable degrees (Fig 5.11A). Knockdown of CG4572_05.1 could not be validated, because samples from cells treated with dsRNA against CG4572_05.1 produced a stronger signal for CG4572_05.1 by RT-PCR compared to NTC. As it is unlikely that expression would increase upon treatment with sequence-specific dsRNA, the explanation for the increase in PCR product is likely to be 'contamination' with unprocessed dsRNA which served as template during PCR. New primer sets were designed and tested, in order to amplify other regions of the CG4572_05.1 cds, which should not amplify remaining dsRNA, but the primers did not amplify a product. The problem occurred repeatedly and was not solved within the timeframe of the present study. Due to the intriguing results obtained, further experiments were performed without validation of knockdown efficiency. For future experiments or publication, a method to determine knockdown efficiency will have to be established.

As expected, addition of dsRNA targeting *Rluc* significantly reduced *Rluc* activity to no more than background levels (Fig 5.11B). Knockdown of egghead resulted in a small non-significant decrease in *Rluc* activity compared to the GFP control. However, addition of dsRNA targeting CG4572_05.1 increased *Rluc* activity significantly by 3.6-fold. Knockdown of CG4572_56.1 also increased *Rluc* activity, but only by 1.5-fold and the increase was not statistically significant. When a mixture of dsRNA targeting both CG4572s was added, *Rluc* activity was 3-fold increased, but when both CG4572 and egghead were targeted *Rluc* activity was not significantly different from the GFP control. This may be a result of variations in knockdown efficiency; alternatively, knockdown of egghead somehow blocked or reversed the beneficial effect CG4572 knockdown had on virus replication.

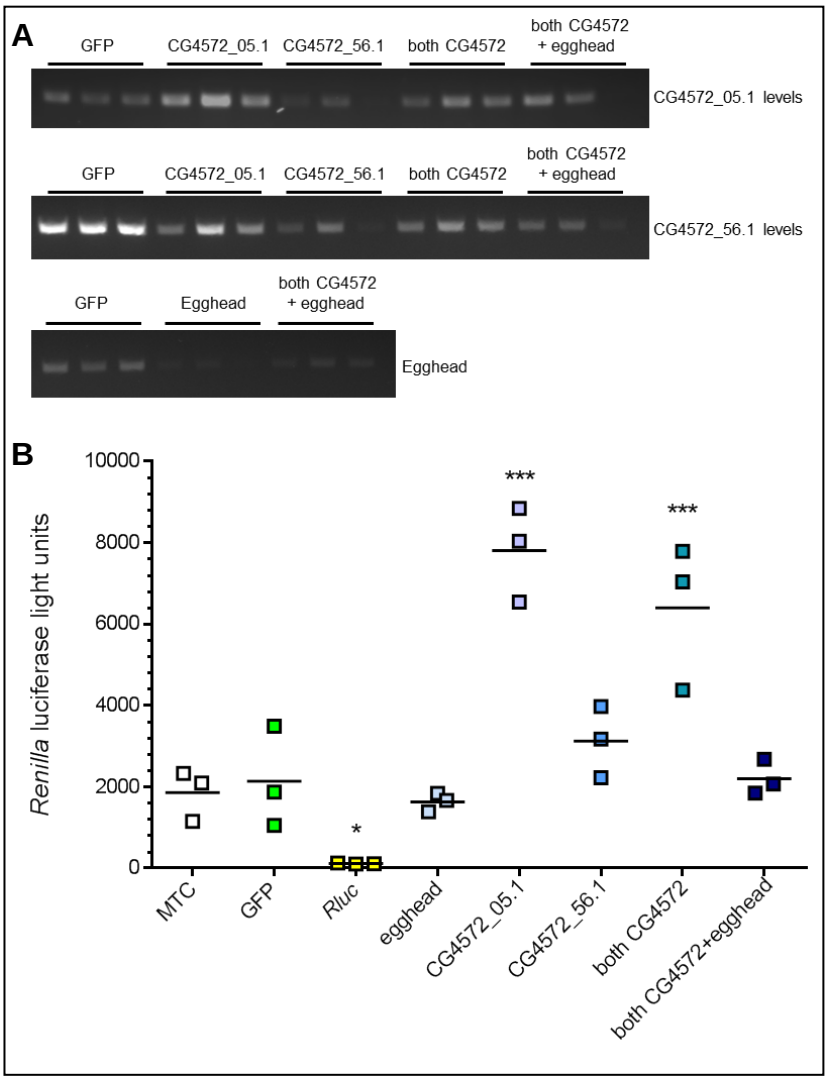

Figure 5.11: Knockdown of egghead and CG4572 orthologues in Aag2 cells and infection with SFV at MOI 0.01. Aag2 cells were mock-transfected (MTC) or transfected with dsRNA targeting GFP, *Rluc*, egghead, CG4572_05.1, CG4572_56.1, both CG4572s, and both CG4572s and egghead. 24 h post transfection, cells were infected with SFV4(3H)-*Rluc* at MOI 0.01. Cells were harvested 48 h p.i.. for RNA extraction and RT-PCR (A) and for luciferase assay (B). Statistical significance as indicated (***p≤0.0001; *p<0.05) was determined by One-way ANOVA with multiple comparisons to the GFP control (Fisher's LSD).

If CG4572 was only involved in spread of the RNAi response through the culture, it should affect virus replication in cells that become infected at a later stage of infection of the culture, once the first infected cells have initiated an antiviral RNAi response which spreads to uninfected cells. It was thus hypothesised that a stronger effect on virus replication would be observed in experiments performed with low

MOI compared to high MOI. Since the first experiment was performed with a low MOI infection, another experiment was performed in the same way, but using an MOI of 1 to infect Aag2 cells with SFV4(3H)-*Rluc*.

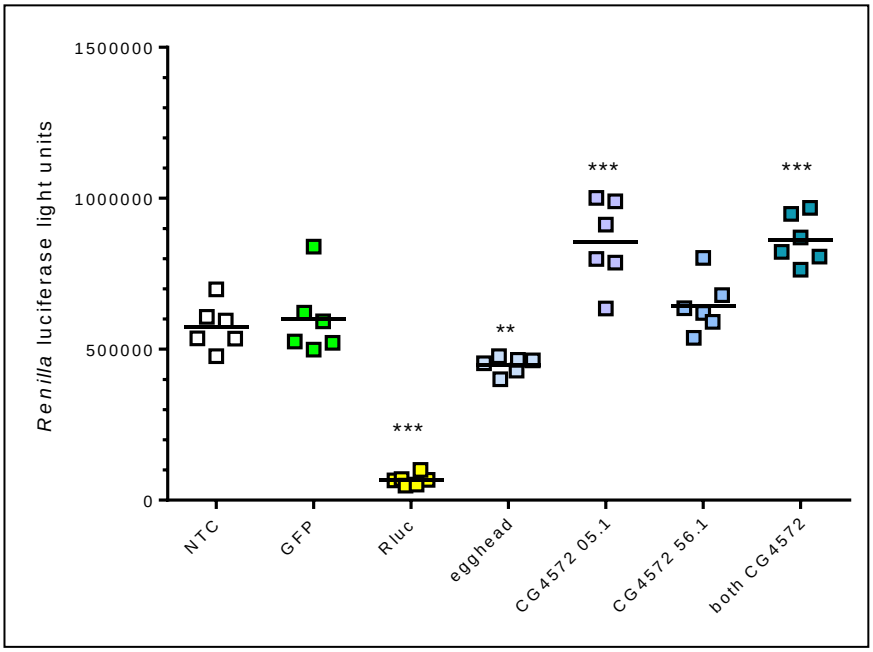

Figure 5.12: Knockdown of egghead and CG4572 orthologues in Aag2 cells and infection with SFV at MOI 1. Aag2 cells were mock-transfected (MTC) or transfected with dsRNA targeting GFP, *Rluc*, egghead, CG4572_05.1, CG4572_56.1 or both CG4572s. 24 h post transfection, cells were infected with SFV4(3H)-*Rluc* at MOI 1. Cells were harvested 48 h p.i. for luciferase assay. Statistical significance as indicated (***p≤0.0001; *p<0.05) was determined by One-way ANOVA with multiple comparisons to the GFP control (Fisher's LSD).

While there was again a significant increase in *Rluc* activity in Aag2 cells treated with dsRNA against CG4572_05.1 and with dsRNA targeting both CG4572 orthologues compared to the GFP control, the increase was only 1.4-fold (Fig 5.12). There was no significant increase in cells treated with dsRNA targeting CG4572_56.1. Interestingly, there was again a decrease in *Rluc* activity after treatment of cells transfected with dsRNA targeting egghead, confirming the previous result that egghead may be a pro-viral factor in mosquito cells. However, due to the variability between results, it could not be concluded whether the less prominent effect of CG4572 knockdown on SFV was due to the higher MOI used, a

less efficient knockdown or general variation between experiments caused by other confounding factors.

Further experiments were performed to address this question. Expression of CG4572 orthologues, including CG4572_06.1, was knocked down in Aag2 cells and cells were infected with SFV4(3H)-*Rluc* at MOI 0.01. Cells were then lysed at 48 and 72 h p.i. for luciferase assay.

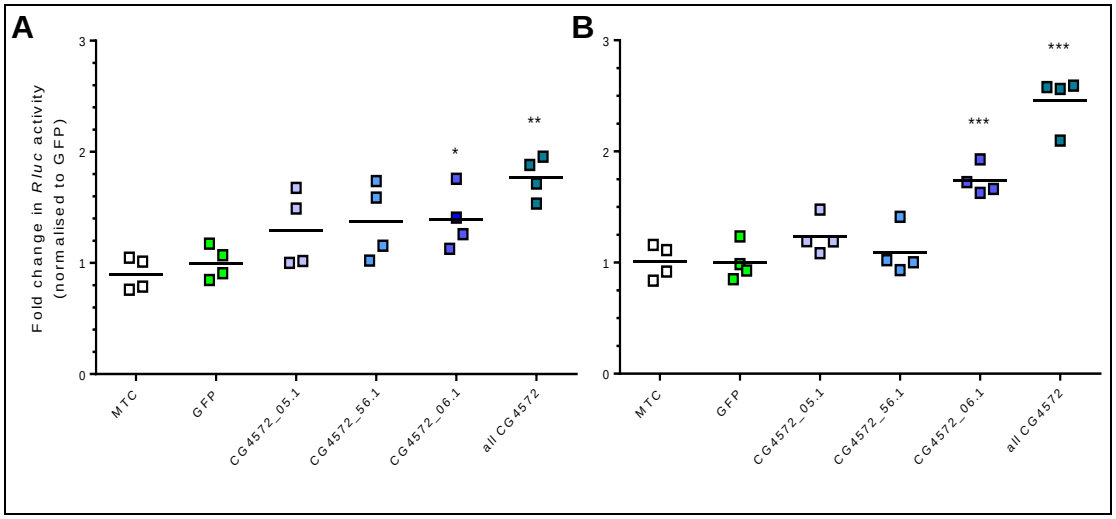

Figure 5.13: The effect of CG4572 knockdown in Aag2 cells on *Rluc* activity 48 and 72 h p.i. with SFV4(3H)-*Rluc*. Aag2 cells were mock-transfected (MTC) or transfected with dsRNA targeting GFP, *Rluc*, CG4572_05.1, CG4572_56.1, CG4572_06.1 or all CG4572 orthologues. 24 h after transfection, cells were infected with SFV4(3H)-*Rluc* at MOI 0.01. Cells were harvested 48 h (A) or 72 h (B) p.i. for luciferase assay. Values were normalised to the GFP control. Statistical significance as indicated (***p≤0.0001; **p<0.01; *p<0.05) was determined by One-way ANOVA with multiple comparisons (Fisher's LSD).

At 48 h p.i., *Rluc* activity was increased in cells transfected with dsRNA targeting any of the CG4572 orthologues, but the increase was small and only significant in cells transfected with dsRNA targeting CG4572_06.1 (1.4-fold) or all three CG4572s (1.8-fold) (Fig 5.13A). At 72 h p.i., *Rluc* activity was also increased significantly in cells transfected with dsRNA targeting CG4572_06.1 and all three CG4572 orthologues (Fig 5.13B), and the increase was greater (1.7 and 2.5-fold, respectively) than at 48 h p.i. consistent with greater spread of SFV through these cultures. CG4572_05.1 and CG4572_56.1 knockdown had no significant effect on SFV replication in this experiment; however as knockdown efficiency was not validated

(see above), it is possible that expression was not significantly reduced. Furthermore, *Rluc* readings in all samples were high (over 10^5 light units) compared to the previous SFV4(3H)-*Rluc* infection with MOI 0.01 (Fig 5.11), suggesting that the MOI used here was effectively higher than in the previous experiment, which may explain the generally smaller effect of CG4572 knockdown on SFV replication in this experiment compared to Fig 5.11. This putative variation in MOI could be the result of small variations in the titre of virus stock aliquots caused by handling during stock preparation (differences between aliquots) or accidental freeze-thawing during laboratory moves. Other factors which may have affected MOI are differences in cell susceptibility to infection caused by different culture passages, cell density or the formation of clumps, which are often observed in Aag2 cell culture. Efforts were made to minimise these variations.

In order to investigate if the observed effect may indeed be caused by increased spread of virus through the culture, Aag2 cells were mock-transfected or transfected with dsRNA targeting *Rluc* (control), CG4572_05.1, CG4572_56.1, CG4572_06.1 or all CG4572 orthologues in two independent experiments (the combination of all CG4572s was only knocked down in one of the two experiments). Cells were then infected with SFV4(3F)ZsGreen at MOI 0.01 and harvested 48 h p.i. for flow cytometry to quantify the number of ZsGreen-positive cells (see 2.8.2). Knockdown of all CG4572 orthologues individually and combined resulted in a significant increase in the proportion of ZsGreen-positive cells (Fig 5.14). The increase seen with knockdown of the CG4572 orthologues individually was only between 1.3 and 1.4-fold, but the proportion of ZsGreen-positive cells was increased 1.7-fold in cells in which all CG4572 orthologues were knocked down. Overall, these results show that more cells become infected in an Aag2 culture with reduced expression of CG4572 proteins compared to a control culture by 48 h p.i.. Optimisation of MOI, time-point and knockdown validation/efficiency might provide more persuasive results.

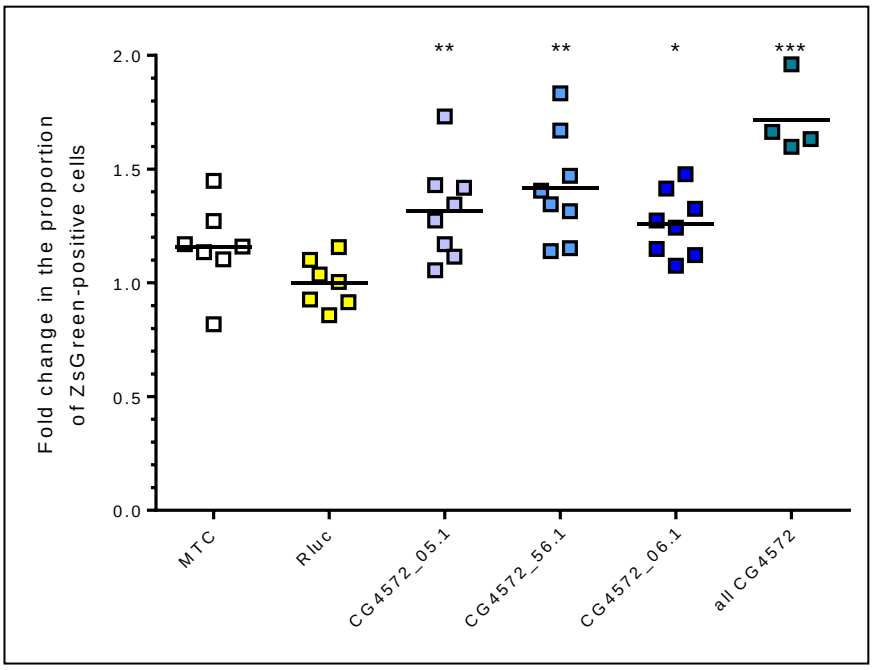

Figure 5.14: The effect of CG4572 knockdown on the proportion of ZsGreen-positive Aag2 cells after infection with SFV4(3F)-ZsGreen. Aag2 cells were mock-transfected (MTC) or transfected with dsRNA targeting *Rluc*, CG4572_05.1, CG4572_56.1, CG4572_06.1 or all CG4572 orthologues. 24 h after transfection, cells were infected with SFV4(3F)-ZsGreen at MOI 0.01. Cells were harvested 48 h p.i. for flow cytometry. Values were normalised to the *Rluc* control and two independent experiments were combined. Statistical significance as indicated (***p≤0.0001; **p<0.01; *p<0.05) was determined by One-way ANOVA with multiple comparisons (Fisher's LSD).

5.2.5 The role of CG4572 in antiviral defences of U4.4 cells

Aag2 cells can be difficult to work with as they can be sensitive to harsh treatment and have a tendency to form clumps and grow in three dimensions, instead of an even distribution across the well surface. *Ae. albopictus* U4.4 cells, however, grow in even monolayers and are generally easy to culture and use in experiments, often resulting in much smaller SDs compared to experiments using Aag2 cells. Some experimental conditions that have been established for U4.4 cells proved unsuitable for Aag2 cells (author's unpublished observation). Since the *Ae. albopictus* genome has not been published, the whole cds sequences of the putative CG4572 orthologues would have to be amplified and sequenced to ensure the genes are highly conserved between *Ae. aegypti* and *Ae. albopictus*. An attempt to amplify the full length cds was made, but the primers did not amplify a PCR product (from either *Ae. aegypti* or

Ae. albopictus). dsRNA was generated from U4.4-derived cDNA using primers designed for the *Ae. aegypti* CG4572 orthologues, and PCR products for CG4572_05.1 and CG4572_56.1 were amplified. U4.4 cells were then mock-transfected or transfected with dsRNA targeting GFP, CG4572_05.1, CG4572_56.1 or a mixture of dsRNA targeting both CG4572s, and infected 24 h later with SFV4(3H)-*Rluc* at MOI 0.001 in two independent experiments. The normalised and combined data are presented (Fig 5.15).

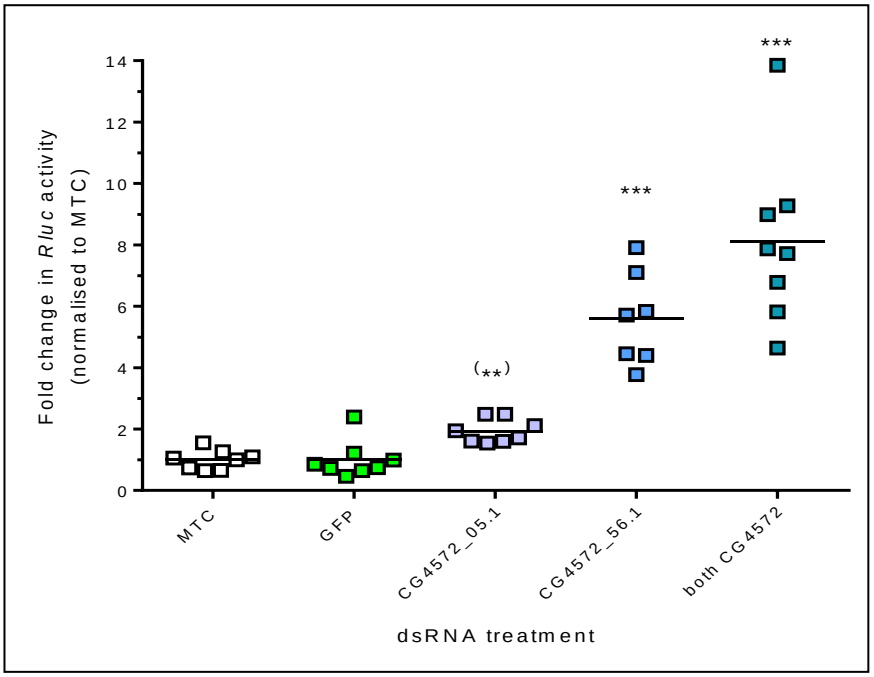

Figure 5.15: The effect of CG4572 knockdown on *Rluc* activity in U4.4 cells infected with SFV4(3H)-*Rluc*. U4.4 cells were mock-transfected (MTC) or transfected with dsRNA targeting GFP, CG4572_05.1, CG4572_56.1 or both CG4572 orthologues. 24 h after transfection, cells were infected with SFV4(3H)-*Rluc* at MOI 0.001. Cells were harvested 48 h p.i. for luciferase assay. Results from two independent experiments were normalised to the GFP control and combined. Statistical significance as indicated was determined by One-way ANOVA with multiple comparisons (Fisher's LSD) (***p≤0.0001) and Student's t-test ($^{(**)}$p<0.01).

Knockdown of the putative CG4572_05.1 resulted in a 1.9-fold increase in *Rluc* activity, which was not significant by One-way ANOVA, but statistically significant by Student's t-test (p=0.0033) compared to the GFP control. *Rluc* activity was significantly increased (5.6-fold) in cells treated with dsRNA targeting putative

CG4572_56.1 and the increase was even more prominent when U4.4 cells were treated with dsRNA targeting both CG4572 orthologues (8.1-fold). Overall, these results suggest that *Ae. albopictus* CG4572 orthologues are also involved in controlling SFV infection in U4.4 cell culture.

5.2.6 Spread of the RNAi response in Aag2 and IDE8 cells

CG4572 is likely to be involved in the antiviral response of tick and mosquito cells through a role in dsRNA uptake and spread of the RNAi response. In *Drosophila* and U4.4 mosquito cells, it is known that dsRNA in the form of long dsRNA (*Drosophila*) and/or siRNA (U4.4 cells) can spread through the body of the fly or from cell to cell through a culture, respectively. While uptake of dsRNA and siRNA by tick cells has been demonstrated (Barry et al., 2013), it is unknown whether dsRNA and/or siRNA molecules induced by virus infection can spread from cell to cell in Aag2 or IDE8 cultures. Experiments were performed to determine whether there is cell-to-cell spread of dsRNA and/or siRNA in Aag2 and IDE8 cells. The following experiments are based on the idea that adding/transfecting dsRNA against *Rluc* will reduce SFV(3H)-*Rluc* replication and measured *Rluc* activity. To determine if dsRNA or siRNA can spread through a culture, one population of cells was treated with dsRNA targeting *Rluc* (or a control/no dsRNA) and mixed with another population of cells infected with *Rluc*-encoding virus or virus replicon particles. Reduction of *Rluc* activity, compared to the controls, is an indication that *Rluc* dsRNA and/or siRNA has spread from the first cell population to the second cell population.

U4.4, Aag2 and IDE8 cells were seeded into two 24-well plates each. In the first plate, 8 wells of each cell line were not treated (NTC), 8 wells were transfected (U4.4, Aag2) or treated (IDE8) with dsRNA targeting GFP, and 8 wells were transfected/treated with dsRNA targeting *Rluc*. Medium was changed 5 h (U4.4, Aag2) or 24 h (IDE8) after transfection/addition of dsRNA. 48 h after treatment with dsRNA, 12 wells of each cell line in the second plate were infected with SFV4(3H)-*Rluc* at MOI 5 and 12 wells at MOI 1. dsRNA-treated cells in the first plate were harvested 3 h later, centrifuged (300 x g, 5 min) and resuspended in new complete

culture medium. Cells from each well of plate 1 were then added to the equivalent well of infected cells in plate 2 (Fig 5.16A). 24 h p.i. with SFV, the cells were lysed and *Rluc* activity was measured.

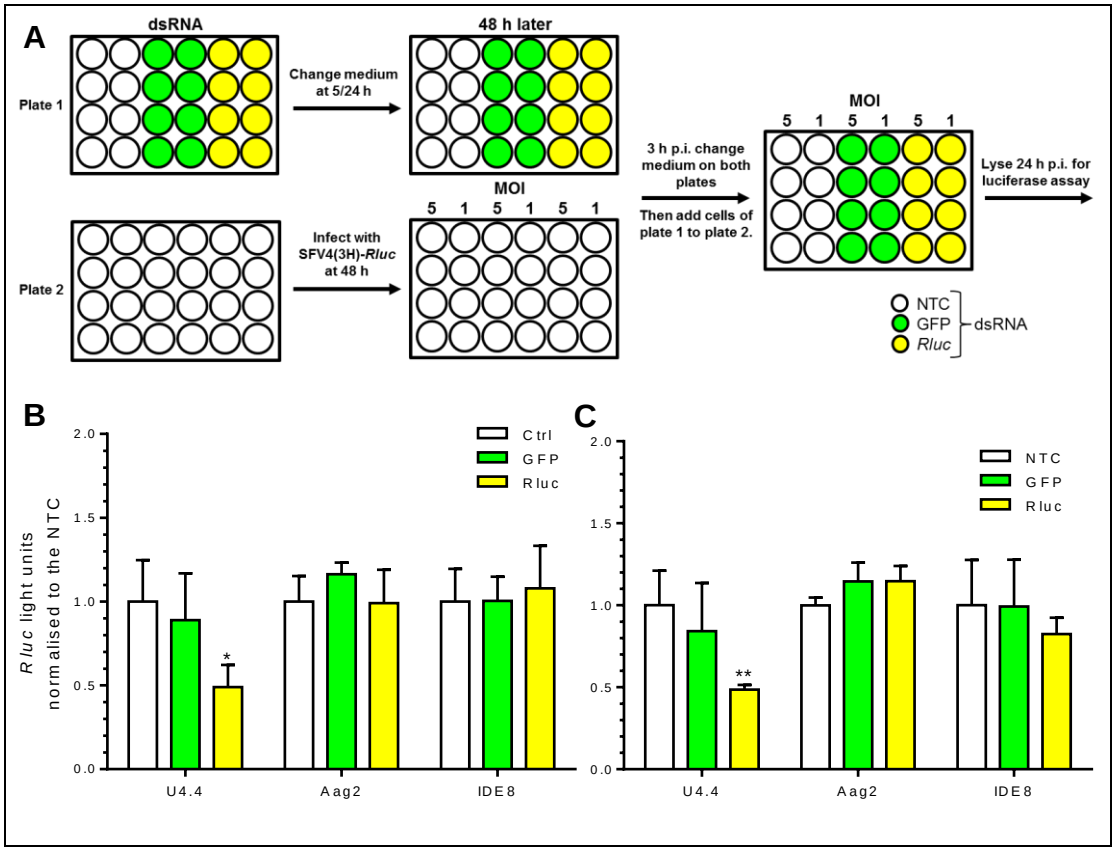

Figure 5.16: Potential spread of dsRNA/siRNA was detected in U4.4, but not in Aag2 or IDE8 cells. U4.4, Aag2 and IDE8 cells were seeded in two 24-well plates for each cell line. (A) Depicts the experimental design. Cells of plate 1 were not treated or transfected with dsRNA targeting either GFP or *Rluc*. For IDE8 cells dsRNA was added to the cells without transfection reagent. Medium of plate 1 was changed twice and on day 2, cells of plate 2 were infected with SFV4(3H)-*Rluc* at (B) MOI 5 or (C) MOI 1. 3 h p.i. medium was changed and the dsRNA-treated cells were harvested and added to the infected cells. 24 h p.i. cells were lysed for luciferase assay. Each data point represents the mean of four individual cultures and error bars indicate SD. Statistical significance as indicated (**p<0.01; *<0.05) was determined by One-way ANOVA with multiple comparisons (Fisher's LSD).

In U4.4 cells, addition of the cells containing *Rluc* dsRNA resulted in significantly decreased *Rluc* activity (51%) compared to the NTC control at both MOI used (Fig 5.16B,C). There was also a small non-significant decrease after addition of cells transfected with dsRNA targeting GFP. However, no significant difference in *Rluc*

activity was observed in Aag2 or IDE8 cells between the three conditions. In cells infected at MOI 1, there was only a small (18%) non-significant decrease in *Rluc* activity after addition of cells treated with *Rluc* dsRNA (Fig 5.16C). Overall, these results suggest that siRNA or dsRNA spreads from cell to cell in U4.4 cells but not in Aag2 or IDE8 cells.

Using SFV4(3H)-*Rluc*, which produces new virus particles after infection, may have made the results of this experiment difficult to interpret, because the virus produced by cells in plate 2 will infect new cells from plate 1 which have been treated with dsRNA against either GFP or *Rluc* (or none, NTC). Cells transfected with dsRNA targeting *Rluc* should be less able to support SFV4(3H)-*Rluc* replication. Thus the observed difference in *Rluc* activity in U4.4 cells could be due to inefficient virus spread through the culture as opposed to spread of dsRNA/siRNA targeting *Rluc* expression. In a follow-up experiment SFV1-*Rluc* VRPs were used to infect cells. These VRPs encode the non-structural proteins of SFV and *Rluc* under the subgenomic promoter, but encode no structural proteins and cannot generate new virus particles. In a test infection of IDE8 cells with VRPs using MOIs ranging from 0.05 to 5, high expression of *Rluc* activity (>50,000 light units) was detected in IDE8 cells (Fig 5.17) even at a low MOI of 0.05. MOI 0.05 was selected for the following experiment.

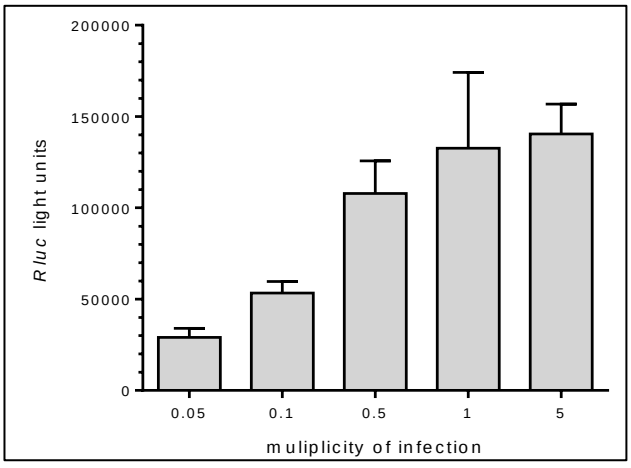

Figure 5.17: Test infection of IDE8 with SFV1-*Rluc* VRPs at different MOI. IDE8 cells were infected with SFV1-*Rluc* VRPs at MOI 0.05, 0.1, 0.5, 1 and 5 and harvested 24 h p.i. for luciferase assay. Each data point represents triplicate cultures and the error bars indicate SD.

U4.4, Aag2 and IDE8 cells were seeded into two 6-well plates each. Two wells of each cell line in the first plate were not treated (NTC), two wells were transfected (U4.4, Aag2) or inoculated (IDE8) with dsRNA targeting GFP, and two wells with dsRNA targeting *Rluc*. Medium was changed once at 5 h and twice at 24 h after transfection/addition of dsRNA. Then six wells of each cell line in the second plate were infected with SFV1-*Rluc* VRPs at MOI 0.05, and 2 h p.i. cells were harvested and washed twice with medium to remove remaining virus. In parallel, the cells treated with dsRNA in the first plate were harvested (Fig 5.18A). Equal numbers of infected cells and dsRNA treated cells for each condition were then mixed and seeded into 24-well plates at either a high cell density (U4.4/Aag2: $1x10^6$ cells/well; IDE8: $2x10^6$ cells/well) or a low cell density (U4.4/Aag2: $2x10^5$ cells/well; IDE8: $3x10^5$ cells/well). Two independent experiments were performed in triplicate, normalised to the NTC and combined.

The aim of using both high and low cell densities was to determine whether cell-to-cell contact is necessary for spread of the RNAi response, if any such response was observed in Aag2 and/or IDE8 cells. In both experiments, however, cells seeded at the designated 'low density' still had a high proportion of cell-to-cell contacts. In U4.4 cultures, adding cells containing *Rluc* dsRNA significantly decreased *Rluc* activity compared to the NTC control at both cell densities. No difference between conditions was observed in Aag2 cells seeded at high density. At the lower cell density, a small but significant decrease compared to the NTC was observed in Aag2 cells, when cells containing dsRNA targeting GFP or *Rluc* were added. Since the effect was not specific to *Rluc* dsRNA, the decrease may have been caused by downstream signalling events activated by dsRNA in general. In IDE8 cells, no significant difference between conditions was observed. In retrospect, a useful control would have been to directly infect cells transfected/inoculated with dsRNA targeting *Rluc* to provide evidence for efficient uptake and processing of dsRNA.

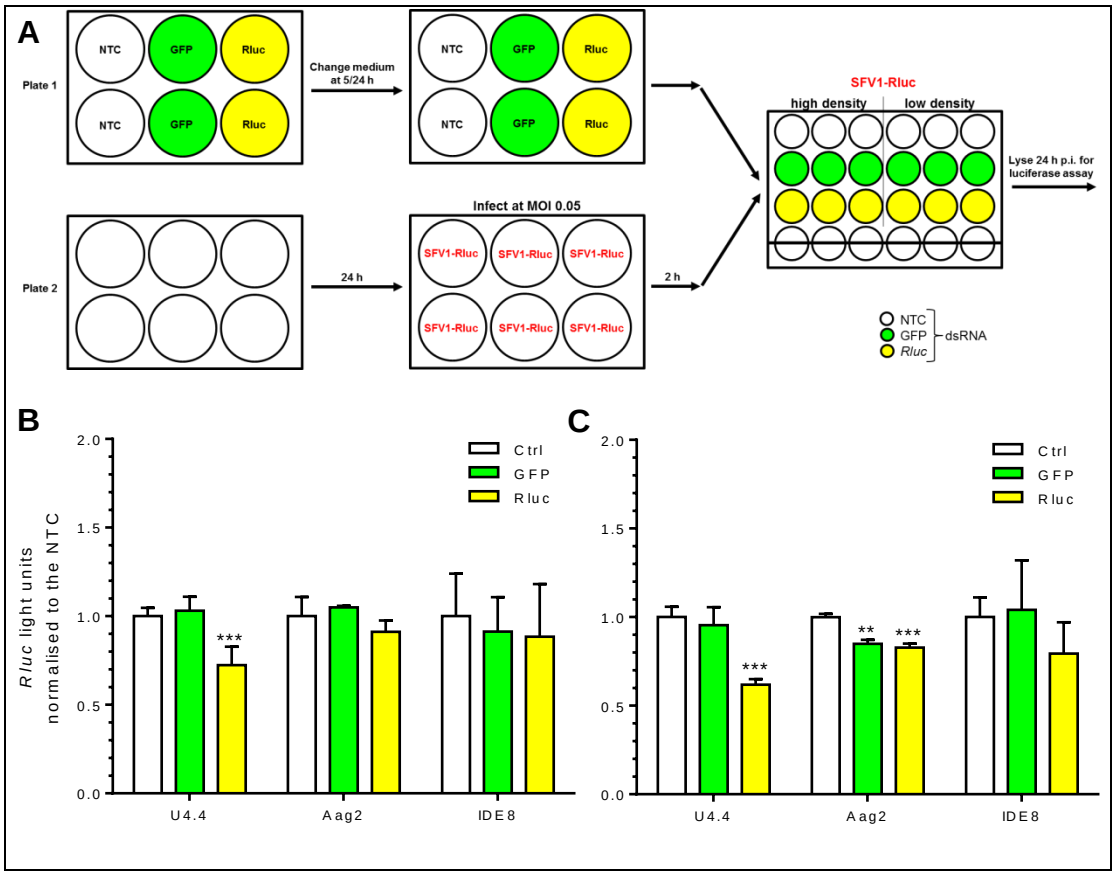

Figure 5.18: Spread of the RNAi response was detected in U4.4, but not Aag2 and IDE8 cells. U4.4, Aag2 and IDE8 cells were seeded into 6-well plates. 2 wells of each cell line were not treated (NTC), 2 wells were transfected (U4.4, Aag2) or inoculated (IDE8) with dsRNA targeting GFP, and 2 wells with dsRNA targeting *Rluc*. Medium was changed once at 5 h and twice at 24 h after addition of dsRNA. 6 wells of each cell line were infected with SFV1-*Rluc* VRPs at MOI 0.05, and 2 h p.i. cells were harvested and washed twice with medium to remove remaining virus. At the same time, the cells treated with dsRNA were harvested, equal numbers of infected/dsRNA treated cells were mixed and seeded at (A) high density or (B) low density. Results from two independent experiments were normalised to the NTC and combined. Statistical significance as indicated (***p≤0.0001; **p<0.01) was determined by One-way ANOVA with multiple comparisons (Fisher's LSD).

Overall these results do not suggest cell-to-cell spread of dsRNA/siRNA through Aag2 or IDE8 cell cultures. A more direct attempt to visualise spread of siRNAs between cells was performed using fluorescently labelled siRNA. In this experiment, the three cell lines were 'scrape loaded' with fluorescent siRNA as described previously (Attarzadeh-Yazdi et al., 2009), mixed with fresh untreated cells and the spread of fluorescent siRNA over 5 h was to be measured by confocal microscopy (and later flow cytometry). The experiment was inconclusive due to the sensitivity of

Aag2 and IDE8 cells to scrape loading and loss of viable cells. U4.4 cells were viable after treatment and siRNAs could be visualised, but the experimental protocol was not suitable for the other two cell lines.

5.2.7 Summary of results

- The *I. scapularis* genome appears to encode components of the miRNA, piRNA and dsRNA uptake pathways
- CG4572 and egghead orthologues are encoded in the *Ae. aegypti* and *I. scapularis* genomes and expressed in Aag2 mosquito and IDE8 tick cell lines
- RNAi appears to be involved in controlling SCRV, SFV and LGTV in tick cells. Knockdown of expression of the RNAi pathway component Ago30 resulted in a large increase in SFV replication and production.
- Inoculation of tick cells with dsRNA targeting a CG4572 orthologue increased replication of SFV and LGTV
- Knockdown of mosquito CG4572 orthologues resulted in increased SFV replication and spread through the culture
- In contrast to U4.4 cells, no cell-to-cell spread of dsRNA and/or siRNA was observed in Aag2 and IDE8 cells

5.3 DISCUSSION

RNAi is undoubtedly an important antiviral mechanism in arthropods. In tick cells it was previously proposed as an antiviral mechanism (Garcia et al., 2005; Garcia et al., 2006), but direct evidence for this through knockdown of components of the RNAi pathway has only recently been provided by Schnettler et *al*. (2014, submitted) and by the present study. Schnettler and colleagues showed that knockdown of specific Dcr and Ago proteins, including Ago16 and Ago30, increased LGTV replication. Similar results were observed with LGTV for knockdown of Ago16 and Ago30 in the present study. Furthermore, the present study provided evidence for a role of Ago16 and Ago30 in controlling replication of SCRV, an orbivirus which persistently infects IDE8 tick cells. Particularly noticeable was the effect of Ago30

knockdown on SFV replication in IDE8 tick cells. Depending on the MOI used to infect, SFV replication was 10-fold to over 100-fold increased in cells with reduced Ago30 expression, indicating that Ago30 plays an important role in the RNAi response controlling SFV replication in IDE8 cells. In future studies it would be interesting to investigate all the identified players in the RNAi system to see if other Ago proteins are important for antiviral RNAi controlling SFV and/or SCRV and if Dcr knockdown would result in a similar effect. Since alphaviruses are not known to be tick-borne, it would be interesting to see whether the difference in sensitivity of the virus to the tick cell RNAi system is an important factor in vector competence. While alphaviruses have been isolated from ticks (Al-Khalifa et al., 2007; Lwande et al., 2013), they are not known to be transmitted by ticks in nature. VEEV has been experimentally transmitted between guinea pigs by ticks (Linthicum and Logan, 1994), but other alphaviruses have only been isolated or detected by RT-PCR from field-collected whole ticks and may have been contained in the blood meal without replicating in the tick itself. SFV appears to replicate well in most tissues of tick explants *in vitro*, except in the midgut (Lesley Bell-Sakyi, personal communication). This could indicate that a host factor necessary for virus entry or replication is missing in the midgut (for example the receptor to which SFV binds) or that the antiviral immune response is particularly strong in the midgut. Since Ago30 knockdown had such a strong effect on SFV replication, it would be interesting to see how important the role of the RNAi response is *in vivo* and whether it may be one of the crucial factors determining vector competence. Transmission studies could show whether RNAi may be a factor limiting alphavirus transmission by ticks in nature.

In order to further determine the role of RNAi in controlling SCRV replication, experiments over a longer time period would be beneficial. Due to the time limitations of this study only a single time-point, 72 h after inoculation with dsRNA, was investigated, but effects on SCRV replication may be slow and the increase in SCRV replication after Ago16/30 knockdown might be much larger at later time-points.

Besides the general involvement of RNAi in controlling virus replication in tick cells, two putative components of the dsRNA uptake machinery were investigated in tick and mosquito cells. While egghead, which had high sequence homology with *D. melanogaster* egghead, appeared to have no antiviral effect in either tick or mosquito cells, orthologues of the *Drosophila* serine carboxypeptidase CG4572 appeared to be important for the antiviral response in both tick and mosquito cells. In a number of experiments it was shown that treatment of Aag2, U4.4 and IDE8 cells with dsRNA targeting orthologues of CG4572 resulted in an increase in SFV replication, and also in LGTV replication in tick cells, though not to the same extent in each experiment performed. In mosquito cells it appeared that the three identified CG4572 orthologues all played a role in antiviral defences and the strongest effect was observed when all three orthologues were targeted concurrently. The impact of the results presented suffers from the technical difficulties experienced during attempted knockdown validation. No evidence was obtained that expression of these genes was in fact reduced in the present experiments. In retrospect, putting more effort into the establishment of a conclusive knockdown validation would have been beneficial and possibly more important than the large number of repeat experiments performed. For example, further primer sets could have been tested for validation, or a second region of the genes could have been used to knockdown gene expression. If dsRNA targeting the same genes, but derived from a different sequence had a comparable effect on virus replication, the probability of the observed effect being the result of an off-target effect would be lower. However, the present study and the work of others (Goic et al., 2013; Saleh et al., 2009) have collectively shown an antiviral role for CG4572 in three different arthropod species, namely *D. melanogaster*, *Ae. aegypti* and *I. scapularis*. What remains unclear, however, is the exact mechanism by which CG4572 contributes to an antiviral response in arthropod cells. In *D. melanogaster*, some evidence has been provided that the effect is linked to the spread of antiviral dsRNA through the fly (Saleh et al., 2009). However, Goic et *al*. (2013) showed that CG4572 in *Drosophila* was also involved in the control of FHV in flies which were persistently infected; knockdown of CG4572 increased FHV levels to a similar degree as achieved by knockdown of Ago2. The state of persistent infection

is considered one of balance between host cell and virus replication - spread of the virus through the culture to infect new cells would not be expected to play an important role. It is likely that all susceptible cells are already infected and it would be surprising if spread of the RNAi response is important for controlling a persistent virus infection. As none of the experiments performed in the present study provided evidence for cell-to-cell spread of the RNAi response in Aag2 or IDE8 cells, and knockdown of CG4572 still benefitted the virus, this may indicate that CG4572 plays a more general role in the antiviral response than merely uptake of dsRNA. This could be tested by infecting mosquito and tick cells treated with dsRNA targeting CG4572 using an SFV virus expressing the tombusvirus protein p19. p19 blocks the spread of siRNA by binding double-stranded siRNAs in a highly specific manner (Zamore, 2004). It thus inhibits spread of the RNAi response through an infected culture. If the antiviral effect of CG4572 is mediated by spread of the RNAi response, a virus antagonising this process would benefit less from CG4572 knockdown than wild type SFV.

Overall, the results presented in this chapter highlight the importance of RNAi as an antiviral mechanism in tick cells and begin to elucidate the role of specific genes.

6. Concluding remarks

The present study characterised virus infection in selected hard tick cell lines, provided evidence that innate immunity pathways known from insects are present in ticks, and suggested that RNAi is likely to be the most important antiviral mechanism in ticks. It was one of the first studies investigating tick antiviral responses and, overall, it has provided a solid basis for future studies on tick antiviral immunity.

By characterising virus infection of selected tick cell lines, experimental conditions were established and parameters to consider when designing experiments to investigate tick cell-virus interactions were highlighted. This will be beneficial for future work on the characterised cell lines and will provide guidelines for work on other tick cell lines. In addition, as part of this and other studies, the presence and importance of endogenous viruses in tick cell lines has become increasingly apparent over the last few years (Alberdi et al., 2012; Bell-Sakyi and Attoui, 2013). While other studies have detected endogenous tick viruses (Alberdi et al., 2012; Bell-Sakyi and Attoui, 2013), only SCRV has been identified (Attoui et al., 2001). This is the first study in which the interactions between endogenous SCRV, host cell and acutely infecting arboviruses have been investigated. It is apparent from the results that acute arbovirus infection affected replication of the endogenous SCRV with replication of both viruses most probably controlled by the RNAi system. It is not unreasonable to hypothesise that arbovirus replication may also have been affected by SCRV replication, but this was not investigated as 'sterile' non virus-infected tick cell lines are not known to exist. Lesley Bell-Sakyi and Houssam Attoui suggested in their review on endogenous tick viruses that it might be possible to 'cure' tick cells of a persistent virus infection by targeting viral sequences with dsRNA and thus inducing and/or increasing antiviral RNAi (Bell-Sakyi and Attoui, 2013). If IDE8 tick cells were cured of SCRV, it would allow investigation of the effect of SCRV infection on arbovirus replication. Interplay between endogenous microorganisms and arboviruses in nature could have significant effects on tick fitness and/or virus transmission. If endogenous viruses decrease subsequent arbovirus infection, this

could reduce vector capacity of ticks for arbovirus transmission, similar to mosquitoes infected with specific strains of *Wolbachia* bacteria (Iturbe-Ormaetxe et al., 2011). There may also be changes in host cell gene expression in tick cells 'cured' of endogenous virus infections compared to persistently infected cells, which could result in the discovery of pathways and genes involved in antiviral responses in tick cells. Altogether, persistent infection of tick cells with endogenous viruses is a potentially confounding factor for studies on arbovirus-tick cell interactions, such as the present one, but also provides an intriguing subject for future studies.

Understanding of antiviral responses in arthropod vectors has increased immensely over the last decade. Insights into antiviral responses in the model insect *Drosophila* and high throughput sequencing studies have helped to identify antiviral mechanisms in arthropod vectors, but with a focus on mosquitoes (reviewed by Donald et al., 2012; Kingsolver et al., 2013; Merkling and van Rij, 2013; Rückert et al. 2014, in press). While the most important antiviral mechanism in mosquitoes is still considered to be exogenous RNAi, it is becoming more and more evident that the innate immune system of arthropods is complex and that other mechanisms also defend against viruses. In the present study, no evidence for an antiviral role of signalling pathways such as Toll and JAK/STAT was found in tick cells. In insects, considerably different results have been observed in different systems during infection with alphaviruses. In mosquito cells, activation of JAK/STAT and Imd using bacteria reduced SFV replication, but SFV infection itself did not activate the JAK/STAT or Imd pathway (Fragkoudis et al., 2008). In *Drosophila*, however, it was shown that the alphavirus SINV induced expression of antimicrobial peptides mediated by JAK/STAT and Imd, which had an antiviral role in flies (Avadhanula et al., 2009; Huang et al., 2013). These studies show that different insect systems or different alphaviruses can provide different results and it is difficult to draw conclusions from individual studies. While the present study is one of the first to investigate tick antiviral responses, only selected components of the pathways were silenced and only SFV and for some experiments LGTV were used to infect the cells. In fact, evidence suggests that there are significant differences between the different arbovirus families which need to be taken into consideration. A number of flaviviruses have the ability to suppress RNAi (Kakumani et al., 2013; Schnettler et

al., 2012; Schnettler et al. 2014, submitted); thus it is not surprising that other innate immunity pathways such as JAK/STAT and Toll are involved in controlling flavivirus infection in mosquitoes (Paradkar et al., 2012; Souza-Neto et al., 2009; Xi et al., 2008). In contrast, alphaviruses are not known to actively suppress RNAi, though they may have evolved decoy mechanisms to evade the RNAi response (Siu et al., 2010). It is possible that antiviral RNAi is more efficient in controlling alphavirus replication than flavivirus replication and that innate immunity signalling pathways may play only a small role in controlling alphavirus replication in arthropods. In tick cells, based on results of the present study, the alphavirus SFV appears to be controlled mainly by RNAi. While many aspects of innate immunity were not investigated due to the time constraints, none of the signalling pathways investigated could be clearly shown to control virus replication. Further *in vivo* experiments could elucidate whether signalling pathways are involved in antiviral defences *in vivo*, for example in specific tissues or organs. Little is known about defences of arthropods against other arboviruses such as bunyaviruses or reoviruses, apart from RNAi. In the present study, some evidence was provided for a potential role of RNAi in controlling replication of the orbivirus SCRV in IDE8 cells. A surprising and interesting observation during knockdown experiments was the frequently observed increase in SFV replication when cells were treated with non-specific dsRNA (targeting GFP or *Rluc*) compared to the NTC. In mosquito cells, treatment with any dsRNA generally results in a reduction in SFV replication compared to a non-treated control, possibly due to the upregulation of components of the RNAi system or other antiviral responses triggered by PRRs (the present study and Rennos Fragkoudis, personal communication). It is thus surprising that pre-treatment of tick cells with dsRNA did not result in a decrease in virus replication. One explanation could be that the dsRNA-induced activation of signalling pathways such as JAK/STAT has a small beneficial effect on SFV replication as observed during experiments described in Chapter 4. However, there are other possible explanations such as slow processing of dsRNA, which would essentially result in competition for the RNAi response controlling SFV replication. This may also be the explanation for the increase in SCRV RNA 4 days after infection with SFV and LGTV; in this case the high levels of SFV or LGTV RNA compete with the SCRV

RNA for control by RNAi with the consequence that the high SFV/LGTV levels are controlled while the levels of SCRV RNA increase.

A number of other tick immune responses were not covered by the present study. No studies on humoral antimicrobial mechanisms such as encapsulation, nodulation and the complement system were made, which are all implicated in antibacterial defences of ticks (Hajdusek et al., 2013; Kopacek et al., 2010). In a parallel transcriptomic and proteomic study by fellow PhD student Sabine Weisheit, some components of these pathways were shown to be differentially expressed in IDE8 tick cells after infection with TBEV, indicating that these responses could be worth investigating in future. If they have antiviral activity, these responses may also play a role in co-infection scenarios where bacteria trigger humoral responses which then may target arboviruses.

Overall, this project has provided a solid background and basis for further investigation of tick responses to virus infection. Future studies may build on the data obtained here, in particular using *in vivo* systems, or on humoral mechanisms such as nodulation, encapsulation and the complement system, or on other innate immune responses known from insects or crustaceans, such as virus-induced piRNAs or the Down syndrome cell adhesion molecule (Dscam), which was recently implicated in antiviral immunity in crustaceans and may act as a mediator of adaptive immunity in arthropods (Chiang et al., 2013). Eventually, increasing knowledge of antiviral responses in ticks may assist the development of new strategies for the control of tick-borne arboviruses.

7. References

Adelman, Z.N., Anderson, M.A., Liu, M., Zhang, L., Myles, K.M., 2012. Sindbis virus induces the production of a novel class of endogenous siRNAs in *Aedes aegypti* mosquitoes. Insect Mol Biol 21, 357-368.

Ahola, T., Kaariainen, L., 1995. Reaction in alphavirus mRNA capping: formation of a covalent complex of nonstructural protein nsP1 with 7-methyl-GMP. Proc Natl Acad Sci USA 92, 507-511.

Akhrymuk, I., Kulemzin, S.V., Frolova, E.I., 2012. Evasion of the innate immune response: the Old World alphavirus nsP2 protein induces rapid degradation of Rpb1, a catalytic subunit of RNA polymerase II. J Virol 86, 7180-7191.

Al-Khalifa, M.S., Diab, F.M., Khalil, G.M., 2007. Man-threatening viruses isolated from ticks in Saudi Arabia. Saudi Med J 28, 1864-1867.

Alberdi, M.P., Dalby, M.J., Rodriguez-Andres, J., Fazakerley, J.K., Kohl, A., Bell-Sakyi, L., 2012. Detection and identification of putative bacterial endosymbionts and endogenous viruses in tick cell lines. Ticks Tick-borne Dis 3, 137-146.

Altschul, S.F., Gish, W., Miller, W., Myers, E.W., Lipman, D.J., 1990. Basic local alignment search tool. J Mol Biol 215, 403-410.

Anderson, J.F., Main, A.J., Andreadis, T.G., Wikel, S.K., Vossbrinck, C.R., 2003. Transstadial transfer of West Nile virus by three species of ixodid ticks (Acari: Ixodidae). J Med Entomol 40, 528-533.

Andrew, D.R., 2011. A new view of insect-crustacean relationships II. Inferences from expressed sequence tags and comparisons with neural cladistics. Arthropod Struct Dev 40, 289-302.

Arias-Goeta, C., Mousson, L., Rougeon, F., Failloux, A.B., 2013. Dissemination and transmission of the E1-226V variant of chikungunya virus in *Aedes albopictus* are controlled at the midgut barrier level. PloS One 8, e57548.

Arnot, C.J., Gay, N.J., Gangloff, M., 2010. Molecular mechanism that induces activation of Spatzle, the ligand for the *Drosophila* Toll receptor. J Biol Chem 285, 19502-19509.

Asgari, S., 2013. MicroRNA functions in insects. Insect Biochem Mol Biol 43, 388-397.

Attarzadeh-Yazdi, G., Fragkoudis, R., Chi, Y., Siu, R.W., Ulper, L., Barry, G., Rodriguez-Andres, J., Nash, A.A., Bouloy, M., Merits, A., Fazakerley, J.K., Kohl, A., 2009. Cell-to-cell spread of the RNA interference response suppresses Semliki Forest virus (SFV) infection of mosquito cell cultures and cannot be antagonized by SFV. J Virol 83, 5735-5748.

Attoui, H., Mendez-Lopez, M.R., Rao, S., Hurtado-Alendes, A., Lizaraso-Caparo, F., Jaafar, F.M., Samuel, A.R., Belhouchet, M., Pritchard, L.I., Melville, L., Weir, R.P., Hyatt, A.D., Davis, S.S., Lunt, R., Calisher, C.H., Tesh, R.B., Fujita, R., Mertens,

P.P., 2009. Peruvian horse sickness virus and Yunnan orbivirus, isolated from vertebrates and mosquitoes in Peru and Australia. Virology 394, 298-310.

Attoui, H., Mohd Jaafar, F., de Micco, P., de Lamballerie, X., 2005. Coltiviruses and seadornaviruses in North America, Europe, and Asia. Emerg Infect Dis 11, 1673-1679.

Attoui, H., Stirling, J.M., Munderloh, U.G., Billoir, F., Brookes, S.M., Burroughs, J.N., de Micco, P., Mertens, P.P., de Lamballerie, X., 2001. Complete sequence characterization of the genome of the St Croix River virus, a new orbivirus isolated from cells of *Ixodes scapularis*. J Gen Virol 82, 795-804.

Avadhanula, V., Weasner, B.P., Hardy, G.G., Kumar, J.P., Hardy, R.W., 2009. A novel system for the launch of alphavirus RNA synthesis reveals a role for the Imd pathway in arthropod antiviral response. PLoS Path 5, e1000582.

Bancroft, W.H., Scott, R.M., Snitbhan, R., Weaver, R.E., Jr., Gould, D.J., 1976. Isolation of Langat virus from *Haemaphysalis papuana* Thorell in Thailand. Am J Trop Med Hyg 25, 500-504.

Barletta, A.B., Silva, M.C., Sorgine, M.H., 2012. Validation of *Aedes aegypti* Aag-2 cells as a model for insect immune studies. Parasites Vect 5, 148.

Barrero, R.A., Keeble-Gagnere, G., Zhang, B., Moolhuijzen, P., Ikeo, K., Tateno, Y., Gojobori, T., Guerrero, F.D., Lew-Tabor, A., Bellgard, M., 2011. Evolutionary conserved microRNAs are ubiquitously expressed compared to tick-specific miRNAs in the cattle tick *Rhipicephalus (Boophilus) microplus*. BMC Genomics 12, 328.

Barrett, A.D.T., Higgs, S., 2007. Yellow fever: A disease that has yet to be conquered. Ann Rev Entomol 52, 209-229.

Barry, G., Alberdi, P., Schnettler, E., Weisheit, S., Kohl, A., Fazakerley, J.K., Bell-Sakyi, L., 2013. Gene silencing in tick cell lines using small interfering or long double-stranded RNA. Exp Appl Acarol 59, 319-338.

Behura, S.K., 2007. Insect microRNAs: Structure, function and evolution. Insect Biochem Mol Biol 37, 3-9.

Belhouchet, M., Mohd Jaafar, F., Firth, A.E., Grimes, J.M., Mertens, P.P., Attoui, H., 2011. Detection of a fourth orbivirus non-structural protein. PloS One 6, e25697.

Bell-Sakyi, L., 2004. *Ehrlichia ruminantium* grows in cell lines from four ixodid tick genera. Journal of comparative pathology 130, 285-293.

Bell-Sakyi, L., Attoui, H., 2013. Endogenous tick viruses and modulation of tick-borne pathogen growth. Front Cell Infect Microbiol 3, 25.

Bell-Sakyi, L., Kohl, A., Bente, D.A., Fazakerley, J.K., 2012. Tick cell lines for study of Crimean-Congo hemorrhagic fever virus and other arboviruses. Vector-borne Zoonot Dis 12, 769-781.

Bell-Sakyi, L., Zweygarth, E., Blouin, E.F., Gould, E.A., Jongejan, F., 2007. Tick cell lines: tools for tick and tick-borne disease research. Trends Parasitol 23, 450-457.

Bennett-Lovsey, R.M., Herbert, A.D., Sternberg, M.J., Kelley, L.A., 2008. Exploring the extremes of sequence/structure space with ensemble fold recognition in the program Phyre. Proteins 70, 611-625.

Berglund, P., Sjoberg, M., Garoff, H., Atkins, G.J., Sheahan, B.J., Liljestrom, P., 1993. Semliki Forest virus expression system: production of conditionally infectious recombinant particles. Biotechnology 11, 916-920.

Betz, A., Lampen, N., Martinek, S., Young, M.W., Darnell, J.E., Jr., 2001. A *Drosophila* PIAS homologue negatively regulates stat92E. Proc Natl Acad Sci USA 98, 9563-9568.

Bhatt, P.N., Rodrigues, F.M., 1967. Chandipura: a new Arbovirus isolated in India from patients with febrile illness. Ind J Med Res 55, 1295-1305.

Bialik, S., Kimchi, A., 2006. The death-associated protein kinases: structure, function, and beyond. Ann Rev Biochem 75, 189-210.

Binnington, K.C., Lane, N.J., 1980. Perineurial and glial cells in the tick *Boophilus microplus* (Acarina: Ixodidae): freeze-fracture and tracer studies. J Neurocytol 9, 343-362.

Black, W.C.t., Bennett, K.E., Gorrochotegui-Escalante, N., Barillas-Mury, C.V., Fernandez-Salas, I., de Lourdes Munoz, M., Farfan-Ale, J.A., Olson, K.E., Beaty, B.J., 2002. Flavivirus susceptibility in *Aedes aegypti*. Arch Med Res 33, 379-388.

Blair, C.D., 2011. Mosquito RNAi is the major innate immune pathway controlling arbovirus infection and transmission. Future Microbiol 6, 265-277.

Blouin, E.E., Manzano-Roman, R., de la Fuente, J., Kocan, K.M., 2008. Defining the role of subolesin in tick cell culture by use of RNA interference. Ann NY Acad Sci 1149, 41-44.

Breakwell, L., Dosenovic, P., Karlsson Hedestam, G.B., D'Amato, M., Liljestrom, P., Fazakerley, J., McInerney, G.M., 2007. Semliki Forest virus nonstructural protein 2 is involved in suppression of the type I interferon response. J Virol 81, 8677-8684.

Briggs, M.S., Gierasch, L.M., 1986. Molecular mechanisms of protein secretion: the role of the signal sequence. Adv Protein Chem 38, 109-180.

Brown, D.T., 1984. Alphavirus growth in cultured vertebrate and invertebrate cells. In: Mayo MA, Herrop KA, editors. Vectors in Virus Biology. New York: Academic Press, pp. 113–133.

Butenko, A.M., Gromashevsky, V.L., L'Vov D, K., Popov, V.F., 1981. First isolations of Barur virus (Rhabdoviridae) from ticks (Acari: Ixodidae) in Africa. J Med Entomol 18, 232-234.

Cabezas-Cruz, A., Vancova, M., Zweygarth, E., Ribeiro, M.F., Grubhoffer, L., Passos, L.M., 2013. Ultrastructure of *Ehrlichia mineirensis*, a new member of the *Ehrlichia* genus. Vet Microbiol 167, 455-458.

Carpenter, S., Groschup, M.H., Garros, C., Felippe-Bauer, M.L., Purse, B.V., 2013. *Culicoides* biting midges, arboviruses and public health in Europe. Antiviral Res 100, 102-113.

Cerenius, L., Lee, B.L., Soderhall, K., 2008. The proPO-system: pros and cons for its role in invertebrate immunity. Trends Immunol 29, 263-271.

Cerenius, L., Soderhall, K., 2004. The prophenoloxidase-activating system in invertebrates. Immunol Rev 198, 116-126.

Cerenius, L., Soderhall, K., 2011. Coagulation in invertebrates. J Innate Immun 3, 3-8.

Charrel, R.N., de Lamballerie, X., Raoult, D., 2007. Chikungunya outbreaks--the globalization of vectorborne diseases. N Engl J Med 356, 769-771.

Chauvin, A., Moreau, E., Bonnet, S., Plantard, O., Malandrin, L., 2009. *Babesia* and its hosts: adaptation to long-lasting interactions as a way to achieve efficient transmission. Vet Res 40, 37.

Chen, R., Vasilakis, N., 2011. Dengue--quo tu et quo vadis? Viruses 3, 1562-1608.

Chen, S., Chahar, H.S., Abraham, S., Wu, H., Pierson, T.C., Wang, X.A., Manjunath, N., 2011. Ago-2-mediated slicer activity is essential for anti-flaviviral efficacy of RNAi. PloS One 6, e27551.

Chhabra, M., Mittal, V., Bhattacharya, D., Rana, U., Lal, S., 2008. Chikungunya fever: a re-emerging viral infection. Ind J Med Microbiol 26, 5-12.

Chiang, Y.A., Hung, H.Y., Lee, C.W., Huang, Y.T., Wang, H.C., 2013. Shrimp Dscam and its cytoplasmic tail splicing activator serine/arginine (SR)-rich protein B52 were both induced after white spot syndrome virus challenge. Fish Shellfish Immunol 34, 209-219.

Choi, I.K., Hyun, S., 2012. Conserved microRNA miR-8 in fat body regulates innate immune homeostasis in *Drosophila*. Dev Comp Immunol 37, 50-54.

Christensen, B.M., Li, J., Chen, C.C., Nappi, A.J., 2005. Melanization immune responses in mosquito vectors. Trends Parasitol 21, 192-199.

Chuang, M., Chisholm, A.D., 2014. Insights into the functions of the death associated protein kinases from *C. elegans* and other invertebrates. Apoptosis 19, 392-397.

Chumakov, M.P., 1963. Report on the isolation from Ixodes persulcatus ticks and from patients in western Siberia of a virus differing from the agent of tick-borne encephalitis. Acta virologica 7, 82-83.

Cirimotich, C.M., Scott, J.C., Phillips, A.T., Geiss, B.J., Olson, K.E., 2009. Suppression of RNA interference increases alphavirus replication and virus-associated mortality in *Aedes aegypti* mosquitoes. BMC Microbiol 9, 49.

Coates, C.J., Kelly, S.M., Nairn, J., 2011. Possible role of phosphatidylserine-hemocyanin interaction in the innate immune response of *Limulus polyphemus*. Dev Comp Immunol 35, 155-163.

Cordes, E.J., Licking-Murray, K.D., Carlson, K.A., 2013. Differential gene expression related to Nora virus infection of *Drosophila melanogaster*. Virus Res 175, 95-100.

Costa, A., Jan, E., Sarnow, P., Schneider, D., 2009. The Imd pathway is involved in antiviral immune responses in *Drosophila*. PloS One 4, e7436.

Czech, B., Malone, C.D., Zhou, R., Stark, A., Schlingeheyde, C., Dus, M., Perrimon, N., Kellis, M., Wohlschlegel, J.A., Sachidanandam, R., Hannon, G.J., Brennecke, J., 2008. An endogenous small interfering RNA pathway in *Drosophila*. Nature 453, 798-802.

de la Fuente, J., Kocan, K.M., Almazan, C., Blouin, E.F., 2007. RNA interference for the study and genetic manipulation of ticks. Trends Parasitol 23, 427-433.

de la Fuente, J., Maritz-Olivier, C., Naranjo, V., Ayoubi, P., Nijhof, A.M., Almazan, C., Canales, M., de la Lastra, J.M.P., Galindo, R.C., Blouin, E.F., Gortazar, C., Jongejan, F., Kocan, K.M., 2008. Evidence of the role of tick subolesin in gene expression. BMC Genomics 9.

de la Fuente, J., Moreno-Cid, J.A., Canales, M., Villar, M., de la Lastra, J.M., Kocan, K.M., Galindo, R.C., Almazan, C., Blouin, E.F., 2011. Targeting arthropod subolesin/akirin for the development of a universal vaccine for control of vector infestations and pathogen transmission. Vet Parasitol 181, 17-22.

Deddouche, S., Matt, N., Budd, A., Mueller, S., Kemp, C., Galiana-Arnoux, D., Dostert, C., Antoniewski, C., Hoffmann, J.A., Imler, J.L., 2008. The DExD/H-box helicase Dicer-2 mediates the induction of antiviral activity in *Drosophila*. Nature Immunol 9, 1425-1432.

Deiss, L.P., Feinstein, E., Berissi, H., Cohen, O., Kimchi, A., 1995. Identification of a novel serine/threonine kinase and a novel 15-kD protein as potential mediators of the gamma interferon-induced cell death. Genes Dev 9, 15-30.

Depaquit, J., Grandadam, M., Fouque, F., Andry, P.E., Peyrefitte, C., 2010. Arthropod-borne viruses transmitted by Phlebotomine sandflies in Europe: a review. Euro Surveill 15, 19507.

DeTulleo, L., Kirchhausen, T., 1998. The clathrin endocytic pathway in viral infection. EMBO J 17, 4585-4593.

Dixon, L.K., Chapman, D.A., Netherton, C.L., Upton, C., 2013. African swine fever virus replication and genomics. Virus Res 173, 3-14.

Dobler, G., 2010. Zoonotic tick-borne flaviviruses. Vet Microbiol 140, 221-228.

Donald, C.L., Kohl, A., Schnettler, E., 2012. New insights into control of arbovirus replication and spread by insect RNA interference pathways. Insects 3, 511-531.

Dostert, C., Jouanguy, E., Irving, P., Troxler, L., Galiana-Arnoux, D., Hetru, C., Hoffmann, J.A., Imler, J.L., 2005. The Jak-STAT signaling pathway is required but not sufficient for the antiviral response of *Drosophila*. Nature Immunol 6, 946-953.

Dyachenko, V., Geiger, C., Pantchev, N., Majzoub, M., Bell-Sakyi, L., Krupka, I., Straubinger, R.K., 2013. Isolation of canine *Anaplasma phagocytophilum* strains from clinical blood samples using the *Ixodes ricinus* cell line IRE/CTVM20. Vet Microbiol 162, 980-986.

Edgar, R.C., 2004a. MUSCLE: a multiple sequence alignment method with reduced time and space complexity. BMC Bioinform 5, 113.

Edgar, R.C., 2004b. MUSCLE: multiple sequence alignment with high accuracy and high throughput. Nucleic Acids Res 32, 1792-1797.

Everett, R.D., Boutell, C., Hale, B.G., 2013. Interplay between viruses and host sumoylation pathways. Nature Rev Microbiol 11, 400-411.

Fan, Z.H., Wang, X.W., Lu, J., Ho, B., Ding, J.L., 2008. Elucidating the function of an ancient NF-kappaB p100 homologue, CrRelish, in antibacterial defense. Infect Immun 76, 664-670.

Flotho, A., Melchior, F., 2013. Sumoylation: a regulatory protein modification in health and disease. Ann Rev Biochem 82, 357-385.

Fragkoudis, R., Attarzadeh-Yazdi, G., Nash, A.A., Fazakerley, J.K., Kohl, A., 2009. Advances in dissecting mosquito innate immune responses to arbovirus infection. J Gen Virol 90, 2061-2072.

Fragkoudis, R., Breakwell, L., McKimmie, C., Boyd, A., Barry, G., Kohl, A., Merits, A., Fazakerley, J.K., 2007. The type I interferon system protects mice from Semliki Forest virus by preventing widespread virus dissemination in extraneural tissues, but does not mediate the restricted replication of avirulent virus in central nervous system neurons. J Gen Virol 88, 3373-3384.

Fragkoudis, R., Chi, Y., Siu, R.W., Barry, G., Attarzadeh-Yazdi, G., Merits, A., Nash, A.A., Fazakerley, J.K., Kohl, A., 2008. Semliki Forest virus strongly reduces mosquito host defence signaling. Insect Mol Biol 17, 647-656.

Friedman, R.M., Levin, J.G., Grimley, P.M., Berezesky, I.K., 1972. Membrane-associated replication complex in arbovirus infection. J Virol 10, 504-515.

Frolova, E., Frolov, I., Schlesinger, S., 1997. Packaging signals in alphaviruses. J Virol 71, 248-258.

Frolova, E.I., Gorchakov, R., Pereboeva, L., Atasheva, S., Frolov, I., 2010. Functional Sindbis virus replicative complexes are formed at the plasma membrane. J Virol 84, 11679-11695.

Galindo, R.C., Doncel-Perez, E., Zivkovic, Z., Naranjo, V., Gortazar, C., Mangold, A.J., Martin-Hernando, M.P., Kocan, K.M., de la Fuente, J., 2009. Tick subolesin is an ortholog of the akirins described in insects and vertebrates. Dev Comp Immunol 33, 612-617.

Garbuzov, A., Tatar, M., 2010. Hormonal regulation of *Drosophila* microRNA let-7 and miR-125 that target innate immunity. Fly 4, 306-311.

Garcia, S., Billecocq, A., Crance, J.M., Munderloh, U., Garin, D., Bouloy, M., 2005. Nairovirus RNA sequences expressed by a Semliki Forest virus replicon induce RNA interference in tick cells. J Virol 79, 8942-8947.

Garcia, S., Billecocq, A., Crance, J.M., Prins, M., Garin, D., Bouloy, M., 2006. Viral suppressors of RNA interference impair RNA silencing induced by a Semliki Forest virus replicon in tick cells. J Gen Virol 87, 1985-1989.

Garigliany, M.M., Bayrou, C., Kleijnen, D., Cassart, D., Jolly, S., Linden, A., Desmecht, D., 2012. Schmallenberg virus: a new Shamonda/Sathuperi-like virus on the rise in Europe. Antiviral Res 95, 82-87.

Garoff, H., Huylebroeck, D., Robinson, A., Tillman, U., Liljestrom, P., 1990. The signal sequence of the p62 protein of Semliki Forest virus is involved in initiation but not in completing chain translocation. J Cell Biol 111, 867-876.

Ghildiyal, M., Seitz, H., Horwich, M.D., Li, C., Du, T., Lee, S., Xu, J., Kittler, E.L., Zapp, M.L., Weng, Z., Zamore, P.D., 2008. Endogenous siRNAs derived from transposons and mRNAs in *Drosophila* somatic cells. Science 320, 1077-1081.

Glomb-Reinmund, S., Kielian, M., 1998. The role of low pH and disulfide shuffling in the entry and fusion of Semliki Forest virus and Sindbis virus. Virology 248, 372-381.

Gloster, J., Burgin, L., Witham, C., Athanassiadou, M., Mellor, P.S., 2008. Bluetongue in the United Kingdom and northern Europe in 2007 and key issues for 2008. Vet Rec 162, 298-302.

Gogin, A., Gerasimov, V., Malogolovkin, A., Kolbasov, D., 2013. African swine fever in the North Caucasus region and the Russian Federation in years 2007-2012. Virus Res 173, 198-203.

Goic, B., Vodovar, N., Mondotte, J.A., Monot, C., Frangeul, L., Blanc, H., Gausson, V., Vera-Otarola, J., Cristofari, G., Saleh, M.C., 2013. RNA-mediated interference and reverse transcription control the persistence of RNA viruses in the insect model *Drosophila*. Nature Immunol 14, 396-403.

Gomez de Cedron, M., Ehsani, N., Mikkola, M.L., Garcia, J.A., Kaariainen, L., 1999. RNA helicase activity of Semliki Forest virus replicase protein NSP2. FEBS letters 448, 19-22.

Gould, E.A., Solomon, T., 2008. Pathogenic flaviviruses. Lancet 371, 500-509.

Grandadam, M., Caro, V., Plumet, S., Thiberge, J.M., Souares, Y., Failloux, A.B., Tolou, H.J., Budelot, M., Cosserat, D., Leparc-Goffart, I., Despres, P., 2011. Chikungunya virus, southeastern France. Emerg Infect Dis 17, 910-913.

Griffiths-Jones, S., Grocock, R.J., van Dongen, S., Bateman, A., Enright, A.J., 2006. miRBase: microRNA sequences, targets and gene nomenclature. Nucleic Acids Res 34, D140-144.

Grimley, P.M., Berezesky, I.K., Friedman, R.M., 1968. Cytoplasmic structures associated with an arbovirus infection: loci of viral ribonucleic acid synthesis. J Virol 2, 1326-1338.

Grimley, P.M., Levin, J.G., Berezesky, I.K., Friedman, R.M., 1972. Specific membranous structures associated with the replication of group A arboviruses. J Virol 10, 492-503.

Gritsun, T.S., Nuttall, P.A., Gould, E.A., 2003. Tick-borne flaviviruses. Adv Virus Res 61, 317-371.

Gu, J., Hu, W., Wu, J., Zheng, P., Chen, M., James, A.A., Chen, X., Tu, Z., 2013. miRNA genes of an invasive vector mosquito, *Aedes albopictus*. PloS One 8, e67638.

Guglielmone, A.A., Robbins, R.G., Apanaskevich, D.A., Petney, T.N., Estrada-Pena, A., Horak, I.G., Shao, R.F., Barker, S.C., 2010. The Argasidae, Ixodidae and

Nuttalliellidae (Acari: Ixodida) of the world: a list of valid species names. Zootaxa, 1-28.

Haig, D.A., Woodall, J.P., Danskin, D., 1965. Thogoto virus: a hitherto undescribed agent isolated from ticks in Kenya. J Gen Microbiol 38, 389-394.

Hajdusek, O., Sima, R., Ayllon, N., Jalovecka, M., Perner, J., de la Fuente, J., Kopacek, P., 2013. Interaction of the tick immune system with transmitted pathogens. Front Cell Infect Microbiol 3, 26.

Handler, D., Meixner, K., Pizka, M., Lauss, K., Schmied, C., Gruber, F.S., Brennecke, J., 2013. The genetic makeup of the *Drosophila* piRNA pathway. Mol Cell 50, 762-777.

Havlikova, S., Lickova, M., Klempa, B., 2013. Non-viraemic transmission of tick-borne viruses. Acta Virol 57, 123-129.

Helenius, A., Morein, B., Fries, E., Simons, K., Robinson, P., Schirrmacher, V., Terhorst, C., Strominger, J.L., 1978. Human (HLA-A and HLA-B) and murine (H-2K and H-2D) histocompatibility antigens are cell surface receptors for Semliki Forest virus. Proc Natl Acad Sci USA 75, 3846-3850.

Hendrickx, G., Gilbert, M., Staubach, C., Elbers, A., Mintiens, K., Gerbier, G., Ducheyne, E., 2008. A wind density model to quantify the airborne spread of Culicoides species during north-western Europe bluetongue epidemic, 2006. Prev Vet Med 87, 162-181.

Hess, A.M., Prasad, A.N., Ptitsyn, A., Ebel, G.D., Olson, K.E., Barbacioru, C., Monighetti, C., Campbell, C.L., 2011. Small RNA profiling of Dengue virus-mosquito interactions implicates the PIWI RNA pathway in anti-viral defense. BMC Microbiol 11, 45.

Hill, C.A., Wikel, S.K., 2005. The *Ixodes scapularis* Genome Project: an opportunity for advancing tick research. Trends Parasitol 21, 151-153.

Hoa, N.T., Keene, K.M., Olson, K.E., Zheng, L., 2003. Characterization of RNA interference in an *Anopheles gambiae* cell line. Insect Biochem Mol Biol 33, 949-957.

Holland, J., Domingo, E., 1998. Origin and evolution of viruses. Virus Genes 16, 13-21.

Hollidge, B.S., Gonzalez-Scarano, F., Soldan, S.S., 2010. Arboviral encephalitides: transmission, emergence, and pathogenesis. J Neuroimmune Pharmacol 5, 428-442.

Huang, Z., Kingsolver, M.B., Avadhanula, V., Hardy, R.W., 2013. An antiviral role for antimicrobial peptides during the arthropod response to alphavirus replication. J Virol 87, 4272-4280.

Hubalek, Z., Rudolf, I., 2012. Tick-borne viruses in Europe. Parasitol Res 111, 9-36.

Hussain, M., Torres, S., Schnettler, E., Funk, A., Grundhoff, A., Pijlman, G.P., Khromykh, A.A., Asgari, S., 2012. West Nile virus encodes a microRNA-like small RNA in the 3' untranslated region which up-regulates GATA4 mRNA and facilitates virus replication in mosquito cells. Nucleic Acids Res 40, 2210-2223.

Hussain, M., Walker, T., O'Neill, S.L., Asgari, S., 2013. Blood meal induced microRNA regulates development and immune associated genes in the Dengue mosquito vector, *Aedes aegypti*. Insect Biochem Mol Biol 43, 146-152.

Il'enko, V.I., Smorodincev, A.A., Prozorova, I.N., Platonov, V.G., 1968. Experience in the study of a live vaccine made from the TP-21 strain of Malayan Langat virus. Bull WHO 39, 425-431.

Ishizu, H., Siomi, H., Siomi, M.C., 2012. Biology of PIWI-interacting RNAs: new insights into biogenesis and function inside and outside of germlines. Genes Dev 26, 2361-2373.

Ismail, N., Bloch, K.C., McBride, J.W., 2010. Human ehrlichiosis and anaplasmosis. Clin Lab Med 30, 261-292.

Iturbe-Ormaetxe, I., Walker, T., SL, O.N., 2011. *Wolbachia* and the biological control of mosquito-borne disease. EMBO Rep 12, 508-518.

Jaenson, T.G., Jaenson, D.G., Eisen, L., Petersson, E., Lindgren, E., 2012. Changes in the geographical distribution and abundance of the tick *Ixodes ricinus* during the past 30 years in Sweden. Parasites Vect 5, 8.

Jaworski, D.C., Barker, D.M., Williams, J.P., Sauer, J.R., Ownby, C.L., Hair, J.A., 1983. Age-related changes in midgut ultrastructure and surface tegument of unfed adult Lone Star ticks. J Parasitol 69, 701-708.

Jeffries, C., Mansfield, K., Phipps, L.P., Wakeley, P., Mearns, R., Schock, A., Bell, S., Breed, A., Fooks, A., Johnson, N., 2014. Louping Ill virus: An endemic tick-borne disease of Great Britain. J Gen Virol. 95(Pt 5), 1005-14

Kadota, K., Satoh, E., Ochiai, M., Inoue, N., Tsuji, N., Igarashi, I., Nagasawa, H., Mikami, T., Claveria, F.G., Fujisaki, K., 2002. Existence of phenol oxidase in the argasid tick *Ornithodoros moubata*. Parasitol Res 88, 781-784.

Kakumani, P.K., Ponia, S.S., S, R.K., Sood, V., Chinnappan, M., Banerjea, A.C., Medigeshi, G.R., Malhotra, P., Mukherjee, S.K., Bhatnagar, R.K., 2013. Role of RNA interference (RNAi) in dengue virus replication and identification of NS4B as an RNAi suppressor. J Virol 87, 8870-8883.

Karlikow, M., Goic, B., Saleh, M.C., 2014. RNAi and antiviral defense in *Drosophila*: Setting up a systemic immune response. Dev Comp Immunol 42, 85-92.

Kaufmann, B., Rossmann, M.G., 2010. Molecular mechanisms involved in the early steps of flavivirus cell entry. Microbes Infect 13, 1-9.

Keene, K.M., Foy, B.D., Sanchez-Vargas, I., Beaty, B.J., Blair, C.D., Olson, K.E., 2004. RNA interference acts as a natural antiviral response to O'nyong-nyong virus (*Alphavirus*; *Togaviridae*) infection of *Anopheles gambiae*. Proc Natl Acad Sci USA 101, 17240-17245.

Kelley, L.A., Sternberg, M.J., 2009. Protein structure prediction on the Web: a case study using the Phyre server. Nature Protocols 4, 363-371.

Kiiver, K., Tagen, I., Zusinaite, E., Tamberg, N., Fazakerley, J.K., Merits, A., 2008. Properties of non-structural protein 1 of Semliki Forest virus and its interference with virus replication. J Gen Virol 89, 1457-1466.

Kim, M., Lee, J.H., Lee, S.Y., Kim, E., Chung, J., 2006. Caspar, a suppressor of antibacterial immunity in *Drosophila*. Proc Natl Acad Sci USA 103, 16358-16363.

Kingsolver, M.B., Huang, Z., Hardy, R.W., 2013. I Insect antiviral innate immunity: pathways, effectors, and connections. J Mol Biol, 425, 4921-36

Klimstra, W.B., Nangle, E.M., Smith, M.S., Yurochko, A.D., Ryman, K.D., 2003. DC-SIGN and L-SIGN can act as attachment receptors for alphaviruses and distinguish between mosquito cell- and mammalian cell-derived viruses. J Virol 77, 12022-12032.

Klimstra, W.B., Ryman, K.D., Johnston, R.E., 1998. Adaptation of Sindbis virus to BHK cells selects for use of heparan sulfate as an attachment receptor. J Virol 72, 7357-7366.

Kopacek, P., Hajdusek, O., Buresova, V., Daffre, S., 2010. Tick innate immunity. Adv Exp Med Biol 708, 137-162.

Koressaar, T., Remm, M., 2007. Enhancements and modifications of primer design program Primer3. Bioinformatics 23, 1289-1291.

Krober, T., Guerin, P.M., 2007. In vitro feeding assays for hard ticks. Trends Parasitol 23, 445-449.

Kuno, G., Chang, G.J., Tsuchiya, K.R., Karabatsos, N., Cropp, C.B., 1998. Phylogeny of the genus Flavivirus. J Virol 72, 73-83.

Kurata, S., Ariki, S., Kawabata, S., 2006. Recognition of pathogens and activation of immune responses in *Drosophila* and horseshoe crab innate immunity. Immunobiology 211, 237-249.

Kurscheid, S., Lew-Tabor, A.E., Rodriguez Valle, M., Bruyeres, A.G., Doogan, V.J., Munderloh, U.G., Guerrero, F.D., Barrero, R.A., Bellgard, M.I., 2009. Evidence of a tick RNAi pathway by comparative genomics and reverse genetics screen of targets with known loss-of-function phenotypes in *Drosophila*. BMC Mol Biol 10, 26.

Kurtti, T.J., Mattila, J.T., Herron, M.J., Felsheim, R.F., Baldridge, G.D., Burkhardt, N.Y., Blazar, B.R., Hackett, P.B., Meyer, J.M., Munderloh, U.G., 2008. Transgene expression and silencing in a tick cell line: A model system for functional tick genomics. Insect Biochem Mol Biol 38, 963-968.

Kurtti, T.J., Munderloh, U.G., Andreadis, T.G., Magnarelli, L.A., Mather, T.N., 1996. Tick cell culture isolation of an intracellular prokaryote from the tick *Ixodes scapularis*. J Invertebr Pathol 67, 318-321.

La Ruche, G., Souares, Y., Armengaud, A., Peloux-Petiot, F., Delaunay, P., Despres, P., Lenglet, A., Jourdain, F., Leparc-Goffart, I., Charlet, F., Ollier, L., Mantey, K., Mollet, T., Fournier, J.P., Torrents, R., Leitmeyer, K., Hilairet, P., Zeller, H., Van Bortel, W., Dejour-Salamanca, D., Grandadam, M., Gastellu-Etchegorry, M., 2010. First two autochthonous dengue virus infections in metropolitan France, September 2010. Euro Surveill 15, 19676.

Laakkonen, P., Hyvonen, M., Peranen, J., Kaariainen, L., 1994. Expression of Semliki Forest virus nsP1-specific methyltransferase in insect cells and in *Escherichia coli*. J Virol 68, 7418-7425.

Labuda, M., Nuttall, P.A., 2004. Tick-borne viruses. Parasitology 129 Suppl, S221-245.

Labuda, M., Randolph, S.E., 1999. Survival strategy of tick-borne encephalitis virus: cellular basis and environmental determinants. Zentralblatt Bakteriol 289, 513-524.

Lai, E.C., Tomancak, P., Williams, R.W., Rubin, G.M., 2003. Computational identification of *Drosophila* microRNA genes. Genome Biol 4, R42.

Lasecka, L., Baron, M.D., 2013. The molecular biology of nairoviruses, an emerging group of tick-borne arboviruses. Arch Virol, epub ahead of print.

Lawrie, C.H., Uzcategui, N.Y., Armesto, M., Bell-Sakyi, L., Gould, E.A., 2004a. Susceptibility of mosquito and tick cell lines to infection with various flaviviruses. Med Vet Entomol 18, 268-274.

Lawrie, C.H., Uzcategui, N.Y., Gould, E.A., Nuttall, P.A., 2004b. Ixodid and argasid tick species and West Nile virus. Emerg Infect Dis 10, 653-657.

Leake, C.J., Pudney, M., Varma, M.G.R., 1980. Studies on arboviruses in established tick cell lines. Invertebrate Systems In Vitro Amsterdam: Elsevier/North Holland Biomedical Pres, pp. 327-335.

Leblebicioglu, H., 2010. Crimean-Congo haemorrhagic fever in Eurasia. Int J Antimicrob Agents 36 Suppl 1, S43-46.

Leger, P., Lara, E., Jagla, B., Sismeiro, O., Mansuroglu, Z., Coppee, J.Y., Bonnefoy, E., Bouloy, M., 2013. Dicer-2- and Piwi-mediated RNA interference in Rift Valley fever virus-infected mosquito cells. J Virol 87, 1631-1648.

Lemaitre, B., Hoffmann, J., 2007. The host defense of *Drosophila melanogaster*. Ann Rev Immunol 25, 697-743.

Lemaitre, B., Nicolas, E., Michaut, L., Reichhart, J.M., Hoffmann, J.A., 1996. The dorsoventral regulatory gene cassette spatzle/Toll/cactus controls the potent antifungal response in *Drosophila* adults. Cell 86, 973-983.

Letchworth, G.J., Rodriguez, L.L., Del cbarrera, J., 1999. Vesicular stomatitis. Vet J 157, 239-260.

Li, F., Xiang, J., 2013. Signaling pathways regulating innate immune responses in shrimp. Fish Shellfish Immunol 34, 973-980.

Li, S., Mead, E.A., Liang, S., Tu, Z., 2009. Direct sequencing and expression analysis of a large number of miRNAs in *Aedes aegypti* and a multi-species survey of novel mosquito miRNAs. BMC Genomics 10, 581.

Liljestrom, P., Garoff, H., 1991. A new generation of animal cell expression vectors based on the Semliki Forest virus replicon. Biotechnology 9, 1356-1361.

Liljestrom, P., Lusa, S., Huylebroeck, D., Garoff, H., 1991. In vitro mutagenesis of a full-length cDNA clone of Semliki Forest virus: the small 6,000-molecular-weight membrane protein modulates virus release. J Virol 65, 4107-4113.

Linthicum, K.J., Logan, T.M., 1994. Laboratory transmission of Venezuelan equine encephalomyelitis virus by the tick *Hyalomma truncatum*. Trans R Soc Trop Med Hyg 88, 126.

Lipardi, C., Paterson, B.M., 2009. Identification of an RNA-dependent RNA polymerase in *Drosophila* involved in RNAi and transposon suppression. Proc Natl Acad Sci USA 106, 15645-15650.

Lipardi, C., Paterson, B.M., 2011. Retraction for Lipardi and Paterson, "Identification of an RNA-dependent RNA polymerase in *Drosophila* involved in RNAi and transposon suppression". Proc Natl Acad Sci USA 108, 15010.

Liu, L., Dai, J., Zhao, Y.O., Narasimhan, S., Yang, Y., Zhang, L., Fikrig, E., 2012. *Ixodes scapularis* JAK-STAT pathway regulates tick antimicrobial peptides, thereby controlling the agent of human granulocytic anaplasmosis. J Infect Dis 206, 1233-1241.

Livak, K.J., Schmittgen, T.D., 2001. Analysis of relative gene expression data using real-time quantitative PCR and the 2(-Delta Delta C(T)) method. Methods 25, 402-408.

Lu, Z., Beck, M.H., Wang, Y., Jiang, H., Strand, M.R., 2008. The viral protein Egf1.0 is a dual activity inhibitor of prophenoloxidase-activating proteinases 1 and 3 from *Manduca sexta*. J Biol Chem 283, 21325-21333.

Lucas, K., Raikhel, A.S., 2013. Insect microRNAs: biogenesis, expression profiling and biological functions. Insect Biochem Mol Biol 43, 24-38.

Lundstrom, K., 2009. Alphaviruses in gene therapy. Viruses 1, 13-25.

Lwande, O.W., Lutomiah, J., Obanda, V., Gakuya, F., Mutisya, J., Mulwa, F., Michuki, G., Chepkorir, E., Fischer, A., Venter, M., Sang, R., 2013. Isolation of tick and mosquito-borne arboviruses from ticks sampled from livestock and wild animal hosts in Ijara District, Kenya. Vector-borne Zoonot Dis 13, 637-42

Maclachlan, N.J., 2011. Bluetongue: history, global epidemiology, and pathogenesis. Prev Vet Med 102, 107-111.

Maclachlan, N.J., Guthrie, A.J., 2010. Re-emergence of bluetongue, African horse sickness, and other orbivirus diseases. Vet Res 41, 35.

Madani, T.A., Abuelzein el, T.M., Bell-Sakyi, L., Azhar, E.I., Al-Bar, H.M., Abu-Araki, H., Hassan, A.M., Masri, B.E., Ksiazek, T.G., 2013. Susceptibility of tick cell lines to infection with Alkhumra haemorrhagic fever virus. Trans R Soc Trop Med Hyg 107, 806-811.

Mans, B.J., de Klerk, D., Pienaar, R., Latif, A.A., 2011. *Nuttalliella namaqua*: a living fossil and closest relative to the ancestral tick lineage: implications for the evolution of blood-feeding in ticks. PloS One 6, e23675.

Masson, P., Hulo, C., De Castro, E., Bitter, H., Gruenbaum, L., Essioux, L., Bougueleret, L., Xenarios, I., Le Mercier, P., 2013. ViralZone: recent updates to the virus knowledge resource. Nucleic Acids Res 41, D579-583.

Mathiot, C.C., Grimaud, G., Garry, P., Bouquety, J.C., Mada, A., Daguisy, A.M., Georges, A.J., 1990. An outbreak of human Semliki Forest virus infections in Central African Republic. Am J Trop Med Hyg 42, 386-393.

Mattila, J.T., Burkhardt, N.Y., Hutcheson, H.J., Munderloh, U.G., Kurtti, T.J., 2007. Isolation of cell lines and a rickettsial endosymbiont from the soft tick *Carios capensis* (Acari: Argasidae: Ornithodorinae). J Med Entomol 44, 1091-1101.

McLoughlin, M.F., Graham, D.A., 2007. Alphavirus infections in salmonids--a review. J Fish Dis 30, 511-531.

McMullan, L.K., Folk, S.M., Kelly, A.J., MacNeil, A., Goldsmith, C.S., Metcalfe, M.G., Batten, B.C., Albarino, C.G., Zaki, S.R., Rollin, P.E., Nicholson, W.L., Nichol, S.T., 2012. A new phlebovirus associated with severe febrile illness in Missouri. N Engl J Med 367, 834-841.

Medlock, J.M., Hansford, K.M., Bormane, A., Derdakova, M., Estrada-Pena, A., George, J.C., Golovljova, I., Jaenson, T.G., Jensen, J.K., Jensen, P.M., Kazimirova, M., Oteo, J.A., Papa, A., Pfister, K., Plantard, O., Randolph, S.E., Rizzoli, A., Santos-Silva, M.M., Sprong, H., Vial, L., Hendrickx, G., Zeller, H., Van Bortel, W., 2013. Driving forces for changes in geographical distribution of *Ixodes ricinus* ticks in Europe. Parasites Vect 6, 1.

Medlock, J.M., Hansford, K.M., Schaffner, F., Versteirt, V., Hendrickx, G., Zeller, H., Van Bortel, W., 2012. A review of the invasive mosquitoes in Europe: ecology, public health risks, and control options. Vector-borne Zoonotic Dis 12, 435-447.

Menghani, S., Chikhale, R., Raval, A., Wadibhasme, P., Khedekar, P., 2012. Chandipura Virus: an emerging tropical pathogen. Acta Trop 124, 1-14.

Merits, A., Vasiljeva, L., Ahola, T., Kaariainen, L., Auvinen, P., 2001. Proteolytic processing of Semliki Forest virus-specific non-structural polyprotein by nsP2 protease. J Gen Virol 82, 765-773.

Merkling, S.H., van Rij, R.P., 2013. Beyond RNAi: antiviral defense strategies in *Drosophila* and mosquito. J Insect Physiol 59, 159-170.

Mitri, C., Vernick, K.D., 2012. *Anopheles gambiae* pathogen susceptibility: the intersection of genetics, immunity and ecology. Curr Opin Microbiol 15, 285-291.

Moniuszko, A., Ruckert, C., Alberdi, M.P., Barry, G., Stevenson, B., Fazakerley, J.K., Kohl, A., Bell-Sakyi, L., 2014. Coinfection of tick cell lines has variable effects on replication of intracellular bacterial and viral pathogens. Ticks Tick-borne Dis, epub ahead of print.

Morazzani, E.M., Wiley, M.R., Murreddu, M.G., Adelman, Z.N., Myles, K.M., 2012. Production of virus-derived ping-pong-dependent piRNA-like small RNAs in the mosquito soma. PLoS Pathog 8, e1002470.

Morrison, W.I., 2009. Progress towards understanding the immunobiology of *Theileria* parasites. Parasitology 136, 1415-1426.

Moudy, R.M., Meola, M.A., Morin, L.L., Ebel, G.D., Kramer, L.D., 2007. A newly emergent genotype of West Nile virus is transmitted earlier and more efficiently by *Culex* mosquitoes. Am J Trop Med Hyg 77, 365-370.

Moutailler, S., Roche, B., Thiberge, J.M., Caro, V., Rougeon, F., Failloux, A.B., 2011. Host alternation is necessary to maintain the genome stability of Rift Valley fever virus. PLoS Negl Trop Dis 5, e1156.

Muller, J., Sperl, B., Reindl, W., Kiessling, A., Berg, T., 2008. Discovery of chromone-based inhibitors of the transcription factor STAT5. Chembiochem 9, 723-727.

Munderloh, U.G., Kurtti, T.J., 1989. Formulation of medium for tick cell culture. Exp Appl Acarol 7, 219-229.

Munderloh, U.G., Liu, Y., Wang, M., Chen, C., Kurtti, T.J., 1994. Establishment, maintenance and description of cell lines from the tick *Ixodes scapularis*. J Parasitol 80, 533-543.

Munz, E., Reimann, M., Mahnel, H., 1987. Nairobi sheep disease virus and Reovirus-like particles in the tick cell line TTC-243 from *Rhipicephalus appendiculatus*: experiences with the handling of the tick cells, immunoperoxidase and ultrahistological studies. Arboviruses in Arthropod Cells In Vitro I, 133–147.

Muta, T., Iwanaga, S., 1996. The role of hemolymph coagulation in innate immunity. Curr Opin Immunol 8, 41-47.

Myles, K.M., Wiley, M.R., Morazzani, E.M., Adelman, Z.N., 2008. Alphavirus-derived small RNAs modulate pathogenesis in disease vector mosquitoes. Proc Natl Acad Sci USA 105, 19938-19943.

Nagai, T., Kawabata, S., 2000. A link between blood coagulation and prophenol oxidase activation in arthropod host defense. J Biol Chem 275, 29264-29267.

Najm, N.A., Silaghi, C., Bell-Sakyi, L., Pfister, K., Passos, L.M., 2012. Detection of bacteria related to *Candidatus Midichloria mitochondrii* in tick cell lines. Parasitol Res 110, 437-442.

Nakamoto, M., Moy, R.H., Xu, J., Bambina, S., Yasunaga, A., Shelly, S.S., Gold, B., Cherry, S., 2012. Virus recognition by Toll-7 activates antiviral autophagy in *Drosophila*. Immunity 36, 658-667.

Nandi, S., Negi, B.S., 1999. Bovine ephemeral fever: a review. Comp Immunol Microbiol Infect Dis 22, 81-91.

Naranjo, V., Ayllon, N., Perez de la Lastra, J.M., Galindo, R.C., Kocan, K.M., Blouin, E.F., Mitra, R., Alberdi, P., Villar, M., de la Fuente, J., 2013. Reciprocal regulation of NF-kB (Relish) and Subolesin in the tick vector, *Ixodes scapularis*. PloS One 8, e65915.

Nasar, F., Palacios, G., Gorchakov, R.V., Guzman, H., Da Rosa, A.P., Savji, N., Popov, V.L., Sherman, M.B., Lipkin, W.I., Tesh, R.B., Weaver, S.C., 2012. Eilat virus, a unique alphavirus with host range restricted to insects by RNA replication. Proc Natl Acad Sci USA 109, 14622-14627.

Nellaiappan, K., Sugumaran, M., 1996. On the presence of prophenoloxidase in the hemolymph of the horseshoe crab, *Limulus*. Comp Biochem Physiol Part B Biochem Mol Biol 113, 163-168.

Normile, D., 2013. Tropical medicine. Surprising new dengue virus throws a spanner in disease control efforts. Science 342, 415.

Nunn, M.A., Barton, T.R., Wanless, S., Hails, R.S., Harris, M.P., Nuttall, P.A., 2006. Tick-borne Great Island Virus: (I) Identification of seabird host and evidence for co-feeding and viraemic transmission. Parasitology 132, 233-240.

Offerdahl, D.K., Dorward, D.W., Hansen, B.T., Bloom, M.E., 2012. A three-dimensional comparison of tick-borne flavivirus infection in mammalian and tick cell lines. PloS One 7, e47912.

Okamura, K., Chung, W.J., Ruby, J.G., Guo, H., Bartel, D.P., Lai, E.C., 2008. The *Drosophila* hairpin RNA pathway generates endogenous short interfering RNAs. Nature 453, 803-806.

Ooi, J.Y., Yagi, Y., Hu, X., Ip, Y.T., 2002. The *Drosophila* Toll-9 activates a constitutive antimicrobial defense. EMBO Rep 3, 82-87.

Oura, C., 2013. African swine fever virus: on the move and dangerous. Vet Rec 173, 243-245.

Page, R.D., 1996. TreeView: an application to display phylogenetic trees on personal computers. Comput Appl Biosci 12, 357-358.

Panas, M.D., Varjak, M., Lulla, A., Eng, K.E., Merits, A., Karlsson Hedestam, G.B., McInerney, G.M., 2012. Sequestration of G3BP coupled with efficient translation inhibits stress granules in Semliki Forest virus infection. Mol Biol Cell 23, 4701-4712.

Paradkar, P.N., Trinidad, L., Voysey, R., Duchemin, J.B., Walker, P.J., 2012. Secreted Vago restricts West Nile virus infection in *Culex* mosquito cells by activating the Jak-STAT pathway. Proc Natl Acad Sci USA 109, 18915-18920.

Paredes, A.M., Brown, D.T., Rothnagel, R., Chiu, W., Schoepp, R.J., Johnston, R.E., Prasad, B.V., 1993. Three-dimensional structure of a membrane-containing virus. Proc Natl Acad Sci USA 90, 9095-9099.

Passos, L.M.F., 2012. In vitro cultivation of *Anaplasma marginale* and *A. phagocytophilum* in tick cell lines: a review. Rev Brasil Parasitol V 21, 81-86.

Patel, A., Roy, P., 2013. The molecular biology of Bluetongue virus replication. Virus Res 182, 5-20.

Peleg, J., 1968. Growth of arboviruses in monolayers from subcultured mosquito embryo cells. Virology 35, 617-619.

Petersen, T.N., Brunak, S., von Heijne, G., Nielsen, H., 2011. SignalP 4.0: discriminating signal peptides from transmembrane regions. Nature Meth 8, 785-786.

Petterson, E., Sandberg, M., Santi, N., 2009. Salmonid alphavirus associated with *Lepeophtheirus salmonis* (Copepoda: Caligidae) from Atlantic salmon, *Salmo salar* L. J Fish Dis 32, 477-479.

Powers, A.M., Brault, A.C., Shirako, Y., Strauss, E.G., Kang, W., Strauss, J.H., Weaver, S.C., 2001. Evolutionary relationships and systematics of the alphaviruses. J Virol 75, 10118-10131.

Pudney, M., 1987. Tick cell lines for the isolation and assay of arboviruses. In: Yunker CE, editor. Arboviruses in Arthropod Cells In Vitro I. Boca Raton: CRC Press; 1987. pp. 87–101.

Puthiyakunnon, S., Yao, Y., Li, Y., Gu, J., Peng, H., Chen, X., 2013. Functional characterization of three MicroRNAs of the Asian tiger mosquito, *Aedes albopictus*. Parasites Vect 6, 230.

Ratinier, M., Caporale, M., Golder, M., Franzoni, G., Allan, K., Nunes, S.F., Armezzani, A., Bayoumy, A., Rixon, F., Shaw, A., Palmarini, M., 2011. Identification and characterization of a novel non-structural protein of bluetongue virus. PLoS Pathog 7, e1002477.

Ready, P.D., 2013. Biology of phlebotomine sand flies as vectors of disease agents. Annu Rev Entomol 58, 227-250.

Reinert, J.F., Harbach, R.E., Kitching, I.J., 2009. Phylogeny and classification of tribe Aedini (Diptera: Culicidae). Zool J Linn Soc-Lond 157, 700-794.

Renault, P., Solet, J.L., Sissoko, D., Balleydier, E., Larrieu, S., Filleul, L., Lassalle, C., Thiria, J., Rachou, E., de Valk, H., Ilef, D., Ledrans, M., Quatresous, I., Quenel, P., Pierre, V., 2007. A major epidemic of chikungunya virus infection on Reunion Island, France, 2005-2006. Am J Trop Med Hyg 77, 727-731.

Ribeiro, M.F., Bastos, C.V., Vasconcelos, M.M., Passos, L.M., 2009. *Babesia bigemina*: in vitro multiplication of sporokinetes in *Ixodes scapularis* (IDE8) cells. Exp Parasitol 122, 192-195.

Rider, M.A., Zou, J., Vanlandingham, D., Nuckols, J.T., Higgs, S., Zhang, Q., Lacey, M., Kim, J., Wang, G., Hong, Y.S., 2013. Quantitative proteomic analysis of the *Anopheles gambiae* (Diptera: Culicidae) midgut infected with O'nyong-nyong virus. J Med Entomol 50, 1077-1088.

Rodriguez-Andres, J., Rani, S., Varjak, M., Chase-Topping, M.E., Beck, M.H., Ferguson, M.C., Schnettler, E., Fragkoudis, R., Barry, G., Merits, A., Fazakerley, J.K., Strand, M.R., Kohl, A., 2012. Phenoloxidase activity acts as a mosquito innate immune response against infection with Semliki Forest virus. PLoS Pathog 8, e1002977.

Ronquist, F., Teslenko, M., van der Mark, P., Ayres, D.L., Darling, A., Hohna, S., Larget, B., Liu, L., Suchard, M.A., Huelsenbeck, J.P., 2012. MrBayes 3.2: efficient Bayesian phylogenetic inference and model choice across a large model space. System Biol 61, 539-542.

Rose, P.P., Hanna, S.L., Spiridigliozzi, A., Wannissorn, N., Beiting, D.P., Ross, S.R., Hardy, R.W., Bambina, S.A., Heise, M.T., Cherry, S., 2011. Natural resistance-associated macrophage protein is a cellular receptor for sindbis virus in both insect and mammalian hosts. Cell Host Microbe 10, 97-104.

Rückert, C., Bell-Sakyi, L., Fazakerley, J.K., Fragkoudis, R., 2014. Antiviral responses of arthropod vectors: an update on recent advances. VirusDisease, in press.

Ruzek, D., Bell-Sakyi, L., Kopecky, J., Grubhoffer, L., 2008. Growth of tick-borne encephalitis virus (European subtype) in cell lines from vector and non-vector ticks. Virus Res 137, 142-146.

Ryu, S.W., Chae, S.K., Lee, K.J., Kim, E., 1999. Identification and characterization of human Fas associated factor 1, hFAF1. Biochem Biophys Res Commun 262, 388-394.

Ryu, S.W., Kim, E., 2001. Apoptosis induced by human Fas-associated factor 1, hFAF1, requires its ubiquitin homologous domain, but not the Fas-binding domain. Biochem Biophys Res Commun 286, 1027-1032.

Saleh, M.C., Tassetto, M., van Rij, R.P., Goic, B., Gausson, V., Berry, B., Jacquier, C., Antoniewski, C., Andino, R., 2009. Antiviral immunity in *Drosophila* requires systemic RNA interference spread. Nature 458, 346-350.

Saleh, M.C., van Rij, R.P., Hekele, A., Gillis, A., Foley, E., O'Farrell, P.H., Andino, R., 2006. The endocytic pathway mediates cell entry of dsRNA to induce RNAi silencing. Nature Cell Biol 8, 793-802.

Salonen, A., Ahola, T., Kaariainen, L., 2005. Viral RNA replication in association with cellular membranes. Curr Top Microbiol Immunol 285, 139-173.

Sanchez-Vargas, I., Travanty, E.A., Keene, K.M., Franz, A.W., Beaty, B.J., Blair, C.D., Olson, K.E., 2004. RNA interference, arthropod-borne viruses, and mosquitoes. Virus Res 102, 65-74.

Savage, H.M., Godsey, M.S., Jr., Lambert, A., Panella, N.A., Burkhalter, K.L., Harmon, J.R., Lash, R.R., Ashley, D.C., Nicholson, W.L., 2013. First detection of Heartland virus (bunyaviridae: phlebovirus) from field collected arthropods. Am J Trop Med Hyg 89, 445-452.

Schnettler, E., Donald, C.L., Human, S., Watson, M., Siu, R.W.C., McFarlane, M., Fazakerley, J.K., Kohl, A., Fragkoudis, R., 2013a. Knockdown of piRNA pathway proteins results in enhanced Semliki Forest virus production in mosquito cells. J Gen Virol 94, 1680-1689.

Schnettler, E., Ratinier, M., Watson, M., Shaw, A.E., McFarlane, M., Varela, M., Elliott, R.M., Palmarini, M., Kohl, A., 2013b. RNA interference targets arbovirus replication in *Culicoides* cells. J Virol 87, 2441-2454.

Schnettler, E., Sterken, M.G., Leung, J.Y., Metz, S.W., Geertsema, C., Goldbach, R.W., Vlak, J.M., Kohl, A., Khromykh, A.A., Pijlman, G.P., 2012. Noncoding flavivirus RNA displays RNA interference suppressor activity in insect and mammalian cells. J Virol 86, 13486-13500.

Schnettler, E., Tykalová, H., Watson, M., Sharma, M., Sterken, M.G., Obbard, D.J., Lewis, S.H., McFarlane, M., Bell-Sakyi, L., Barry, G., Weisheit, S., Best, S.M., Kuhn, R.J., Pijlman, G.P., Chase-Topping, M.E., Gould, E.A., Grubhoffer L., Fazakerley, J.K., Kohl, A., 2014. Induction and suppression of tick cell antiviral RNAi responses by tick-borne flaviviruses. Submitted to Nucleic Acid Research.

Scoles, G.A., 2004. Phylogenetic analysis of the *Francisella*-like endosymbionts of *Dermacentor* ticks. J Med Entomol 41, 277-286.

Scott, J.C., Brackney, D.E., Campbell, C.L., Bondu-Hawkins, V., Hjelle, B., Ebel, G.D., Olson, K.E., Blair, C.D., 2010. Comparison of dengue virus type 2-specific small

RNAs from RNA interference-competent and -incompetent mosquito cells. PLoS Negl Trop Dis 4, e848.

Senigl, F., Grubhoffer, L., Kopecky, J., 2006. Differences in maturation of tick-borne encephalitis virus in mammalian and tick cell line. Intervirology 49, 239-248.

Shin, S.W., Kokoza, V., Ahmed, A., Raikhel, A.S., 2002. Characterization of three alternatively spliced isoforms of the Rel/NF-kappa B transcription factor Relish from the mosquito *Aedes aegypti*. Proc Natl Acad Sci USA 99, 9978-9983.

Shin, S.W., Kokoza, V., Bian, G., Cheon, H.M., Kim, Y.J., Raikhel, A.S., 2005. REL1, a homologue of *Drosophila* dorsal, regulates toll antifungal immune pathway in the female mosquito *Aedes aegypti*. J Biol Chem 280, 16499-16507.

Shirako, Y., Strauss, J.H., 1994. Regulation of Sindbis virus RNA replication: uncleaved P123 and nsP4 function in minus-strand RNA synthesis, whereas cleaved products from P123 are required for efficient plus-strand RNA synthesis. J Virol 68, 1874-1885.

Shuai, K., 2006. Regulation of cytokine signaling pathways by PIAS proteins. Cell Res 16, 196-202.

Silaghi, C., Kauffmann, M., Passos, L.M., Pfister, K., Zweygarth, E., 2011. Isolation, propagation and preliminary characterisation of *Anaplasma phagocytophilum* from roe deer (*Capreolus capreolus*) in the tick cell line IDE8. Ticks Tick-borne Dis 2, 204-208.

Simser, J.A., Palmer, A.T., Fingerle, V., Wilske, B., Kurtti, T.J., Munderloh, U.G., 2002. *Rickettsia monacensis* sp. nov., a spotted fever group *Rickettsia*, from ticks (*Ixodes ricinus*) collected in a European city park. Appl Environ Microbiol 68, 4559-4566.

Simser, J.A., Palmer, A.T., Munderloh, U.G., Kurtti, T.J., 2001. Isolation of a spotted fever group *Rickettsia*, *Rickettsia peacockii*, in a Rocky Mountain wood tick, *Dermacentor andersoni*, cell line. Appl Environ Microbiol 67, 546-552.

Singh, I., Helenius, A., 1992. Role of ribosomes in Semliki Forest virus nucleocapsid uncoating. J Virol 66, 7049-7058.

Singh, K.R.P., 1967. Cell cultures derived from larvae of *Aedes Albopictus* (Skuse) and *Aedes Aegypti* (L). Curr Sci India 36, 506-&.

Siomi, M.C., Sato, K., Pezic, D., Aravin, A.A., 2011. PIWI-interacting small RNAs: the vanguard of genome defence. Nature Rev Mol Cell Biol 12, 246-258.

Siu, R.W., Fragkoudis, R., Simmonds, P., Donald, C.L., Chase-Topping, M.E., Barry, G., Attarzadeh-Yazdi, G., Rodriguez-Andres, J., Nash, A.A., Merits, A., Fazakerley, J.K., Kohl, A., 2010. Antiviral RNA interference responses induced by Semliki Forest virus infection of mosquito cells: characterization, origin, and frequency-dependent functions of virus-derived small interfering RNAs. J Virol 85, 2907-2917.

Skalsky, R.L., Vanlandingham, D.L., Scholle, F., Higgs, S., Cullen, B.R., 2010. Identification of microRNAs expressed in two mosquito vectors, *Aedes albopictus* and *Culex quinquefasciatus*. BMC Genomics 11, 119.

Smardon, A., Spoerke, J.M., Stacey, S.C., Klein, M.E., Mackin, N., Maine, E.M., 2000. EGO-1 is related to RNA-directed RNA polymerase and functions in germ-line development and RNA interference in *C. elegans*. Curr Biol 10, 169-178.

Smerdou, C., Liljestrom, P., 1999. Two-helper RNA system for production of recombinant Semliki forest virus particles. J Virol 73, 1092-1098.

Smith, C.E., 1956. A virus resembling Russian spring-summer encephalitis virus from an ixodid tick in Malaya. Nature 178, 581-582.

Smith, D.R., Adams, A.P., Kenney, J.L., Wang, E., Weaver, S.C., 2008. Venezuelan equine encephalitis virus in the mosquito vector *Aedes taeniorhynchus*: infection initiated by a small number of susceptible epithelial cells and a population bottleneck. Virology 372, 176-186.

Smith, T.J., Cheng, R.H., Olson, N.H., Peterson, P., Chase, E., Kuhn, R.J., Baker, T.S., 1995. Putative receptor binding sites on alphaviruses as visualized by cryoelectron microscopy. Proc Natl Acad Sci USA 92, 10648-10652.

Smithburn, K.C.H.A.J., 1944. Semliki Forest Virus I. Isolation and Pathogenic Properties. J Immunol 49, p141-157.

Soonsawad, P., Xing, L., Milla, E., Espinoza, J.M., Kawano, M., Marko, M., Hsieh, C., Furukawa, H., Kawasaki, M., Weerachatyanukul, W., Srivastava, R., Barnett, S.W., Srivastava, I.K., and Cheng H.R., 2010. Structural evidence of glycoprotein assembly in cellular membrane compartments prior to alphavirus budding. J Virol 84, 11145–11151.

Souza-Neto, J.A., Sim, S., Dimopoulos, G., 2009. An evolutionary conserved function of the JAK-STAT pathway in anti-dengue defense. Proc Natl Acad Sci USA 106, 17841-17846.

Spuul, P., Balistreri, G., Hellstrom, K., Golubtsov, A.V., Jokitalo, E., Ahola, T., 2011. Assembly of alphavirus replication complexes from RNA and protein components in a novel trans-replication system in mammalian cells. J Virol 85, 4739-4751.

Spuul, P., Balistreri, G., Kaariainen, L., Ahola, T., 2010. Phosphatidylinositol 3-kinase-, actin-, and microtubule-dependent transport of Semliki Forest Virus replication complexes from the plasma membrane to modified lysosomes. J Virol 84, 7543-7557.

Spuul, P., Salonen, A., Merits, A., Jokitalo, E., Kaariainen, L., Ahola, T., 2007. Role of the amphipathic peptide of Semliki forest virus replicase protein nsP1 in membrane association and virus replication. J Virol 81, 872-883.

Stephenson, J.R., 1988. Flavivirus vaccines. Vaccine 6, 471-480.

Strauss, J.H., Strauss, E.G., 1994. The alphaviruses: gene expression, replication, and evolution. Microbiol Rev 58, 491-562.

Stricker, R.B., Johnson, L., 2011. Lyme disease: the next decade. Infect Drug Resist 4, 1-9.

Su, L., David, M., 2000. Distinct mechanisms of STAT phosphorylation via the interferon-alpha/beta receptor. Selective inhibition of STAT3 and STAT5 by piceatannol. J Biol Chem 275, 12661-12666.

Takkinen, K., 1986. Complete nucleotide sequence of the nonstructural protein genes of Semliki Forest virus. Nucleic Acids Res 14, 5667-5682.

Tamang, D., Tseng, S.M., Huang, C.Y., Tsao, I.Y., Chou, S.Z., Higgs, S., Christensen, B.M., Chen, C.C., 2004. The use of a double subgenomic Sindbis virus expression system to study mosquito gene function: effects of antisense nucleotide number and duration of viral infection on gene silencing efficiency. Insect Mol Biol 13, 595-602.

Tamberg, N., Lulla, V., Fragkoudis, R., Lulla, A., Fazakerley, J.K., Merits, A., 2007. Insertion of EGFP into the replicase gene of Semliki Forest virus results in a novel, genetically stable marker virus. J Gen Virol 88, 1225-1230.

Theilmann, D.A., Stewart, S., 1992. Tandemly repeated sequence at the 3' end of the IE-2 gene of the baculovirus *Orgyia pseudotsugata* multicapsid nuclear polyhedrosis virus is an enhancer element. Virology 187, 97-106.

Thirugnanasambantham, K., Hairul-Islam, V.I., Saravanan, S., Subasri, S., Subastri, A., 2013. Computational approach for identification of *Anopheles gambiae* miRNA involved in modulation of host immune response. Appl Biochem Biotechnol 170, 281-291.

Thompson, J.D., Higgins, D.G., Gibson, T.J., 1994. CLUSTAL W: improving the sensitivity of progressive multiple sequence alignment through sequence weighting, position-specific gap penalties and weight matrix choice. Nucleic Acids Res 22, 4673-4680.

Tomasello, D., Schlagenhauf, P., 2013. Chikungunya and dengue autochthonous cases in Europe, 2007-2012. Travel Med Infect Dis 11, 274-284.

Tsai, C.W., McGraw, E.A., Ammar, E.D., Dietzgen, R.G., Hogenhout, S.A., 2008. *Drosophila melanogaster* mounts a unique immune response to the Rhabdovirus sigma virus. Appl Environ Microbiol 74, 3251-3256.

Tumban, E., Mitzel, D.N., Maes, N.E., Hanson, C.T., Whitehead, S.S., Hanley, K.A., 2010. Replacement of the 3' untranslated variable region of mosquito-borne dengue virus with that of tick-borne Langat virus does not alter vector specificity. J Gen Virol 92, 841-848.

Tuppurainen, E.S., Lubinga, J.C., Stoltsz, W.H., Troskie, M., Carpenter, S.T., Coetzer, J.A., Venter, E.H., Oura, C.A., 2013. Evidence of vertical transmission of lumpy skin disease virus in *Rhipicephalus decoloratus* ticks. Ticks Tick-borne Dis 4, 329-333.

Tuppurainen, E.S., Stoltsz, W.H., Troskie, M., Wallace, D.B., Oura, C.A., Mellor, P.S., Coetzer, J.A., Venter, E.H., 2010. A potential role for ixodid (hard) tick vectors in the transmission of lumpy skin disease virus in cattle. Transboundary Emerg Infect Dis 58, 93–104.

Ulvila, J., Parikka, M., Kleino, A., Sormunen, R., Ezekowitz, R.A., Kocks, C., Ramet, M., 2006. Double-stranded RNA is internalized by scavenger receptor-mediated endocytosis in Drosophila S2 cells. J Biol Chem 281, 14370-14375.

Untergasser, A., Cutcutache, I., Koressaar, T., Ye, J., Faircloth, B.C., Remm, M., Rozen, S.G., 2012. Primer3 - new capabilities and interfaces. Nucleic Acids Res 40, e115.

Vagin, V.V., Sigova, A., Li, C., Seitz, H., Gvozdev, V., Zamore, P.D., 2006. A distinct small RNA pathway silences selfish genetic elements in the germline. Science 313, 320-324.

Valanne, S., Wang, J.H., Ramet, M., 2011. The *Drosophila* Toll signaling pathway. J Immunol 186, 649-656.

Varma, M.G., Pudney, M., Leake, C.J., 1975. The establishment of three cell lines from the tick *Rhipicephalus appendiculatus* (Acari: Ixodidae) and their infection with some arboviruses. J Med Entomol 11, 698-706.

Vazeille, M., Moutailler, S., Coudrier, D., Rousseaux, C., Khun, H., Huerre, M., Thiria, J., Dehecq, J.S., Fontenille, D., Schuffenecker, I., Despres, P., Failloux, A.B., 2007. Two Chikungunya isolates from the outbreak of La Reunion (Indian Ocean) exhibit different patterns of infection in the mosquito, *Aedes albopictus*. PloS One 2, e1168.

Vijayendran, D., Airs, P.M., Dolezal, K., Bonning, B.C., 2013. Arthropod viruses and small RNAs. J Invert Pathol 114, 186-195.

Vodovar, N., Bronkhorst, A.W., van Cleef, K.W., Miesen, P., Blanc, H., van Rij, R.P., Saleh, M.C., 2012. Arbovirus-derived piRNAs exhibit a ping-pong signature in mosquito cells. PloS One 7, e30861.

Vogel, R.H., Provencher, S.W., von Bonsdorff, C.H., Adrian, M., Dubochet, J., 1986. Envelope structure of Semliki Forest virus reconstructed from cryo-electron micrographs. Nature 320, 533-535.

Voinnet, O., 2005. Non-cell autonomous RNA silencing. FEBS letters 579, 5858-5871.

Waldock, J., Olson, K.E., Christophides, G.K., 2012. *Anopheles gambiae* antiviral immune response to systemic O'nyong-nyong infection. PLoS Negl Trop Dis 6, e1565.

Walker, A.R., Bouattour, A., Camicas, J.-L., Estrada-Peña, A., Horak, I. G., Latif, A. A., Pegram, R. G. & Preston, P. M. , 2003. Ticks of domestic animals in Africa. Bioscience Reports, Edinburgh ISBN: 0-9545173-0-X.

Wang, K.S., Kuhn, R.J., Strauss, E.G., Ou, S., Strauss, J.H., 1992. High-affinity laminin receptor is a receptor for Sindbis virus in mammalian cells. J Virol 66, 4992-5001.

Wang, P.H., Gu, Z.H., Huang, X.D., Liu, B.D., Deng, X.X., Ai, H.S., Wang, J., Yin, Z.X., Weng, S.P., Yu, X.Q., He, J.G., 2009. An immune deficiency homolog from the white shrimp, *Litopenaeus vannamei*, activates antimicrobial peptide genes. Mol Immunol 46, 1897-1904.

Wang, P.H., Wan, D.H., Gu, Z.H., Deng, X.X., Weng, S.P., Yu, X.Q., He, J.G., 2011. *Litopenaeus vannamei* tumor necrosis factor receptor-associated factor 6 (TRAF6) responds to *Vibrio alginolyticus* and white spot syndrome virus (WSSV) infection and activates antimicrobial peptide genes. Dev Comp Immunol 35, 105-114.

Wang, X.W., Tan, N.S., Ho, B., Ding, J.L., 2006. Evidence for the ancient origin of the NF-kappaB/IkappaB cascade: its archaic role in pathogen infection and immunity. Proc Natl Acad Sci USA 103, 4204-4209.

Waterhouse, R.M., Kriventseva, E.V., Meister, S., Xi, Z., Alvarez, K.S., Bartholomay, L.C., Barillas-Mury, C., Bian, G., Blandin, S., Christensen, B.M., Dong, Y., Jiang,

H., Kanost, M.R., Koutsos, A.C., Levashina, E.A., Li, J., Ligoxygakis, P., Maccallum, R.M., Mayhew, G.F., Mendes, A., Michel, K., Osta, M.A., Paskewitz, S., Shin, S.W., Vlachou, D., Wang, L., Wei, W., Zheng, L., Zou, Z., Severson, D.W., Raikhel, A.S., Kafatos, F.C., Dimopoulos, G., Zdobnov, E.M., Christophides, G.K., 2007. Evolutionary dynamics of immune-related genes and pathways in disease-vector mosquitoes. Science 316, 1738-1743.

Weaver, S.C., Reisen, W.K., 2010. Present and future arboviral threats. Antiviral Res 85, 328-345.

Williams, M.C., Woodall, J.P., Corbet, P.S., Gillett, J.D., 1965. O'nyong-Nyong Fever: An Epidemic Virus Disease in East Africa. 8. Virus Isolations from *Anopheles* Mosquitoes. Trans R Soc Trop Med Hyg 59, 300-306.

Wilson, A.J., Mellor, P.S., 2009. Bluetongue in Europe: past, present and future. Phil Trans R Soc London Series B Biol Sci 364, 2669-2681.

Winter, F., Edaye, S., Huttenhofer, A., Brunel, C., 2007. *Anopheles gambiae* miRNAs as actors of defence reaction against *Plasmodium* invasion. Nucleic Acids Res 35, 6953-6962.

Wise, L.N., Kappmeyer, L.S., Mealey, R.H., Knowles, D.P., 2013. Review of Equine Piroplasmosis. J Vet Internal Med 27, 1334-46.

Wu, L.P., Anderson, K.V., 1998. Regulated nuclear import of Rel proteins in the *Drosophila* immune response. Nature 392, 93-97.

Wu, Q., Luo, Y., Lu, R., Lau, N., Lai, E.C., Li, W.X., Ding, S.W., 2010. Virus discovery by deep sequencing and assembly of virus-derived small silencing RNAs. Proc Natl Acad Sci USA 107, 1606-1611.

Xi, Z., Ramirez, J.L., Dimopoulos, G., 2008. The *Aedes aegypti* toll pathway controls dengue virus infection. PLoS Pathog 4, e1000098.

Yang, S.J., Carter, S.A., Cole, A.B., Cheng, N.H., Nelson, R.S., 2004. A natural variant of a host RNA-dependent RNA polymerase is associated with increased susceptibility to viruses by *Nicotiana benthamiana*. Proc Natl Acad Sci USA 101, 6297-6302.

Yu, X.J., Liang, M.F., Zhang, S.Y., Liu, Y., Li, J.D., Sun, Y.L., Zhang, L., Zhang, Q.F., Popov, V.L., Li, C., Qu, J., Li, Q., Zhang, Y.P., Hai, R., Wu, W., Wang, Q., Zhan, F.X., Wang, X.J., Kan, B., Wang, S.W., Wan, K.L., Jing, H.Q., Lu, J.X., Yin, W.W., Zhou, H., Guan, X.H., Liu, J.F., Bi, Z.Q., Liu, G.H., Ren, J., Wang, H., Zhao, Z., Song, J.D., He, J.R., Wan, T., Zhang, J.S., Fu, X.P., Sun, L.N., Dong, X.P., Feng, Z.J., Yang, W.Z., Hong, T., Zhang, Y., Walker, D.H., Wang, Y., Li, D.X., 2011. Fever with thrombocytopenia associated with a novel bunyavirus in China. N Engl J Med 364, 1523-1532.

Zacks, M.A., Paessler, S., 2010. Encephalitic alphaviruses. Vet Microbiol 140, 281-286.

Zamore, P.D., 2004. Plant RNAi: How a viral silencing suppressor inactivates siRNA. Curr Biol 14, R198-200.

Zhang, G., Hussain, M., O'Neill, S.L., Asgari, S., 2013. *Wolbachia* uses a host microRNA to regulate transcripts of a methyltransferase, contributing to dengue virus inhibition in *Aedes aegypti*. Proc Natl Acad Sci USA 110, 10276-10281.

Zhang, X., Fugere, M., Day, R., Kielian, M., 2003. Furin processing and proteolytic activation of Semliki Forest virus. J Virol 77, 2981-2989.

Zhang, Y.Z., Zhou, D.J., Qin, X.C., Tian, J.H., Xiong, Y., Wang, J.B., Chen, X.P., Gao, D.Y., He, Y.W., Jin, D., Sun, Q., Guo, W.P., Wang, W., Yu, B., Li, J., Dai, Y.A., Li, W., Peng, J.S., Zhang, G.B., Zhang, S., Chen, X.M., Wang, Y., Li, M.H., Lu, X., Ye, C., de Jong, M.D., Xu, J., 2012. The ecology, genetic diversity, and phylogeny of Huaiyangshan virus in China. J Virol 86, 2864-2868.

Zhao, L., Zhai, S., Wen, H., Cui, F., Chi, Y., Wang, L., Xue, F., Wang, Q., Wang, Z., Zhang, S., Song, Y., Du, J., Yu, X.J., 2012. Severe fever with thrombocytopenia syndrome virus, Shandong Province, China. Emerg Infect Dis 18, 963-965.

Zhioua, E., Yeh, M.T., LeBrun, R.A., 1997. Assay for phenoloxidase activity in *Amblyomma americanum*, *Dermacentor variabilis*, and *Ixodes scapularis*. J Parasitol 83, 553-554.

Zhou, J., Zhou, Y., Cao, J., Zhang, H., Yu, Y., 2013. Distinctive microRNA profiles in the salivary glands of *Haemaphysalis longicornis* related to tick blood-feeding. Exp Appl Acarol 59, 339-349.

Zintl, A., Mulcahy, G., Skerrett, H.E., Taylor, S.M., Gray, J.S., 2003. *Babesia divergens*, a bovine blood parasite of veterinary and zoonotic importance. Clin Microbiol Rev 16, 622-636.

Zou, Z., Shin, S.W., Alvarez, K.S., Kokoza, V., Raikhel, A.S., 2010. Distinct melanization pathways in the mosquito *Aedes aegypti*. Immunity 32, 41-53.

Zweygarth, E., Josemans, A.I., Steyn, H.C., 2008. *In vitro* isolation of *Ehrlichia ruminantium* from ovine blood into *Ixodes scapularis* (IDE8) cell cultures. The Onderstepoort J Vet Res 75, 121-126.

8. Appendix

8.1 ADDITIONAL INFORMATION FOR CHAPTER 2

8.1.1 Tick cell medium - preparation of L-15B

L15B medium was kindly prepared and provided by either Lesley Bell-Sakyi or Pilar Alberdi. Ingredients for the stock solutions were dissolved in distilled water in the order listed, and the volume of each stock solution was brought to 100 ml. Trace mineral stock solutions A,B and C were prepared and used to make up stock solution D (Table 8.1).

Table 8.1: Composition of trace mineral stock solution D.

Ingredient	Weight (mg/100ml)	Final molarity in L-15B
Stock solution A		
$CoCl \cdot 6H_2O$	20	$8.4x10^{-9}$
$CuSO_4 \cdot 5H_2O$	20	$8.0x10^{-9}$
$MnSO_4 \cdot H_2O$	160	$9.5x10^{-8}$
$Zn\ SO_4 \cdot 7H_2O$	200	$7.0x10^{-8}$
Stock solution B		
$NaMoO_4 \cdot 2H_2O$	20	$8.3x10^{-9}$
Stock solution C		
Na_2SeO_3	20	$1.2x10^{-8}$
Stock solution D		
Glutathione (reduced)	1000	$3.3x10^{-5}$
Ascorbic acid	1000	$7.5x10^{-5}$
$FeSO_4 \cdot 7H_2O$	50	$1.8x10^{-6}$
Stock solution A	1ml	
Stock solution B	1ml	
Stock solution C	1ml	

Aliquots of stock solution D and the vitamin stock (Table 8.2) were stored in 1 ml amounts at -20°C. Stock solutions A, B and C were stored as larger aliquots at -20°C.

Table 8.2: Composition of vitamin stock solution.

Ingredient	Weight (mg/100ml)	Final molarity in L-15B
p-aminobenzoic acid	100	7.3x10-3
Cyanocobalamine (B12)	50	3.7x10-4
d- Biotin	10	4.1x10-4

L-15 powder for 1 litre of medium (Invitrogen/Life Technologies Cat No.41300-021) was dissolved in approximately 900 ml distilled water, then the components listed in Table 8.3 were added and the solution was brought to a final volume of one litre. The medium was sterilised by filtration (0.22 µm) and stored at 4°C for up to 4 months. Before use, pH was adjusted using 1M NaOH to obtain a neutral-mildly acidic pH as judged by colour of the pH indicator in the medium (desired colour was orange).

Table 8.3: Components added to L-15 medium to generate L-15B medium.

Ingredient	Weight or volume
aspartic acid	299 mg
glutamic acid	500 mg
proline	300 mg
α-ketoglutaric acid	299 mg
D-glucose	2239 mg
Mineral stock D	1 ml
Vitamin stock	1 ml

8.1.2 Settings of BD LSRFortessa lasers for flow cytometry (Pirbright)

The laser configuration of the BD LSRFortessa was as depicted in Fig 8.1 using the 488nm laser for ZsGreen and the 640nm laser for the LIVE/DEAD stain.

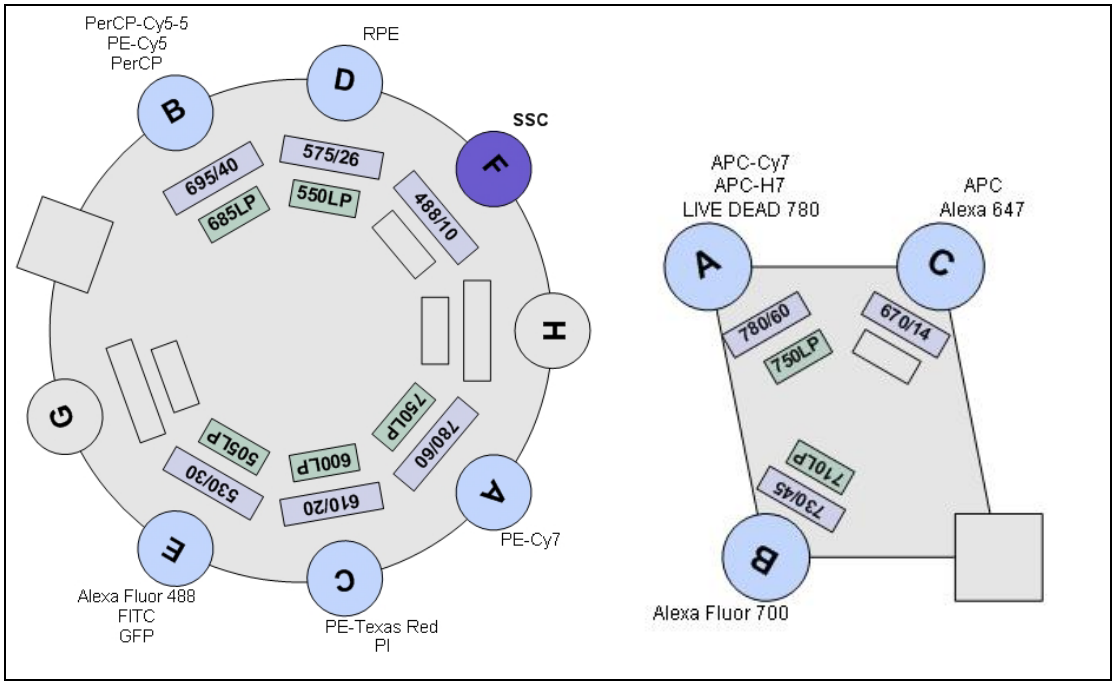

Figure 8.1: BD LSRFortessa (A) 488nm and (B) 640nm laser configuration.

8.1.3 Additional primer sequences

Table 8.4: Primer sequences used on IDE8 cells that did not amplify a target sequence.

primer name	sequence (5' to 3')	gene/origin
Ixodes_Toll2_F	TAATACGACTCACTATAGGGCATTCACGCAGCTTGTTGTT	IxToll-2 (this study)
Ixodes_Toll2_R	TAATACGACTCACTATAGGGTTGCTGCTGAACGATAGGAA	
noT7_Ixodes_Toll2_F#	CATTCACGCAGCTTGTTGTT	IxToll-2 (this study)
noT7_Ixodes_Toll2_R#	TTGCTGCTGAACGATAGGAA	
noT7_Ixodes_Toll3_F#	TGGTGTCGCTTCATTCTCTG	IxToll-3 (this study)
noT7_Ixodes_Toll3_R#	AACCGTGACACGTTGTTGAA	
noT7_Ixodes_Toll5_F#	CCGACGTGGTATGTCATCTG	IxToll-5 (this study)
noT7_Ixodes_Toll5_R#	ACGAAGGTGGCGTTATTCAC	
noT7_Ixodes_Toll6_F#	CCGACTCCAGAACCTGGATA	IxToll-6 (this study)
noT7_Ixodes_Toll6_R#	CGTGGACATGTTGTGGAAAG	
noT7_Ixodes_MyD88_F#	CTCCATCCTCAGCTCCAGAC	IxMyD88 (this study)
noT7_Ixodes_MyD88_R#	CTTGCACCACTTCTCCATGA	
gene15F	TCCGTAACCGTTTTCATCGTTA	gene15* (Liu et al 2012)
gene15R	CCTTCCTTGCATTCGTCATCTC	
gene-7F	TGCCGTAACCATTTTCATCGTT	gene7 (Liu et al 2012)
gene-7R	CCCTGTTTTGCAGTCTTCATCT	
gene-9F	AAAGCCCGAACCAGGACCCGC	gene9* (Liu et al 2012)
gene-9R	TGGCAATAGTGTCGCCCCAC	
Ixodes_CG4572_1_F	TAATACGACTCACTATAGGGCAATACGAGCGACGAAGACA	IxCG4572_1 (this study)
Ixodes_CG4572_1_R	TAATACGACTCACTATAGGGAGCATATTTTCCGCCATACG	
Ixodes_CG4572_2_F	TAATACGACTCACTATAGGGCGCTGTACCTAACGCCTCTC	IxCG4572_2 (this study)
Ixodes_CG4572_2_R	TAATACGACTCACTATAGGGGTGTAGGCGAGAGCAGGAAC	
Ixodes_CG4572_5_F	TAATACGACTCACTATAGGGTATGCGACGAAGTCAAGCAC	IxCG4572_5 (this study)
Ixodes_CG4572_5_R	TAATACGACTCACTATAGGGAAGTGTCCGGCATTTCTCAC	
Ixodes_CG4572_6_F	TAATACGACTCACTATAGGGGGTTTCAGCTTCACCGAGAC	IxCG4572_6 (this study)
Ixodes_CG4572_6_R	TAATACGACTCACTATAGGGTACAGCTCTTGGGGCAACTT	
Ixodes_CG4572_7_F	TAATACGACTCACTATAGGGAGATTGGACTGGTGGACAGC	IxCG4572_7 (this study)
Ixodes_CG4572_7_R	TAATACGACTCACTATAGGGCCTCTCCACTTGGAGTCAGC	
Ixodes_CG4572_8_F	TAATACGACTCACTATAGGGTTTACGAAATTGGCCTGGTC	IxCG4572_8 (this study)
Ixodes_CG4572_8_R	TAATACGACTCACTATAGGGCGGTGAAGTTGGCTACCTGT	
Ixodes_CG4572_9_F	TAATACGACTCACTATAGGGGCGAACTCCTCTACCAGACG	IxCG4572_9 (this study)
Ixodes_CG4572_9_R	TAATACGACTCACTATAGGGCTCTCCGTGGCCTTGTACTC	
Ixodes_CG4572_10_F	TAATACGACTCACTATAGGGGTACAGGAGACTCCCCACCA	IxCG4572_10 (this study)
Ixodes_CG4572_10_R	TAATACGACTCACTATAGGGGTGGGAGTTATAGCCCGTCA	
Ixodes_CG4572_neu_1_F	TAATACGACTCACTATAGGGCGTATGGCGGAAAATATGCT	IxCG4572_1 (this study)
Ixodes_CG4572_neu_1_R	TAATACGACTCACTATAGGGCTCCAAGTAGGGCTTTGCAG	
Ixodes_CG4572_neu_2_F	TAATACGACTCACTATAGGGGTTCCTGCTCTCGCCTACAC	IxCG4572_2 (this study)
Ixodes_CG4572_neu_2_R	TAATACGACTCACTATAGGGACCACTGAAGGGTGGAGATG	

Ixodes_CG4572_neu_5_F	TAATACGACTCACTATAGGGAACCTGACATGGGAAGCAAC	IxCG4572_5 (this study)
Ixodes_CG4572_neu_5_R	TAATACGACTCACTATAGGGGTGCTTGACTTCGTCGCATA	
Ixodes_CG4572_neu_6_F	TAATACGACTCACTATAGGGAGTGGATCTGGAATCCATGC	IxCG4572_6 (this study)
Ixodes_CG4572_neu_6_R	TAATACGACTCACTATAGGGGTCTGACGTAGCCAGCAACA	
Ixodes_CG4572_neu_7_F	TAATACGACTCACTATAGGGGAATCGTACGCCGGAAAATA	IxCG4572_7 (this study)
Ixodes_CG4572_neu_7_R	TAATACGACTCACTATAGGGTGAGATCATGTTGGCCGTTA	
Ixodes_CG4572_neu_8_F	TAATACGACTCACTATAGGGGAGCATTTCAAGCCAGAAGC	IxCG4572_8 (this study)
Ixodes_CG4572_neu_8_R	TAATACGACTCACTATAGGGCGCACTCGTGTTGTCTGAAT	
Ixodes_CG4572_neu_9_F	TAATACGACTCACTATAGGGAAGGTGAAGGGCCTGATTCT	IxCG4572_9 (this study)
Ixodes_CG4572_neu_9_R	TAATACGACTCACTATAGGGCTCTCCGTGGCCTTGTACTC	
Ixodes_CG4572_neu_10_F	TAATACGACTCACTATAGGGGAGACTCCCCACCATTCAGA	IxCG4572_10 (this study)
Ixodes_CG4572_neu_10_R	TAATACGACTCACTATAGGGTATAGCCCGTCAGGTTCTGG	

these primers were all first tested with T7 promoter, then without;
*primer sequences did not match to gene sequence;

8.2 ADDITIONAL INFORMATION FOR CHAPTER 3

8.2.1 EM of SFV replication in tick cells

Some structures in BDE/CTVM16 cells infected with SFV, showed similar morphology to replication complexes observed in mammalian cells, but the images are not entirely convincing (Fig 8.2).

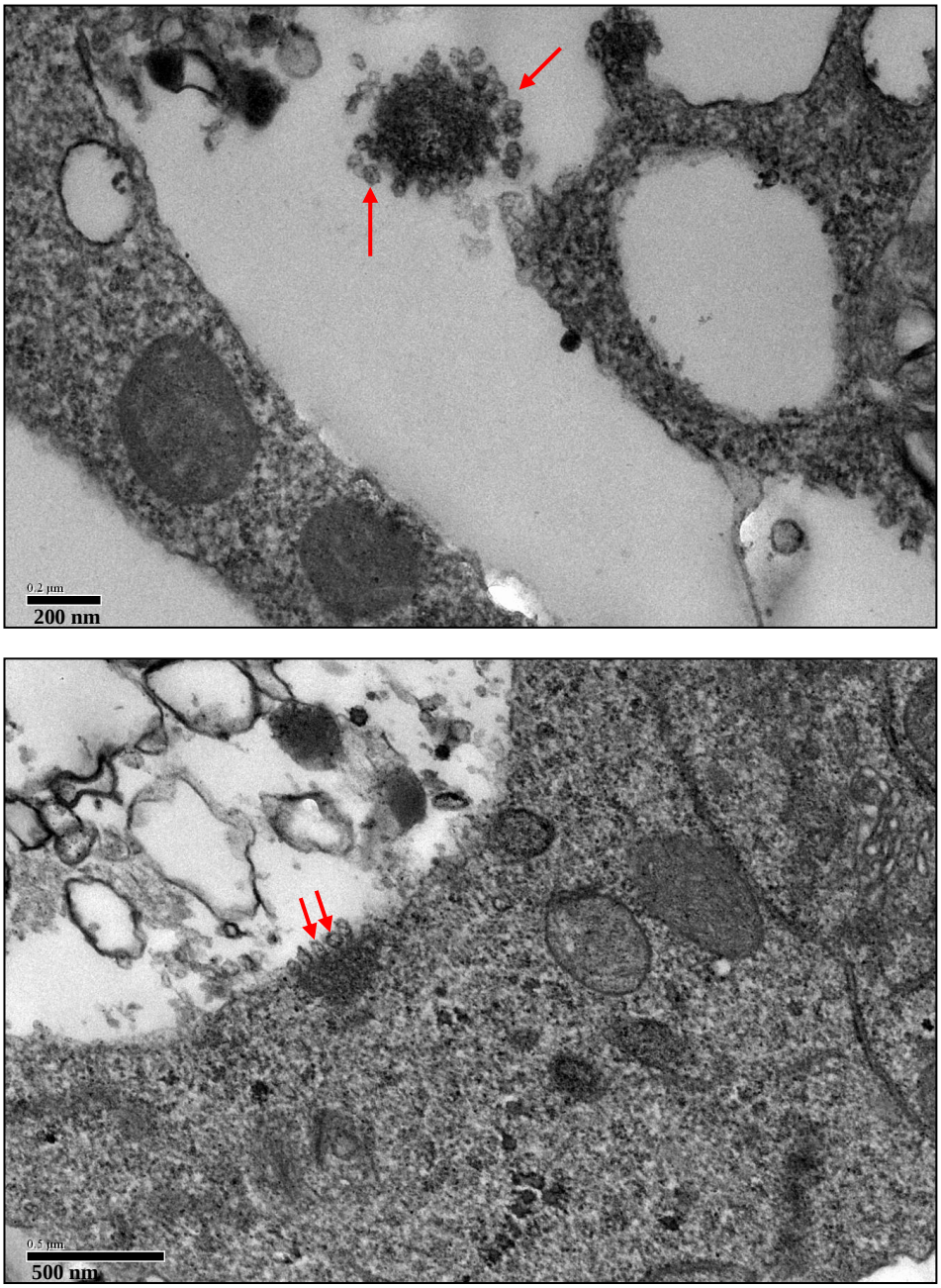

Figure 8.2: Tick BDE/CTVM16 cells infected with SFV4(3F)-ZsGreen and visualised by EM Arrows indicate potential CPV-I type replication complexes of SFV.

8.3 ADDITIONAL INFORMATION FOR CHAPTER 4

8.3.1 SUMO alignments

The sequences of two putative *I. scapularis* SUMO orthologues, namely IxSUMO-1 (XP_002434373) and IxSUMO2/3 (XP_002411230.1), were identified by BLAST search using human sequences. This finding is in contrast to *Drosophila* and mosquitoes, which appear to have only one SUMO protein (Susan Jacobs, personal communication). The sequences are highly conserved (Fig. 8.2) and both human SUMO1 and SUMO2/3 antibodies detected the putative tick SUMO proteins.

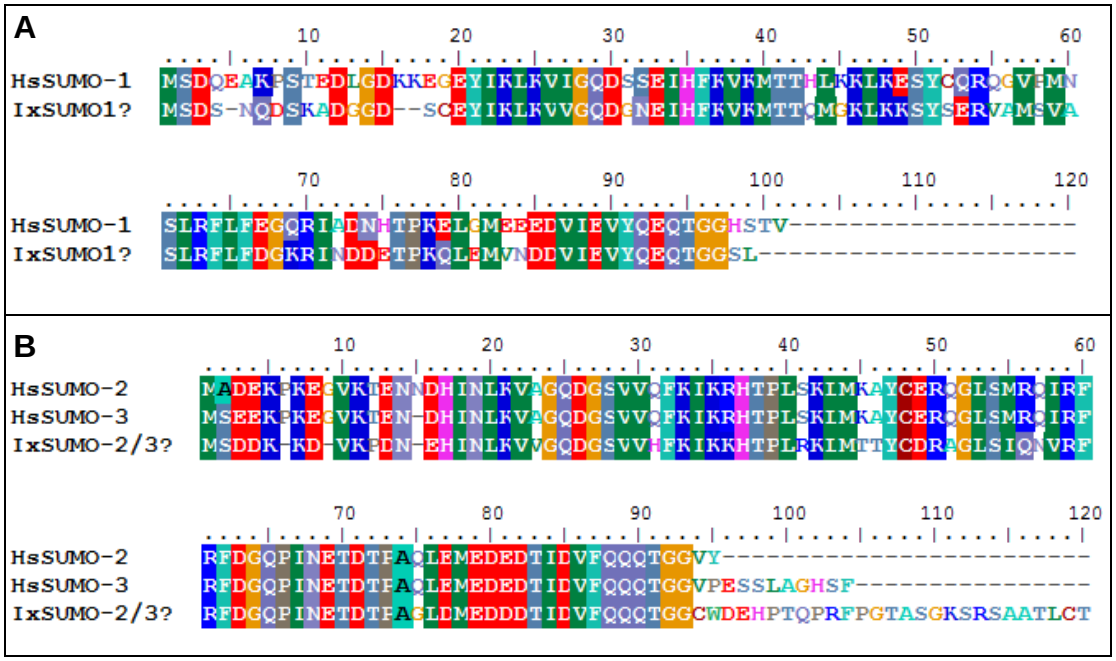

Figure 8.3: Alignment of human (Hs) and putative *I. scapularis* (Ix) SUMO1 (A) and SUMO2/3 (B).

8.3.2 IxVago modelling

During identification of Vago orthologues in *I. scapularis*, the structure of putative orthologues was modelled for the prediction of VWC domains (Fig 8.3).

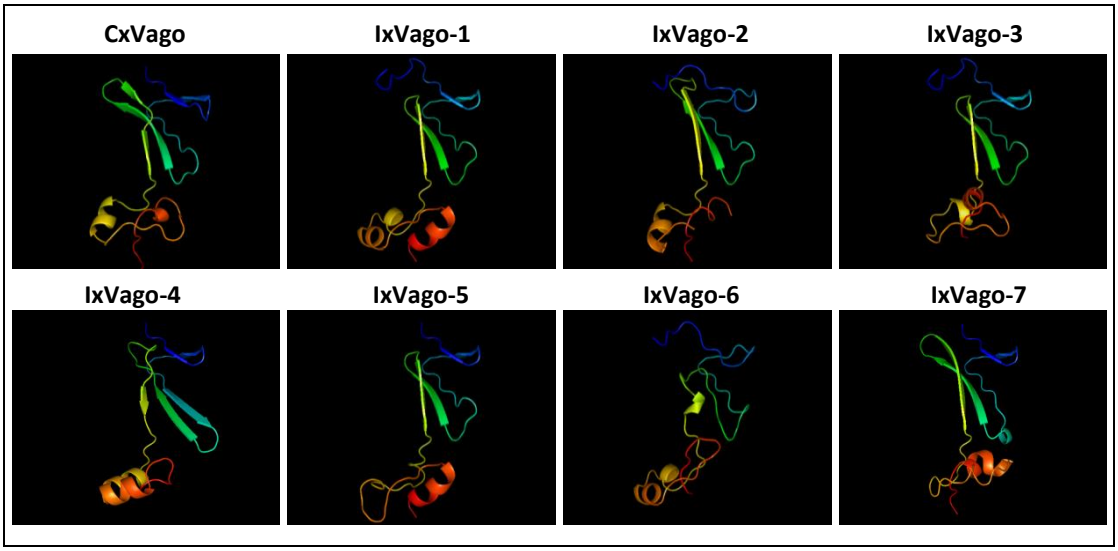

Figure 8.4: 3D-modelling of IxVago structures of the full length *C. quinquefasciatus* Vago and *I. scapularis* vago sequences before cleavage at the signal peptide sequence.

8.4 ADDITIONAL INFORMATION FOR CHAPTER 5

8.4.1 U4.4 sequences for CG4572 orthologues

Provided below are the contig sequences found in the *Ae. albopictus* U4.4 cell transcriptomic study performed by Julio Rodriguez-Andres (AAHL, CSIRO, Geelong).

CG4572_56.1 orthologue (AAEL009291-RA)

>contig09733; length=211; numreads=3
gttttcggtgaacaGgCCATACATAGATGAAGCCCCGGGACCACCTTGGAGCCAGATGACCAC
CGGAGCGTCATCCTgAACATCGTGTTCAGCCACAAAGTACCAGAaGAAAaGATTGGAGT
TGAGCTTTTCGTCTACGGTcAGGTAACCGGAGTAGCTCTCgATGTTCGCCGGGATGgCa
GAATGGTtCaCTttGgCCGCATTaCGTCCa

>contig10450; length=230; numreads=3
TTAAATaTATCtATtGTTtgAACTatATtATTCAaTCTtCCTTctCAaCTGAATtGTTcCGAATTCC
ACcAGCACTaatCTAGCCCcAACcGCTCAGGCATAaCCTTTACCGTGGgTGAGTCTCATCA
GTAGATCCAGCGCCCACTtGGGTTGATCCTTCGGAaCCATGTGGCCTGCGTTTCGGACC
AaCACCTCGGCCAAaTTtCcGGCcTCcTTtGcgTaCCcGgcaa

>contig04052 length=702 numreads=23
agcagtggtatcaacgcagagtaCGGGggagTTttcttctanncntnngntnnnnnngnnnnnnnnnnaaannnnnt
ncccnntnntnnncnnnnannnnnnnnnnnnnttaggtgcagcagcagtgtatGTaattgaattatccctctgtgtcgtttcatt
gcgttggtcgaagatgcgagcccattcatacgggtcgctcgcGGTACTCGCCTTATCGTTGATGATAGGAAC
CGCCaGCGCcAAACTGTTCGTCAATCCCTATCCGAGCTACcAGCATCTGAAGAGCTACA
GCTCTGCTTTCGCTTTGGACGGAGGGGACGTCGGTGAACCGCTGTTtCTGTCGCCCTTt
ATTTTtAATGGTTCCGtCGAaGCTGgACGTAATGCGGCCAAAGTGAACcATTCTGCCATCC
CGGCgAACATCGAGAGCTACTCCGGTTACCTGACCGTAGACgAAAaGCTCAACTCCAAc
TTTTCTTCTGGTACTTTGTGGCTGAACACGATGTTCAGGATGACGCTCCGGTGGTCAtCT
GGCTCcAAGGTGGTCCcGGGGCTTCaTCTATGTATGGCcTGTTCACCGAAAACGGACCG
TTCTCGGTGGATAACAAGATGAAGTTGCATCCcCGGAAGTACTCGTGGCACTTCAACCA
TCATaTGATCTACTTCGACAACCCcGTTGGAACAGGCTTTAGCTtCACcGa

CG4572_05.1 orthologue (AAEL006542-RA)

>contig00521 length=858 numreads=19
gcAaTCTCACCGTCCACCTTCCAGATGTAGCgaGGGGCCTTCTTGTACTGAtcccggcccggg
aagttctaatttttgcacgtagttcatggtcaatgggtaggccccaatgatatccagctgaccgttgtagatcaccactcggtaggag
ttcaaaagttcctccaggtagggcaccaccgacttcatcacgtCCAGCTTCAGaTGTTCTtCAACcTTGTtCtCA
CTgTCcAACTCgTGGAAGgTgTTATtGCcGAcATGgATTgctctacgggtttccggcagctctaggaacttca
ccatgtaatcgtccttgggatccggcttggtttgtaggtagttGAAGTAaGTCTCGAAGCCGGAGACGTTTTTAA
ACAGCGATCCGCTGGAATACATGTCTCCGTTGATCAGCGCgTCGAACGCCTCGAATGC
GCAGTTCATGTCGTTCTTGGTGATACAGTCCCGTCCTTtCTTTTCGTACGCGtGGAaCTC
GTCGCGGGCATTGGAATCGATCAACCCCAGCTGATAAaGgTAATCTCCGTAGACAAGTT
GGTGGAGCGGATCACACAGCCCGTTGCCAATGgCCAATCcTTTGAGgTTTAtCTTGACCT
TGGCgTTATCGTtGtAGCGgTgAaTGGCaTGCGACACaGCcGGGACGTACTTTCCTCCaTA
AgaCTCACCAGTAACGTAGAAATTGCGTTTCTGTaGATCAGGGAACAACAGGAAGAACT
GCACCAAAGCgTTGTGAAGGTTGTTGCCTACTTGCGTTTCGTTGGTGCTGTAGCcTTCG
TCGTGATCGGTGAAGCTAAaGCCTGTtCCAaCGGGGTTGTCGAAGTAGATCATATGATG
GTTGAAGTG

>contig00177 length=587 numreads=14
GTCTCCGGCTTCGAGAngtACTTCAACTACCTACAAACCAAGCCGGATCCCAAGGACGA
TTACATGGTGAAGTTCCTAGAGCtGCCGGAAACCCGTAgagCAATCCATGTCGGCAATAA
CACCTTCCACGAGTTGGAcAGTGAGAACAAGGTTGAAGAACATCTGAAGCTGGACGTGA
TGAAGTCGGTGGTGCCCTACCTGGAGGAACTTTTGAACTCCTACCGAGTGGTGATCTA
CAACGGTCAGCTGGATATCATTGTGGCCTACCCATTGACCATGAACTACGTGCAAAAAT
TGAACTTCCCGGGCCGGGATCAGTACAAGAAGGCCCCTCGCTACATCTGGAAGGTGGA
CGGTGAGATtGCcGggTACGCAAAGGAGGCCGGAAaTTTGGCTGAGGTGTTGGTTCGAA
ATGCAGGCCATATGGTGCCCAAGGATCAACCcAAgTGGGCGCTGGATCTGCTGATGAG
ACTCACCcAcGGTAAaGgTTATGCCTGaGCGGTTggggctagattagtgctngnnnaantnnnnnannan
tnnnntnnnnangnannntnnannannnnnntnnaannannnnnnnn